ISSN 0385-2520

ROCK MAGNETISM and PALEOGEOPHYSICS

volume 4

1977

Published by the

ROCK MAGNETISM AND PALEOGEOPHYSICS RESEARCH GROUP IN JAPAN

まえがき

本書は、Geodynamics Project (GDP) II-1-(2)「古地磁気学的方法」の研究グループの報告書として刊行されるものである。岩石磁気学・古地球物理学研究グループでは、以前からAnnual Reportの形で英文の報文集を刊行してきた。(Annual Progress Report of the Rock Magnetism (Paleogeophysics) Research Group in Japan, 1963, 1964, 1965, 1967, 1968)。これらの報文集は、諸外国の研究者の間でもかなり広く活用されている。こういった実績を継続するためにも、GDPの研究報告書ではあるが英文によっている。日本国内の研究者の方々にいく分御面倒をおかけすることになるが、このような事情なので御了承いただきたい。

報文の配列の仕方は便宜的なものであるが、一方大まかに(1) 磁性鉱物・熱残留磁化 7編, (2) 堆積残留磁化(DRM)およびpost DRM 7編, (3) 考古磁気学および古地磁気学 13編, (4) アイソトープ地学・希ガス分析 7編という分類がしてある。

"Rock Magnetism and Paleogeophysics" はextended abstract集であるのでここにおさめられた報文はprogress report的なものを除いて、いずれは完全な形の論文としてさまざまな学術誌に投稿・発表される予定である。発表予定が特にはっきりしているものについては、各論文末尾にそのことが付記してある。従ってこの報文集から引用されることは自由であるが、本論文が発表されたものについてはそちらを引用されるよう御配慮をお願いしたい。

本巻は はじめ1976年12月に刊行する予定であったが、主として財政的な理由から出版が大幅におくれた。本書におさめられた研究には 文部省よりGDP特別事業費によって援助を受けた。

1977年10月

古地磁気学・古地球物理学研究グループ

CONTENTS

ROCK MAGNETISM AND PALEOGEOPHYSICS SYMPOSIA

The Eighth Rock Magnetism and Paleogeophysics Symposium was held on 22nd and 23rd September, 1976 at Faculty of Engineering Science, Osaka University.

22 September

N. Fujii (Kanazawa Univ.)	Climate changes deduced from pollen analysis.
S. Sasajima (Kyoto Univ.)	Paleomagnetic studies in Indonesia.
N. Isezaki (Kobe Univ.)	Relation between the frequency of geomagnetic reversals and the rate of sea floor spreading.
H. Inokuchi (Shinshu Univ.)	Normalization of DRM intensity by TRM.
T. Sueishi and N. Kawai (Osaka Univ.)	Fine structure of geomagnetic variation in the first half of Matuyama epoch and normalization of magnetization intensity of sediments.
T. Nishitani (Tokyo Univ.)	Synthesis of titanomaghemites.
H. Domen, H. Muneoka and S. Kuniyoshi (Yamaguchi Univ.)	J_s-T analyses of Japanese iron sands.

23 September

N. Kawai (Osaka Univ.)	Climate and history change because of geomagnetism.
H. Kamiyama (Tohoku Univ.)	An aeronomical consideration of climate changes in times of geomagnetic weakening.
H. Watanabe (Tokyo Univ.)	Turbulence in rotating systems and dynamo process.
H. Sakai, N. Kawai (Osaka Univ.) and K. Kobayashi (Tokyo Univ.)	On the movement of earth's rotational axis.
K. Kobayashi (Tokyo Univ.)	Voyage on Glomar Challenger.
K. Yaskawa (Kobe Univ.)	New method of alternating field demagnetization.
T. Yokoyama (Doshisha Univ.)	Paleomagnetism in Siwalik.
K. Hirooka, C. Tobita (Fukui Univ.), T. Yokoyama (Doshisha Univ.) and S. Nakagawa (Fujimi High School)	Paleomagnetism of Ontake tephra.

The Ninth Rock Magnetism and Paleogeophysics Symposium was held on 25th and 26th July, 1977 at Rakuyu-kaikan of Kyoto University.

25 July

T. Shinjo (Kyoto Univ)	Ferromagnetism of fine particles.
A. Yamamoto (Osaka Tellecom. Coll.)	200m core of Lake Biwa, with special reference to silty sediments.
K. Nakagawa (Osaka City Unig.)	Physical, chemical and kinematic properties of silty sediments.
Y. Hamano (Tokyo Univ.)	Characteristics of magnetic remanence caused by compaction.

Y. Otofuji, I. Katsura and S. Sasajima (Kyoto Univ.) Remanent magnetization in silts.

N. Niitsuma (Tohoku Univ.) Zone magnetization model and depth lag in deep sea sediments.

S. Noboriuchi and K. Kobayashi (Tokyo Univ.) Stability of remanences of deep sea sediments.

H. Inokuchi (Shinshu Univ.) Magnetic properties of deep sea sediments collected from Phillipine Sea.

T. Sato, T. Sueishi, N. Kawai (Osaka Univ.) and K. Kobayashi (Tokyo Univ.) Remanent magnetization of sediments from Melanesia basin.

M. Yoshida (Hokkaido Univ.) Paleomagnetism of Quaternary rocks from Nobeyama region, east of Yatsugatake.

26 July

K. Hirooka (Fukui Univ.) Paleomagnetism of loam layers.

N. Aida (Hokkaido Univ.) Paleomagnetism of younger loam layers distributed on the north-east side of Yatsugatake.

H. Domen (Yamaguchi Univ.) Stability of DRM(?) of volcanic ash.

S. Sasajima (Kyoto Univ.) Paleomagnetic data and Phillipine Sea plate.

K. Kobayashi (Tokyo Univ.) Magnetic anomalies in the Shikoku basin and IPOD project.

K. Hirooka and I. Hattori (Fukui Univ.) Paleomagnetism of paleozoic formations in Mino-Tamba zone.

H. Ito and K. Tokieda (Shimane Univ.) NRM and chemical composition of Cretaceous granites.

T. Furuta and K. Kobayashi (Tokyo Univ.) Magnetic properties of DSDP Leg 49 rocks (Reykjanes Ridge).

H. Sakai and N. Kawai (Osaka Univ.) Geomagnetic field intensity variation in archeological period.

H. Domen and H. Muneoka (Yamaguchi Univ.) Paleointensities from some Quaternary volcanic rocks of western Japan.

H. Domen (Yamaguchi Univ.) Relation between "Jori" divisions and archeomagnetic directions.

H. Domen (Yamaguchi Univ.) Treatment of NRM direction data with large dispersions.

I. Muroi (Osaka Science Education Center) NRM direction and error angle of a single specimen (2).

N. Niitsuma (Tohoku Univ.) Superconducting magnetometer and alternating field demagnetization apparatus.

K. Momose and Y. Inoue (Shinshu Univ.) Thermal stability of titanomaghemites (2).

J. Nishida, S. Sasajima and E. Abe (Kyoto Univ.) Estimation of thickness of Lake Biwa sediments.

N. Niitsuma (Tohoku Univ.) What occurred when the geomagnetic field reversed ?

PREFACE

This volume is the annual progress report of the Rock Magnetism and Paleogeophysics Research Group in Japan for the year 1977. As the previous volumes were so, this volume is a collection of summaries or extended abstracts of various research works carried out in our group. Many of the reports contain substances which may be changed or revised as the research work continues. In this respect, this volume contains many tentative results.

Except for the ones written as pure progress reports, the papers in this volume will be published in academic journals in full detail and length. This volume may be referenced, but if a paper is published in such an academic journal, readers are requested to quote the paper from that journal. We hope that this volume is a useful source of advance information of recent works on rock magnetism and paleogeophysics in Japan.

This volume also constitutes a scientific report of the Rock Magnetism and Paleogeophysics Research Group in the Japanese Geodynamics Project. We would like to acknowledge the partial financial support from the Ministry of Education for this publication and for the investigations included in this volume as a part of the Geodynamics Project.

Publication of this volume was at first scheduled for December 1976. Because of finantial and other difficulties, however, it was postponed for ten months. We apologize to the contributors and the readers for the inconvenience caused by this delay.

October 1977

Masaru KONO
Editor

MAGNETIC PROPERTIES OF TITANOMAGNETITES CONTAINING SPINEL($MgAl_2O_4$)

Tadashi NISHITANI

Geophysical Institute, University of Tokyo,
Bunkyo-ku, Tokyo 113

Hidefumi TANAKA, Takashi KATSURA

Tokyo Institute of Technology
Ookayama, Meguro, Tokyo 152

Introduction

The carriers of remanent magnetization in natural rocks are almost titanomagnetites. For titanomagnetites in basalts it was shown by electron microprobe analysis that they contain Al (0.4 ~ 4.1 % by weight), Mg (0.2~ 3.2 %) and small amounts of Mn, Cr, Ni and Zn (Creer and Ibbetson, 1970). Prevot and Mergoil (1973) pointed out that a considerable amount of Mg and Al exist in titanomagnetites in an alkali basalt. In order to determine the concentration of cations other than Fe and Ti, Sasajima et al.(1975) carried out careful wet chemical analyses of titanomagnetites. Their data show that the amounts of both Al_2O_3 and MgO are too large to be treated as impurities. Creer and Stephenson (1972) considered the distribution of these cations in titanomagnetites and its effect on Curie points. Joshima (1975) studied the effect of Al contamination in titanomagnetites and titanomaghemites. Richards et al.(1973) synthesized two series of solid solutions $Fe_{2.4-\delta}M_\delta Ti_{0.6}O_4$ (where M = Al or Mg) and examined the variation of lattice constant, saturation magnetization and Curie point as a function of substitution parameter δ ($0<\delta<0.25$).

However, it may not be a good procedure to consider the effect of two cations separately. Generally, the ratio of Mg to Al in natural titanomagnetites is close to 1:2 which is the same as that of spinel ($MgAl_2O_4$)(Katsura et al., 1976). It may therfore be worthwhile to examine synthesized titanomagnetites containing various amounts of spinel. Lattice constants of titanomagnetites are considerably affected by the addition of spinel component (Katsura et al., 1976).

The purpose of the present work is to examine the magnetic properties, mainly Curie temperature (T_c) and saturation magnetization (J_s) of the titanomagnetites containing spinel.

Table 1

mole fraction of Fe_2TiO_4 in titanomagnetite x	mole fraction of spinel y	lattice constant (Å)	Curie Temp. (^oC)	Saturation magnetization at 20^oC (emu/g)
0.00	0.1	8.367	520	66.1
	0.2	8.342	449	52.0
	0.3	8.315	346	34.8
	0.5	8.262	144	13.3
	0.7	8.198	-106	0.26
0.1579	0.0	8.412	509	71.3
	0.1	8.403	435	48.9
	0.4	8.267	85	2.03
0.2787	0.0	8.429	427	56.7
	0.1	8.403	340	37.4
	0.3	8.343	174	25.0
0.3333	0.0	8.437	403	46.3
0.4682	0.0	8.457	298	35.4
	0.1	8.430	221	26.1
	0.2	8.397	126	16.7
0.5294	0.0	8.466	248	29.7
	0.1	8.437	172	19.4
	0.2	8.406	81	12.5
0.6364	0.0	8.487	142	19.2
	0.1	8.453	77	12.6
	0.2	-	-21	1.03
0.7037	0.0	8.500	79	13.9
	0.5	8.409 8.147	-151	0.21
0.7736	0.1	8.472	-6	0.62
	0.3	8.418 8.150	-122	0.35
1.0000	0.1	8.492	-162	1.14

Experiment and Result

Titanomagnetites are usually expressed by the formula

$$xFe_2TiO_4 \cdot (1-x)Fe_3O_4$$

where x ($0 \leq x \leq 1$) is the mole fraction of ulvospinel, with x = 0.0 corresponding to magnetite and x = 1.0 to ulvospinel. The titanomagnetites containing spinel can be represented by

$$(1-y)(xFe_2TiO_4 \cdot (1-x)Fe_3O_4) \cdot yMgAl_2O_4$$

where y ($0 \leq y \leq 1$) is the mole fraction of spinel, y = 0.0 represents titanomagnetite solid solution series without impurity.

Curie temperature and saturation magnetization at 20°C were measured using magnetic balance under a magnetic field of about 5 kOe. Samples were heated in vacuum (about 10^{-5} Torr) up to 700°C. When the Curie point of a sample below the room temperature, the change in J_S was examined down to -180°C using liquid nitrogen.

The results are shown in table 1. Lattice parameters were quoted from Katsura et al. (1976).

Fig. 1 shows the variation of Curie temperature as a function of x and y. The Curie points decrease with increasing the amounts of spinel (y) and mole fraction of ulvospinel (x).

Fig. 2. is a variation of saturation magnetization at 20°C (emu/g) as a function of x and y. Saturation magnetization decreases as x and y increase. The values of the series y = 0.0 (titanomagnetites) are in agreement with those of Akimoto et al.(1957).

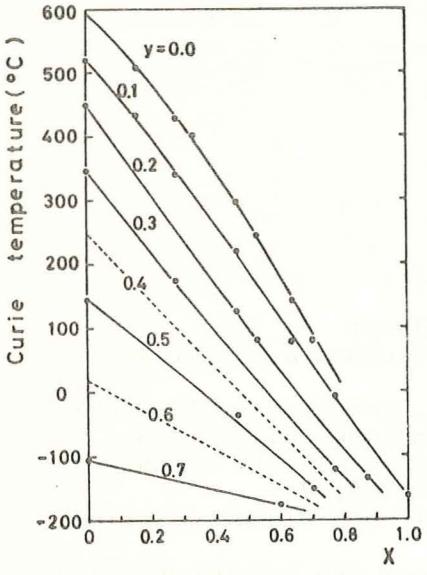

Fig. 1. Curie points of synthetic titanomagnetites containing spinel. Dotted line represent interpolated curves.

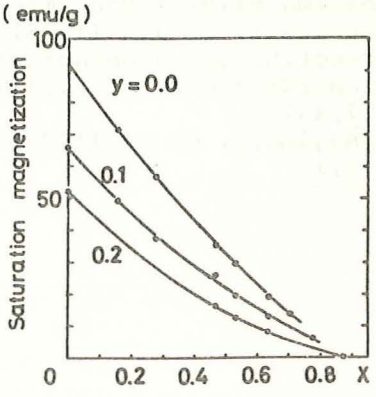

Fig. 2.
Saturation magnetization at 20°C.

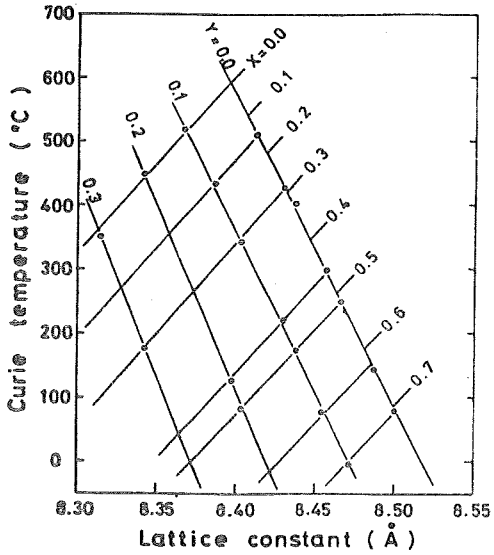

Fig. 3. The relation between lattice constant and Curie temperature. Solid circles represent experimental data.

In Fig. 3 horizontal axis is lattice constant and vertical axis is Curie point. This figure shows that the changes in the composition of titanomagnetites (x,y) affect both Curie temperature and lattice constant in a systematic way. Therfore, the chemical composition of natural titanomagnetites containing impurities may be estimated by measuring Curie temperature and lattice constant, provided that the impurities are really of spinel composition and that the titanomagnetite is not oxidized.

References

Akimoto,S et al.(1957) J.Geomag.Geoelectr. 9, 165.
Creer,K.M. and J.D. Ibbetson (1970) Geophys.J.R.astr.Soc. 21,485.
Creer,K.M. and A. Stephenson (1972)J.Geophys.Res. 77, 3698.
Joshima,M(1975) Rock magnetism and Paleogeophysics 3,5.
Katsura,T. et al. (1976) J.Volcanology 21,31.(in Japanese)
Prevot,M. and J.Mergoil (1973) MIN.Mag.39,474.
Richards,J.C.W. et al.(1973)Phys.Earth and Planet.Interiors, 7,437.
Sasajima,S. et al.(1975) rock magnetism and Paleogeophysics 3,1.

A SHORT NOTE ON THERMO-MAGNETIC AND X-RAY ANALYSES OF JAPANESE IRON SANDS.

Haruo DOMEN

Institute of Physical Sciences, Faculty of Education,
Yamaguchi University, Yamaguchi 753, Japan.

Iron sand specimens sampled at about one hundred and fifty sites in overall Japan were submitted to the thermo-magnetic analysis. And some of those were examined by means of an X-ray analyzer. The test specimens were classified into seven locality groups accoding to geographic districts at where the specimens were collected, such as; (1) Hokkaido, (2) Tohoku·Hokuriku (northern Main Island), (3) Kwanto (east central), (4) Chubu·Kinki (west central), (5) San-in (northwestern coastal region of the Sea of Japan), (6) San-yo (southwestern coastal region of the Seto Inland Sea) and (7) Kyushu districts respectively. A map showing the location of sampling sites, excluding Iwo-Jima Islet in Bonin Islands, is presented in Fig. 1.

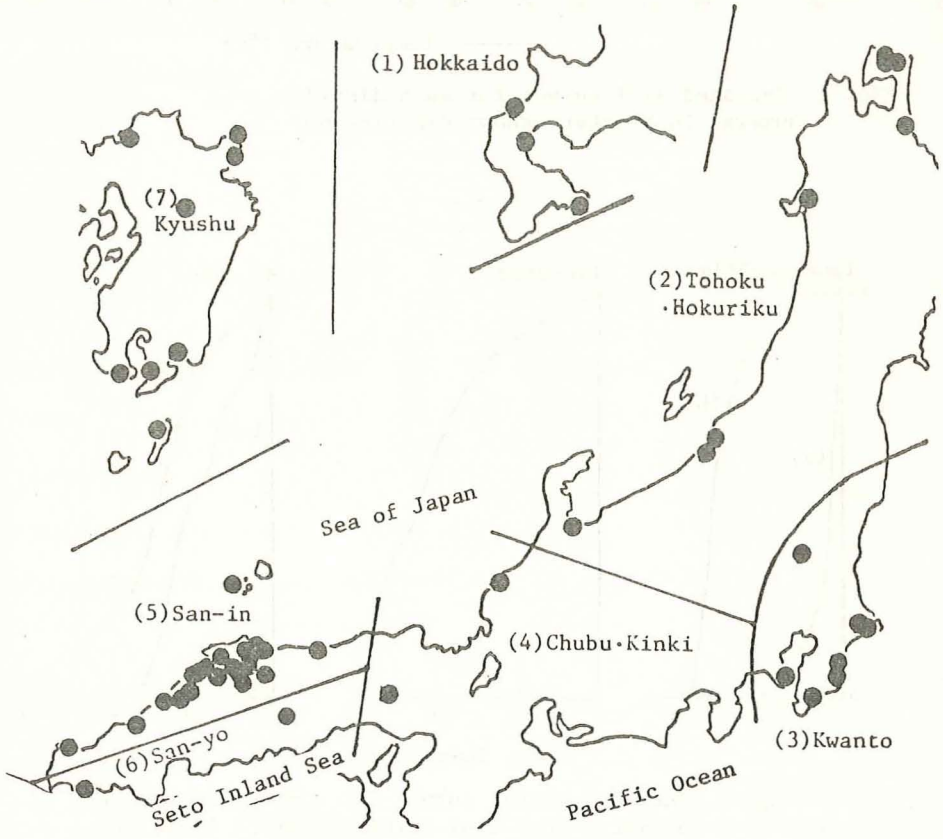

Fig. 1. Map showing sampling locations with zonning of geographic districts (Iwo-Jima in Bonin Islands exclusive).

Averaged Js-T curves for each district mentioned above are roughly skeched in Fig. 2.

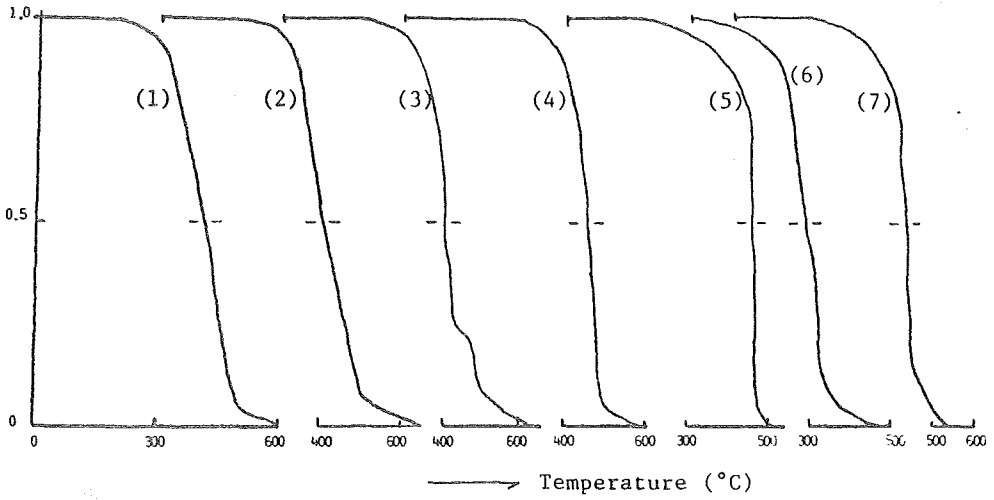

Fig. 2. Averaged Js-T curves for each district.
Numeral in brackets shows district no.

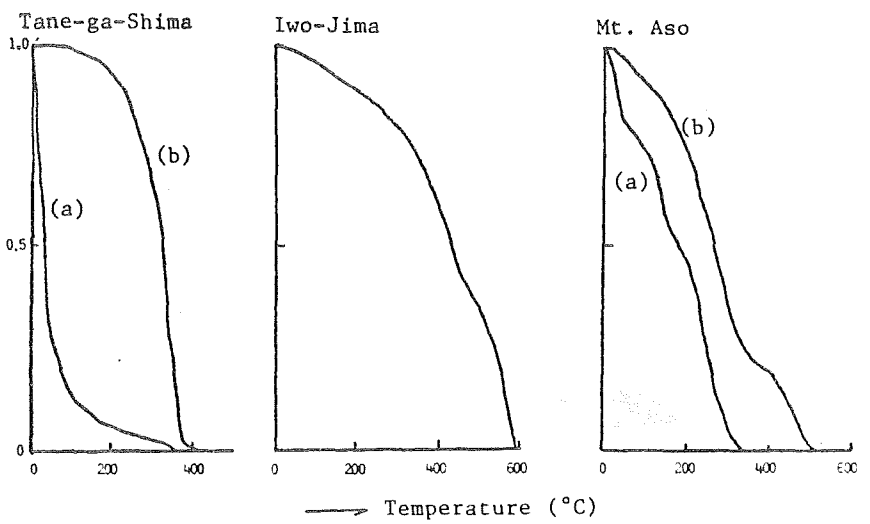

Fig. 3. Thermo-magnetic curves for some characteristic specimens come from three different locations. (a) and (b) are for separat sites within the same location respectively.

Test specimens from both Tane-ga-Shima (nearest south neighboring of Kyushu Island, the most northern island belonged to Ryukyu Islands) and Iwo-Jima show somewhat characteristic Js-T curves, which are illustrated in Fig. 3.

At the summit of Mt. Aso, the famous active volcano at the central Kyushu Island, shallow-sheeted volcanic dusts were sampled at two sites; (a) foot of the central cone, (b) rim of central crater, from which the ferromagnetic minerals as the test specimen were extracted by a hand magnet and these were submitted to the Js-T analysis. The Js-T curves thus obtained are also shown in Fig. 3.

Some of Kyushu and Yamaguchi (belonged to districts (5) and (6), west end of Main Island) samples and also Iwo-Jima sample were submitted to the X-ray analysis. Ferromagnetic constituents of those samples were identified by both Js-T and X-ray analyses mentioned above, which results agreed with each other rather well in general speaking.

THERMOMAGNETIC ANALYSIS OF THOLEIITIC BASALT

Kan-ichi MOMOSE

Department of Geology, Shinshu University
Asahi 3-1-1, Matsumoto 390, Japan

Confirmation of the generation of native iron in volcanic rocks should be important to get a clue to the problem of the oxygen partial pressure or the reducing condition pertinent to the magma within the crust or the mantle of the earth.

As already reported by Momose(1974-5), the occurrence of native iron has been discovered in lava flow at some place of a new-born volcanic island Nishinoshima-shinto. The problem may rather be simplified because the volcano is not the one piled up on the continental crust. Another problem, however, lies in the difficulty of interpreting the origin and the coexistence of both native iron and titanomagnetite within a microscopic extent.

If the occurrence of native iron is peculiar only to the lava flow of Nishinoshima-shinto, the magma reservoir related to this lava flow should have, even partially, once been in a highly reducing condition.

For the purpose of confirming the problem if the occurrence of metallic iron is to be expected generally in such a type of volcanic rocks, first several samples as cited below, were examined (according to an instructive suggestion of Prof. Miyashiro(New York State Univ.) and Prof. Kobayashi(Shinshu Univ.), who advised the reporter to concern more samples from other localities in wider extent) by the thermomagnetic analysis and observed under the reflection microscope. Some of the samples were given from Prof. Sasajima(Kyoto Univ.) and Mr Inokuchi (Shinshu Univ.).

All the experimental samples are of typical tholeiitic basalt and include lava flows with definite date from Kilauea and Mauna Loa, and those of different geologic ages from volcanic islands in the Western Pacific : i.e. Maug, Agrihan, Pagan and Anatahan islands of the Mariana archipelago, and Miyakejima.

The results obtained have prove that these samples do not contain native iron at all.

The results along with the facts that the localities of rock samples are wide in distribution and that the samples are typical of tholeiite lead reasonably to a conclusion : that the occurrence of native iron within the lava of Nishinoshima-shinto demonstrates a peculiar case allowing to assume an existence of local reducing condition in the mantle or the crust.

References

Momose,K. (1974) Rock Mag. Paleogeophys., 2, 1.
Momose,K. (1975) Kagaku, 45, 637. (in Japanese)
Momose,K. (1975) Rock Mag. Paleogeophys., 3, 17.

FERROMAGNETIC MINERALS IN THE DEEP-SEA SEDIMENT CORE COLLECTED FROM THE PHILIPPINE SEA

Hiroo INOKUCHI

Department of Geology, Faculty of Science, Shinshu University, 3-1-1, Asahi, Matsumoto 390, Japan

Preface

In order to trace continuous change of the ancient geomagnetic field, it is effective to measure the direction and intensity of Natural Remanent Magnetization of the sediments. In particular, the sedimentation rate of the deep-sea deposits is, in general, very slow and constant. Therefore, a core log, if not long, affords the information for a relatively long time span. A large number of magnetic studies for deep-sea sediments collected from various localities of the oceans have been made since Johnson et al.(1948). It, however, is still unknown how and when the sediments have acquired the NRM(Natural Remanent Magnetization).

It is important to identify the kind of minerals responsible for NRM of the sediments for the explanation of the magnetism of the oceanic sediments. Haggerty(1970) descrived by the optical observations that the magnetic minerals separated from twenty-two sediment cores from the equatorial and north Pacific, Atrantic, and Indian Oceans and from below the Antarctic ice sheet, variously consisted of titaniferous magnetite, titanomaghemite, hematite, goethite or limonite, pyrite, micro manganese nodules and so on. On the other hand, Kobayashi & Nomura (1974) reported by means of thermomagnetic analysis, X-ray diffraction, X-ray fluorescence analysis and microscopic observation that ferromagnetic minerals, in the deep-sea sediments from the Pacific basin, were titaniferous magnetite and were stable or at least metastable.

In the present study, it is found by the thermomagnetic analysis and microscopic observation, that ferromagnetic minerals in the deep-sea sediment core collected from the Philippine sea are stoichiometric magnetite, maghemite, iron sulphides and a small quantity of hematite.

Sample

Observed core sample(Sample No. st.185 P22, 27°34.5'N, 134° 24.5'E, 4575m deep, 5.39m long) was collected from deep-sea floor, south-east of the Komahashi sea mount, by R/V Hakurei maru on the GH74-7 cruise(Mizuno et al., 1975a) by the Geological Survey of Japan. The core sample, consists mostly of pale yellowish brown clay, and the upper half of the core log is somewhat tuffaceous and contains some volcanic ash layers (Mizuno et al., 1975b). The specimens were picked from non-tuffaceous clay part of the whole core, and examined through the thermomagnetic analysis and the microscopic observations.

Thermomagnetic analysis

As the grain size of the ferromagnetic minerals in the specimens are measured to be mostly smaller than few microns in diameter, the ferromagnetic minerals can not be separated. So, the whole specimens dried at room temperature were examined by means of the magnetic balance.
Thermal changes of saturation magnetization were measured, respectively in vacuum of 10^{-3} torr and in air, through both processes of heating from ordinary temperature up to 600°C, and cooling down to ordinary temperature after keeping at 600°C for about 30min.

The Curie temperatures of the specimens fall with in a range 540°C to 580°C, and their thermomagnetic curves are simple one. (i) The thermomagnetic curve of each primary specimen measured in vacuum, changes irreversibly through heating and cooling process(Fig.1-a). The saturation moment at ordinary temperature (Js(To)) of the specimens after heating in vacuum is approximately two to four times as much as Js(To) of the original specimens. (ii) The specimen once heated in vacuum also changes irreversibly through heating and cooling process in air and the thermomagnetic curve indicates a decrease of Js(To) (Fig.1-b). (iii) The thermomagnetic curve of the specimen thus treated

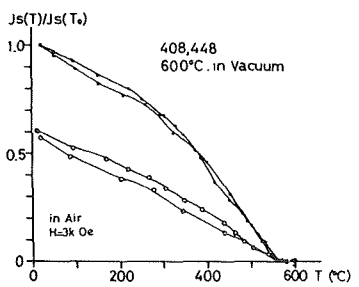

Fig.1-b

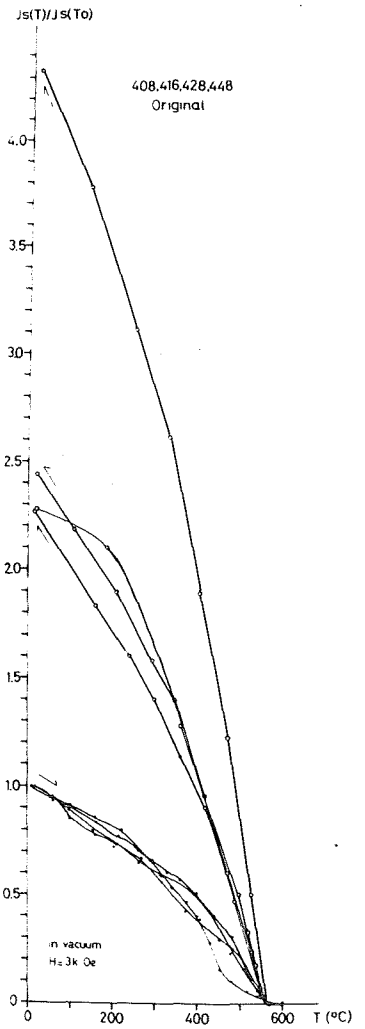

Fig.1-a

Fig.1, a-f. Thermomagnetic curves(Js-T) , heated to 600°C, and cooled after keeping at 600°C for about 30min., in each specimens. Solid and hollow circles respectively indicate heating and cooling.
a-c, the experiments carried out in order of in vacuum(a), in air(b), and in vacuum(c).
d-f, the experiments carried out in order of in air(d), in vacuum(e), and in air(f).

Fig.1-c

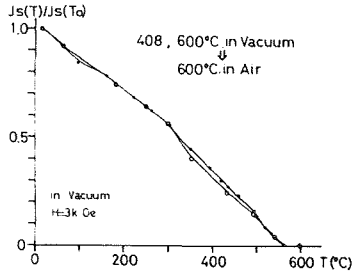

Fig.1-d

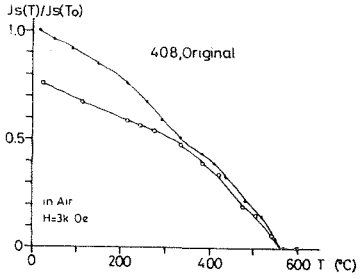

Fig.1-e

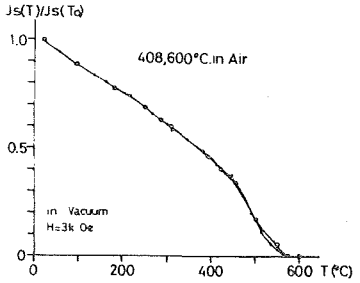

Fig.1-f

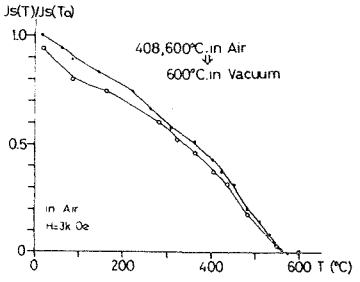

and again measured in vacuum, changes reversibly showing no change of Js(To) in both heating and cooling(Fig.1-c). On the other hand, (iv) the thermomagnetic curve of each primary specimen measured in air changes irreversibly indicating a decrease of Js(To) (Fig.1-d). (v) The thermomagnetic curve of the specimen once heated in air, changes reversibly through heating and cooling process in vacuum(Fig.1-e). Moreover, (vi) the thermomagnetic curve of the specimen thus treated and again measured in air, changes irreversibly indicating a decrease of Js(To) (Fig.1-f).

In all cases mentioned above, specimens hardly show any changes of the Curie temperature after heating. It is considered that the ferromagnetic minerals in the present sample are stoichiometric magnetite, maghemite as a low-temperature oxidized product of magnetite and iron sulphides, based on both the facts that the Curie temperatures range from 540°C to 580°C, and that the specimens are believed to contain little Ti based on the result of the X-ray fluorescence analysis.

On the basis of the results of the thermomagnetic analysis from (i) to (vi), the following conclusions may be deduced, as schematized in Fig.2. The ferromagnetic minerals in the original specimens are identified to be magnetite(Fe_3O_4), maghemite(γ-Fe_2O_3) and iron sulphides as noted in the following. The increase in Js (To) and irreversible change of the thermomagnetic curve in the experimental result (i), can explained as the result of reduction of maghemite to magnetite, and oxidation of iron sulphides to magnetite; but primary magnetite shows no change. The decrease in Js(To) shown in the experimental result (ii) indicates development of hematite by partial oxidation of magnetite. Moreover, though this specimen containing magnetite and hematite was heated and cooled in vacuum, the specimen showed no change of mineral composition in the experimental result (iii). On the other

hand, the decrease in Js(To) shown in the experimental result (iv) can be explained by development of hematite by partial oxidation of magnetite, decomposition of maghemite and oxidation of iron sulphides. The experimental result (v) that showed reversible change in the thermomagnetic curve, doesn't exhibit any alteration of mineral composition, as similarly shown in the result (iii). Moreover, when this specimen (magnetite + hematite) was heated and cooled in air, magnetite partially altered to hematite by partial oxidation; and Js(To) decreases as shown in the experimental result (vi).

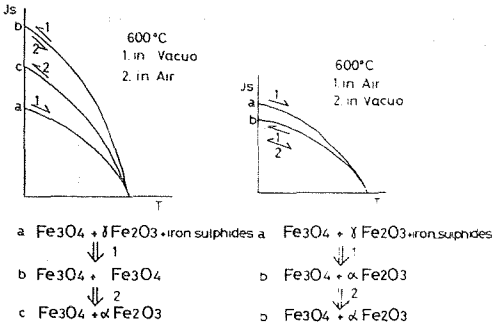

Fig.2 Schematic results of the thermomagnetic analysis. The arrows indicate heating and cooling processes.

The samples heated to 600°C in vacuum have a fairly large value in the intensity of Isothermal Remanent Magnetization (IRM,H=7000 Oe) compared with IRM of the original sample. As shown in Fig.3, the intensity of Partial Thermo-Remanent Magnetization ranging from T°C to ordinary temperature (PTRM, T°C to 20°C, H=intensity of magnetic field in the laboratory 0.5≃Oe, temperature was raised up to every 100°C from 100°C-600°C) increases suddenly over about 500°C. Above-noted two experimental resuls give good agreement with the conclusions derived from the thermomagnetic analysis. The result of the differential thermal analysis, moreover, doesn't indicate an occurrence of iron oxyhydroxides.

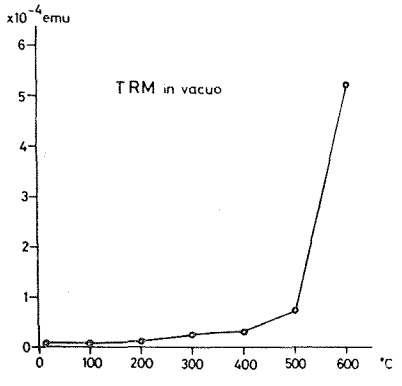

Fig.3 Change of intensity of PTRM from T°C to room temperature. H=intensity of magnetic field in the laboratory 0.5≃Oe.

Microscopic observation

All the specimens used for the thermomagnetic analysis, including the original specimens, the heat-treated specimens at 600°C in air and in vacuum, and heat-treated specimens at 600°C in air after heat-treated at 600°C in vacuum, were fixed in regin, and polished, and so observed with a reflecting microscope.

The grain size of the ferromagnetic minerals in the original specimens ranges below 1μ to about 100μ, and that of nearly half amount of particle is below 3μ. The microscopic observation demonstrates that the ferromagnetic minerals in the original specimens are magnetite, maghemite, iron sulphides and a small quantity of hematite. No grains are found that partially altered from magnetite to maghemite in rims or along cracks. But, it is considered that maghemite grain is wholly oxidated at low temperature. The ferromagnetic minerals in the specimens heat-treated in vacuum, are observed to be magnetite and a small quantity of hematite; and the ferromagnetic minerals in the specimens both heat-treated in air and heat-treated in air after heat-treated in vacuum, are observed to be hematite and magnetite. The microscopic and the thermomagnetic results are in good agreement with each other, too.

Discussion

As mentioned above, the present study suggests that the ferromagnetic minerals in the sample mainly consist of β-phase (magnetite) and γ-phase(maghemite) of magnetic minerals. However, it is hardly known to which extent this γ-phase mineral may contribute to NRM of the sediments. It is important in the study of the magnetism of the sediments, that γ-phase fraction does occur as oxidized from β-phase fraction in mineral assemblage. In the case when the γ-phase minerals were produced before acquisition of DRM, it is explained that the sort of γ-phase minerals may be responsible for NRM. However, if γ-phase minerals were formed after acquisition of DRM, the problem whether or not the γ-phase succeeded the remanence of the β-phase, still remains, similarly in the case of the γ-phase of the igneous minerals.

References

Haggerty, S.E. (1970) Carnegie Inst. Year Book Ann. Rep. Geophys. Lab., 68, 332-335.

Johnson, E.A., T.Murphy and O.W.Torreson (1948) Terr. Mag. Atmos. Electr., 53, 349-372.

Kobayashi, K. and M.Nomura (1974) J. Geophys., 40, 501-512.

Mizuno, A., Y.Okuda, K.Tamaki, Y.Kinoshita, M.Nohara, M.Yuasa, N.Nakajima, F.Murakami, S.Terashima and K.Ishibashi(1975a) Marine Sci., 7, 484-491, 543-548.(in Japanese)

Mizuno, A., M.Nohara, Y.Kinoshita, N.Nakajima, Y.Okuda, K.Tamaki, and K.Ishibashi (1975b) Geological Problems of the Philippine Sea Area (Papers presented at the Symposium of the 82nd General Meeting of the Geol. Soc. of Japan, Kyoto, 1975), 105-111.(in Japanese)

FERROMAGNETIC MINERALS IN PYROCLASTIC DEPOSITS IN SOUTHEAST HOKKAIDO AND CENTRAL HONSHU, JAPAN

Yoshiki FUJIWARA*, Shomei OKADA** and Nobuyuki AIDA*

* Dept. of Geology, Hokkaido University, Sapporo, Japan
** Faculty of Education, Tottori Univ. Tottori, Japan

For an aid of correlation of pyroclastic deposits such as pumice flow deposit and pumice fall deposit, we have carried out both magnetic and mineralogical analysis on ferromagnetic minerals extracted from some Quaternary pyroclastic deposits widely developed in southeastern Hokkaido and also central Honshu. Thermomagnetic analysis, X-ray diffraction analysis, refractive microscope analysis, electron probe analysis and heavy mineral assemblage analysis were undertaken. Of them, the experimental results of thermomagnetic analysis and X-ray analysis are briefly given in this short note.

Ferromagnetic minerals in the pyroclastic deposits in Shikotsu and Noboribetsu area, Hokkaido.

The pyroclastic plateaus arround this area are comprise from at least eight volcanic Formations which composed of mainly pumiceous volcanic products. Each Formation comprises from several layers of pumice or ash fall deposits and one pumice flow deposit. The pumice flow member is always overlain on the pumice or ash fall deposits.

More than 100 hundred thermomagnetic analysis were made on the ferromagnetic minerals extracted from many layers of pyroclastic sequences arround this area. Most of their thermomagnetic curves may classified into two types as illustrated in Fig.1, Type A and Type B.

Fig.1.

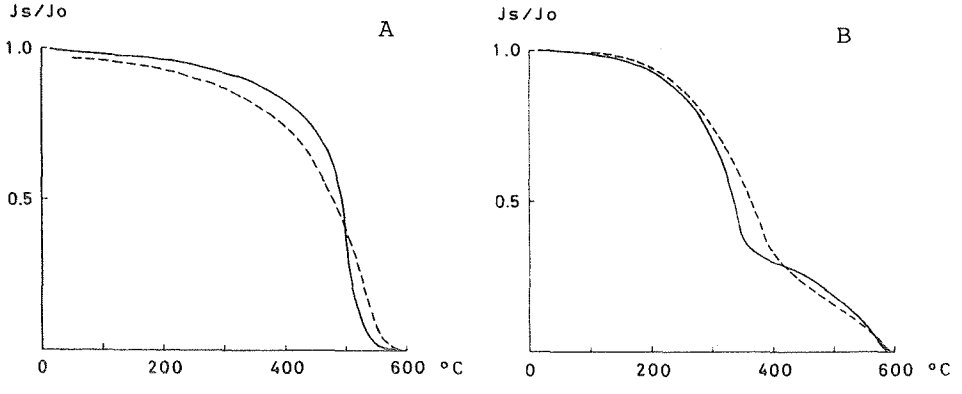

In Fig.1, solid line indicates the magnetization change in heating process and dotted line indicates in cooling process. The results of these analysis are shown in Fig.2 in compiled form. Solid circles in Fig.2 indicate the Curie temperatures at higher temperature phase. In this case, thermomagnetic curve of such specimen is always coincide with Type B in Fig. 1. Ilmenite lamellas are common. Double circles indicate the Curie points which are regarded as those of main ferromagnetic phase. As clearly shown in Fig.2, Curie temperatures of the lower phase are gradually shift from lower to higher temperature with lower to higher stratigraphic position, except in case of Shikotsu Volcanic Formation. Curie temperatures of the flow member of each volcanic Formation always show most high temperature among the Formation.

Ferromagnetic minerals of the pyroclastic deposits in the Yatsugadake area, Central Honshu.

Various types of pyroclastic deposits ranging from lower Pleistocene to Recent, widely develop arround the eastern part of Yatsugadake area, Central Honshu. In the present note, the experimental results of ferromagnetic minerals extracted from pyroclastic deposits which belonging to the upper part

Fig.2.

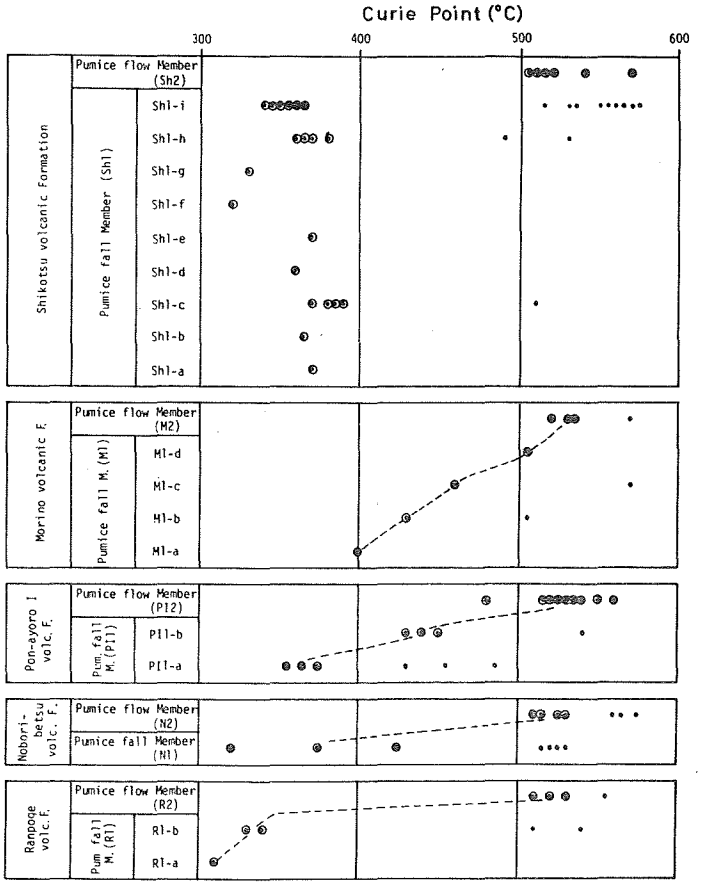

of the Yatsugadake volcanic sequence are briefly given in the following.

Fig.3 shows the variation of Curie temperatures with stratigraphic sequence. KwP, Pm-I and YPm-I, II, III, IV the name key layers of ash fall member, as was described by Nakaya (1971). Of them, Pm-I is originated from Ontake volcano about 90 km southwest from this area. Thermomagnetic properties of Pm-I was already described by Momose et al. (1972). Most of thermomagnetic curves may classified into Type B (Fig.1). Ilmenite lamellasare also common in almost all specimens. In the stratigraphic succession of volcanic ash and pumice fall members in Yatsugadake area, the Curie point variation of lower temperature phase also shows gradually shift to high temperature in one volcanic unit as clearly shown in Fig.3.

X-ray diffraction analysis

The results of lattice parameter calculation and Curie temperatures of main phase are plotted on Fig.4. All ferromagnetic minerals in the present work considered to be cubic structure. Some mutual relation between lattice parameters and Curie points may recognized in Fig.4. However, correlation between Curie temperature and lattice parameter is different from the results of synthetic samples described by Lindsley (1962) and Akimoto (1962). These difference may probably arise from the reason that ferromagnetic minerals of the present samples may considered to be mixture of multi phase titanomagnetite and almost pure magnetite with ilmenite lamella.

Fig.3.

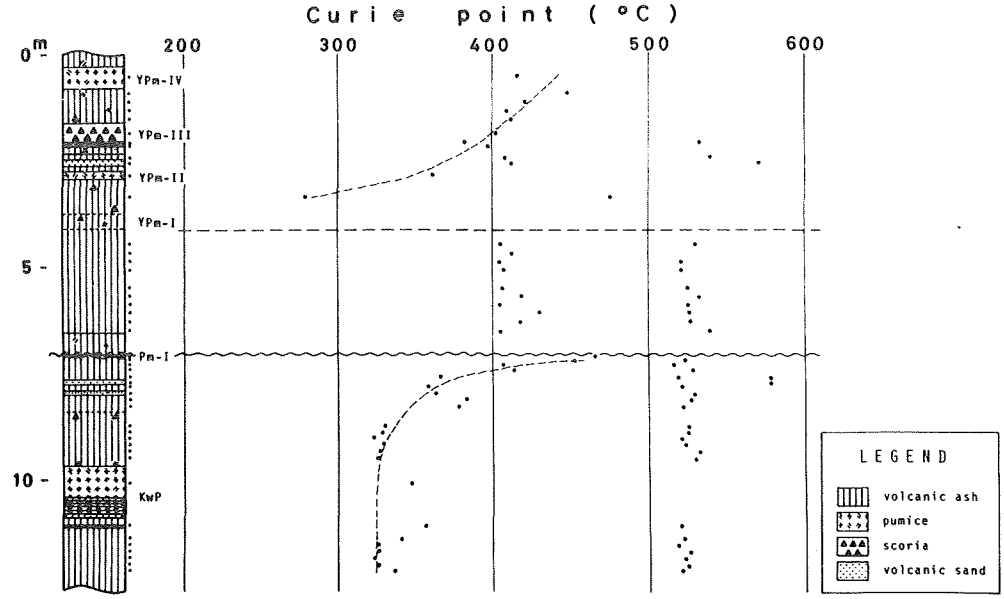

Fig.4.

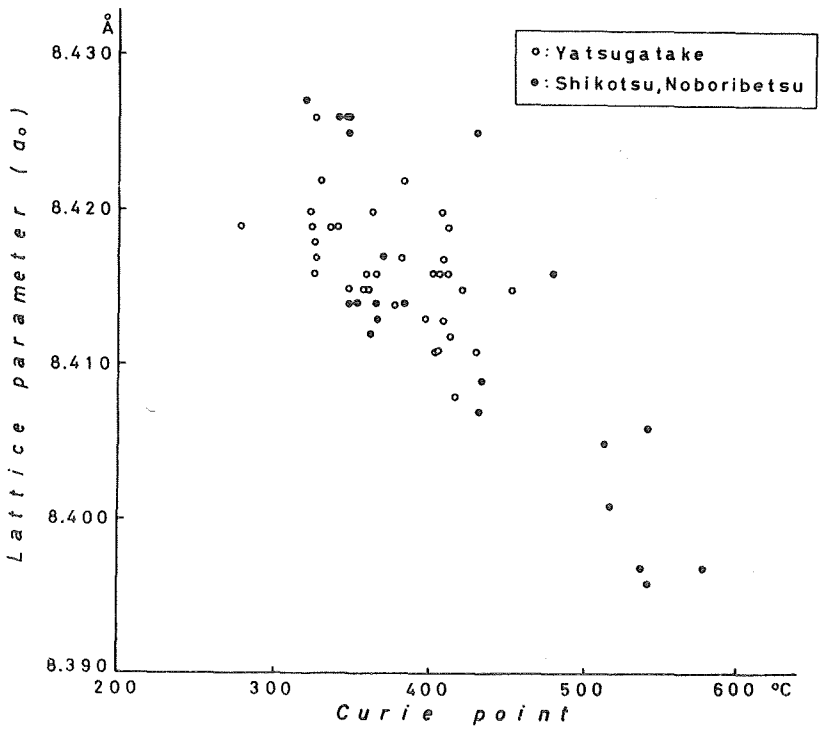

Conclusions and discussions

The Curie temperatures of the pyroclastic deposits in both Shikotsu, Noboribetsu area and also Yatsugadake area are gradually increase from the bottom to the top in one unit of volcanic Formation. This suggests that slightly but constantly changes of chemical compositions of the volcanic products had occurred during in one series of activity.

Generally, the main ferromagnetic minerals in the fall members have two Curie temperatures while the flow members have a single phase of very high Curie temperatures.

The Curie temperatures of nine fall members of the Shikotsu Volcanic Formation do not show any remarkable regular variation. Probably these fall members were the products from something different type of volcanism in comparison with another five volcanic Formation in the present note.

Reference

Akimoto, S. (1962) J. Phys. Soc. Japan 17, 1.
Lindsley, D. H. (1961) Geophys. Lab. Carnegie Inst. Year Book 61.
Momose, K. and K. Kobayashi (1972) J. Geomag. Geoelect. 24, 1.
Nakaya, S. (1971) Quaternary, 16, 55.

CHANGES IN MAGNETIC PROPERTIES OF A BASALT INDUCED BY HEATING IN AIR

Masaru KONO

Geophysical Institute, University of Tokyo, Bunkyo-ku, Tokyo 113, Japan.

Introduction

Because of the fact that the mechanism of acquisition is not only understood fairly well but also is reproducible in a laboratory, thermoremanent magnetization (TRM) of volcanic rocks is the most reliable source of information on paleomagnetic field intensities. All the paleointensity methods used today are based on the comparison of some fractions (in coercivity or in blocking temperature) of natural remanent magnetization (NRM) and TRM in the same sample. However, it is commonly observed that heatings carried out to induce a total or partial TRM cause changes in magnetic properties of samples.

Khodair and Coe (1975) proposed that the risks of such inconvenient changes can be greatly reduced by heating samples in vacuum. Kono and Tanaka (1977) systematically investigated the changes in TRM properties using oxygen fugacity-controlled furnace, and concluded that TRM properties of basaltic rocks are best preserved when the atmosphere of the furnace is moderately reducing. However, even the use of these sophisticated furnaces has some drawbacks of its own. Apart from the cost of gases, there are facts that fugacity-controlled furnaces are best operated in a vertical position, which is very inconvenient for paleomagnetic experiments, and that the time needed to heat a sample is considerably lengthened by flowing gas mixtures. In the case of vacuum furnaces, it is very difficult to cool samples in a short time. Compared to these, ordinary furnaces heated in air can have very short thermal cycling time and also have merits of ease of construction and operation.

In the present study, changes in magnetic properties of a basalt was investigated. The samples were taken from the 1950-1951 lava flow of Oshima island, Izu, Japan. These samples contain titanomagnetites with about 40 mol percent ulvospinel, and their NRM is very stable to alternating field (AF) demagnetization (Kono, 1977). Samples were prepared as cylinders about 2.5 mm in diameter and 3 mm long. The very small size of the samples were necessitated because both the hysteresis properties and the remanence properties were to be measured on the same samples.

Experimental Procedures

For the measurements of hysteresis properties, a Princeton Applied Research vibration magnetometer was used. Magnetic remanences were measured by a Schonstedt magnetometer. Thermomagnetic curves were obtained by a Naruse magnetic balance in a magnetic field of about 5 kOe and under a vacuum of 1-5 x 10^{-5} Torr. Heatings were carried out in a furnace preheated to 640°C, which was placed in a solenoid coil set in a two-layer magnetic shield.

First, the NRM of each sample was measured. After this measurement, the hysteresis properties were measured by the vibration magnetometer and a saturation remanence ($J_r = IRM_s$) given to the sample. The saturation remanence was again measured by the spinner magnetometer. Then the sample was heated in the furnace for a period between 3 minutes and 300 minutes and rapidly cooled in the magnetic field (0.5 Oe) produced by the solenoid. The same set of measurements were repeated on the heated sample to determine the hysteresis and remanence properties. After all these measurements, the same sample was used in thermomagnetic analysis. As the size of samples was quite small, they quickly reached to the ultimate temperatures.

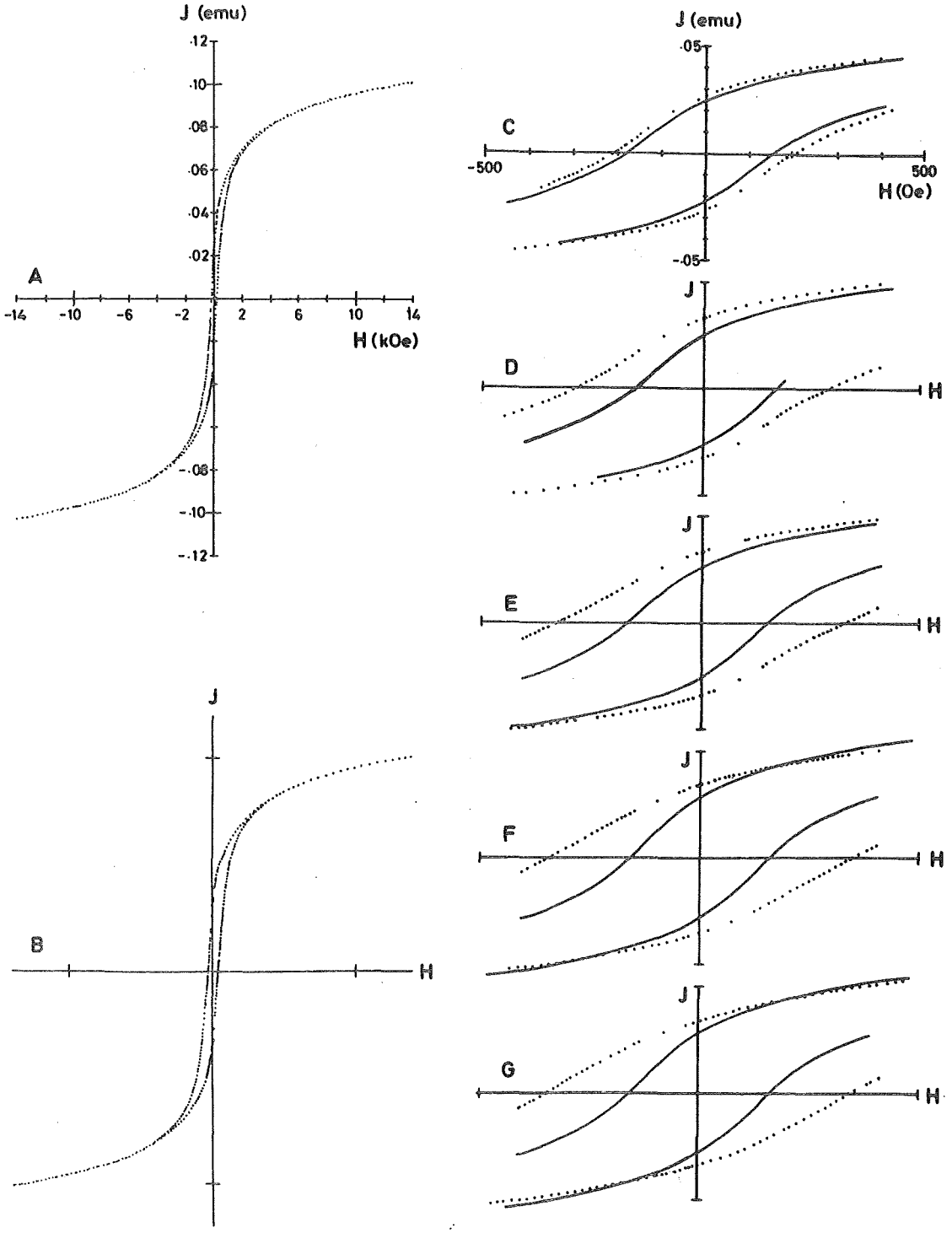

Fig. 1. Magnetic hysteresis curves of unheated and heated samples. (A) Original sample. (B) The same sample heated to 640°C for 30 min. (C)-(G) Hysteresis curves of original (continuous curves) and heated samples (dotted curves, for heating times of (C) 3 min., (D) 10 min., (E) 30 min., (F) 100 min. and (G) 300 min.

Results

Fig. 1 shows hysteresis curves of samples before and after the heating. On the left of the figure, A shows a hysteresis of an original sample, and B that of the same sample after it was heated to 640°C for 30 minutes. On the right, the continuous curves show hystereses of original samples and dotted curves are those for the same samples heated to 640°C for (C) 3 minutes, (D) 10 minutes, (E) 30 minutes, (F) 100 minutes and (G) 300 minutes. Only the portion of figures near the origin is shown in (C) through (G). Some features are easily to be noted in these figures; increase in coercive force (H_c) and saturation remanence (J_r) and very similar values of saturation magnetization(J_s). That these changes proceed with time is clearly demonstrated by the curves in (C) to (G). It is also seen that the change apparently is larger in the period of 3 to 10 minutes than any other interval and that after 100 minutes heating, it is practically terminated.

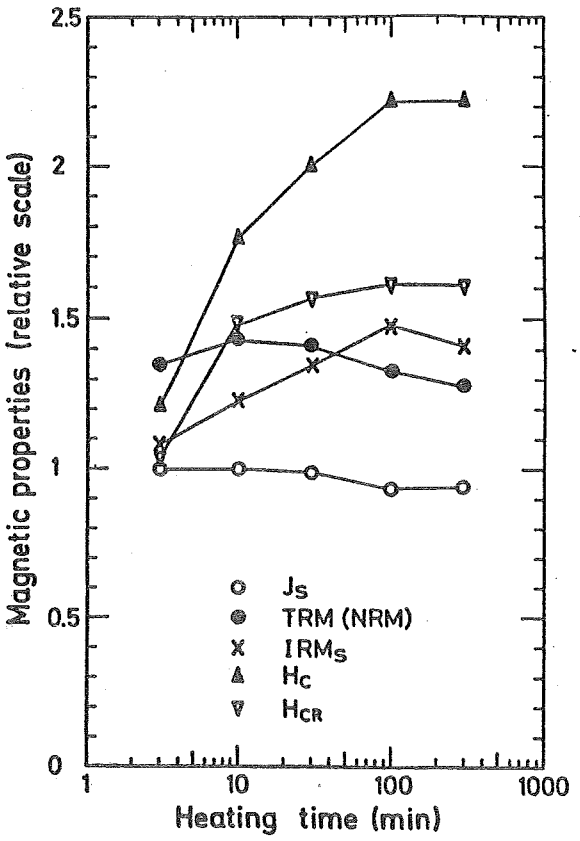

Fig. 2. Change in hysteresis parameters and intensity of remanences.

Fig. 2 shows the changes in hysteresis parameters and the magnitudes of remanences as a function of heating time. The intensity of the original NRM, TRM and IRM_S was measured on the same samples, so that these ratios truly represent the changes induced by the heating.

H_c and remanence coercive force (H_{CR}) increase steadily until they reach a saturation at about 100 minutes. On the other hand, J_s hardly changes by heating and TRM magnitude (compared to the NRM) increases by heating but it reaches to a maximum at about 10 minutes, after which the magnitude decreases again.

Figure 3 shows the change in the ratio TRM/NRM in various samples of the same size. The samples used in the hysteresis measurements are shown by filled circles. Although the data are considerably scattered, it seems that the maximum at about 10 minutes heating time is a real feature. It may therefore be pointed out that when some change occurs by heating, its effect on TRM magnitude is not similar to the magnetic properties measured in strong fields; i.e., J_s, J_r, H_c or H_{CR}.

Figure 4 summarizes the thermomagnetic curves for the heated and unheated samples. Only the heating curves are shown here for clarity. The original,

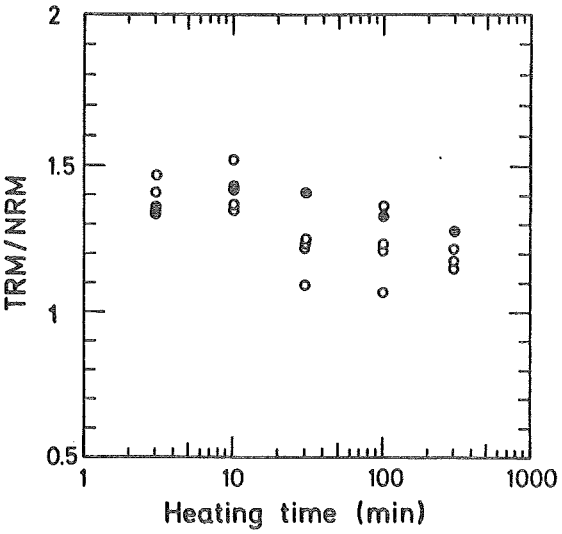

Fig. 3. TRM/NRM ratio.

unheated sample shows two Curie points near 300°C and 540°C. The lower Curie point is consistent with the chemical composition of titanomagnetite in this basalt, i.e., about 40 mol percent ulvospinel and 60 percent magnetite (Akimoto, 1955). By the heating, the lower Curie temperature is raised and the proportion of high Curie point fraction increased until the sample became single-phased, with a Curie point near 540°C.

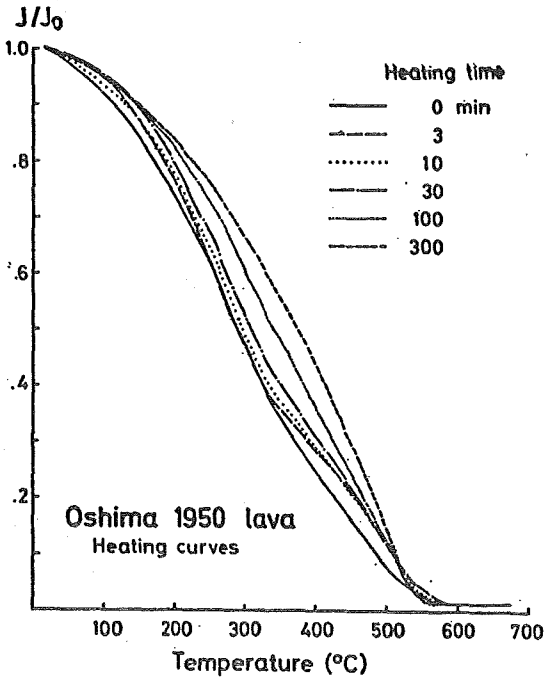

Fig. 4. Change in thermomagnetic curves of samples by heating in air. Only the heating curves are shown. J_s is normalized by the values at room temperature.

Interpretation and Discussion

The basic process operating in the heating experiment is undoubtedly that of high-temperature oxidation of titanomagnetites. When oxidized at high temperatures, titanomagnetites break down to intergrowths of Ti-poor magnetite solidsolution and Ti-rich ilmenite solid solution (Buddington and Lindsley, 1964). The ilmenites thus produced exsolve on (111) planes of magnetites and effectively divide magnetites into plane or rod shaped regions. Davis and Evans (1976) studied such changes by electron micrographs and by magnetic measurements and concluded that magnetite-ilmenite intergrowths behave as interacting single domain particles.

Fig. 4 clearly shows that such oxidation proceeded with time in the present samples. The main Curie point changes from about 300°C to about 540°C by the heating. This suggests that the ulvospinel mol fraction x of the magnetic phase decreased from about 0.4 to about 0.5 by oxidation, which is in good agreement with the data of Buddington and Lindsley (1964). The magnetic hardness increases remarkably because of the reduction of the effective grain size due to the exsolution of ilmenite lamellae. The increase in H_c and H_{CR} shown in Fig. 2 is in good agreement with this scheme. The similar increase of saturation remanence (IRM_s) reflects the increase in the J_r/J_s ratio as the fraction of single domained regions increased. On the other hand, J_s stays nearly constant as its value in titanomagnetites depends mostly on the mole fraction of magnetite, which is little changed in the process of high-temperature oxidation.

Thus the changes in hysteresis parameters can be conveniently explained by the evolution of magnetite-ilmenite intergrowths. The change in TRM magnitude is quite dissimilar to those of hysteresis parameters. Therfore, it seems quite difficult to normalize the magnitude of TRM by parameters such as IRM_s, as has been done by some authors in paleointensity experiments.

References

Akimoto, S. (1955) Jap. J. Geophys. 1, 1.
Buddington, A.F. and D.H. Lindsley (1964) J. Petrol. 5, 310.
Davis, P.M. and M.E. Evans (1976) J. Geophys. Res. 81, 989.
Khodair, A.A. and R.S. Coe (1975) Geophys. J. Roy. Astr. Soc. 42, 107.
Kono, M. (1977) Geophys. J. Roy. Astr. Soc., in press.
Kono, M. and H. Tanaka (1977) Phys. Earth Planet. Interiors 13, 276.
Strangway, D.W., E.E. Larson and M. Goldstein (1968) J. Geophys. Res. 73, 3787.

Results

Fig. 1 shows hysteresis curves of samples before and after the heating. On the left of the figure, A shows a hysteresis of an original sample, and B that of the same sample after it was heated to 640°C for 30 minutes. On the right, the continuous curves show hystereses of original samples and dotted curves are those for the same samples heated to 640°C for (C) 3 minutes, (D) 10 minutes, (E) 30 minutes, (F) 100 minutes and (G) 300 minutes. Only the portion of figures near the origin is shown in (C) through (G). Some features are easily to be noted in these figures; increase in coercive force (H_c) and saturation remanence (J_r) and very similar values of saturation magnetization(J_s). That these changes proceed with time is clearly demonstrated by the curves in (C) to (G). It is also seen that the change apparently is larger in the period of 3 to 10 minutes than any other interval and that after 100 minutes heating, it is practically terminated.

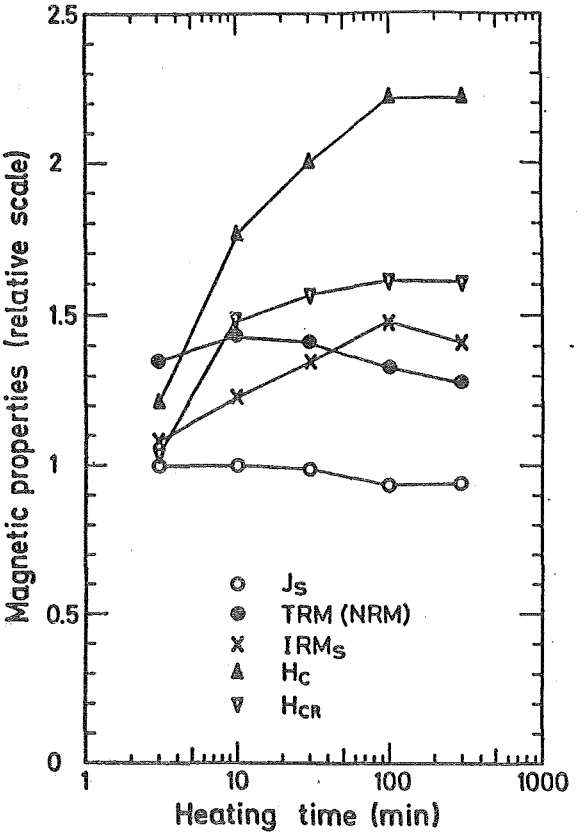

Fig. 2. Change in hysteresis parameters and intensity of remanences.

Fig. 2 shows the changes in hysteresis parameters and the magnitudes of remanences as a function of heating time. The intensity of the original NRM, TRM and IRM_S was measured on the same samples, so that these ratios truly represent the changes induced by the heating.

H_c and remanence coercive force (H_{CR}) increase steadily until they reach a saturation at about 100 minutes. On the other hand, J_s hardly changes by heating and TRM magnitude (compared to the NRM) increases by heating but it reaches to a maximum at about 10 minutes, after which the magnitude decreases again.

Figure 3 shows the change in the ratio TRM/NRM in various samples of the same size. The samples used in the hysteresis measurements are shown by filled circles. Although the data are considerably scattered, it seems that the maximum at about 10 minutes heating time is a real feature. It may therefore be pointed out that when some change occurs by heating, its effect on TRM magnitude is not similar to the magnetic properties measured in strong fields; i.e., J_s, J_r, H_c or H_{CR}.

Figure 4 summarizes the thermomagnetic curves for the heated and unheated samples. Only the heating curves are shown here for clarity. The original,

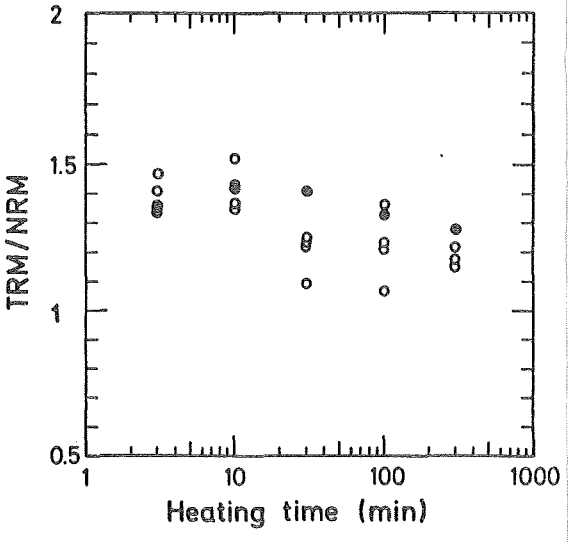

Fig. 3. TRM/NRM ratio.

unheated sample shows two Curie points near 300°C and 540°C. The lower Curie point is consistent with the chemical composition of titanomagnetite in this basalt, i.e., about 40 mol percent ulvospinel and 60 percent magnetite (Akimoto, 1955). By the heating, the lower Curie temperature is raised and the proportion of high Curie point fraction increased until the sample became single-phased, with a Curie point near 540°C.

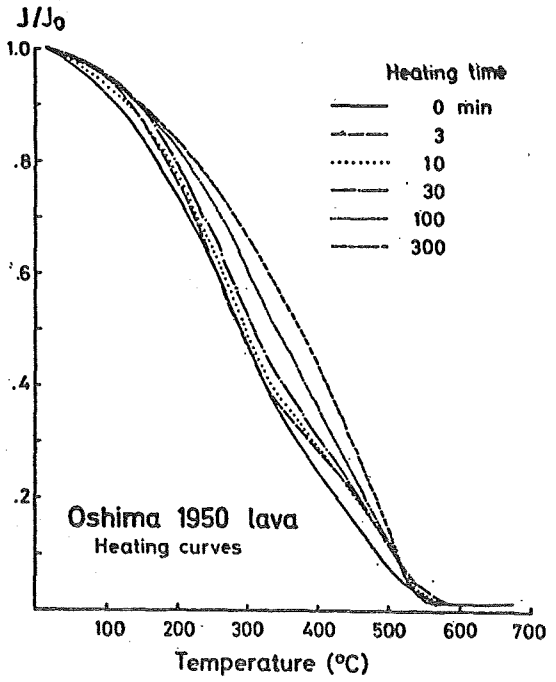

Fig. 4. Change in thermomagnetic curves of samples by heating in air. Only the heating curves are shown. J_s is normalized by the values at room temperature.

Interpretation and Discussion

The basic process operating in the heating experiment is undoubtedly that of high-temperature oxidation of titanomagnetites. When oxidized at high temperatures, titanomagnetites break down to intergrowths of Ti-poor magnetite solidsolution and Ti-rich ilmenite solid solution (Buddington and Lindsley, 1964). The ilmenites thus produced exsolve on (111) planes of magnetites and effectively divide magnetites into plane or rod shaped regions. Davis and Evans (1976) studied such changes by electron micrographs and by magnetic measurements and concluded that magnetite-ilmenite intergrowths behave as interacting single domain particles.

Fig. 4 clearly shows that such oxidation proceeded with time in the present samples. The main Curie point changes from about 300°C to about 540°C by the heating. This suggests that the ulvospinel mol fraction x of the magnetic phase decreased from about 0.4 to about 0.5 by oxidation, which is in good agreement with the data of Buddington and Lindsley (1964). The magnetic hardness increases remarkably because of the reduction of the effective grain size due to the exsolution of ilmenite lamellae. The increase in H_C and H_{CR} shown in Fig. 2 is in good agreement with this scheme. The similar increase of saturation remanence (IRM_S) reflects the increase in the J_r/J_s ratio as the fraction of single domained regions increased. On the other hand, J_s stays nearly constant as its value in titanomagnetites depends mostly on the mole fraction of magnetite, which is little changed in the process of high-temperature oxidation.

Thus the changes in hysteresis parameters can be conveniently explained by the evolution of magnetite-ilmenite intergrowths. The change in TRM magnitude is quite dissimilar to those of hysteresis parameters. Therfore, it seems quite difficult to normalize the magnitude of TRM by parameters such as IRM_S, as has been done by some authors in paleointensity experiments.

References

Akimoto, S. (1955) Jap. J. Geophys. 1, 1.
Buddington, A.F. and D.H. Lindsley (1964) J. Petrol. 5, 310.
Davis, P.M. and M.E. Evans (1976) J. Geophys. Res. 81, 989.
Khodair, A.A. and R.S. Coe (1975) Geophys. J. Roy. Astr. Soc. 42, 107.
Kono, M. (1977) Geophys. J. Roy. Astr. Soc., in press.
Kono, M. and H. Tanaka (1977) Phys. Earth Planet. Interiors 13, 276.
Strangway, D.W., E.E. Larson and M. Goldstein (1968) J. Geophys. Res. 73, 3787.

RELIABILITY OF PALEOINTENSITY METHODS USING ALTERNATING FIELD DEMAGNETIZATION AND ANHYSTERETIC REMANENCE

Masaru KONO

Geophysical Institute, University of Tokyo
Tokyo 113, Japan

1. Introduction

Paleointensity methods using alternating field (AF) demagnetization require only one heating to a temperature higher than the Curie point of the sample, so that the entire experiment can be performed within a short time. It is a great advantage over the standard method of Thellier and Thellier (1959) which requires a considerable number of heatings before any meaningful results are obtained. Therefore, if it can be shown that alteration does not occur when the sample is heated, or if the effect of such alteration can be accounted for by some appropriate means, these methods may be equally useful as the Thellier method in studying paleointensities. An obvious extension of vanZijl et al.'s (1962) original method is to compare the components of the natural remanent magnetization (NRM) with those of the artificial thermoremanent magnetization (TRM) at many demagnetizing steps (Smith, 1967a) or even over the whole coercivity spectra (Symons and Schwarz, 1970), assuming that it is unlikely for an altered sample to exhibit a coercivity spectrum similar in shape to the original one. Others used samples or data which satisfy some criteria; e.g., reversibility of thermomagnetic curve, certain range of oxidation index (Smith, 1967b), etc. Carmichael (1967) tried to account for the effect of alteration by dividing the NRM and TRM by saturation remanence before and after the heating.

Recently, Shaw (1974) proposed that anhysteretic remanent magnetization (ARM) may be used to monitor the occurrence of alteration during heating. It is well known that ARM has characteristics quite similar to those of TRM, including the proportionality with direct magnetic field and the additivity of partial ARM's (Patton and Fitch, 1962). It can therefore be assumed that TRM is unchanged in the coercivity range where ARM is the same before and after heating.

It is the main purpose of the present study to examine and evaluate the assumptions of Shaw's method and to demonstrate its ability in determining paleointensities. Shaw's method was applied to 22 samples taken from 11 volcanic rocks ranging from basalt to rhyolite in chemical composition and from 1962 A.D. to 34 m.y. old in age. All of these rocks have already given well-defined paleointensity estimates by the Thellier method (Table 1).

Secondly, an attempt was made to evaluate the possibility of obtaining paleointensities solely from the TRM-ARM relationship. A relation of the general form

$$\frac{TRM}{ARM} = f\,\frac{F_t}{F_a}$$

Table 1. The samples

Sample Number(s)	Lock Type and Locality	Age	Paleointensity (Oe) Observed	Thellier Method
1-3	Miyake-jima basalt	1962 A.D.	0.46±0.01	0.468±0.011
4-5	Oshima basalt	1951 A.D.	0.46±0.05	0.517±0.017
6	Hawaii basalt	1926 A.D.	*	0.37
7-8	Hawaii basalt	1907 A.D.	*	0.32 ±0.02
9-10	Hawaii basalt	1750 A.D.	*	0.32 ±0.01
11-14	Asama andesite	2000 y.B.P.		0.843±0.012
15-16	Hakone andesite	∿ 0.5 m.y.		0.71
17	Hakone andesite	∿ 0.5 m.y.		0.89 ±0.01
18	Usami andesite	1.0 m.y.		0.73 ±0.06
19	San Juan Rhyolite	27 m.y.		0.48 ±0.03
20-22	San Juan Rhyodacite	34 m.y.		0.16 ±0.03

* Coe and Gromme (1973) estimated the recent field intensity on the island of Hawaii to be 0.36±0.02 Oe from magnetic charts.

has been proposed by Stephanson and Collinson (1974) and by Banerjee and Mellema (1974), where F_t and F_a are direct fields used to induce TRM and ARM, and f is a numerical constant or a parameter determined by the magnetic properties of the sample at room temperature and at blocking temperature. If indeed such relation can be used in paleointensity determination, it may be that we need not heat a sample to Curie temperature and that we can completely avoid the effect of alteration during heating. The problem is, therefore, whether we can estimate the numerical factor f with enough accuracy without heating samples.

2. Results of Shaw's Method

The experimental procedures in the present study were quite similar to those of the original author (Shaw, 1974). First, the NRM of a sample was AF demagnetized at 50 Oe steps to 500 Oe and thereafter at 100 Oe steps to 1500 (or 1700) Oe. After this, an ARM was given to the sample using a direct field between 0.5 and 5 Oe and a peak alternating field of 1500 (or 1700) Oe. This ARM (called ARM 1) was AF demagnetized at the same steps as in the case of NRM. Second, the sample was heated to a temperature higher than the Curie point and cooled in a magnetic field of 0.5 Oe. The TRM thus acquired and the ARM induced afterwards in the same way as ARM 1 (called ARM 2) were AF demagnetized in the same manner.

Results from these experiments can be divided into several classes according to the relations in ARM 1 - ARM 2 plot and NRM-TRM plot. The criteria for the classification are

(1) ARM 1 - ARM 2 relation is linear, gradient is one.
(2) ARM 1 - ARM 2 relation is linear, gradient is not one.

Table 2. Results of Field Intensity Determination by Shaw's Method

Sample No.	F_a	ARM1 - ARM2 H_1	H_2	N	Slope	T_{max}	NRM - TRM H_1	H_2	N	Slope	Field Intensity Expected	Obtained	Class
1	1	Nonlinear			0.69-1.10[a]	640	Nonlinear			0.82-1.32[a]		0.37-0.96	3c
2	1	150	1500	18	1	450[c]	150	1500	18	2.073	0.47	(1.036)[d]	PTRM
3	1	600	1500	10	0.720	600	600	1500	10	0.735		0.510[b]	2a
4	2	200	1500	17	1	450[c]	600	1500	10	1.147	0.49	0.523	1a
5	2	200	1500	17	0.706	640	150	1500	18	0.662		0.469[b]	2a
6	5	200	1500	14	0.332	600	250	1500	14	0.162	0.37	0.244[b]	2b
7	2	100	1500	19	1	300[c]	150	1500	17	3.101	0.32	(1.550)[d]	PTRM
8	2	600	1500	10	1	640	Nonlinear			———		———	1c
9	0.5	200	1700	17	1.256	600	200	1700	20	0.974	0.32	0.388[b]	2b
10	0.5	300	1700	11	1.291	640	700	1700	7	1.002		0.388[b]	2b
11	2	0	1700	21	1	600	300	1700	15	1.694		0.847	1a
12	4	200	1700	20	1	640	300	1700	18	1.766	0.84	0.883	1a
13	2	Nonlinear			0.96-1.48[a]	640	200	1700	9	1.715		0.58-0.89	3a
14	4	0	1700	15	1	450[c]	50	1700	14	3.298		(1.649)[d]	PTRM
15	2	900	1500	7	1	600	900	1500	7	1.027	0.71	0.513	1b
16	2	900	1500	7	1	640	Nonlinear			———		———	1c
17	5	800	1500	8	1	600	Nonlinear			———	0.89	———	1c
18	4	Nonlinear			—	600	700	1500	8	1.434	0.73	0.717[e]	3b
19	2	Nonlinear			—	640	Nonlinear			———	0.48	———	3c
20	2	0	1700	16	1	640	300	1700	11	0.463		0.231	1b
21	2	500	1700	7	1	450[c]	Nonlinear			———	0.16	———	PTRM
22	2	0	1700	17	1	600	Nonlinear			0.23-0.58[a]		0.12-0.29	1c

Explanation: F_a, static field used to induce ARM. H_1, H_2, N, coercivity interval in which ARM1-ARM2 (NRM-TRM) is linear and number of measurements in the interval. T_{max}, maximum temperature reached when the sample was heated to induce TRM. Magnetic fields in Oe, temperature is degrees Celsius.

a A range of gradient was estimated when the change of slope is gradual and smooth.

b Intensity values after slope correction.

c Heating below the highest Curie point of the sample (see Table 1).

d Apparent "paleointensity" derived from NRM-PTRM relation.

e Intensity value obtained by assuming the absence of change in TRM coercivity spectrum.

(3) ARM 1 - ARM 2 relation is non-linear.

and

(a) NRM - TRM curve is linear, goes through the origin.
(b) NRM - TRM curve is linear, does not go throuth the origin.
(c) NRM-TRM curve is non-linear.

All the results are summarized in Table 2. Some of the examples of ARM 1 - ARM 2 plots and NRM - TRM plots are given in Figs. 1-4. In these figures, circled numbers refer to the sample numbers and small numerals indicate peak AF in oersteds. To save space, the graphs are displaced in the horizontal direction by arbitrary distances but the origins are indicated by thick vertical lines in NRM-TRM diagrams. The data points belonging to the portion of coercivity spectra in which ARM 1 - ARM 2 or NRM - TRM relations are linear are shown by filled circles and others by open circles.

Fig. 1 shows the Class la results. The intensity estimates obtained from the NRM - TRM slopes are very close to the expected values (Table 2). From the ARM 1 - ARM 2 diagram, it can be concluded that the heating did not cause appreciable changes in the coercivity spectrum of ARM-type remanences. In the NRM - TRM diagram, deviation from linearity is observed below 600 Oe (sample 4) and 300 Oe (samples 11 and 12), suggesting some viscous effects in the low coercivity portion of the NRM. It is to be noted that the points in the interval of 200 and 600 Oe for sample 4 define a straight line with a gradient about 60% larger thant that between 600 and 1500 Oe. Since the ARM relation is the same for both of these intervals, there is no reason to reject the 60% larger intensity estimate of 0.79 Oe if the demagnetization was terminated at 600 Oe, except that the NRM - TRM relation does not go through the origin. Therefore, the use of high demagnetization field appears essential for the successful application of Shaw's method.

Fig. 2 shows Class 2a results. In these samples the ARM relation is linear but the gradient is significantly different from unity; i.e., the shape of ARM coercivity spectrum is unchanged but the magnitude is different before and after the heating. If we estimate field intensity from the linear portion of NRM - TRM diagram of these samples, the resulting values are too low or too high depending on the gradient of the ARM 1 - ARM 2 curve. However, if we assume that the change in TRM capacity is the same as the change

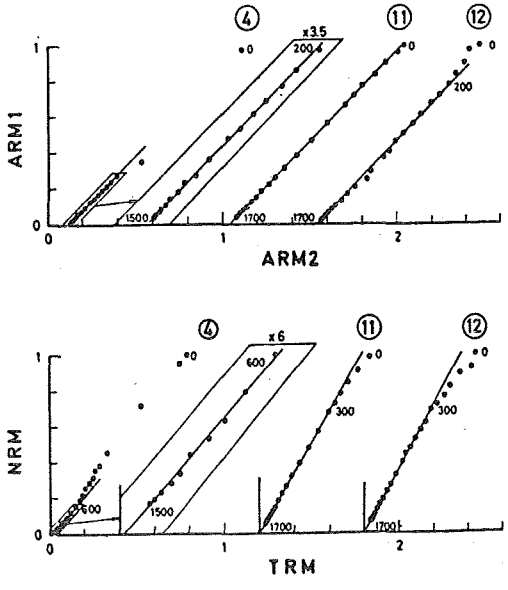

Fig. 1. Class la samples.

in ARM capacity, we can obtain "slope-corrected" paleointensities

$$F = F_{LAB} \times (\text{NRM-TRM slope})/(\text{ARM 1-ARM 2 slope})$$

which are much closer to the expected values (Table 2). Although Shaw (1974) rejected such data, they may be good estimates of field intensities if the ARM capacity change is not very great and if the internal consistency is as good as shown in Fig. 2.

Fig. 3 shows Class 2b results in which not only ARM capacty change is observed but also NRM - TRM curve does not go through the origin. The slope corrected field intensity is again very close to the expected value (Table 2). This suggests that the above assumption is justified and that grains with coercivities higher than 1500 Oe (or 1700 Oe) were selectively destroyed by the heating but not much affected otherwise. It seems reasonable to determine field intensities from the gradients of straight lines in Fig. 3 with appropriate slope correction. The same conclusion applies to Class 1b samples.

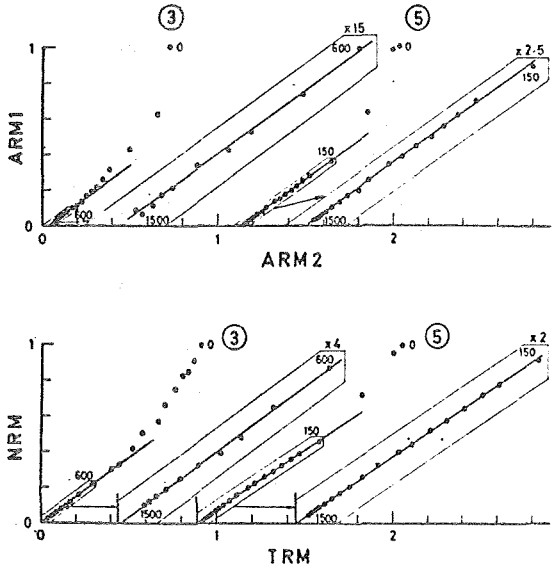

Fig. 2. Class 2a samples.

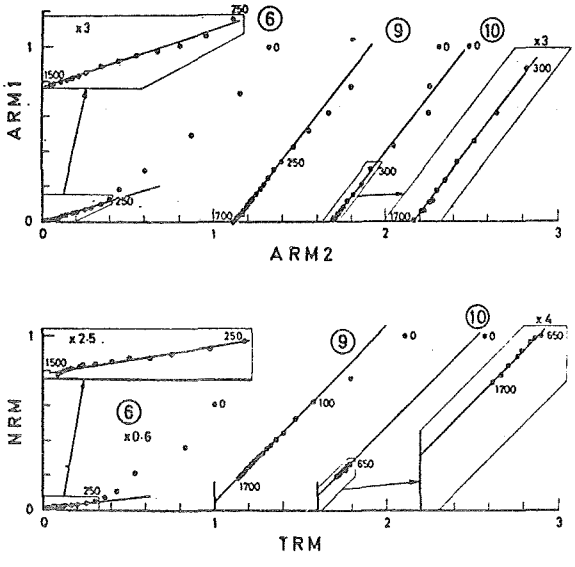

Fig. 3. Class 2b samples.

3. Reliabiligy of Shaw's Method

The comparison of ARM's induced in samples before and after heating proved to be a very powerful method for detecting changes in coercivity spectra. For samples belonging to Class 1a, the estimated field intensities were within 7% of the expected values. It seems reasonable to conclude that Class 1a results are just as reliable as those from successful Thellier experiments.

Somewhat surprisingly, satisfactory results were obtained from many of the samples which apparently

were affected by alteration effects during heating (Class 1b, 2a, 2b). This indicates that the ARM and TRM are very similar and even when some change occurs in heating, they affect the two remanences in a very similar manner.

One of the serious sources of error in Shaw's method is insufficient heating of samples. Fig. 4 shows the results when the samples were heated to a temperature lower than the highest Curie point. Because the heating temperature was low, chemical changes seem to be absent from all the samples. The ARM's are therefore almost identical except very low coercive force portion. The lower diagram in Fig. 4 shows that the partial TRM acquired in an insufficient heating may have coercivity spectrum indistinguishable from that of the total TRM. Field estimates obtained from samples 2, 7 and 14 are between two to five times as large as the expected values (Table 2). It is certainly not possible to reject these results without knowing that the heating did not reach the highest Curie temperture. The exact knowledge of Curie points in samples in essential not to obtain such spurious results as shown in Fig. 4.

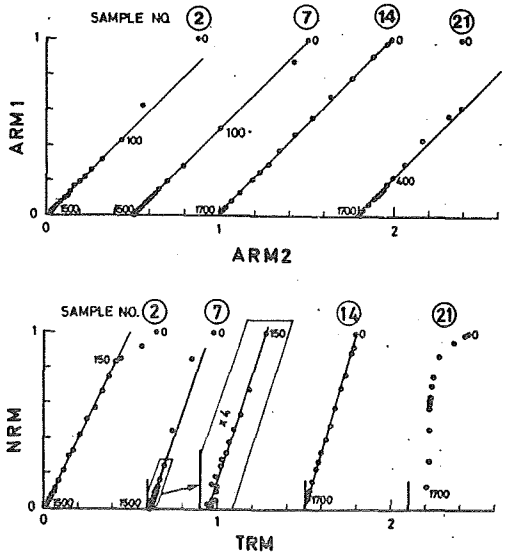

Fig. 4. Result of Shaw's method with insufficient heating.

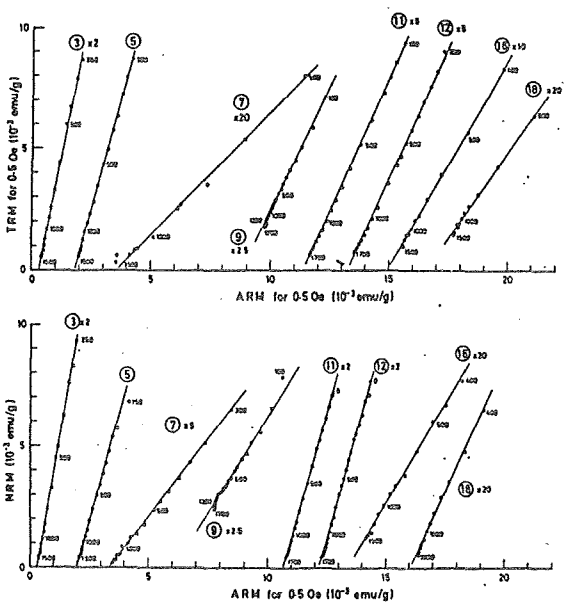

Fig. 5. Samples for which linearity was observed both between NRM and ARM 1 and between TRM and ARM 2 .

4. ARM-TRM relations

The gross similarity between the properties of TRM and ARM is the basis of paleointensity methods proposed by Banerjee and Mellema (1974) and by Stephanson and Collinson (1974). Fig. 5 summarizes the results for samples in which both NRM - ARM 1 and TRM - ARM 2 relations were linear for comparable coercivity ranges. Remarkably linear relations were

observed in many samples but the slope f between TRM and ARM defined earlier is quite different among various samples. Levi and Merrill (1976), using grain size controlled magnetite samples, demonstrated that the slope f varies between 0.5 and 10 and concluded that the application of ARM-TRM paleointensity methods may lead to order of magnitude errors. The present samples contain titanomagnetites with unknown grain size distribution and the f-value varies between 1 and 5.

Thus we may conclude that the ratio between the TRM and ARM magnitudes differs from sample to sample among volcanic rocks so that for paleointensity determination it is necessary to experimentally determine the value of f for individual samples. To determine f, a heating to the Curie temperature and measurements of TRM and ARM coercivity spectra are needed. But when we know coercivity spectra of NRM, TRM and ARM's before and after heating, there is no reason why we should use the ARM-NRM relation instead of the more direct NRM-TRM relation as in Shaw's method.

References

Banerjee, S.K. and J.P. Mellema (1974) Earth Planet. Sci. Lett. 23, 177.

Carmichael, C.M. (1967) Earth Planet. Sci. Lett. 3, 351.

Levi, S. and R.T. Merrill (1976) Earth Planet. Sci. Lett. 32, 171.

Patton, B.J. and J.L. Fitch (1962) J. Geophys. Res. 67, 307.

Shaw, J. (1974) Geophys. J. Roy. Astro. Soc. 39, 133.

Smith, P.J. (1967a) Geophys. J. Roy. Astr. Soc. 12, 239.

Smith, P.J. (1967b) Earth Planet. Sci. Lett. 2, 99.

Stephanson, A. and D.W. Collinson (1974) Earth Planet. Sci. Lett. 23, 220.

Symons, D.J.A. and E.J. Schwarz (1970) Canad. J. Earth Sci. 7, 176.

Thellier, E. and O. Thellier (1959) Ann. Géophys. 15, 285.

Van Zijl, J.S.V., K.W.T. Graham and A.L. Hales (1962) Geophys. J. Roy. Astr. Soc. 7, 169.

(In press in Geophys. J. Roy. Astr. Soc., 1977)

MAGNETIC STABILITY OF DEEP-SEA SEDIMENTS

Tsutomu SUEISHI, Naoto KAWAI

Department of Physics, Faculty of Engineering Science,
Osaka University, Toyonaka, Japan

Kazuo KOBAYASHI

Ocean Research Institute, University of Tokyo,
Nakano-ku, Tokyo, Japan

Introduction

In a companion paper (Sueishi et al., this issue), detailed variations of geomagnetic direction and intensity from 1.01 m.y.BP to 2.03 m.y.BP have been revealed by measuring the natural remanent magnetization of sliced sections of the deep-sea calcareous sedimentary core KH73-4-7.

Magnetic stability of the sedimentary core with 6 m length has been tested by AF demagnetization of Saturation IRM (SIRM) and ARM, and also tested by acquired ARM in the laboratory. SIRM (9 kOe) and ARM (peak AF field ; 1 kOe, bias direct field ; 0.83 Oe) are used to estimate the amount of magnetic minerals in the specimens.

Fundamental Data of Artificial Magnetization

The result of the acquisition curve of IRM is shown in Fig 1. The IRM is almost saturated in the field of a few kOe. It is safety to regard the IRM in the field of 9 kOe as SIRM.

The acquisition curve of ARM for alternating field is shown in Fig 2. The ARM is almost saturated with the peaking AF field of 1 kOe under the constant direct field. This data is not inconsistent with the result by Rimbert (1958).

The acquisition curve of ARM for direct field is shown in Fig 3. According to the data by Patton and Fitch (1962) or Rimbert (1958), the ARM in the same peak field is initially proportional to the direct field up to about several tens Oe, but according to our result for deep-sea sediment , the relation is linear in the range of only less than 1 Oe. There may be some possible causes ; (1) the density of ferromagnetic mineral is dilute . (2) the magnetic hardness of the ferromagnetic grain seems to be large (Jaep, 1971).

The result of the progressive AF demagnetization curve of IRM (1 kOe) and ARM (1 kOe) is shown in Fig 4. Johnson et al. (1975) considered that the estimation of the domain state of the main carrier for remanent magnetization can be possible by comparing the stability of ARM with that of SIRM in the stepwise AF demagnetization (Lowrie-Fuller test). While SIRM is ascribed by the large multi-domain particles, ARM as well as TRM is thought to be caused by single-domain grains. Perhaps the predominant magnetic minerals in this sedimentary core have the size of single or pseudosingle domain (Dunlop, 1973).

The Change of ARM and SIRM along the Core Depth

The variations of ARM and SIRM versus time scale from 449 cm to 638 cm are shown in Fig 5. SIRM (9 kOe) and ARM (1 kOe) are formed every two thin sliced sections throughout the 6 m length.

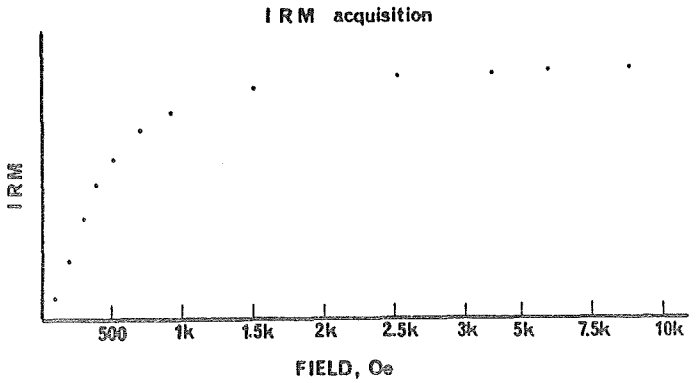

Fig 1. Acquisition of IRM for direct field
The IRM intensity is in the arbitrary unit.

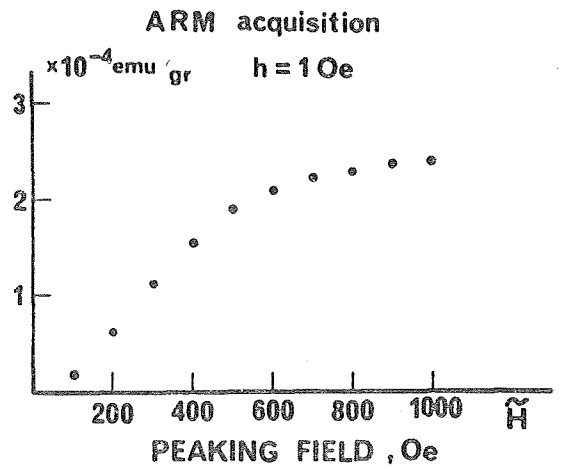

Fig 2. Acquisition of ARM for alternative peak field

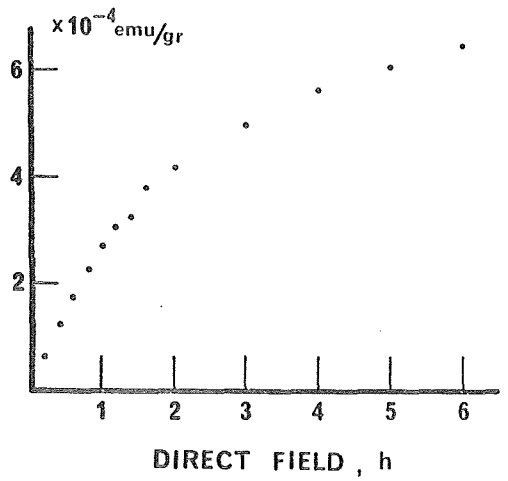

Fig 3. Acquisition of ARM for direct field

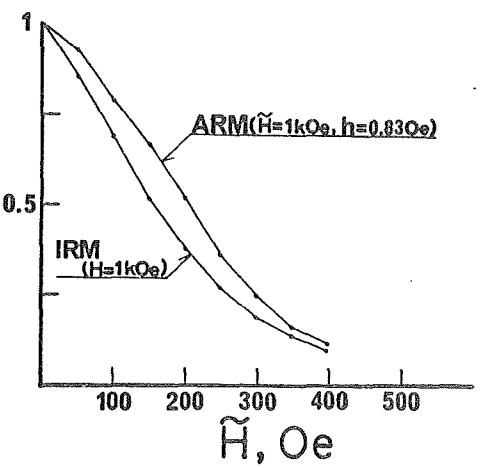

Fig 4. Lowrie-Fuller test

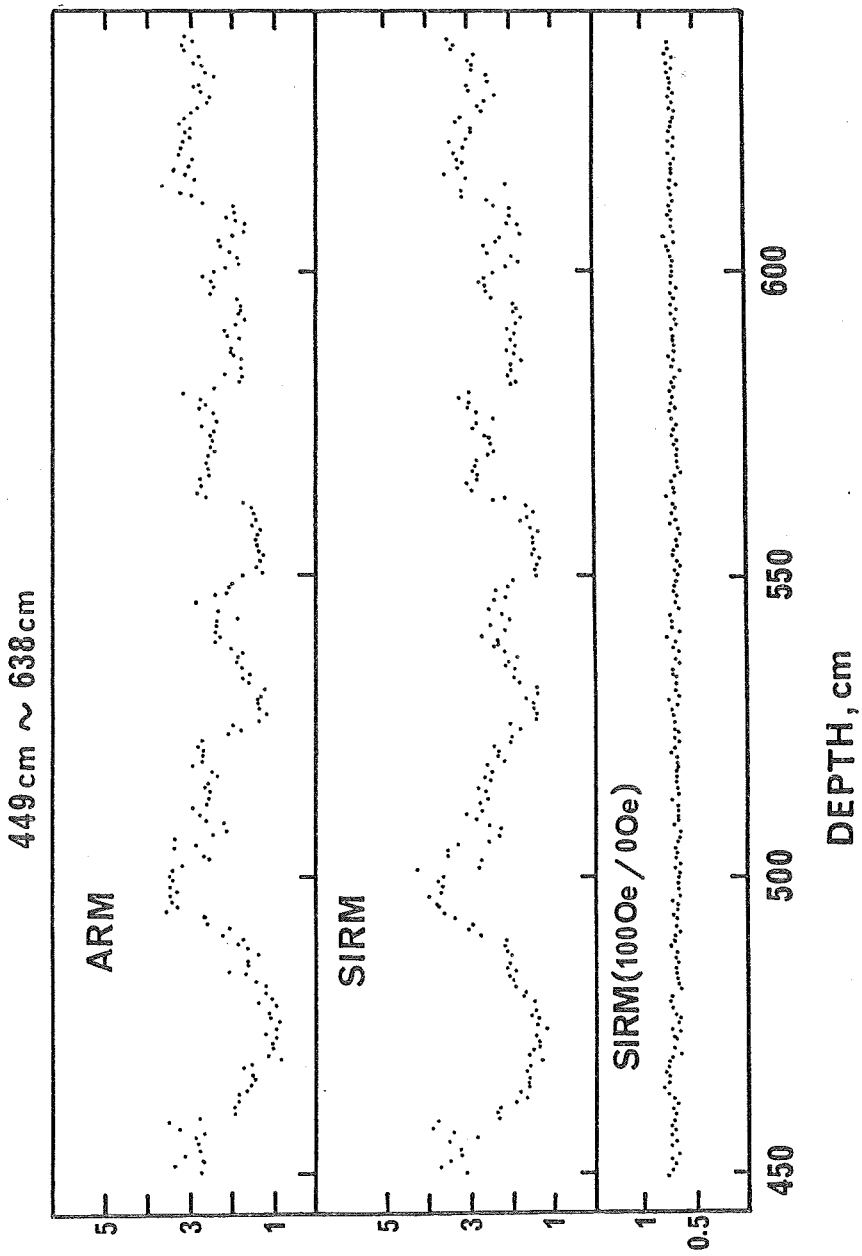

Fig 5. Result of artificial magnetization measurement at depths from 449 cm to 638 cm
The INTENSITY of ARM is in unit of 10^{-4} emu/gr and SIRM is in unit of 10^{-3} emu/gr. Both ARM and SIRM are demagnetized in the field of 100 Oe.

The ARM is measured after the specimen is cleaned up by AF field of 100 Oe. The SIRM is measured twice before and after AF demagnetization in the field of 100 Oe. The spectrum of ARM and SIRM are extremely similar in shape. This tendency also appears in other part of the core as shown in Fig 6. and Fig 7.

The ratio SIRM (100 Oe) to SIRM (0 Oe) is very constant, so the coecivity of SIRM is stable along the core depth. The result means that magnetic minerals of the sedimentary core have been invariable with respect to the grains' size distribution or other physical conditions for about 1 million years. It is a surprising matter that the ratio ARM / SIRM is continuously constant for about 1 million years in our detailed measurement using thin sliced sections.

In the method of relative palaeointensity which is obtained by dividing NRM intensity by the amount of the magnetic minerals, it should be discussed in the range where the ratio ARM / SIRM is continuously constant. ARM (SIRM) can be reliable as a normalizing parameter in the range where the grains' size distribution of the magnetic minerals is fairly constant, even if the amount of magnetic mineral varies.

The Magnitude of the Ratio ARM / SIRM

The ratio ARM / SIRM is also calculated on other sedimentary cores KH73-4-8 (calcareous) and GDP-15-12 (red caly), and from data in other reports (Opdyke et al., 1973 ; Levi and Banerjee, 1976). The comparison of the ratio is shown in Table.

KH73-4-7	KH73-4-8 (calcareous)	GDP-15-12 (red clay)	RC-14-14	1232.5/1 1232.5/2	1066/1 1066/2 926/1 926/2
11.0%	6.2%	1.2%	3.3%	0.7%	2.5%

Table. The magnitude of the ratio ARM / SIRM

Both ARM and SIRM are demagnetized in the alternating field of 100 Oe, and the ratio in the Table is averaged value.

Discussion

When it is taken into consideration that ARM represents the quantity of single (or pseudo-single) domain particle and that SIRM, on the other hand, represents the amount of the multi-domain one, ARM / SIRM can be regarded as a parameter of magnetic stability. The ratio ARM / SIRM will be large when single-domain grain is predominant in an assemblage of ferromagnetic particles. This ratio is essentially able to estimate the grains' size distribution as the method of Lowrie-Fuller test.

As shown in the Table, the magnitude of the ratio in KH73-4-7 is very large. Therefore it is possible to say that the change in NRM of KH73-4-7 is reliable for palaeomagnetism (Otofuji, 1975 ; Sato, 1976 ; Sueishi, 1977 ; also see our companion paper). The fact that the ratios ARM / SIRM are different according to the cores collected at the different places is very interesting.

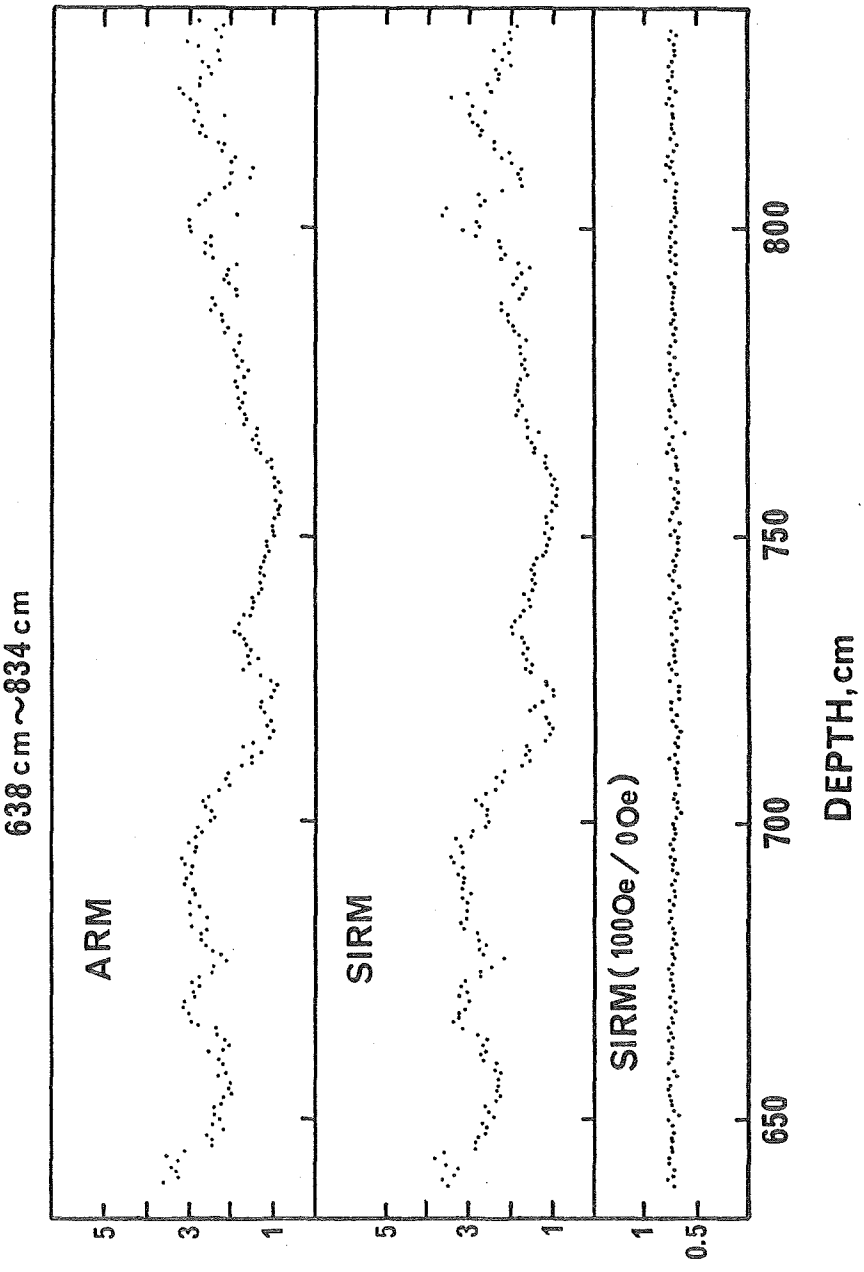

Fig 6. Result of artificial magnetization measurement at depths from 638 cm to 834 cm
The INTENSITY of ARM is in unit of 10^{-4} emu/gr and SIRM is in unit of 10^{-3} emu/gr. Both ARM and SIRM are demagnetized in the field of 100 Oe.

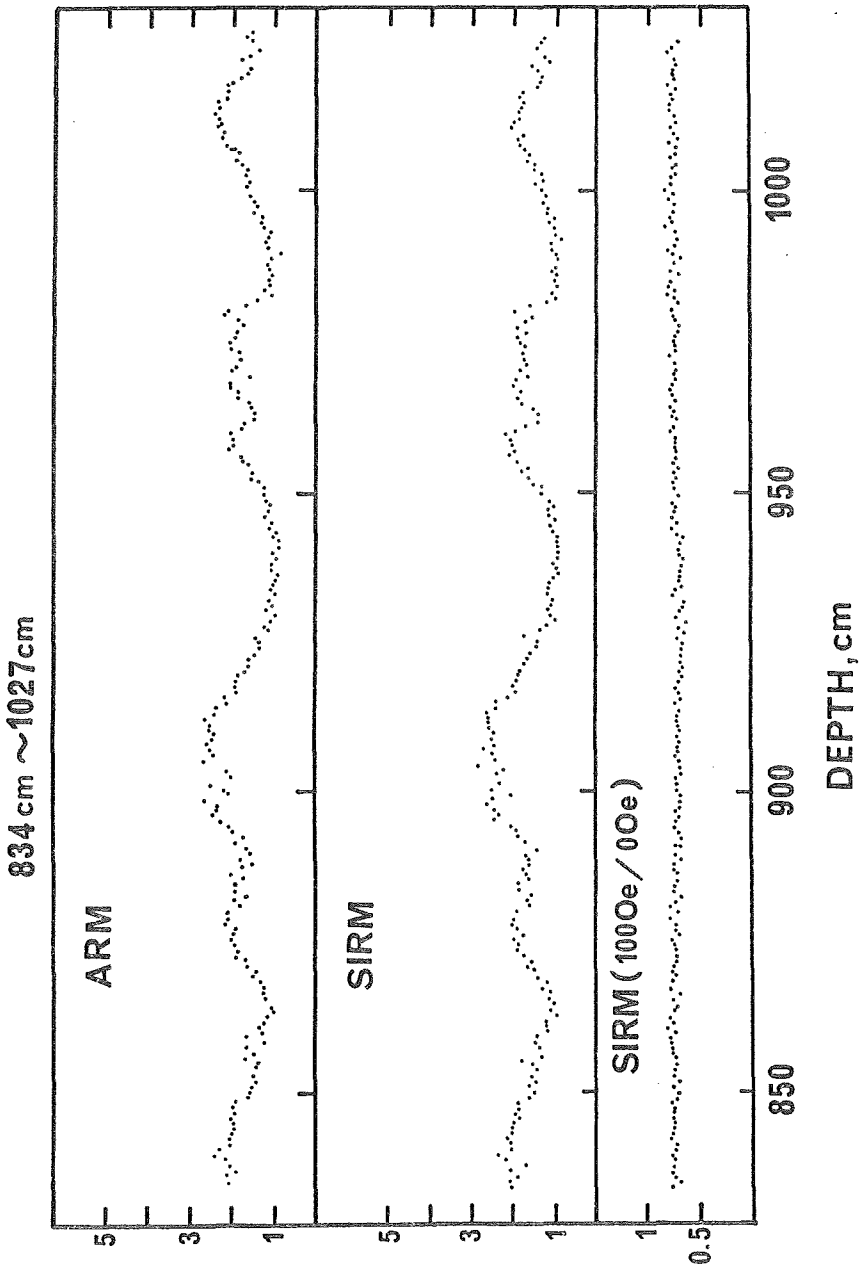

Fig 7. Result of artificial magnetization measurement at depths from 834 cm to 1027 cm
The INTENSITY of ARM is in unit of 10^{-4} emu/gr and SIRM is in unit of 10^{-3} emu/gr. Both ARM and SIRM are demagnetized in the field of 100 Oe.

A plausible explanation may be that magnetic particles derived from volcanoes acquired induced anisotropy at high temperature and thereafter were directly deposited in deep sea. The difference of ARM / SIRM depending on core is originally caused by geometric configuration of volcanoes in the sea or land. From another viewpoint, one million years are only a short period compared with the " time constant " of the geological change of ocean floor.

References

Dunlop.D.J. (1973) J. Geophys. Res., 78, 1780.
Jaep,W.F. (1971) J. Appl. Phys., 42, 2790.
Johnson,H.P., Lowrie,W. and Kent,D.V. (1975) Geophys.J.R.Astr.Soc., 41,1.
Sueishi,T., Kawai,N. and Kobayashi,K. (1977) Rock Magnetism and Paleogeophysics, this issue.
Levi,S. and Banerjee,S.K. (1976) Earth Planet. Sci. Lett., 29, 219.
Opdyke,N.D., Kent,D.V. and Lowrie,W. (1973) Earth Planet. Sci. Lett., 20, 315.
Otofuji,Y. (1975) M.Sc.Thesis, Osaka Univ.
Patton,B.J. and Fitch,J.L. (1962) J. Geophys. Res., 67, 307.
Rimbert,F. (1958) Ph.D.Thesis, Paris Univ.
Sato,T. (1976) M.Sc.Thesis, Osaka Univ.
Sueishi,T. (1977) M.Sc.Thesis, Osaka Univ.

(To be submitted to Phys. Earth Planet. Inter.)

PRELIMINARY REPORT ON THE STABILITY OF NATURAL REMANENT MAGNETIZATION OF DILUVIAL ASH OF CENTRAL YAMAGUCHI PREFECTURE, WEST JAPAN.

Haruo DOMEN

Institute of Physical Sciences, Faculty of Education,
Yamaguchi University, Yamaguchi 753, Japan.

Diluvial ash deposits are widely spreaded in Yamaguchi Prefecture, west Japan; mainly in south-central and -west of it. Some magnetic properties on these samples were previously reported by the present author (Domen 1971, 1975, Domen and Kawano 1969, Domen et al 1970, Kawano and Domen 1971). The present article shows a preliminary study on the stability of the NRM of such tephra sample taken from the Diluvial ash deposit at a part of the famous Akiyoshi limestone plateau in the central Yamaguchi Prefecture. The directional and intensity changes of NRM of the test specimen which was stored within the geomagnetic field at the laboratory in room temperature had been examined during three-month duration. Slight changes of both direction and intensity of NRM were recognized during the storing.

The original NRM of the test specimen shows oblique direction such as D(E) = +88°, I(D) = -50°. Ferromagnetic constituents are mainly titanomagnetites which were identified by Js-T and X-ray analyses.

Soon after the sampling, the tephra sample was cut at rectrangles into block having an extent of 5 x 5 x 1 cm^3, such a way that a long side of block specimen should be in parallel to its NRM direction (as X-axis). Therefore other sides to be along Y- and Z-axes of right-hand coordinate respectively (Fig. 1 (1)). The test specimen thus prepared was tightly sealed by plastic container in which the test specimen was saturated by pure water filled up as long as the experiment was performed. The test specimen thus sealed was stored its X-axis towards the geomagnetic east and the Y-Y plane in horizontal as shown in Fig. 1 (2).

Magnetic measurements were carried out only within the X-Y plane at any suitable time duration of storing by means of an astatic magnetometer, and the test specimen was restored *in situ* as quick as possible after every magnetic measurement. The sealing efficiency of the container was examined by weighing a bulk mass of the sealed specimen before and after magnetic measuring. Any change of mass could be recognized less than the measuring error at every weighing so far as the present experiment was continued. The fluctuations of room temperature, in which the test specimen sealed up was stored, did not exceed by 10°C over a long time span of storing up to about 3 months.

During the storing, however, the orientation of the test specimen was sometimes modified such a way that; firstly the container in which the test specimen was saturated with pure water had been kept its X-axis in horizontal east (in X-Z plane the NRM of specimen lay on at first) as shown in Fig. 1 (1). After 700-hour storing, the sealed container was opened once and the specimen was exposed in the open air, then the specimen was dried somewhat for 100 hours. Next, the specimen was saturated with pure water and sealed again, and moreover the container was overturned upside-down keeping the X-axis in horizontal east (Fig. 1 (3) → (4)). Such an overturned orientation was kept 1000 hours. After this duration past, the container was restored in the initial orientation again (Fig. 1 (4) → (3)).

Magnetic measurement during the above-mentioned storing was carried

out up about 3 months. In this duration, slight changes of the magnetic moment of the specimen was recognized.

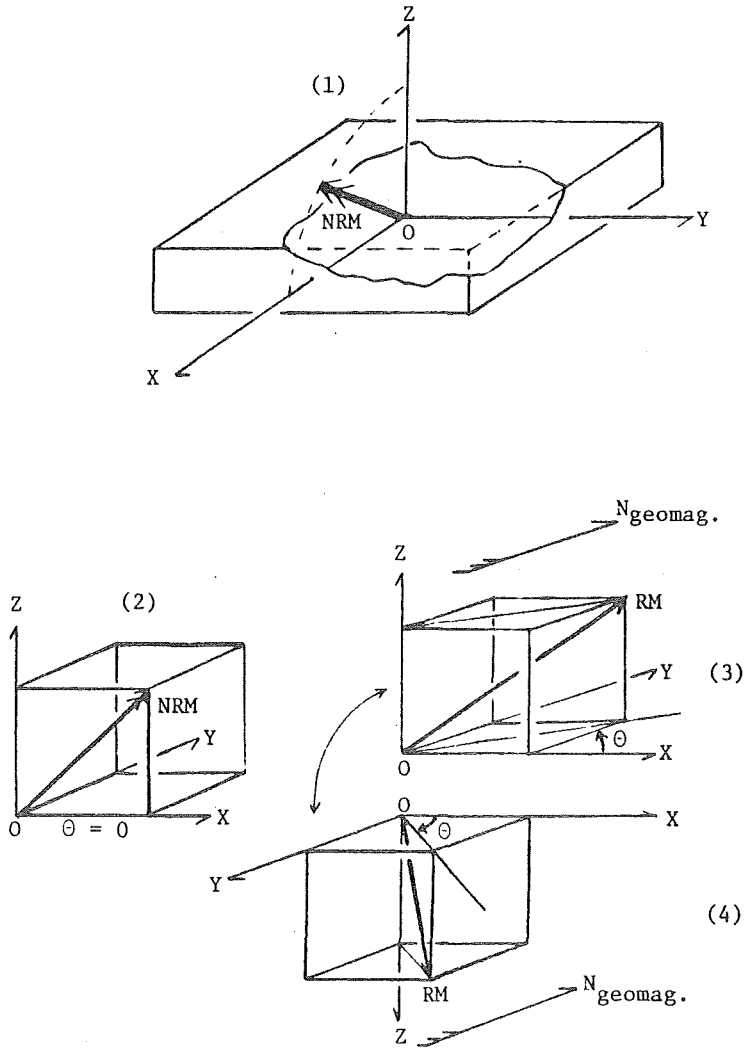

Fig. 1. Sample preparation and orientains during storing.

Such movements of NRM were illustrated in Fig. 2, in which storing orientations mentioned above is also shown. Top of this illustration is for the change of the angle measured from X-axis (geomagnetic horizontal east) to the remanent magnetic component within X-Y plane; $\Theta = \tan^{-1}(Y/X)$, and the bottom for the X component of magnetic vector.

The present preliminary study on time change of NRM of tephra sample was carried out about 3 months of total duration of storing. However it is very hard to draw any essential conclusion from the result obtained, the

NRM which might be a kind of DRM seems to have been changed slightly in wet and dried conditions.

A precise experiment on the stablity of NRM such ash deposit under several controled conditions is now being planned.

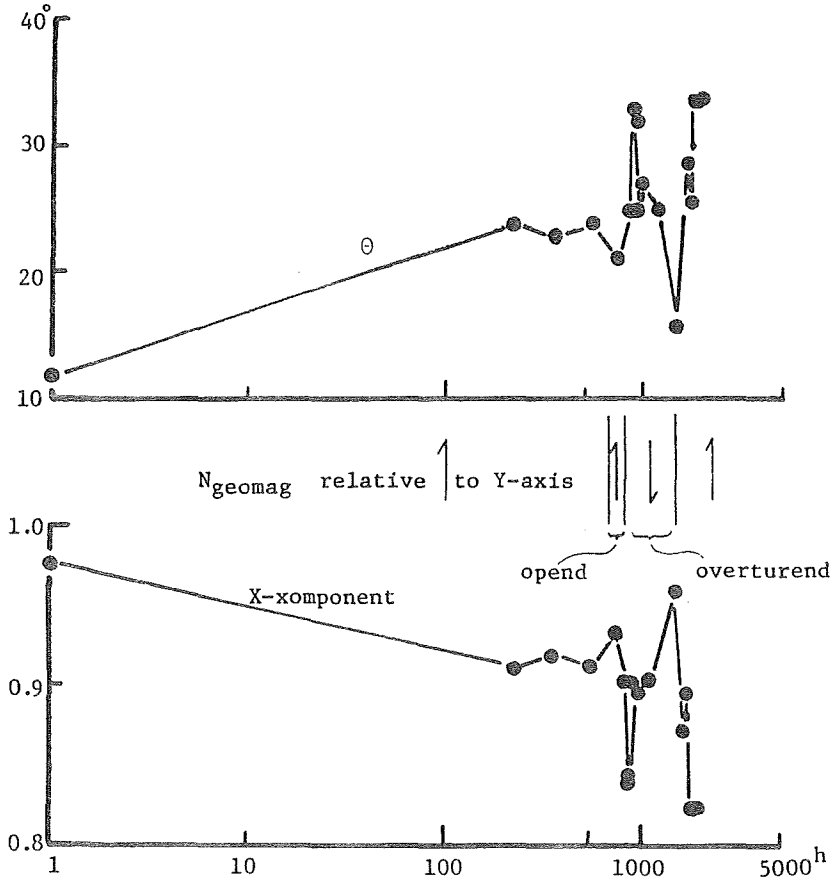

Fig. 2. Directional and intensity changed during storing of Diluvial tephra specimen, the central Yamaguchi, Japan.

References.

Domen, H. (1971) Bull. Fac. Educ., Yamaguchi Univ. 21 (Part 2), 1-14.
Domen, H. (1975) ibid. 25 (Part 2), 63-66.
Domen, H. and M. Kawano (1969) ibid. 18 (Part 2), 23-33 (in Japanese).
Domen, H., H. Muneoka and M. Kawano (1970) ibid. 19 (Part 2), 23-26 (in Japanese).
Kawano, M. and H. Domen (1971) Dai-yonki (Quaternary) No. 16 (in Japanese).

ATTEMPT TO NORMALIZE THE NRM INTENSITY OF SEDIMENT BY TRM

Hiroo INOKUCHI

Department of Geology, Faculty of Science, Shinshu University,
3-1-1, Asahi, Matsumoto 390, Japan

Preface

To obtain the intensity of the ancient geomagnetic field is important for the discussion of the origin of the geomagnetic field, and it is concerned with an interesting problem in paleomagnetism. A method of using igneous rocks is the most effective to obtain the paleointensity, and this way of study has variously been made since earlier works by Koenigsberger (1938). Absolute paleointensity is able to be determined by this method, while its continuous change can not be traced by igneous rocks. Therefore, for this purpose, some other methods have been tried to get continuous change of paleointensity by using samples from a sequence of sediments.

Relative paleointensity may be obtained by normalizing the intensity of Natural Remanent Magnetization (NRM) with remanent magnetization variously acquired in the labolatory. To normalize the NRM intensity, Johnson et al. (1948) used isothermal remanence (IRM, H=2000 Oe), Nakajima & Kawai (1973) used SIRM (saturation IRM), and Nesbitt (1966) and Harrison (1966) used initial susceptibility, respectively. Opdyke et al. (1973) compared the NRM fluctuations with fluctuations of NRM, anhysteretic remanence (ARM) and initial susceptibility, and discussed a decrease of geomagnetic intensity during a field reversal.

In the present study, a method of using the ratios of the NRM intensity to the TRM (thermo-remanent magnetization) intensity (Dr K.Momose, Shinshu Univ., private suggestion) was applied to assess paleointensity based on the consideration that the ferromagnetic minerals in the sediments had acquired TRM primarily (Kobayashi & Nomura, 1974), and compared with the result by the method of using SIRM.

Observed core sample (sample No. st.185, P-22, 5.39m long) was collected from the deep-sea floor (27°34.5'N, 134°24.5'E, 4575m deep), south-east of the Komahashi sea mount, by R/V Hakurei maru on the GH74-7 cruise (Mizuno et al., 1975a) by the Geological Survey of Japan. The core sample consists mostly of pale yellowish brown clay, and upper half of the core log is somewhat tuffaceous and contains some volcanic ash layers (Mizuno et al., 1975b). The core log indicates normal polarity from top to bottom (Inokuchi & Mizuno, 1977). The experiments were made on the samples from the lower half of this core log, and the lowest layer of several centimeters consists of volcanic ash and the overlying other part is clay.

Experimental methods

TRM was acquired in vacuum of about 10^{-3} torr by heating the specimen dried in room temperature. IRM was acquired in the magnetic field $\underline{H}$ for 2 min. by means of the electromagnet. The

IRM intensity doesn't depend on the applied time length of the magnetic field, provided the magnetic field is over more than a few thousand Oe. As the IRM intensity of the specimen got saturated in over 7000 Oe (Fig.1), SIRM was acquired in 7000 Oe. The SIRM intensity once acquired decreased with a lapse of time (Fig.2). As the SIRM intensity of the specimen after AF demagnetization in the field of 100 Oe had been constant with time, the SIRM intensity after demagnetization was used for calculation. Each intensity of the specimen about 2 cm cubic was measured by means of the astatic magnetometer.

The experiments were divided into the following three parts. After the NRM intensities were respectively measured first, the intensity of each remanence was measured in the following order: (I) SIRM (H=7000 Oe) → drying → TRM (T=600°C, 30 min.) → again SIRM (with respects to some of the specimens), (II) SIRM → drying → TRM (T=300°C, 30 min.) → again SIRM (with respects to some of the specimens), and (III) drying → TRM (T=300°C, 30 min.) → SIRM. The NRM intensity obtained indicates similar values with respect to each specimen before and after drying. By using the wet weight, all the intensities measured are descrived in emu/g.

Results

The result of the experiment I, II and III are shown in Fig.3. The ferromagnetic minerals in the specimen are magnetite, maghemite, iron sulphides and so on. As maghemite and iron sulphides were shown to alter to magnetite by heating up to 600°C in vacuum (Inokuchi, 1977), it is impossible to utilize TRM (600°C) (experiment I) for normalizing of the NRM intensity. In this situation, TRM can be acquired by heating to 300°C, because both heating and cooling thermomagnetic curves between 350°C and normal temperature are reversible showing no altera-

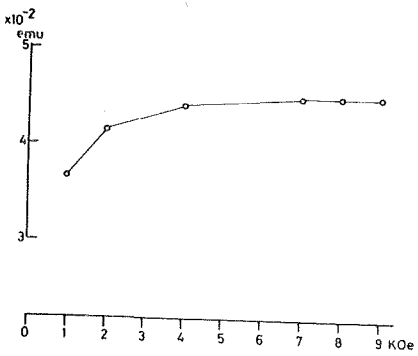

Fig.1 Change in IRM intensity with the applied magnetic field.

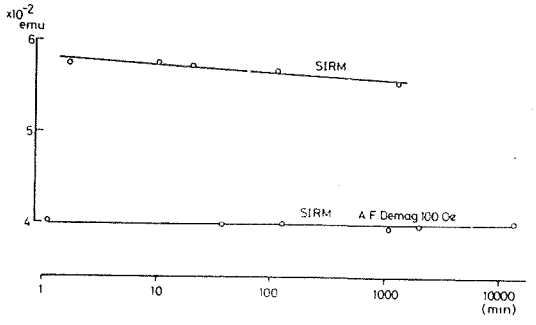

Fig.2 Decrease of the SIRM intensity by time effect before and after AF demagnetization.

Fig.3 Variations in the intensities of NRM, SIRM, TRM(600°C), TRM(300°C), SIRM,T.Demag.300°C and SIRM - SIRM,T.Demag.300°C, and the ratios J(NRM)/J(SIRM), J(NRM)/J(TRM) and J(NRM)/(J(SIRM) - J(SIRM,T.Demag.300°C)). The termomagnetic curves of the specimens indicated with the symbole → are shown in Fig.4, and changes of partial AF demagnetization of the specimens indicated with the symbole ⇒ are shown in Fig.5.

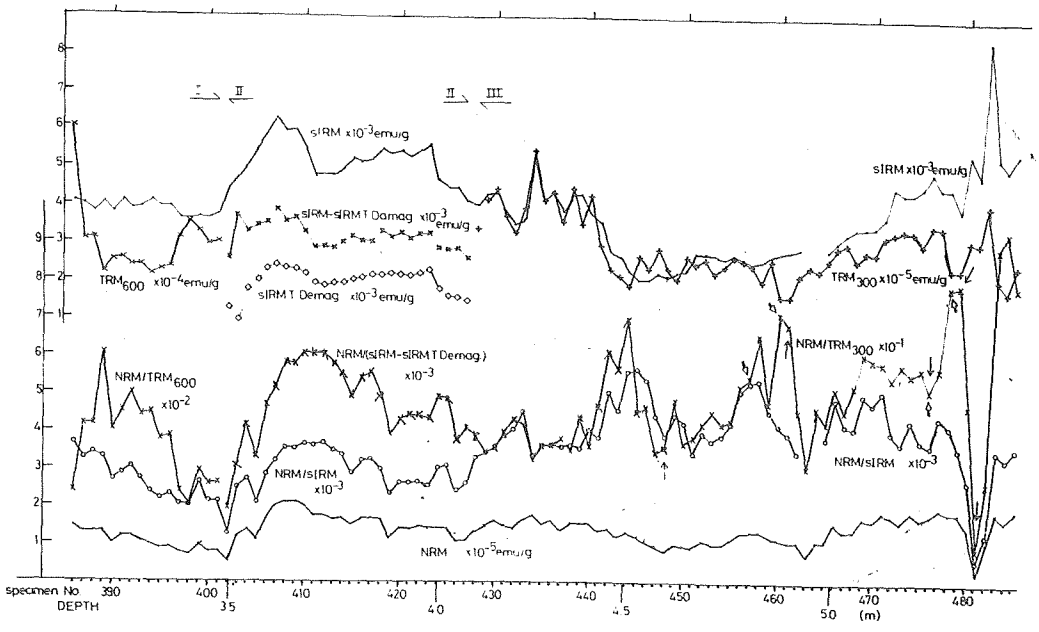

tion of minerals.

As the SIRM intensity (J(SIRM)) shows a value higher than a few hundred times as large as the TRM intensity (J(TRM)), the fact that the specimen having SIRM acquired TRM(300°C) (experiment II) is in a sense similar to the thermal demagnetization at 300°C. This SIRM,T.Demag.300°C corresponds with the remaining part of above 300°C of SIRM, and the part of below 300°C may be expressed by SIRM - SIRM,T.Demag.300°C. The mode of variation in the curve J(SIRM) is similar to that in the curve J(SIRM) - J(SIRM,T.Demag.300°C) (Fig.3, experiment II), and the variation in the SIRM intensity of specimens that previously acquired TRM(300°C) (experiment III) connects smoothly to the variation in the SIRM intensity of specimens having NRM (experiment I and II). Both two facts mentioned above prove that the ferromagnetic minerals don't alter by heating to 300°C.

The variations in the respective ratios J(NRM)/(J(SIRM) - J(SIRM,T.Demag.300°C)), J(NRM)/J(TRM) and J(NRM)/J(SIRM) are shown in Fig.3. The meaning of the variation in J(NRM)/(J(SIRM) - J(SIRM,T.Demag.300°C)) is interpreted to be similar to that in J(NRM)/J(TRM,300°C). The variations in J(NRM)/(J(SIRM) - J(SIRM,T.Demag.300°C)) and J(NRM)/J(TRM,300°C) prove, in their mode, to be roughly similar to that in J(NRM)/J(SIRM), but there are recognized some inconsistencies between the curves J(NRM)/

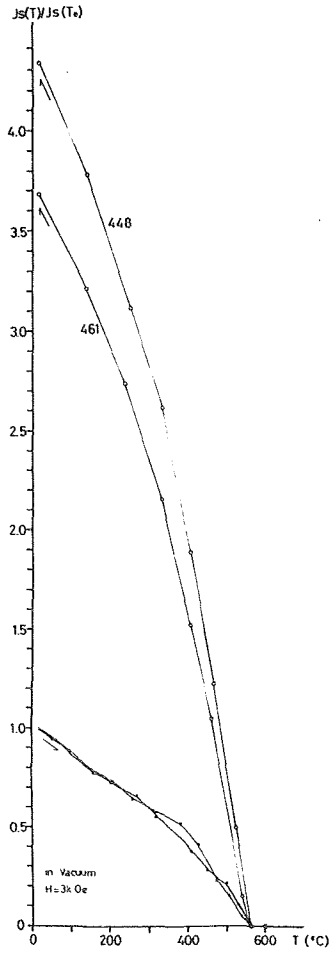

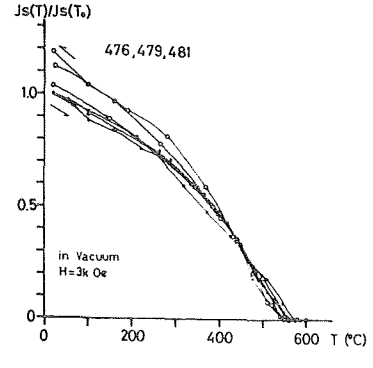

Fig.4 Examples of the thermomagnetic curves. The arrows indicate heating and cooling processes.

J(TRM,300°C) and J(NRM)/J(SIRM) (e.g. specimen No. 460, 461, 478, 479 &c). The thermomagnetic curves of the specimens at this inconsistent part of the core are quite similar to those of the specimens from other part (consistent part) (Fig.4). The thermomagnetic curves of several bottom specimens that consist of volcanic ash change reversibly through both heating and cooling processes, and there is no difference between two parts mentioned above. In the change of partial AF demagnetization from 100 Oe to 400 Oe (Fig.5) and in granumetric measurement of the ferromagnetic minerals under the microscope, the results show a good agreement respestively between two parts mentioned above. As proved in the present experiments, the difference revealed between the consistent and the inconsistent parts should not be ascribed to a difference in the ferromagnetic minerals and their grain-size composition. It remains unexplained what causes existence of the different parts.

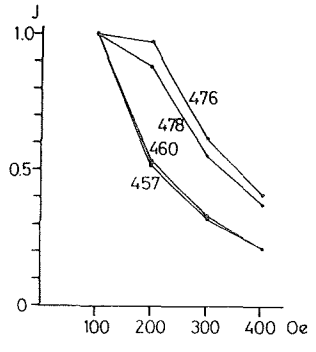

Fig.5 Examples of change in partial AF demagnetization.

Conclusions

In conjecturing the paleointensity from sediments, it is found that the result based on TRM to normalize the NRM intensity is mostly similar to the result based on SIRM. However, there are some inconsistent parts between the results normalized by TRM and by SIRM, and the reason for this inconsistency is still unknown. In the present study, the specimens in which the ferromagnetic minerals alter by heating to 600°C in vacuum are used; but it is necessary to make analogous experiments by using the specimens in which the ferromagnetic manerals don't alter by heating to the Curie temperature. In any case, the method of normalizing the NRM intensity by TRM appears to be one of the most effective methods to assess the paleointensity from sediments. Moreover, as most minerals holding DRM seem to have TRM primarily, the method of using TRM is considered to be more suitable than that of using SIRM in view of the weakness of the applied field.

References

Harrison, C.G.A. (1966) J. Geophys. Res., 71, 3033-3043.

Inokuchi, H. (1977) Rock Mag. Paleogeophys., 4, (submitted).

Inokuchi. H., and A.Mizuno (1977) J. Geol. Soc. Japan, 83, 191-192.(in Japanese)

Johnson, E.A., T.Murphy, and O.W.Torreson (1948) Terr. Magnet. Atmos. Electr., 53, 349-372.

Kobayashi, K., and M.Nomura (1974) J. Geophys., 40, 501-512.

Koenigsberger, J.G. (1938) Terr. Mag., 43, 119-130 & 299-320.

Mizuno, A., Y.Okuda, K.Tamaki, Y.Kinoshita, M.Nohara, M.Yuasa, N.Nakajima, F.Murakami, S.Terashima, and K.Ishibashi (1975a) Marine Sci.(Kaiyo Kagaku), 7, 484-491.(in Japanese)

Mizuno, A., M.Nohara, Y.Kinoshita, N.Nakajima, Y.Okuda, K.Tamaki, and K.Ishibashi (1975b) Geological Problems of the Philippine Sea Area (Papers presented at the Symosium of the 82nd General Meeting of the Geol. Soc. of Japan, Kyoto, 1975), 105-111.(in Japanese)

Nakajima, T., and N.Kawai (1973) Rock Mag. Paleogeophys., 1, 34-38.

Nesbitt, J.D. (1966) Nature, 210, 618.

Opdyke, N.D., D.V.Kent, and W.Lowrie (1973) Earth Planet. Sci. Lett., 20, 315-324.

REMANENT MAGNETIZATION OF SLUMPED MARINE SEDIMENTARY ROCKS

Nobuaki NIITSUMA

Department of Earth Sciences, Tohoku University
Kawauchi, 980 SENDAI, Japan

Generally the intensity of remanent magnetization of sedimentary rocks (ranging from 10^{-4} to 10^{-7}emu/cc) is weak and thus it is possible that secondary component such as viscous remanent magnetization (VRM) and chemical remanent magnetization (CRM) may contribute significantly to the measured remanent magnetization. In contrast to the thermo-remanent magnetization (TRM) in volcanic rocks, the mechanism of acquisition of remanence by sedimentary rock is not well understood. However, sedimentary rocks have the advantage in that it is possible to investigate the continuous history and details of short term changes in the geomagnetic field, particularly if the rate of sedimentation has been high. Furthermore, the bedding plane represents a valuable horizontal frame of reference against which the direction of remanent magnetization can be composed. Fossils in the sediments provide geologic ages and can be used for correlation between widely seperated sections. Thus the mode of acquisition and resultant stability of the remanent magnetization is important, if sedimentary rocks are to be used successfully to investigate the history of the Earth's magnetic field.

This paper deals with the characteristics of remanent magnetization of some sedimentary rocks cropping out in the Boso and Choshi areas of central Japan. Demagnetization experiments have been applied to the source and stability of VRM and CRM. The fixation time of the remanent magnetization, i.e. whether during deposition and consolidation or afterwards, was studied by measuring the remanent magnetization of sedimentary rocks in different parts of an intraformational deformation ("slumping"), here after refered to as the "slumping test of remanent magnetization".

1. Stability test for remanent magnetization of sedimentary rocks

The Neogene and Pleistocene sedimentary rocks in Boso area were first studied paleomagnetically by Kawai (1951), who reported that the natural remanent magnetization (NRM) of all measured rocks exhibited normal polarity. However, Nakagawa and others (1969) found numerous horizons where the remanent magnetization was reversed after AF demanetization in peak fields of 90 Oe. Fig. 1 shows the result of measurement of magnetization of sedimentary rocks of the Boso area during stepwise AF demagnetization. This result demonstrates that an apparently unstable component can be eliminated by AF demagnetization at 60-90 Oe. Fig. 2. shows the change in intensity of remanent magnetization of the

same samples as in Fig. 1, during stepwise AF demagnetization. Also shown is the change in intensity of VRM given to the sedimentary rocks under 10 Oe in 40 minuts. The two curves are very similar; between 30 and 150 Oe the NRM and VRM curves change slope and at higher levels of AF demagnetization they decrease slowly or do not change. Thus these results suggest that the VRM can be eliminated by AF demagnetization.

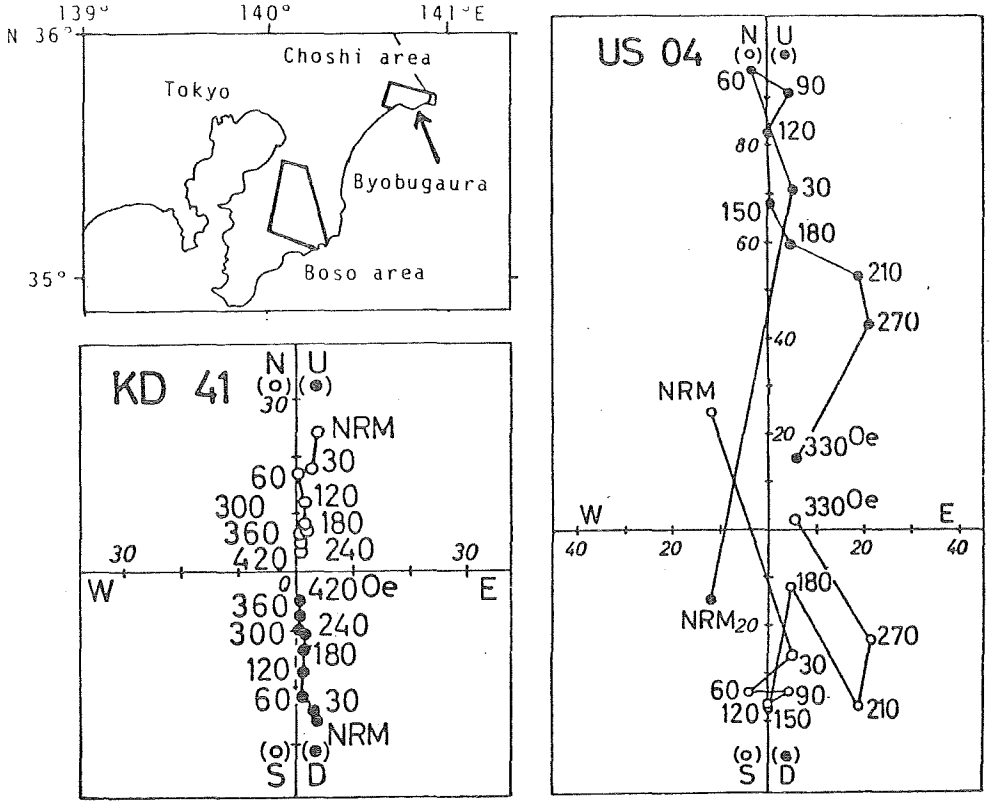

Fig. 1 Index map and stepwise AF demagnetization curves of remanent magnetization of sedimentary rocks of the Boso area (Nakagawa and others, 1969). Each unit on either axis represents 1×10^{-5}emu/cc for KD 41 and 1×10^{-6}emu/cc for US 04.

Fig. 3 illustrated that the VRM of sedimentary rocks increases with time and strength of field, and is parallel to the applied field. From these results, it can be concluded that the unstable remanence of the sedimentary rocks is due to VRM growing in the present magnetic field of the Earth.

In these areas the sedimentary sequences are intercalated frequently by volcanic ash layers, which are useful in layer by layer correlation since they represent a very short interval in geological time. Using these tuff layers as time markers, the preservation of the original remanent magnetization can be

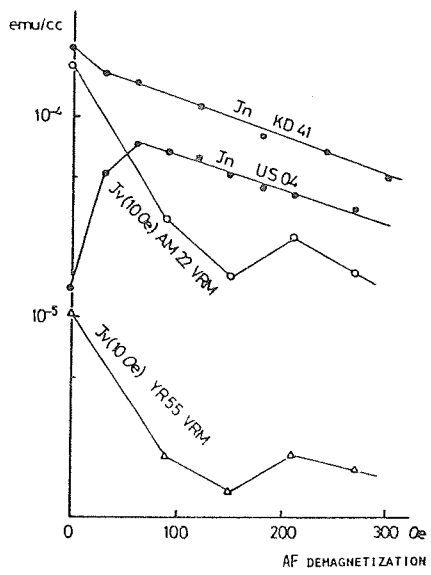

Fig. 2 Stepwise AF demagnetization curves of NRM (Jn) and VRM (Jv) of sedimentary rocks of the Boso area

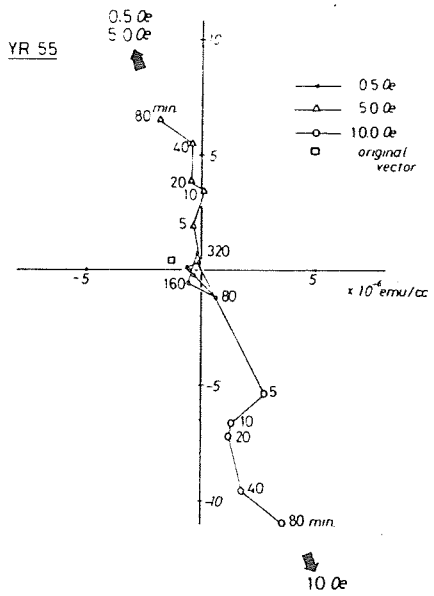

Fig. 3 Growing curves of VRM of sedimentary rock of the Boso area. ⇧: direction of the applied field.

examined. Specifically, variable NRM directions meaned immediately below the same tuff layer but at different localities, imply the existence of a non-uniform secondary component. Intensities of remanent magnetization such samples are less than 5×10^{-6} emu/cc, and the remanence is generally of normal polarity. These samples have a stable direction with normal polarity after 60 to 180 Oe AF demagnetization, but this direction changes after 100 to 200°C thermal demagnetization. Thermal demagnetization was carried out in air and in magnetic free space (a few tens of gamma or less) using a permalloy shield and coil system, as shown in Fig. 4. The component of remanent magnetization removed by the thermal demagnetization was not VRM, since the VRM could be removed by 60-150 Oe AF demagnetization as discussed earlier. It is believed that the remanence was not due to partial thermo-remanent magnetization (PTRM), since the intensity of PTRM acquired by heating at 100°C in the presence of the Earth's magnetic field is 5-10 times larger than what was removed. It is concluded that the remanence results from the CRM of the magnetic minerals crystalized after sedimentation. Such a magnetic component would be expected to have the direction of the present geomagnetic field and a relating low intensity of magnetization. Assumming the component to be heating experiments suggest that the Curie temperature or temperature of decomposition of causal mineral phase should be in the range 100-200°C. Rock samples with this component have been carefully removed from the outcrop after eliminating surficial weathered portion. Reflective

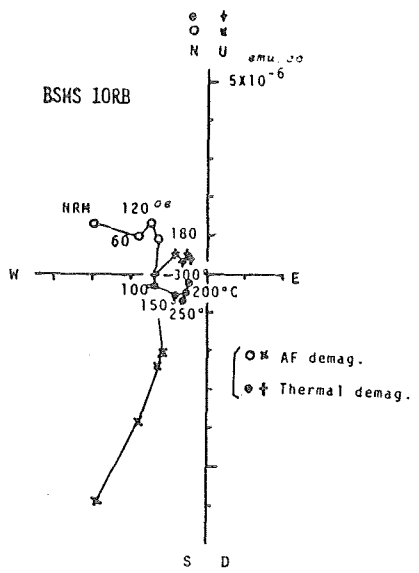

Fig. 4 Stepwise AF and thermal demagnetization curve of sedimentary rock of the Boso area.

microscope reveals the presence of goethite (oxy-hydroxide of iron). It is known that goethite has a weak remanent magnetization with a Curie temperature of 120°C (Strangway, 1967), and generally grows under weathering conditions. Thus it was concluded that this component of the remanent magnetization resulted from CRM of secondary goethite precipitated at the outcrop. With the exception of extremely weathered specimens, the intensity of CRM of goethite was generally less than $5x10^{-6}$emu/cc due to the range of intensity of CRM and the limited amount of goethite.

The development of goethite during weathering of sedimentary rocks emphasizes the need to acquire relatively fresh samples from outcrops. It has been shown that AF demagnetization of 60-150 Oe is necessary for elimination of VRM, and in the case of intensities less than $5x10^{-6}$emu/cc thermo-demagnetization at 200°C may be needed for elimination CRM of goethite.

2. Slumping test of remanent magnetization

For paleomagnetic studies of sedimentary rock, it is important to determine the fixation time of the remanent magnetization of sediments. This problem should be soluble by measurements of the remanent magnetization of sediments at each stage of deposition and consolidation. Another approach is to consider sediments which had been redeposited by submarine slumping shortly after original deposition and consolidation. If the components of remanent magnetization of pre- and post-redeposition were distinguishable, the ratio of pre-redepositional remanence to post-redepositional component is considered to represent the grade of fixing of the remanent magnetization.

Fig. 5 shows a large-scale intraformational deformation observed on the cliff along Byobugaura Coast in the Choshi area, central Japan. The deformed beds are in the basal part of Kasuga Formation stratigraphically directly below the "Oldvai event" (sens Ophdyke, 1972) of magnetic stratigraphy (Niitsuma and others, 1972). Field evidence indicates that the intraformational deformation resulted from submarine slumping. The upper part of the deformed sections characterized by plastic deformation, the lower part of the

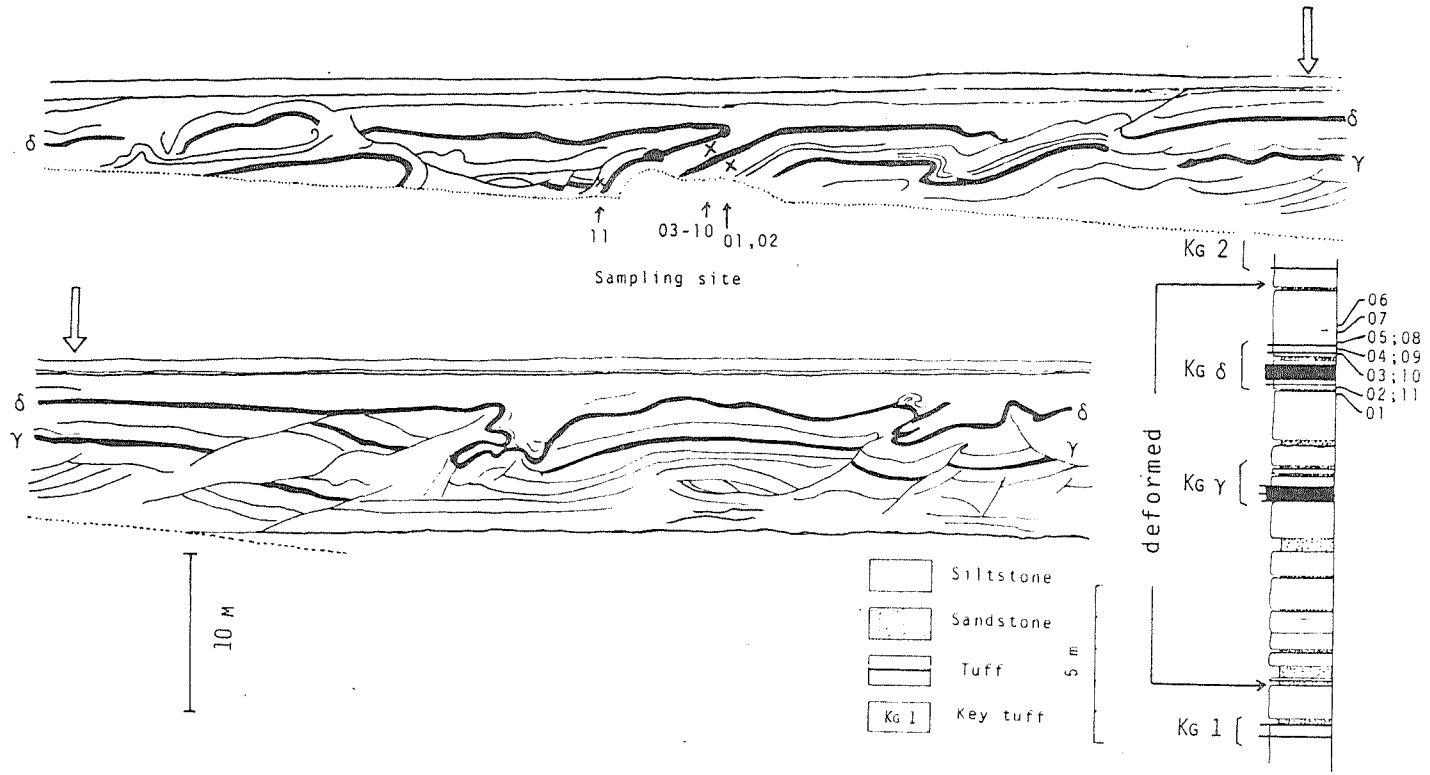

Fig. 5 The large-scale intraformational deformation and restored columnar section in the lowest part of the Kasuga Formation at the Byobugaura Coast in the Chosi area.

deformed beds by relative brittle deformation, suggesting differences in the degree of consolidation of the sediments at the time of slumping. Several interbedded layers of volcanic ash mark original depositional surfaces. From the deformed beds, 27 cored samples were collected at 12 sites, as shown in Fig. 5. In the 12 sites, the contemporanity of 4 paired coeval sites was indicated by the intercalated tuffs. The remanent magnetization of the samples was measured with a shielded parastatic magnetometer after thermal demagnetization at 200°C and AF demagnetization at peak field of 180 Oe. The intensity of remanent magnetization ranged from 2×10^{-6} to 5×10^{-5} emu/cc. The results of measurements at the 4 paired sites are shown in Table 1.

Table 1 Result of measurements and calculations for "slumping test".

paired samples normal side ; overturned side		05	08	04	09	03	10	02	11	06
Direction of RM after correction for bedding	(D)	158°	141°	178°	115°	232°	77°	224°	204°	170°
	(I)	-32°	-24°	-32°	4°	-40°	-38°	-22°	-36°	-62°
after correction for deformation	(D)	172°	140°	183°	113°	213°	84°	211°	190°	
	(I)	-14°	-3°	-31°	23°	-45°	-14°	-22°	12°	
number of samples		4	4	4	4	4	4	4	4	4
k		22	50	30	50	50	6	19	11	35
α_{95}		20°	13°	17°	13°	13°	40°	22°	30°	16°
intensity ($\times 10^{-6}$ emu/cm^3)		43	38	16	13	17	7	16	13	5
angles between measured direction and post-deformational component	(A)	29°	43°	29°	77°	42°	58°	53°	48°	
and pre-deformational component	(B)	8°	11°	3°	6°	37°	50°	8°	8°	
sin B / sin A		0.348		0.093		0.900		0.176		
post-deformational component (%)		25.8		8.5		47.4		15.0		
calculated direction of pre-deformational component	(D)	167°	138°	182°	110°	244°	48°	219°	194°	
	(I)	-8°	8°	-28°	28°	-27°	27°	-17°	17°	
direction of overturn axis		153°		146°		138°		207°		

Fig. 6 shows schematically the declination and inclination in the overturned beds for the case in which the remanence is fixed before deformation. In this case, the declination after deformation varies with the sense of rotation of the bedding plane, which in our case could not be accurately estimated by field observation. Therefore, corrections were made only for dip, even for the case of overturned beds. If the entire remanence had been fixed prior to deformation, then the inclinations of all the samples should be the same after correction for deformation. Also in the case of overturned portion of the section, samples taken from the reversed part should have parallel and opposite inclinations to those from the normal part. On the other hand if the remanence had been fixed after deformation, the uncorrected inclinations and declinations of

the samples should be the same throughout the exposure.

The present results show that before correction the directions of remanent magnetization do not have the same direction, and after correction inclinations are a few tens of degrees upward in the normal part and a few degrees downward in the reversed part of recumbent deformation (Fig. 7). The declinations are southwest in the normal part and southeast in the reversed part. Thus the remanence of these sediments is not characteristic of either the first or the second case discussed above. Estimates can be made on the magnitude and direction of the post-deformational component assuming that 1) the remanent magnetization is composed of two components, a single pre- and post-deformational component, 2) the direction of the pre-deformational component was uniform over the same horizon before deformation, 3) the direction of post-deformational component is uniform throughout the deformed beds, and 4) the ratio between the magnitudes of the two components is the same throughout a given horizon.

In Fig. 7, the enclosed line gives the limits in directions for the post-deformational component of magnetization. If the two angles between the direction of post-deformational component and the measured directions at a given paired site are A and A', and the angles between the direction of pre-deformational component and measured directions are B and B', the relationship between these angles can be written as

$$\frac{\sin A}{\sin B} = \frac{\sin A'}{\sin B'}$$

because the proortion of the two components is the same in the paired sites (Fig. 8). Because the inclination of pre-deformational component should be the same in paired sites, the

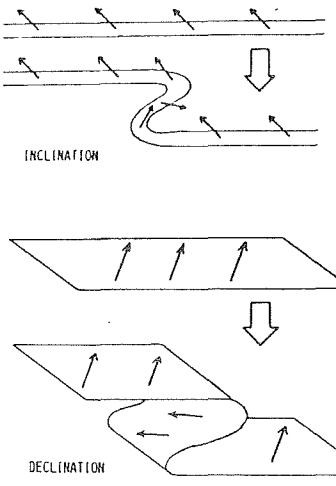

Fig. 6 The changes of the inclination and declination of remanent magnetization by the overturned deformation.

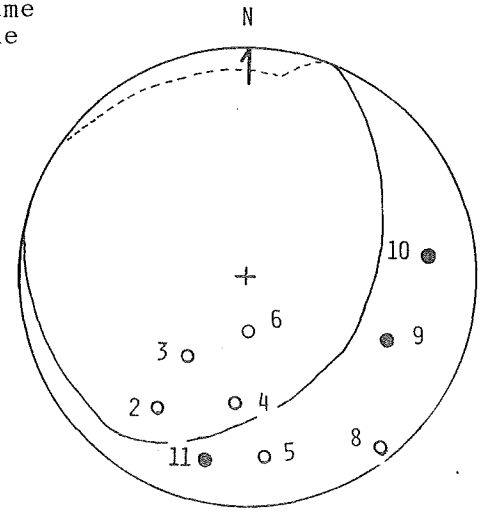

Fig. 7 The pojection of the remanent magnetization after correction for deformation on Wulff net. The enclosed line shows the limits of direction of the post-deformational component of manetization. Open circles for upper hemisphere; closed circules for lower hemisphere.

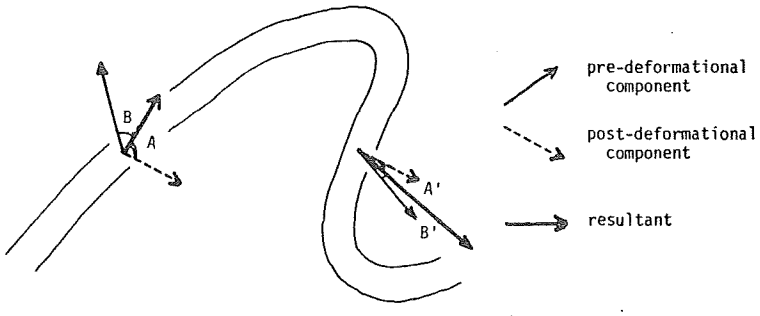

Fig. 8 The relationship among pre-deformational, post-deformational components and resultant of those components. A,A': angles between the directions of post-deformational component and resultant. B,B': angles between the directions of pre-deformational component and resultant.

direction of pre-deformational components could be calcurated. The mean direction of the declinations of the pre-deformational components at paired sites represents the direction of axis of the overturn. Now, the direction of the remanent magnetization of site 06 is taken as the direction of post-deformational component (Table 1), because the site is on the axial plane of recumbent slumping and in this part the primary structure of pre-deformation was completely lost by redeposition. The results of the calculations are shown in Table 1. The proportion of post-deformational component to measured remanence ranges from 8 to 47% depending on horizon. The recumbent fold axis trends SSE-NNW with the exception of beds near site 11 which is near a fault as shown in Fig. 5: the declination of the pre-deformational component is considered to have been rotated not only by the overturning but also by the fault.

The present results suggest that the pre-deformational component of remanent magnetization represents one half or more of the measured remanent magnetization. The deformed structure such as the present one will be one of the worst conditions for preserving pre-deformational remanence, because magnetic grains in the sediments could have a chance to reorientate during deformation. In undeformed sediments the proportion of original remanence in the total remanence is expected to be still higher.

3. Conclusion

Studies made on the sedimentary rocks using demagnetization tests and VRM growing tests show that a large proportion of NRM of sedimentary rocks consists of a secondary remanent magnetization. These secondary components are concluded to be VRM and CRM of goethite grown under the present geomagnetic field. The VRM was found to be eliminated by AF demagnetization at 60-180 Oe and the CRM by thermo-demagnetization at 200°C. The primary remanent magnetization could be measured after the aforementioned demagnetizations;

however, in the case of low intensities of remanent magnetization (less than 5×10^{-6} emu/cc) very careful demagnetization was found to be nessecery.

The results of a "slumping test" were used to examine when fixation of the remanent magnetization of sedimentary rock occurred during the processes of deposition and consolidation. Results indicated that one half or more of remanent magnetization had been fixed before the consolidation, when the sediments could be deformed as plastic material by slumping. The horizons of the measured samples are considered to be 1.8-3.5m below the sea bottom before the slumping. Because the rate of sedimentation has been estimated magnetostratigraphically to be 80-100 cm/1000 years for the studied horizon (Niitsuma and others, 1972), the fixation of the remanence was accomplished within 2000 years after deposition.

References

Kawai, N. (1951) J. Geophys. Res. 56, 73.
Nakagawa, H., Niitsuma, N. and Hayasaka, I. (1969) Geol. Soc. Japan, Jour. 75, 267.
Niitsuma, N., Kimura, K., and Sakai, T. (1972) Japanes Assoc. Petrol. Technol., Jour. 37, 411.
Opdyke,N.D. (1972) Rev. Geophys. Space Phys. 10, 213.
Strangway, D.W., McMahaon, B.E. and Honea, R.M. (1967) Science, 158, 785.

(to be submitted to J. Geomag. Geoelectr.)

EXPERIMENTAL STUDY ON POST-DEPOSITIONAL REMANENT MAGNETIZATION

Yo-ichiro OTOFUJI and Sadao SASAJIMA

Department of Geology and Mineralogy, University of Kyoto
606, Kyoto, Japan

1. Introduction

Some of previous re-deposition experiments have demonstrated that post-depositional alignments of fine grained ferromagnetic minerals in both synthetic (Irving and Major, 1964) and marine sediments (Kent, 1973) produce a stable remanent magnetization with no systematic deviation of the direction from the applied field. Kent (1973) showed in his experiments that the remanent intensities thus obtained were linealy proportional to various intensities of the applied field up to 1.2 Oe. It is well-known that the intensity depends on the content of ferromagnetic minerals contained in the sediments (Nagata et al., 1945). Løvlie (1974) showed, however, experimentally that the magnitude of the remanence was not necessarily concordant with any increase of the susceptibility. This evidence suggests that the acquisition of a stable post-DRM is controlled by any other factors (environmental condition during the accumulation) than the field intensity or ferromagnetic mineral concentration. It is important, therefore, to examine what kinds of condition effectively act upon the alignment of magnetic grains;i.e., magnitude of the remanent intensity.

Previous studies have been recourse to dehydration by artifitial drying-up on their experiments. As Yaskawa pointed out (1974), the actual sedimentation process in natural did not result from dehydration by drying-up but result from gradual dehydration accompanying gravitational compaction. And Johnson et al. (1975) suggested that the remanence already acquired in wet condition was considerably disturbed by the effects of drying. So one should be careful in post-depositional experiment, in strict sense of the word, not to bring the other remanence origins.

There are three major methods of extracting interstitial fluid from sediments; (1) centrifuging, (2) squeezing out, and (3) washing out. The first method is based on the principle of compressing the sediment particles with an appropriate acceleration. This method have merits of, (1) rapidly compacting the sediments, (2) simple control to change the accumulation or compaction rate, (3) scarcely suffering from effects of drying. We have conducted experiments with "Centrifuge" to simulate the actual condition of the gravitational compaction. In the present paper, results of re-deposition experiments so far obtained with "Centrifuge" under various kinds of conditions are reported.

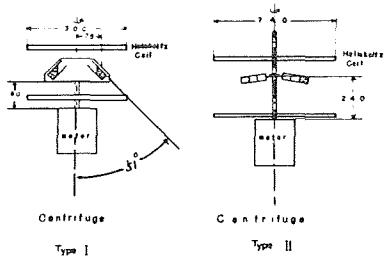

Fig. 1 Centrifuges.

2. Apparatus and methods

Two types of the "Centrifuge" were used to form dehydrated sediments. The apparatuses are shown in Fig. 1. The first type is for high speeds rotation from 3,000 rpm to 10,000 rpm and the cylinder in a non-magnetic cylinder box is fixed on the rotational axis inclined fifty-one degrees. In this type, the direction of acceleration is that of the resultant vector of the centrifugal and gravitational forces, so that the direction of the accumulation and the compaction changes from the vertical to the horizontal with increasing rotational speeds. The second type is for low speeds rotation from 300 rpm to 3,000 rpm. The connection between the cylinder case and the rotational axis moves smoothly, so that the direction of acceleration relative to the bottom of the vessel is unchangeable despite of the increase in rotational speeds.

Rotational speeds were checked with the tachometer consisting of the photoelectric probe connected with the F-V converter. Monitering them frequently, they were maintained constant for several hours within accuracy of 5% in variation.

Single Helmholtz coil covering outside of centrifuge was arranged to provide various intensities of vertical field in each apparatus. The horizontal component of geomagnetic field does not affect the magnetic particles to align definitely, because the horizontal component for the rotation coordinate system is not DC field but AC field. The part of the compaction in the cylinder is apart from the electric motor more than 80 mm. The electric motor generate the magnetic noise only 500 gamma just above it, therefore it dose not disturbe experiment magnetically.

Deep-sea and also lake sediments were used for starting material in this experiments. Deep-sea sediments (GDP-11-16) were dredged from Amami Rise at the depth 2,200 m in the West Pacific and lake sediments were from Lake Biwa at the depth 60 m. These sediments were dissolved and brought into suspension in distilled water using an ultrasonic agitator. And further, sediments were well dispersed by the aid of sodium hexametaphosphate as a peptizer. Suspended sediments were poured into the cylinder which was placed on the glass vessel (diameter 23 mm, height 23 mm). They were then compacted into the vessel in centrifuging and the dehydrated sediments in it were taken off from the cylinder without any deformation. Instantaneously, they were placed in the field free space for 30 minutes until the specimen became

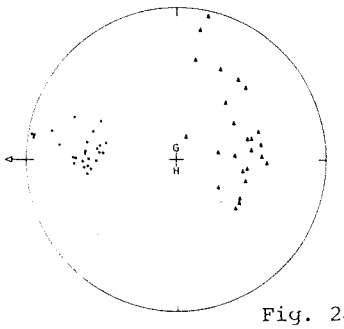

Fig. 2a

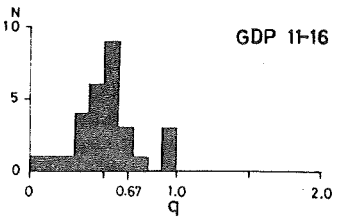

Fig. 2b

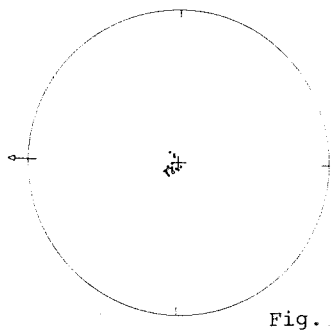

Fig. 2c

cohesive enough to measure the remanence or the magnetic anisotropy with spinner magnetometer (SSM-1A).

Water content in the sediments, before and after the compaction, was measured. Water content; W, was defined as $W = W_W / W_S$, where W_W and W_S are the weight of water and solid in the sediments respectively. The sediments were dried up in the oven at 110°C for longer than 24 hours and weighed by using the balance with accuracy of ± 0.002 gr. For simplicity, water content was represented with the density of the sediments, i.e.,

$$\rho = \frac{1 + W}{1/\rho_s + W}$$

where ρ_s and ρ are the density of the solid and the sediments. In this paper, ρ_s is assumed to be 2.6 gr/cc.

3. Origin of the remanence of the centrifuged sample

The susceptibility anisotropy and the remanent direction of centrifuged sample were measured with a spinner magnetometer. Samples were made by using the Type I centrifuge rotated at 3,000 rpm, corresponding to the acceleration 750 times as large as that of the gravity, for thirty minutes. The ambient field was the geomagnetic vertical component field around the apparatus (strength 0.34 Oe).

The susceptibility ellipsoids of specimens made from the deep-sea sediments were of a type similar to those previously found in natural and laboratory-deposited sediments by Rees (1965) and Løvlie et al. (1971). The value of the q parameter in almost all samples were smaller than 0.67. The minimum axis lay uniformly on the locus of acceleration which changed from vertical (direction of gravity) to horizontal. The lake sediments, however, had the weak susceptibility and produced measurement data unreliable.

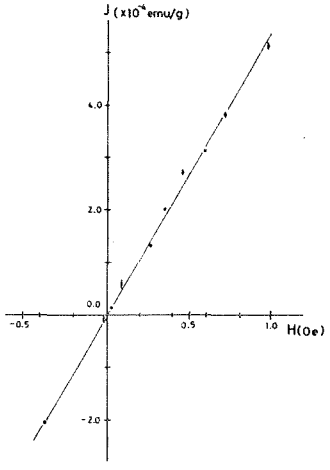

Fig. 2d

The remanent direction agreed reasonably well to that of the control field and well grouped in both sediments. The remanence acquired was of a stable type. Only 8% of remanence in the lake sediments and 20% in deep-sea sediments were randomized by AF demagnetization of 100 Oe. Alternating field demagnetization curves of individual specimens showed median destructive fields around 300 Oe in the lake sediments, accompanying with direction

Fig. 2 Results of the anisotropy and the remanence of the specimens made from the GDP-11-16 ooze. (a) Orientation of minimum (closed circle) and maximum (triangle) axes. The orientations of the initial acceleration (G) and the magnetic field (H) is vertical and the orientation of the final acceleration is shown by the arrow. (b) Distribution of the parameter q. (c) Orientation of the remanence. (d) Intensities of the control field and the remanence.

Table 1

	Remanence	Anisotropy Minimum axis
N	14	25
Decli.	240.4°	275.1°
Incli.	86.5°	35.1°
α_{95}	2.5°	5.6°

changes within the error of measurements. The NRM of the core from the Lake Biwa (Yaskawa et al. 1973) and the remanence of the reconstructed sediments showed similar behavior in the demagnetization curve and the median destructive field. The remanent intesities of both sediments were lineally proportional to the magnitude of control fields, at least up to 1.05 Oe. This relationshop was held also in the experiments under an inversed magnetic field. These results are shown in Fig. 2 and Table 1.

As mentioned above, the remanent properties of the sample made up with the centrifuge agree well with the results of laboratory-deposited experiments previouly done by many workers (Kent, 1973; Rees, 1965 and others) on the magnetic fabric and the remanence. There remain, however, possibilities that the centrifuged sample may acquire an ARM (anhysteretic remanent magnetization) and/or a RRM (rotational remanent magnetization, Wilson and Lomax, 1974), because the magnetic field environment in our experiment is quite similar to those in the acquisition of the ARM and/or the RRM; as for the rotation coordinate system, the horizontal component of the geomagnetic field acts of the sample as AC magnetic field and the vertical component as DC field. But similar experiments proved no production of remanence in the dried up sediments. In the other words, the considerable water content was necessary for the specimen to acquire a definite remanence by the centrifuging. Therefore the remanence acquired in this experiments cannot be ascribed to the ARM or the RRM but to DRM and/or post-DRM.

There is a significant difference between the directions of the anisotropy minimum axis and the remanence by 51.4 degrees. This difference suggests that the time of fixation of the magnetization is not coincident with the time of fixation of the anisotropy; i.e., the former occurs at the later stage from the

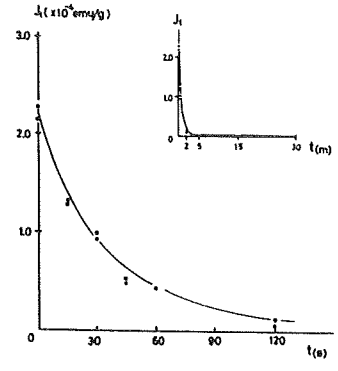

Fig. 3a

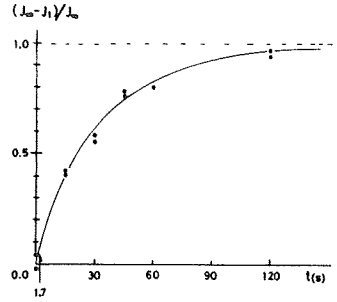

Fig. 3b

Fig. 3
(a) Relationship between J_{t_0} and t_0.

(b) Relationship between $J(t_0)$ and t_0.

beginning of the rotation than the latter. It took only 1.7 seconds from the beginning of the rotation until the direction of the acceleration had reached that of the anisotropy minimum axis. This means that the major part of carrires of the anisotropy cannot rotate after 1.7 seconds. The magnitude of the remanence acuired after the fixation of anisotropy can be estimated by this fixation time and by the following experiment.

Experiment

After the deep-sea sediment slurry (density = 1.18) was poured into cylinder of centrifuge (Type II), it was compacted by rotation for thirty minutes with the acceleration 750 times as large as the gravity.

The magnetic field around the apparatus was controlled at zero field from the beginning of the rotation to the given time (t_0), then the magnetic field was applied at a constant value of 0.34 Oe; that is,

$$H = 0 \text{ Oe} \qquad 0 \leqq t \leqq t_0$$
$$H = 0.34 \text{ Oe} \qquad t_0 < t \leqq 30 \text{ min} \quad .$$

The remanence acquired in such field condition is denoted by J_{t_0}, e.g., J_0 represents the remanence acquired in the constant field 0.34 Oe from the beginning to the end of the centrifuging. The result is shown in Fig. 3a.

Using this J_{t_0}, the processes acquiring the DRM and/or post-DRM intensity can be determined by a function of the time t_0, that is,

$$J(t_0) = (J_0 - J_{t_0}) / J_0 \quad .$$

Because the $J(t_0)$ is considered to be the relative magnitude of the remanence acquired in the following field condition,

$$H = 0.34 \text{ Oe} \qquad 0 \leqq t < t_0$$
$$H = 0 \text{ Oe} \qquad t_0 \leqq t \leqq 30 \text{ min} \quad .$$

So the $J(t_0)$ means the relative magnitude acquired from the beginning to time t_0. The relationship between $J(t_0)$ and t_0 is shown in Fig. 3b. Taking into consideration of this result and the fixation time of the anisotropy (illustrated by the arrow in Fig. 3b) , it seems likely that only 5% of the remanence was acquired until the fixation of the anisotropy had completed.

Stupavsky et al. (1974) suggested that the fine magnetic particles (<37μ) were free to align themselves in the ambient field whereas the coaser material (>37μ) was not significant aligned. If the movement of the carrirer of the anisotropy represents that of the non-magnetic particles whose size is more than 37 microns, 95% of the remanence may be acquired after the fixation of the most portion of particles. In the other words, the remanence acquired in our experiments is almost post-depositional origin. Therefore the experimental apparatus utilizing the centrifugal force can be expected to provide successfully the post-depositional remanence

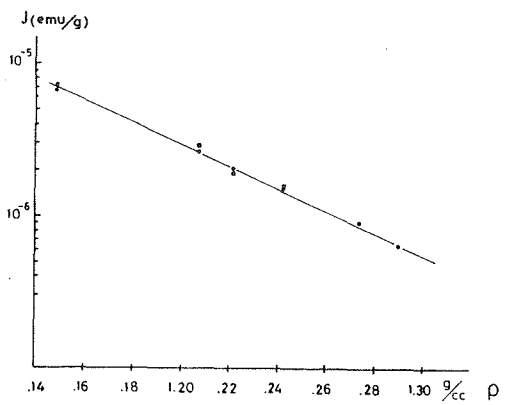

Fig. 4 Remanent intensity acquired between the densiy states from ρ to the final density (ρ_{fin} = 1.30)

without suffering from the remanence effects caused by the drying.

4. Note on the experimental results of post- DRM

Experiments are now in progress and the following properties have been found out until now. Details and discussion will be reported in the near future.

(1) The field dependency of the remanent intensity

As shown in the previous section, the intensity is lineally proportional to the intensity of the ambient field, at least up to 1.05 Oe.

(2) Fixation of the remanence

Fixation of the remanence of wet deep-sea sediments associated with the time was already shown in Fig. 3. By the use of the centrifuge (Type II), the fixation of the remanence of lake sediments was investigated. In this case, variation of the acquisition of the remanence was shown as a function of the density corresponding to the time at which a certain ambient field was applied; i.e., the following field control was operated,

H = 0 Oe from initial density (1.15) to a certain density ρ,

H = 0.34 Oe from ρ to final density (1.30).

Table 2

	Intensity
$J(0 \leq t \leq 200)$	3.97
$J(0 \leq t < 10)$	2.82
$J(10 \leq t \leq 200)$	1.09
$J(0 \leq t < 10) + J(10 \leq t \leq 200)$	3.91

Intensities in units of 10^{-5} emu/gr (dried up weight).

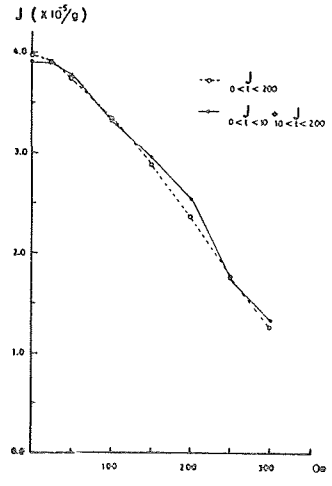

Fig. 5 Demagnetization curves of $J(0 \leq t \leq 200)$ and $J(0 \leq t < 10) + J(10 \leq t \leq 200)$.

The acquisition of the remanence illustrated in Fig. 4 seems to decrease in increase of specimen density. This result seems to be plausible, because the increase in density may decrease the freedom of magnetic particles to rotate interstitially among the already fixed grains. At the present stage, it is noted that the acquisition of the remanence is found to decrease exponentially with the increase in density.

(3) Additive property of partial post-DRM

If, during compaction, field applied only a time interval between t_1 and t_2, we define the component as the partial post-DRM. Using with the centrifuge (Type II), three remanences were formed by varing the time interval of aplication of the field, 1) from the beginning of rotation to 10 min. $[J(0 \leq t < 10)]$, 2) after 10 min. up to 200 min. $[J(10 \leq t \leq 200)]$, and 3) from the beginning to 200

min. [J(0≦ t ≦200)]. Results obtained are shown in Table 2 and Fig. 5. Whithin the error of measurement, J(0≦ t ≦200) was expressed as the sum of J(0≦ t <10) and J(10≦ t ≦200), i.e.,

$$J(0 \leqq t \leqq 200) = J(0 \leqq t < 10) + J(10 \leqq t \leqq 200) \quad .$$

And remanence of J(0≦ t ≦200) and the sum of J(0≦ t <10) and J(10≦ t ≦200) were similar in each other in their demagnetization behavior. Therefore the total post-DRM could be equal to the sum of the partial post-DRM acquired in each consecutive compaction stage. This relation suggests that the depositional remanence once fixed in sediments cannot be easily randomized in further compaction.

(4) Change in magnetization with compaction speed

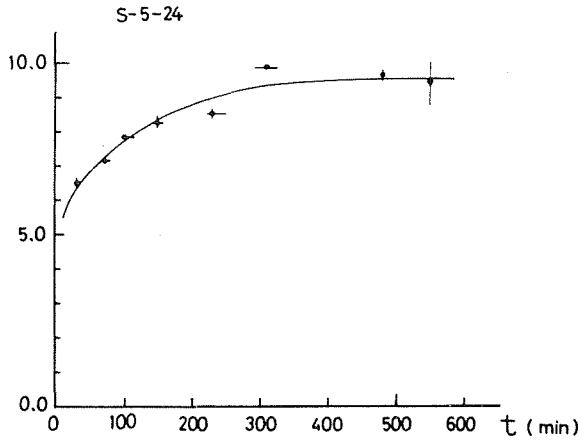

Fig. 6

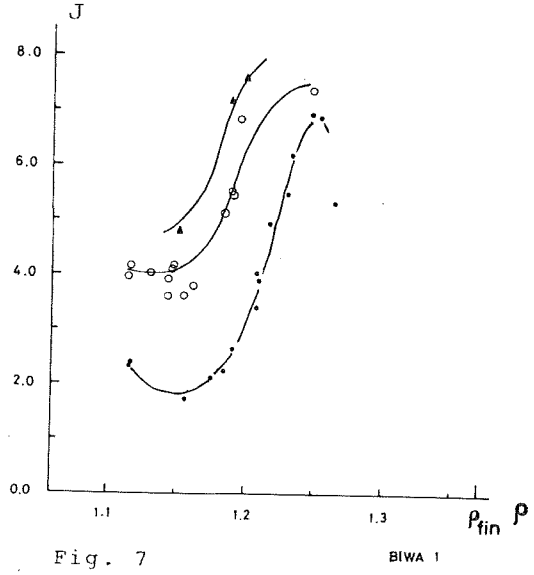

Fig. 7

Various compaction speeds can be easily obtained by changing the rotational speeds of the centrifuge. The remanence intensity was shown as a function of the requiring time in which the sediments had been compacted from the initial density state (ρ =1.12) to the final state (ρ =1.25). The results show that the remanent intensity is attained in its saturation state after a longer time interval, say about 400 min. As in actual sediments the compaction rate must be much slower than that of this experiment, the remanence intensity of actual sediment may not be considered to be influenced by the compaction rate. However, this straightforward supposition cannot be ensured yet,

Fig. 6 Relationship between the remanent intensity and the requiring time to compact the sediments to the final density state.

Fig. 7 Relationship between the remanent intensity and the initial density. Magnitude of the ambient fields are 0.34 Oe (closed circle), 0.68 Oe (open circle), and 1.02 Oe (triangle).

because the following strange phenomenon was discovered.

(5) Strange phenomenon in magnetization

As shown in (2), the remanence was fixed with increasing in the density of the specimen. So the following experiment was carried out to confirm the fixation in detail.

Experiments

The lake sediments slurry initialy poured into the cylinder was varied in *its density* and these were compacted into the same final density (ρ =1.37). It is needless to say that the rotational speeds and the ambient field intensity were always kept constant.

We are tempted to deduce from the result(2) that if the initial density value is higher, the remanent intensity acquired may be smaller. But the results betrayed our presumption. As shown in Fig. 7, the intensity increases abruptly as the initial density being increased and it is found to have the maximum intensity at the initial density value 1.24 gr/cc. Such a phenomenon is also observed in deep-sea sediments.

At the present, we cannot explain this phenomenon by any model. We are urgent to investigate thoroughly the cause of this phenomenon.

References

Irving, E. and A. Major (1964) Sedimentology 3, 135.

Johnson, H. P., H. Kinoshita and R. T. Merrill (1975) Geol. Soc. Amer. Bull. 86, 412.

Kent, D. V. (1973) Nature 246, 32.

Løvlie, R., W. Lowrie and M. Jacobs (1971) Earth Planet. Sci. Lett. 15, 157

Løvlie, R. (1974) Earth Planet. Sci. Lett. 21, 315.

Nagata, T., Y. Harada and K. Hirao (1945) Bull. Earthq. Res. Inst. 23, 79.

Rees, A. I. (1965) Sedimentology 4, 257.

Stupavsky, H., D. T. A. Symons and C. P. Gravenor (1974) Geol. Soc. Amer. Bull. 85, 141.

Wilson, R. L. and R. Lomax (1974) Geophys. J. R. astr. Soc. 30, 285.

Yaskawa, K., N. Nakajima, M. Torii, N. Natsuhara and N. Kawai (1973) J. Geomag. Geoelet. 25, 447.

Yaskawa, K. (1974) Rock Mag. Paleogeophys. 2, 15.

CONSOLIDATION PROCESS IN THE MAGNETIZATION OF ARTIFICIAL SEDIMENTS

Yozo HAMANO

Geophysical Institute, University of Tokyo
Bunkyo-ku, Tokyo 113

1. Introduction

Remanent magnetization possessed by deep-sea sediments has provided a useful information about the record of reversals of the earth's magnetic field. But the mechanism by which these sediments acquired their natural remanent magnetization is not fully understood yet. Recent studies in experiments and observations have shown that the mechanism is a complex phenomena and suggested an importance of a post-depositional process (e.g. Kobayashi et al.,1971; Kent,1973). It is my purpose in this paper to show results of experiments in which I investigated how the remanent magnetization in sediments are acquired while they are being consolidated.

2. Experiment and results

A sketch of the apparatus employed in the present study is given in Fig. 1. This apparatus was designed to consolidate sediments in a magnetic field of known direction and strength. The field is controlled by a helmholtz coil system, where the coil cancels out the ambient geomagnetic field and generates a constant field around the sample site. The field strength was 0.5 oe in a vertical direction through the present study. The pressure to consolidate sediments is exerted by water in a water tank. The tank is placed on the top of the sample system and is counter-balanced when it is empty. Pressure increases linearly from zero as water is poured into the tank with a constant rate.

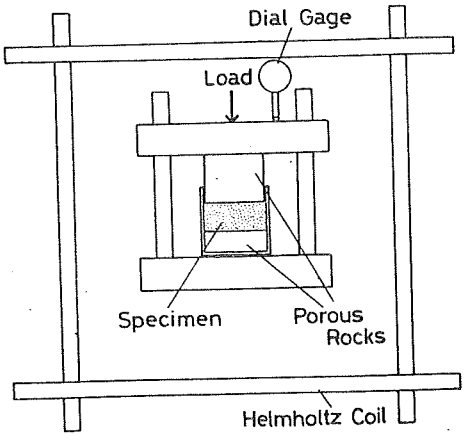

Fig.1 Apparatus to consolidate sediments in a controlled magnetic field.

The synthesized sediments were prepared by mixing magnetite and non-magnetic talc powder with a ratio of 1/200 by weight. The grain diameter of magnetite is about 0.1μ and that of talc ranges from 10μ to 50μ. For each run of the present experiment, a constant amount of the prepared sediments was saturated with distilled water, and then held between two porous rocks inside a plastic tube. The tube prevents the specimen from collapsing. As pressure

exerted on the specimen increases, water in the specimen flows out through the porous rocks, and the specimen is gradually consolidated. Volume change of the specimen during the consolidation process was measured by a dial gage attached on the top of the sample system. Void ratio, which is defined as a ratio of a void volume in the specimen to the rest of the volume occupied by solid grains, has been commonly used to indicate a degree of consolidation. This ratio can be calculated from the observed sample volume and the known densities of talc and magnetite.

In general the volume is a function of a pressure and a loading rate. But if the rate is slow enough, the volume depends on the pressure only. Water flow through the specimen and the porous rocks determines the critical rate. A loading rate smaller than the critical value was employed in the present study to avoid disturbance of the specimen. The rate was about 1.0 bar/hour. The variation of the void ratio with that of the exerted pressure is shown in Fig. 2, where the results for mica and talc powder with a different grain diameter are also shown. Initial value of the void ratio in the present specimen is about 1.85, and the ratio decreases as pressure increases.

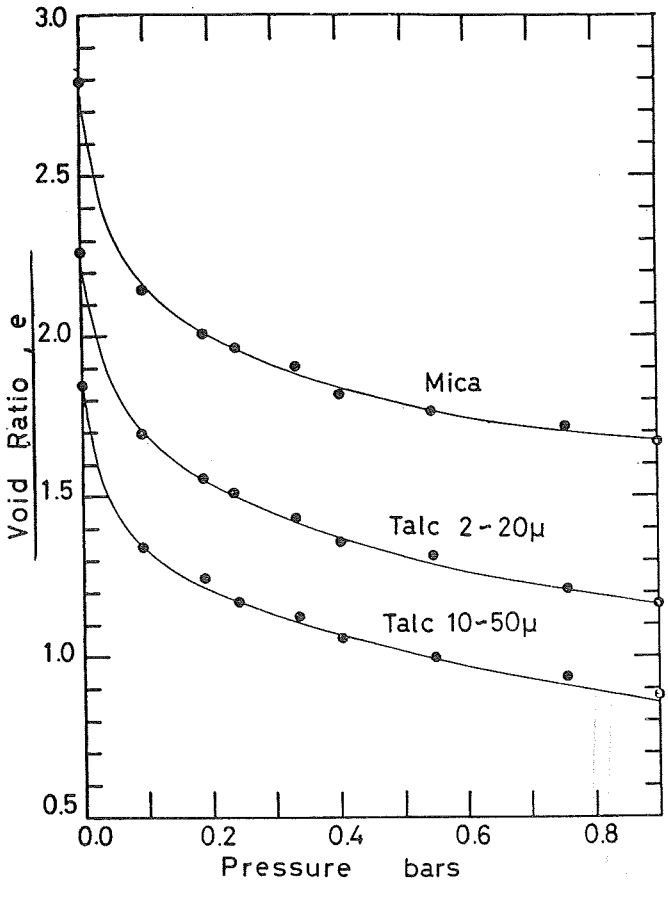

Fig.2 Consolidation curves for some synthesized sediments.

Measurements of the remanent magnetization were made for the specimens with the same void ratio e_o (=0.88), which corresponds to a exerted pressure of about 0.9 bar. The specimen with this void ratio was well consolidated so that the measurement by a spiner magnetometer was possible without disturbing the magnetization. An ambient magnetic field was kept zero while the void ratio of the specimen decreases from the initial value to a value of e_1, and then a constant field with a intensity of 0.5 oe was applied. The void ratio e_1 varies for each specimen. After the void ratio attained to the final value e_o, the specimen was taken out of the apparatus. Then

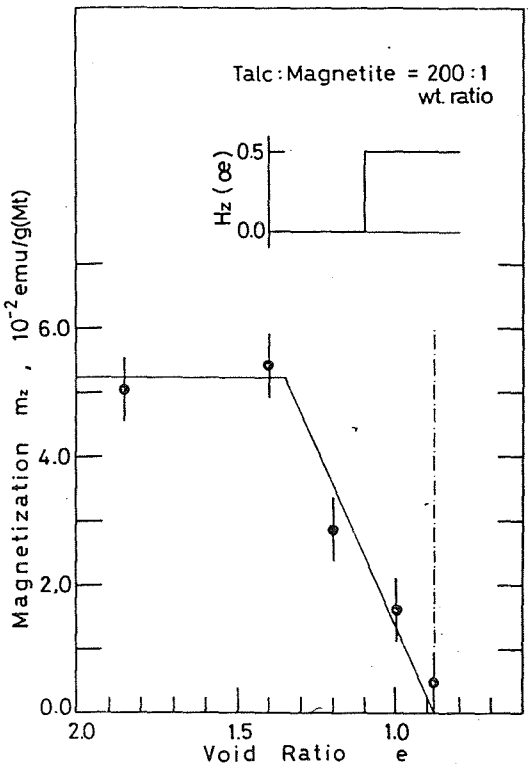

Fig.3 Remanent magnetizations for consolidated specimens.

it was sealed by silicon rubber to avoid a further water-loss, and the remanent magnetization was measured by a spinner magnetometer. The observed magnetization is the remanence acquired while the void ratio decreases from e_1 to e_0. The remanent magnetization as a function of the void ratio e_1 is shown in Fig. 3, where the magnetization is normalized to a unit mass of magnetite contained in the specimen. A decrease of the magnetization with that of the void ratio is evident from the figure. This will be discussed in a later section.

The remanent magnetization is of a stable type. Re-measurements were made after the specimens had been kept in an approximately zero magnetic field for about two weeks. The obtained values were within 5% of the first measurements. The stability is also shown by the results of demagnetization in alternating magnetic field. Demagnetization curves for these specimens are given in Fig.4. These curves are similar one another and show a stable character of the remanence. In order to examine the origin of the stability, one specimen was prepared by using gypsum powder in place of talc. The specimen mixed with water was kept in a known magnetic field until it solidified, and then taken out for magnetic measurements. AF demagnetization curve for this specimen are also shown in Fig. 4 with a dotted line. Because a rotation of magnetic grains in this specimen is essentially impossible, the demagnetization curve should be caused by a rotation of magnetic moments within the grains. The similarity of other demagnetization curves to this one suggests that the rotation of magnetic grains in consolidated sediments is also prevented by adjacent grains.

3. Discussions

In the previous section the remanent magnetization acquired during a consolidation process of artificial sediments were examined. The result can be interpreted by analogy with an established theory of TRM (e.g. Neel,1949). Remanent magnetization arise when distributed magnetic moments change from

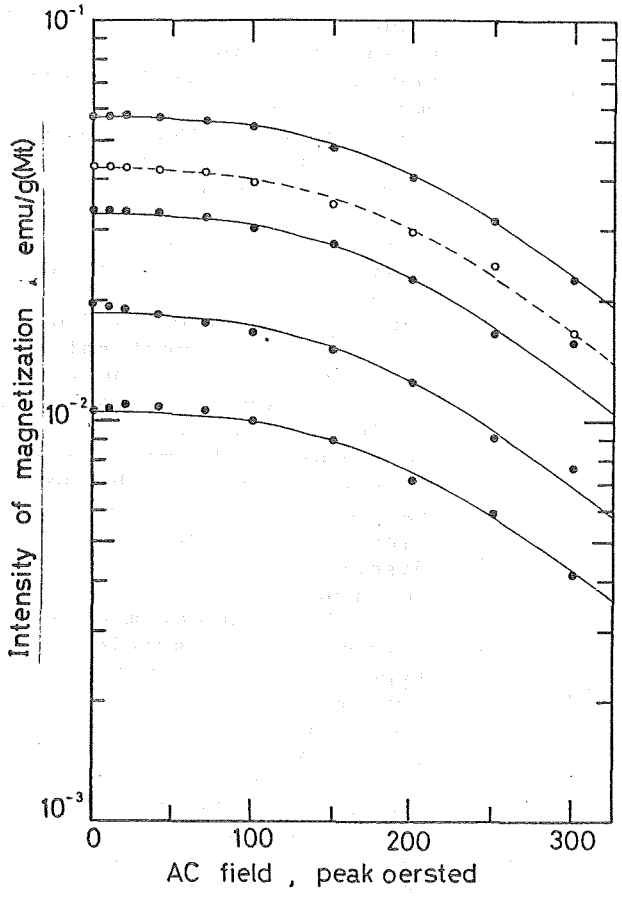

Fig.4 Demagnetization curves for specimens magnetized during a consolidation process.

a free state to a bound state. In the theory of TRM, a decrease of temperature causes this change of state. Due to a distribution of the blocking temperature, the remanent magnetization observed at room temperature is a sum of the remanence acquired during each step of the temperature decrease. In the remanence of consolidated sediments, the void ratio plays the same role as temperature in TRM. A decrease of the void ratio corresponds to that of temperature.

Each magnetic grain becomes unable to follow an ambient magnetic field when the bulk void ratio of the specimen decreases to a certain value. It is reasonable to assume that this 'blocking' void ratio is distributed within a range due to distributions of a grain size and a void volume for each magnetic grain. Then, if a constant magnetic field is applied when the void ratio decreases to e1, some magnetic grains fixed before this stage do not contribute the remanent magnetization. The decrease of the remanent magnetization observed in Fig.3 can be explained by this mechanism.

A spectrum of the 'blocking' void ratio depends on grain sizes and shapes of constituents in sediments. Re-consolidation experiment on natural sediments seems helpful to investigate the origin of the natural remanent magnetization.

4. References

Kent,D.V.(1973) Nature,246,32
Kobayashi,K. et al.(1971) Deep-Sea Res.,18, 1045
Neel,L.(1949) Ann. Geophys., 5,99

ZONE-MAGNETIZATION MODEL AND DEPTH LAG OF NRM IN DEEP-SEA SEDIMENTS

Nobuaki NIITSUMA

Department of Earth Sciences, Tohoku University
Kawauchi, 980 SENDAI, Japan

The depth lag for the fixation of remanent magnetization in deep-sea sediments has been examined, using a zone-magnetization model. The model has been developed from the study of deep sea sediment core B 21-2 which was taken from the Nazca Ridge, southeastern Pacific (17°05'S, 77°34'W).

Paleomagnetism was measured continuously along the length of the core using the cryogenic magnetometer of the University of California, Santa Barbara. The measured value was read at 1 cm interval. NRM and after partial AF demagnetization of 100, 200 and 500 Oe, and ARM made under earth magnetic field and 700 Oe alternative field, were measured. The intensity and direction of remanent magnetization were calculated by the deconvolution program (Dodson and others, 1977).

The remanent magnetization of this core was very stable. The difference among NRM and after 100 Oe AF demagnetization was 10% and among 100 and 500 Oe was a few % in intensity. The intensity range of remanent magnetization after 200 Oe is between 2×10^{-5} and 2×10^{-7} emu/cc, the range for ARM is between 2×10^{-2} and 2×10^{-4} emu/cc. This core has 5 magnetic polarity reversal horizons and one so-called excursion horizon (Fig. 1). Using ARM intensity data, we can divide this sediments into two sections whose boundary is located at 500 cm below the surface. In the upper section, the intensity of ARM shows changing more than 1 order of magnitude of variation, while, in the lower section, the intensity is almost constant. The reversal horizons are located in the lower section. The intensity of NRM after 200 Oe AF demagnetization, shows a very good correlation with the intensity of ARM generally (Fig. 1). Six intervals where the intensity of NRM curve shows a V-shaped change were found as shown in Fig. 1. In these six intervals, four correspond to the magnetic reversal horizons, and one is located on the so-called excursion horizon. The intensity of NRM decreases 1 to 2 orders of magnitude near the reversal horizons. The pattern of intensity change assumes a V-valley shape at every reversal horizon. The width of the V-valley is approximately 30 cm.

Such type of intensity change in NRM of deep-sea sediments has also been noted earlier by several investigatores (Ninkovich and others, 1966; Kobayashi and others, 1971; Opdyke and others, 1973; Kawai and others, 1976). In order to explain such characteristics of intensity variations in deep-sea sediments, two magnetization models can be introduced; one is a plane-magnetization model, and the other is zone-magnetization model (Fig. 2).

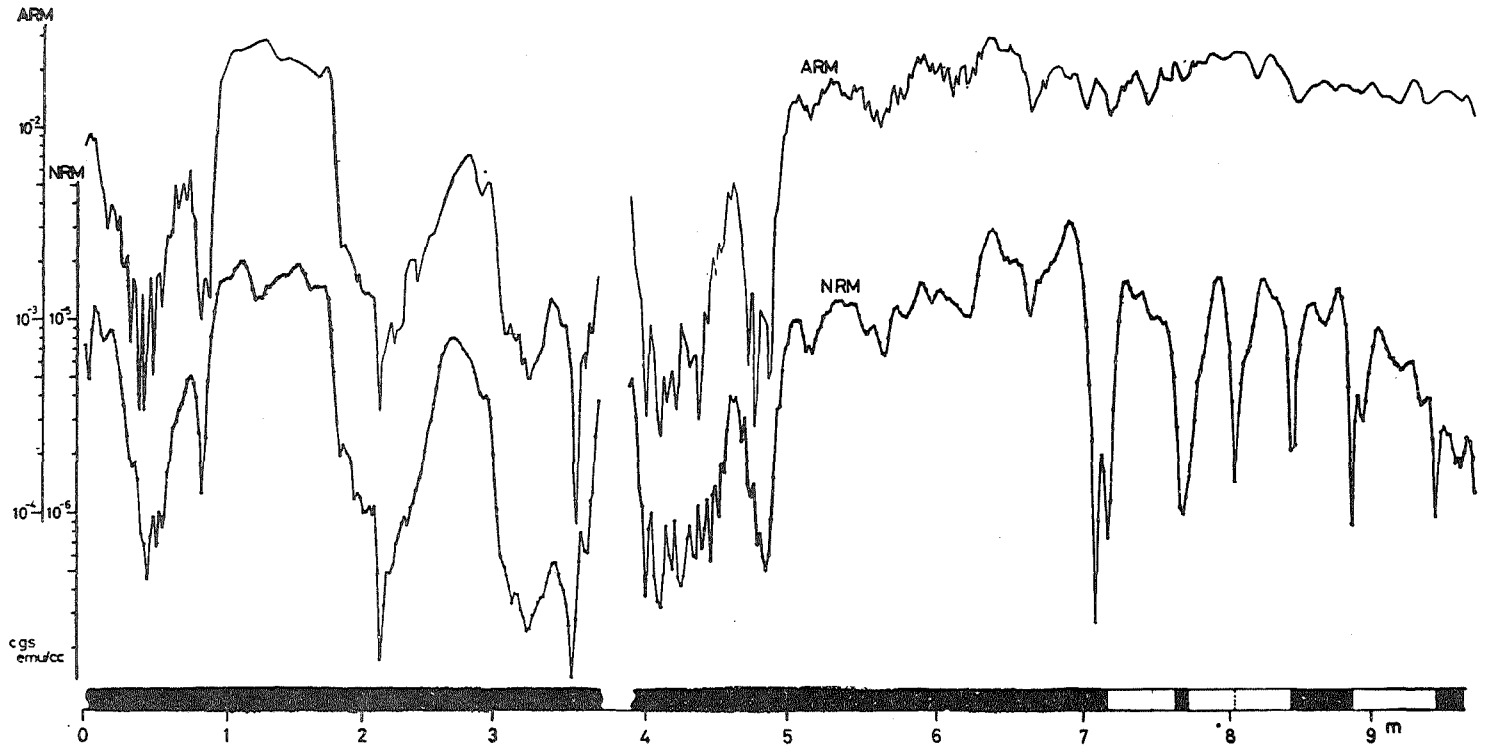

Fig. 1 Paleomagnetic results of deep-sea core B21-2.
NRM: remanent magnetization after 200 Oe AF demagnetization
ARM: made under earth magnetic field and 700 Oe AF.

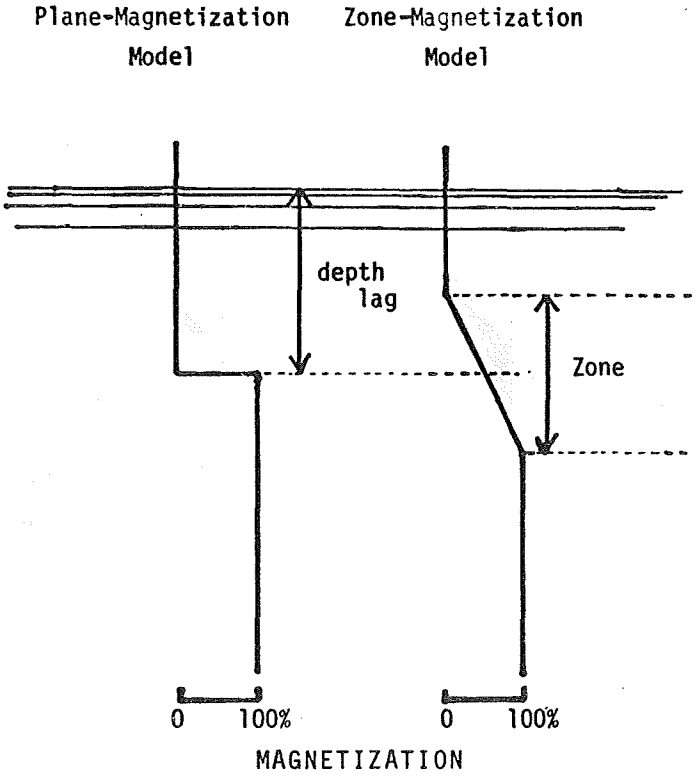

Fig. 2 Two magnetization models for explaining the remanent magnetization in sediments.

In plane-magnetization model, 100% fixation of remanent magnetizationoccures on a plane. In the zone-magnetization model, magnetization is locked gradually within a finite thickness of sediments. The plane magnetization model can be treated as a special case of the zone-magnetization model in which the thickness of the zone is zero. It is possible to have several variations of the zone-magnetization model, corresponding to several different modes of proportion of locked remanent magnetization with depth. The simplest one is that the lock-in of remanent magnetization increases linealy with depth.

If it can be assume in the linear zone-magnetization model that 1) the thickness of the zone is constant (=a), 2) content of magnetic material in the sediments is constant, 3) Earth's magnetic field had only two direction (normal and reversed polarity) and the strength was same or time interval during which intensity drop accompanied with reversals is short enough when compared with the time interval corresponding to the same thickness of the magnetization zone, and 4) the rate of sedimentation was constant (=R), we can consider the direction and intensity of remanent magnetization during a short magnetic polarity event whose time interval is notated as b (Fig. 3);

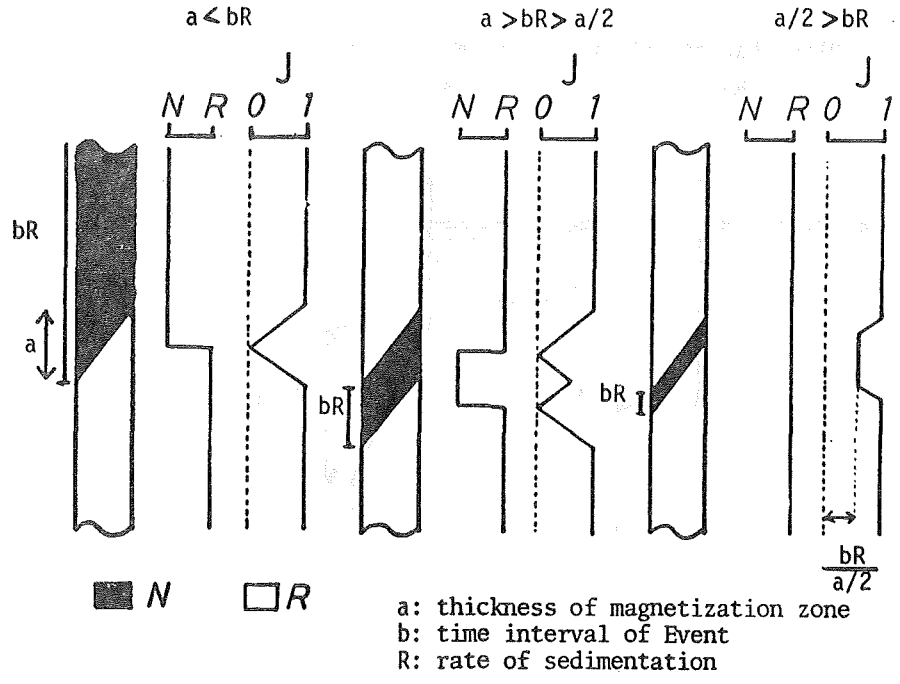

Fig. 3 The direction and intensity (J) of remanent magnentization during some events. N: normal, R: reversed polarity direction.

1) $a < bR$: we can find a reversal at end of the polarity event, and this event has a V-shapec intensity drop at the boundary.
2) $a > bR > a/2$: we can find a polarity event, but we cannot find a true intensity any longer.
3) $a/2 > bR$: we cannot find any kind of excursion and reversal. We can only find the intensity drop. The amount of decrease in intensity of remanent magnetization is equal to $2bR/a$.

It is easy to find exapmles of this kind of intensity change of NRM in many reported cores. The thickness of the magnetization zone should be equal to the width of the intensity drop interval. In core B21-2, this width is about 30 cm.

Opdyke and others (1973) reported similar intensity changes at reversal horizons in the Indian Ocean core RC14-14. The thickness of the intensity drop intervals they observed is about 40 cm. Since the sedimentation rate of core RC14-14 is ten times faster than that of core B21-2, it is difficult to explain the intensity drop by the plane-magnetization model. Rather, these results show that the thickness of the zone is 30-40 cm, and the linear zone-magnetization model seems to be suitable in this case.

If the zone-magnetization model could be accepted for the

explanation of NRM in deep-sea sediments, there should be the depth lag which is larger than one half of the thickness of the magnetization zone. The depth lag is important not only for the consideration of the magnetization mechanism of sediments, but also for comparison of the magnetostratigraphic horizons with the biostratigraphically or Oxygen-isotope stratigraphically dated horizons. If we could determine the ages of sediments (=t) which records magnetic reversal, and with different rates of sedimentation, we can calculate the depth lag, as follow;

$$t = \frac{d}{R} + t'$$

t': true age of the magnetic reversal
d : thickness of depth lag
R : rate of sedimentation

This equation shows that if we plot the age of sediments in which magnetic recersal is recorded against the reciprocal rate of sedimentation, all points should be arranged on a line in the case of constant d. For this calculation, Oxygen-isotope stratigraphy should be useful, because the Oxygen-isotope ($\delta^{18}O$) changes mainly reflect ice volume changes on the Earth, which has periods of about 100 ky.

Fig. 4 shows the results of isotopic measurements of B21-2 core. There are available several sediment cores whose magnetostratigraphy and Oxygen isotope stratigraphy are known, reported by Shakleton and Opdyke (1973, 1976), van Donk (1976), and Oba (MS).

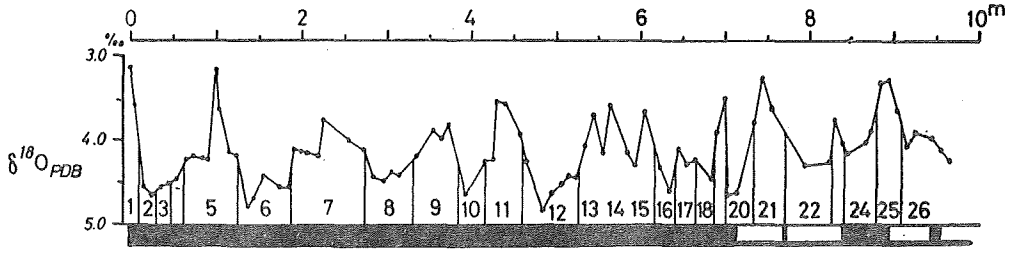

Fig. 4 Oxygen isotope stratigraphy and magnetostratigraphy of B21-2.

In Fig. 5, the apparent ages for the Brunhes-Matuyama Polarity Epoch boundary, marked as cross, can be calculated using oxygen isotope stratigraphy, and plotted aginst the reciprocal rate of sedimentation for those cores, as shown in Fig. 6. In this graph, the averaged normalized thickness (present is 0 and boundary between Stage 22 and 23 coresponds to be 1000) is used as age. These plots give a linear relationship and the correlation coefficent is 0.93. The equation of the line is;

$$t = \frac{39.9}{R} + 827$$

This equation gives us the thickness of the depth lag to be 39,9 cm and the magnetic reversal between Brunhes and Matuyama

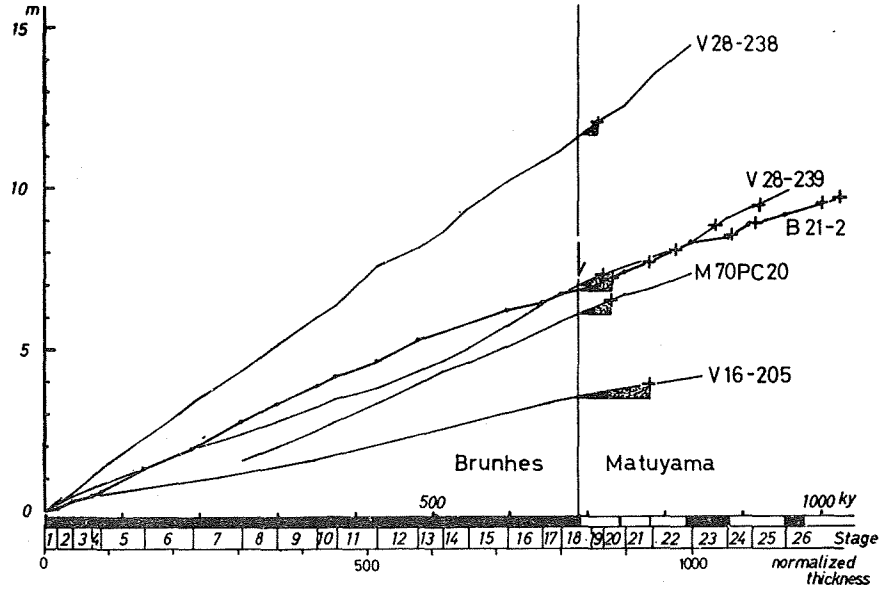

Fig. 5 Oxygen isotope stratigraphy of several cores. Vertical axis: depth of core sediments in m. Horizontal axis: age, averaged normalized thickness, division by oxygen isotope stratigraphy, and magneto-stratigraphy. Cross: magnetic reversal horizons. Dotted triangle: correspond to the calculate depth lag. V28-238 (Shakleton and Opdyke, 1973), V28-239 (Shakleton and Opdyke, 1976), M70PC20 (Oba, MS), V16-205 (van Donk, 1976).

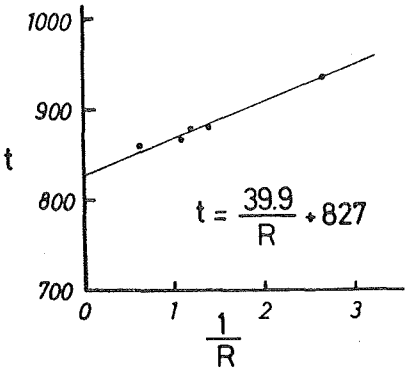

Fig. 6 Plotting of apparent age for the Brunhes-Matuyama boundary against the reciprocal rate of sedimentation for several cores (Fig. 5).

occured at 827 of the averaged normalized thickness.

The mechanism of magnetization in deep-sea sediments should be related to mechanical properties such as bulk density of the sediments. Generally such properties will change with depth in the core due to overburden pressure. The bulk density data derived from in situ measurements by Preiss (1968) showed that major changes in bulk density appeared in the interval between 20 and 60 cm deep in the core, he studied. This observation agrees well with the zone-magnetization model which depicts a thickness of 30-40 cm for the zone, with a depth lag of 40 cm.

References

Dodson, R.E., Fuller, M.D., and Kean, W.F. (1977) Earth Planet. Sci. Lett. 34, 387.
Kawai, N., Otofuji, Y., and Kobayashi, K. (1976) J. Geomag. Geoelectr. 28, 395.
Kobayashi, K., Kitazawa, K., Kanaya, T., and Sakai, T. (1971) Deep-Sea Res. 18, 1045.
Ninkovich, N., Opdyke, N.D., Heezen, B.C., and Foster, J.H. (1966) Earth Planet. Sci. Lett. 1, 476.
Oba, T. (MS) M70PC20 was taken from 14°40'S, 177°12'W, and 2840m.
Opdyke, N.D., Kent, D.V., and Lowrie, W. (1973) Earth Planet. Sci. Lett. 20, 315.
Preiss, K. (1968) Deep-Sea Res. 15, 637.
Shakleton, N.J., and Opdyke, N.D. (1973) Quaternary Res. 3, 39.
---------- (1976) Geol. Soc. America Mem. 145, 449.
van Donk, J. (1976) Geol. Soc. America. Mem. 145, 147.

ON NATURAL REMANENT MAGNETIZATION OF HISTORICAL LAVA AT SAKURA-JIMA KAGOSHIMA, SOUTHERN KYUSHU ISLAND, JAPAN.

Haruo DOMEN and Hiroshi MUNEOKA

Institute of Physical Sciences, Faculty of Education,
Yamaguchi University, Yamaguchi 753, Japan.

One of the historical lava flows at Sakura-Jima in Kagoshima, south end of Kyushu Island, west Japan was attacked and twenty six rock samples were sampled for a purpose of paleomagnetic study. And these NRM were measured by means of an astatic magnetometer.

The mean NRM direction thus obtained is as follows;

$$D(E)^* = +10°, \quad I(D) = +22°, \quad \kappa = 39, \quad \alpha = 5°$$

* measured from the astronomical north.

However these samples submitted to the magnetic measurement were collected from several spots which are not so closely located each other and from an observation with nacked eyes in the field, those seem rather randomly oriented *in situ* with some disturbances at the time the lava was flowed, those NRM directions are rather well concentrated as has been seen above.

The questioned lava flow was erupted in the early Taisho Era (AD 1912 -1926) as the lava flow is so called "Taisho 1st lava flow". But, so far as the present study is concerned, the mean direction of NRM obtained does not coincide with that of the value already known during this era; that is, the geomagnetic field declination was westwards and the inclination was deeper than +40° (Kawai and Hirooka 1967, Kawai et al 1967, Watanabe 1959, Yukutake 1961, Yukutake et al 1964).

The magnetic stability test on these samples is now being studied.

References.

Kawai, N. and K. Hirooka (1967) J. G. G. 19, 217-227.
Kawai, N., K. Hirooka, K. Tokieda and T. Kishi (1967) 1967 Annual Progress Report of Paleogeophys. Res. in Japan 81-85.
Watanabe, N. (1959) Jour. Faculty of Sci., U. of Tokyo, Sect. V, 2, 1-188.
Yukutake, T. (1961) Bull. Earthq. Res. Inst., U. of Tokyo 39, 467-476.
Yukutake, T., K. Nakamura and K. Horai (1964) J. G. G. 16, 183-193.

DETERMINATION OF GEOMAGNETIC PALEOINTENSITIES FROM THE HISTORICAL LAVA FLOWS OF HAWAII

Naoko UENO and Masaru KONO

Natural Science Laboratory, Toyo University, Hakusan, Bunkyo-ku, Tokyo 112 and Geophysical Institute, University of Tokyo, Bunkyo-ku, Tokyo 113, Japan

In a previous report (Kono and Ueno 1975), it was found that the modified Thellier method gives satisfactory result to some Hawaiian basalt and rhyolite of San Luan Volcanics. In the present experiments, the improved modified method by adding occasional zero field heating to test the reproducibility of PTRM was used for 12 historical lava flows of Hawaii. Comparison of the results were made with other authors' and direct observatory data.

31 specimens cylindrical 2.5 cm in diameter by 2.3 cm long were cut from 12 lava flows. Stability of the direction of NRM of each lava flow were convinced by AF demagnetization. It can be assumed that the direction of NRM of them are not change much in thermal demagnetization process. Specimens divided into three groups were set in sample holder made of cupper such as NRM vector being in a plane perpendicular to the furnace tube. They were heated and cooled under the magnetic field of 0.5 Oe applied parallel to the furnace set inside a permalloy shield. Experiments were carried out for one group with low Curie temperature from room temperature at intervals of 30 degree. Others were started at intervals of 50 degree after eliminating the secondary component by heating up to 100 degree in non-magnetic field. To reduce the chemical change N_2 atomosphere was used over 200 degree. Remanent maghetization at each temperature were measured by spinner magnetometer.

Calculations were done to separate remanence to NRM and TRM which made orthogonally each other. The typical example of the result is given in Fig. 1. Open circle represents the remanent magnetization in applied field, cross indicates the remanence in non-magnetic field. Solid circle corresponds to the repeating step in applied field after the experiment has proceeded in non-magnetic field. Cross on the NRM axis indicates that the PTRM added previously has completely been eliminated. Ideally, open circle and solid circle at the same temperature lie on the vertical line, and open circle and cross lie on the horizontal line. The slope of the open circles represents the ratio of the ancient intensity of the geomagnetic field to the intensity of the artificial field.

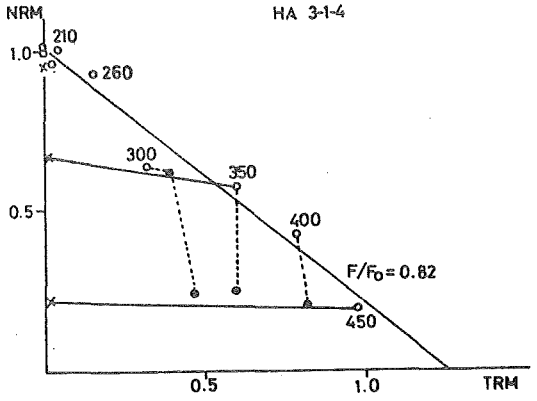

Fig.1. An example of the results of the modified Thellier method. open circle=remanence in applied field; cross=remanence in non-magnetic field; solid circle=remanence in repeated applied field.

In the modified Thellier method, stability of the direction of NRM is the essential condition. Fig.2 shows the small change of the NRM direction through the present experiment. The successful results are summarized in Fig.3 and Table 1. The comparison with other authors' results(Fig. 3) indicate that the modified Thellier method is successful in Hawaiian historical lava flows. Further experiment is performed for the older Hawaiian lava flows.

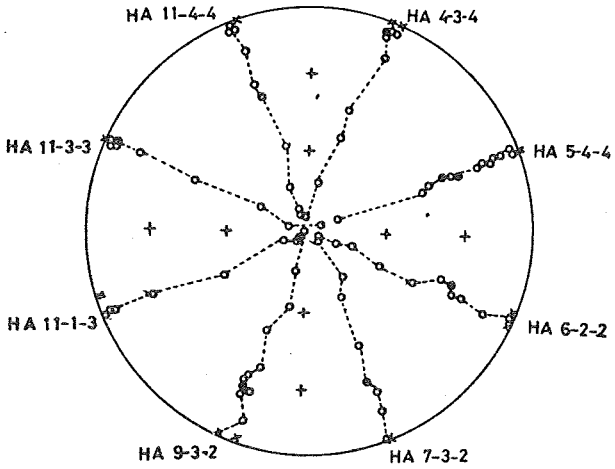

Fig.2 Change in the direction of NRM.

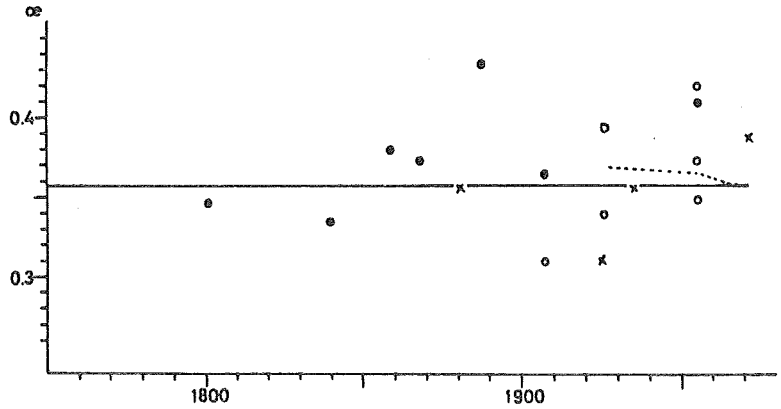

Fig.3 Compilation of the paleointensity data from Hawaii. open circle=other authors'(Doell and Smith 1969, Coe and Grommé 1973, Shaw 1974);dotted line=Oahu observatory;solid circle=present investigation($-r>0.980$);cross=present investigation($-r<0.980$).

References

Doell,R.R. and P.J. Smith (1969) J.Geomag.Geoelectr.21,579.
Coe,R.S. and C.S.Grommé (1973) J.Geomag.Geoelectr.25,415.
Shaw,J. (1974) Geophys.J.R.astr.Soc.39,133.
Kono,M.and N.Ueno (1975) Rock mag.Paleogeophy.3,61.

Sample	Year of Eruption	T_1	T_2	N	-b	S_b	-r	F_{oe}	
HA 9-3-2	1801	20	500	10	0.692	0.048	0.982	0.346	
HA 4-3-4	1840	100	550	10	0.670	0.042	0.985	0.335	
HA11-1-2	1859	20	350	10	0.771	0.028	0.995	0.386	
HA11-1-3		20	400	11	0.777	0.027	0.995	0.388	0.380
HA11-3-3		20	450	12	0.758	0.018	0.997	0.379	
HA11-4-4		20	350	10	0.733	0.029	0.994	0.366	
HA 5-1-4	1868	20	350	10	0.735	0.047	0.984	0.367	0.374
HA 5-4-4		20	350	10	0.763	0.022	0.997	0.381	
HA 6-2-2	1887	20	550	11	0.868	0.044	0.989	0.434	
HA 7-3-2	1907	20	350	10	0.731	0.034	0.992	0.365	
HA 3-1-4	1955	20	450	9	0.823	0.062	0.981	0.411	
HA 2-1-5	1750	20	400	8	0.880	0.104	0.961	0.440	
HA13-3-2	1881	20	350	10	0.711	0.076	0.957	0.356	
HA 8-4-3	1926	20	400	8	0.623	0.058	0.975	0.311	
HA12-3-3	1935	55	450	11	0.713	0.066	0.964	0.357	
HA 1-2-5	1972	20	400	8	0.777	0.071	0.976	0.389	

Table 1. Summary of paleointensity data. T1,T2=temperature interval in which NRM-TRM relation is linear;N=number of points;b=slope of NRM-TRM linear regression line;Sb=standard error of the slope;r=correlation coefficient;F=paleointensity

PALAEOMAGNETISM OF OSAKA BAY SEDIMENTS

Isao MUROI* and Katsumi YASKAWA**

* Department of Earth Science, Science Education Institute of Osaka Prefecture, Osaka 558
** Department of Earth Sciences, Faculty of Science, Kobe University, Kobe 657

1. Introduction

There are not so many palaeomagnetic studies on the past geomagnetic secular variations using the samples from ancient kilns and of water-laid sediments in Japan (Hirooka, 1971; Yaskawa et al., 1973; Domen and Muneoka, 1973; Nakajima and Kawai, 1973; Kawai et al., 1976). In this paper the geomagnetic secular variation will also trace back being based on the measurement of NRM of Osaka Bay sediments.

Recently, the Bottom of the Samondo River, flowing into the Osaka Bay, was dredged by caisson method, to construct piers of a bridge. Taking this opportunity oriented samples for NRM measurement were collected in the caisson at 43 levels of the sediments from 8 m to 25 m in depth (Maeda and Yaskawa, 1976). This sampling method has several advantages in comparison with the coring one, that is

a) Orientating of the sample is easy and sure.
b) As many samples as we want from the same level can easily be taken.

Since age was determined at 16 levels by means of ^{14}C method, palaeomagnetic studies of this sediments will give us a detailed information concerning the secular variation of the past geomagnetic field in Southwest Japan. We will correlate this with the results of the other investigators mentioned above.

2. Geology and age

The sampling site is situated at the mouth of the Samondo River into the Osaka Bay (34°43'N, 135°26'E). The stratigraphic column of this site is shown in Fig. 1. The Umeda Formation is the Holocene sediments with a total thickness of about 17 m. The upper part of this Formation consists mainly of unconsolidated silty clay with small shells. The middle part is homogeneous clay containing shell fossils a little. The lower part is composed of silty clay with ostrea nodule etc. The Nanko Formation is about 1 m or a little more in thickness, being composed of silty clay and/or peaty clay. The upper part of the Itami Formation contains tuff, clay, peaty clay and sandy clay, being regarded as the sediments deposited in the fresh water. Fig. 1 also shows the correlation of depth and age of these sediments (Maeda and Yaskawa, 1976), from which it is clear that the rate of sedimentation was not always constant. The mean value of the sedimentation rate of Umeda Formation in this site is estimated at 1.4 mm/yr in the period from 1200 yr B.P. to 20000 yr B.P.

3. Sampling

Since a magnetic compass can not be used in the caisson, the orientation of each sample was determined on the basis of a caisson's wall direction horizontally declined 3.18°W from the geographic north which was measured outside the caisson. Usually each sample has a column shape with 5 cm in diameter and 7 cm in length. Five or six samples were taken from each level of the sediments. A specimen, 2.5 cm cube, was prepared for NRM measurement from each sample except for the sample (no. 319) 50 cm long, from which 16 specimens were made.

4. Measurement of NRM

The measurement of NRM was made by a Super-conducting Rock Magnetometer. The magnetometer has maximum sensitibity of 10^{-8} emu in total flux. The intensity values of Z and Y components of a specimen observed by the magnetometer is simultaneously indicated on a dizital voltmeter and printed out on a paper. Measurement for one specimen takes less than a minute.

At the beginning of the measurement of all specimens, a stability test of NRM was carried out with a pilot specimen prepared from No. 228. The result is shown in Fig. 2. From this Figure it seems that the NRM of the specimen is stable up to 400 Oe of the ac peak field. All of the specimens were determined to be demagnetized at 100 Oe of ac peak field.

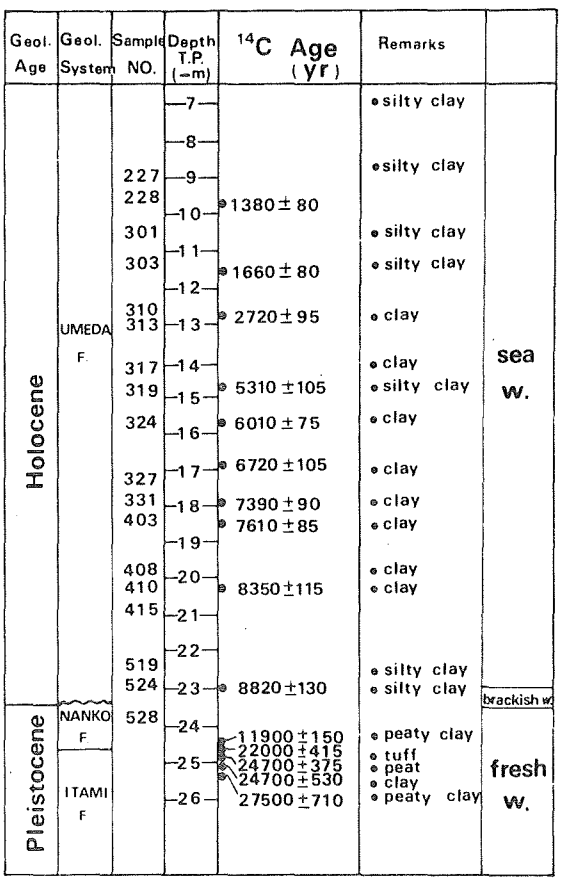

Fig. 1 Stratigraphic column showing geological age and unit, sample no., depth, ^{14}C age etc of this site.

5. Results and discussions

In Fig. 3 are shown the declination, inclination and intensity of NRM outained from 1200 yr B.P. to 9500 yr B.P.. Since the sampling level is not quite continuous, it is not so easy to draw a smoothed curve. In disregard of the detailed variation, solid curves were drawn by free-hand for the declination and inclination.

The declination changes in the range of 10°E to 60°W, the inclination 40° to 70° and the intensity 10^{-5} to 3×10^{-7} (emu/cc). The change

of diclination from 1200 yr B.P. to 1400 yr B.P. (No. 227, 228, 301, 302) is very large. The intensity corresponding to this period also varies considerably in the sense of increasing. In Fig. 4 a part of Fig. 3 was plotted in an enlarged scale with both curves from the ancient kilns (K) and from the water-laid sediments of Lake Biwa (B). The overlapping part of the present result (O) with these two curves (K and B) is not so long and not so frequent. Speaking about declination, the curve K equally fluctuates west- and eastward from the geographic north direction and the curve B deviates eastward against the curve O deviating westward. Speaking about inclination, the curve O, the present result, is vary similar to the curve K, the result from the kilns. The curve B, the Lake Biwa sediments, shows lower value than the others. In sixteen specimens taken from Sample no. 319 which covers the time span from 3900 yr B.P. to 4400 yr B.P., the time interval between each adjacent specimen is about 30 years, and NRM directions of them do not change so much, but the intensity is seen to be increasing in the middle of the sample.

In Fig. 3, the curves for declination and for inclination drawn by free-hand show us more frequent variations in recent than in ancient within the observed period of time except the changes in short period.

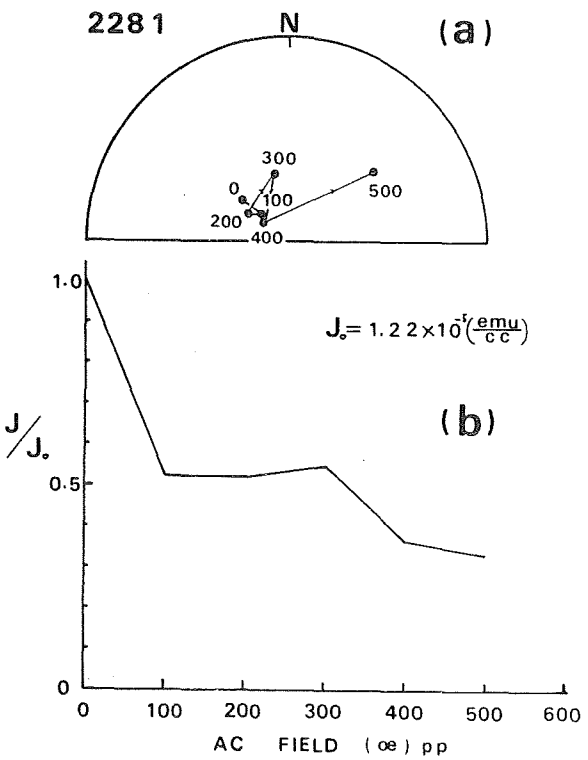

Fig. 2 An example of the change of direction (a) and intensity (b) by alternating field demagnetization.

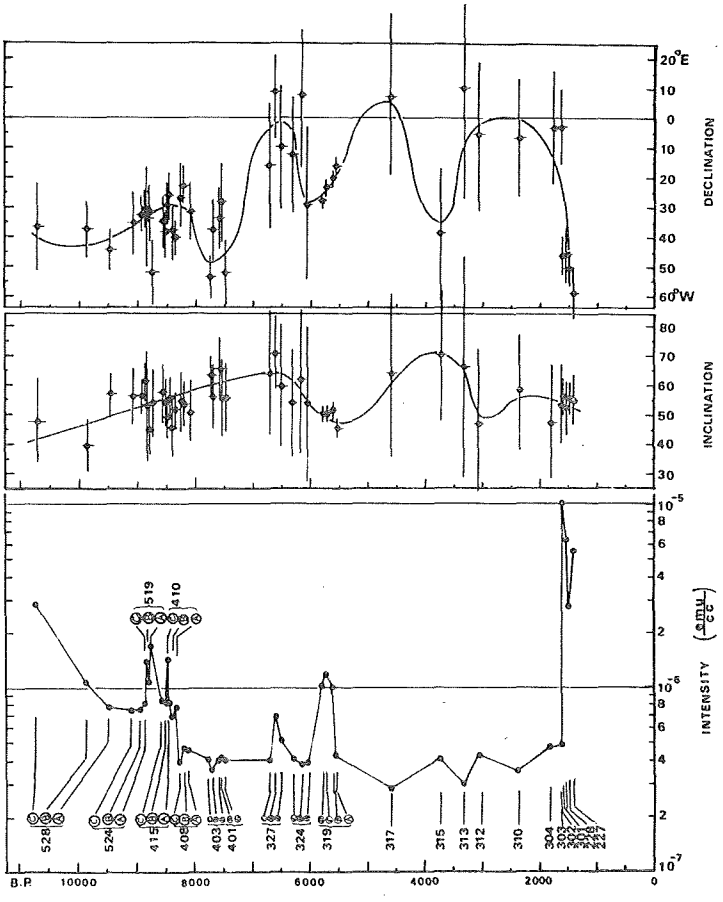

Fig. 3 Declination, inclination and intensity against age from the Samondo River. Smoothed curves are drawned by free-hand.

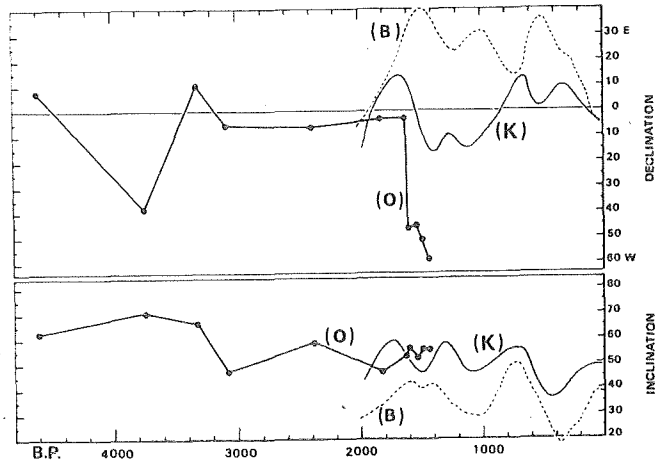

Fig. 4 Curve (O) shows a part of Fig. 3 plotted in an enlarged scale with both curves from the ancient kilns (K) (Hirooka, 1971) and from the water laid sediments of Lake Biwa (B) (Yaskawa et al., 1973).

References

Domen, H. and H. Muneoka (1973) Bull. Fac. Edu., Yamaguchi Univ. 23, 27.
Hirooka, K. (1971) Mem. Fac. Sci., Kyoto Univ., 38, 167.
Kawai, N. Y. Otofuji and K. Kobayashi (1976) J. Geomag. Geoelectr., 28, 395.
Maeda, Y. and K. Yaskawa (1976) Personal communication.
Nakajima, T. and N. Kawai (1973) Rock magnetism and Paleogeophysics 1, 34.
Yaskawa, K., T. Nakajima, N. Kawai, M. Torii, N. Natsuhara and S. Horie (1973) J. Geomag. Geoelectr. 25, 447.

ON THE EXCURSION OF THE LATEST PLEISTOCENE RECORDED IN ONTAKE TEPHRA, INA, CENTRAL JAPAN

Kimio HIROOKA, Chieko TOBITA*

Geological Laboratory, Faculty of Education, Fukui University
Bunkyo 3-9-1, Fukui, 910

Takuo YOKOYAMA

Laboratory of Earth Science, Faculty of Technology, Doshisha University
Kamigyo-Ku, Kyoto, 602

Susumu NAKAYA

Fujimi High School
Fujimi-Cho, Suwa-Gun, Nagano Prefecture, 399-02

Introduction

Recently, precise palaeomagnetic studies of lake- and sea- sediments disclosed several short period excursions in the Brunhes Normal Polarity Epoch. From the geomagnetic point of view, it is very interesting to know how the nature of virtual geomagnetic pole (VGP) paths were during such big geomagnetic fluctuations in the Brunhes Epoch. If the VGP position is assumed to be affected by the dominant local non-dipole field at an excursion when the geomagnetic dipole moment was considerably decreased, the VGP path must show its characteristic locus for the individual excursion. To classify the local VGP paths and to make clear the characteristics of each excursion of known age, will contribute grately to the Pleistocene stratigraphy in correlating the separated formations.

It is the another most interesting problem in the geomagnetic study to clear up the fashion of the palaeo-secular variation right before and after the big geomagnetic fluctuations.

Many precise palaeomagnetic studies of the Pleistocene were carried out by measuring the cored sediments of high sedimentation rate. In these studies, usually, only a single specimen was submitted to the measurement of each of horizons in a core. The variation of the direction of magnetization, therefore, might be exaggerated by the within-horizon scattering. And moreover, the in-situ horizontal orientation of cores cannot be measured. Only the relative declination of each horizon is obtained.

We attempted a palaeomagnetic study of the late Pleistocene terrestrial sediments. It enables us to get as many oriented samples as we need from each one of the horizons, and the study makes us possible to check the amount of scattering of magnetization as well as to get the absolute declination. In the case of young sediments, we allways face dificulties in judging which remanence remained is the original and the stable remanence when we applied stepwise magnetic cleaning. We can decid the most reliable remanence more reasonably by comparing the Fisher's precision parameter k of the steps when we have more than three samples at a horizon.

Sampling and the Stratigraphy of the Site

Palaeomagnetic samples were collected from the late Pleistocene layers

* Present address : Nakago Primary School, Okayama, Tsuruga City, Fukui, 914.

of tephra deposits such as pumice, scoria and volcanic ash, at Rokudo-bara, Ina City, Nagano Prefecture, central Japan (Fig. 1). The geographic coordinates of the site are 35°50'04" N and 137°59'30" E. The volcanic sediments are popularly called "Loam", although the material composition of them is not corresponding to the geological term of "loam" in the strict sence. Such tephras cover a wide area of the central and south part of Nagano Prefecture. These volcanic materials are confirmed to have been derivered mainly from Mt. Ontake, a recent volcano, locating about 50 km west of the site. The layers of the volcanic materials are called "Ontake Tephra" or more commonly "Shinshu Loam". The distribution of one of the pumice bed extends to the region around Tokyo, more than 200 km appert from the volcano.

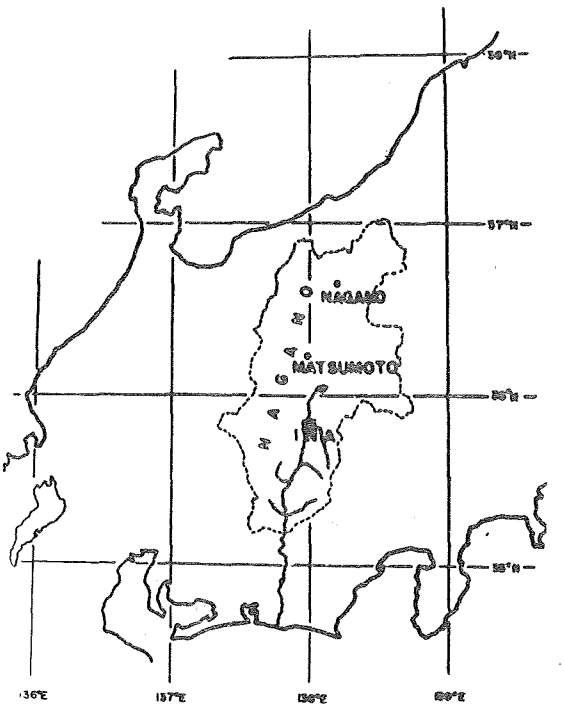

Fig. 1. A locality map of the sampling site. Solid square shows the position of the site.

According to Kobayashi and Shimizu (1962), the Ontake Tephra formation is subdivided into three units, that is, the Younger Loam, the Middle Loam and the Older Loam units. We could get a exposure of the Younger and the Middle Loam units at the site. The volcanic ash beds (so-called "Loam" in the Middle Loam unit at the site) are intercalated by three pumice beds, which are corresponding the pumice bed II (Pm-II), the pumice bed II' (Pm-II'), and the pumice bed III (Pm-III) from the lower to the upper according to Kobayashi's designation. The Younger Loam unit enbeded two pumice beds of Pm-IV and Pm-V (= S2).

Age determination of ^{14}C method was carried out on these five pumice beds. The age of Pm-II' turned out to be older than 42,000 years B.P. (Kobayashi et al., 1971) and that of Pm-III is 35,700±1,400 yr. B.P. (Kobayashi and Shimizu, 1965). In the lower horizon of the Middle Loam unit, there are two distinct pumice beds, Pm-I' and Pm-I. The upper bed, Pm-I, is the bed which has a very wide distribution area as already mentioned. Fission track dating samples for this bed have been collected at a site of Sagamihara City near Tokyo and their ages are 73,000+4,000, 77,000+8,000, 78,000±10,000, 82,000±10,000 and 95,000±5,000 yr. B.P. (Machida and Suzuki, 1971).

The two pumice beds of the Younger Loam unit, Pm-IV and Pm-V, are showing the ^{14}C age of 27,000±2,000 (Quaternary Research Group of Kiso Valley and Kigoshi, 1964) and 15,750±390 yr. B.P. (Kobayashi, 1965) respectively. The Younger Loam unit, therefore, is considered to have been formed in a period between 30,000 to 10,000 years ago (Kobayashi et al., 1967).

About 250 oriented samples were taken from 28 horizons of the Younger and the Middle Loam units. The virtical section of the sampling is shown in Fig. 2. The horizons were numbered SL 9 to SL 34 from the lower to the upper. As the excursion corresponding to the Laschamp Event was expected

at the horizons upper than SL 23, we made a continuous sampling above its level. More than ten samples were collected from each of the horizons except the horizons of SL 10', 27, 28, 30, 31, 33 and 34.

As the samples were oriented by using a magnetic compass, the orientation must be corrected with the present-day geomagnetic declination at the site. To know the varue of this declination, we observed the azimth of the sun at the site using a theodolite. As the result of the observation, the present-day declination (D_{1976}) we got is,

$$D_{1976} = -6.77 \pm 0.02°.$$

Since the sediments sampled here are very loose, sampling was done by using plaster of Paris in order both to protect the sediments from beeing crushed and to attain more accurate orientation of samples. The method of orientating was used the same technique as that of the archaeomagnetic sampling of which detailed procedures were described by Hirooka(1971).

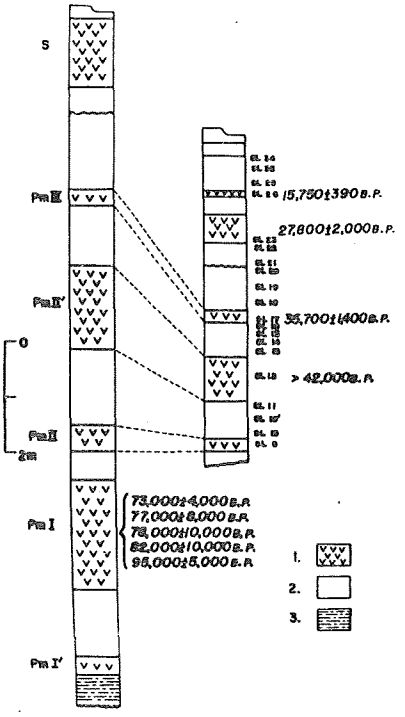

Fig. 2. Stratigraphical section of "Shinshu Loam" and sampling horizons. Left column shows a typical section around Ina City (after Sakai and Shimono,1972), and right column is of the sampling site.
1:pumice fall deposit, 2:"loam", 3:silt

Results of Measurement

After the measurement of n.r.m., one sample for each horizon was selected except 7 horizons of SL 10', 27, 28, 30, 31, 33 and 34, and was submitted to storage test. The samples for the test were placed in a way that their n.r.m. directions became parpendicular to that of the geomagnetic field in the laboratory. The samples were stored for 4 moths meanwhile their magnetization were measured once a month periodically. All the rest of the samples were demagnetized stepwisely by alternating fields of 25, 50, 100 and 150 Oe. As for the each horizon, we decided the optimum step at which the smallest Fisher's circle of confidence (α_{95}) and the muximum varue of the precision parameter (K) were observed. Mean declination and inclination of the optimum step were adopted as the palaeomagntic data. The optimum steps are n.r.m. or 25 Oe for the most of all horizons and usuary no big diference in α_{95} and K was detected between these two steps. There are only three exceptions of horizons of SL 11, 21 and 22, whose optimum demagnetizing field are 100, 50 and 50 Oe respectively.

Detectable direction change of n.r.m. was observed in the case of SL 9, 13, 19 and 20 by the four months storage test. This fact is consistent with the result of A.F. demagnetization. These horizons showed a considerable decrease of α_{95} at 25 Oe. Demagnetizing field of 25 Oe seems to be strong enough to erase out the low coersivity components which changed their direction during 4 months storage.

Natural remanent magnetization of so-called "Shinshu Loam" contains a considerable soft component as is shown by the A.F. demagnetization.

Their usual median decay field (MDF) is about 20 - 30 Oe. Although such a MDF value is very low and seems not desirable for palaeomagnetic study, if we account for the youngness of their age, the sediments were still stable enough and worthwhile for the late Pleistocene palaeomagnetic study.

The results of the measurements were presented in Table 1, and Fig. 3. There is a clear-cut feature in the change of remanent magnetization. That is, in the upper Loam unit (the upper half horizons of the out crop), the obtained directions of remanence show normal polarity while those in the Middle Loam unit indicate anormarous or commonly denoted as "intermediate" directions.

As to know the intensity variation of the geomagnetic field, we applied the same method described in our study of "Kanto Loam" which is also included in this volume (Hirooka et al., 1977). The results is shown in Fig.3 together with the declination and inclination changes. We again find a clear contrast in the ratio of NRM /ISRM, that is, the ratios in the Middle Loam unit show the varues of the order of 10^{-2} while those in the Upper Loam unit are in the order of 10^{-3}.

Discussion

The intermediate directions obtained in this study indicate that a geomagnetic excursion was occurred in the late Pleistocene. This excursion was started at the time older than 60,000 years B.P. and lasted until 35,000 years ago. In the meantime, a very short normal polarity period existed as observed at the horizon SL 11. The virtual pole positions of this excursion are shown in Fig. 4. Its VGP path has a similar locus to that of

Tble 1. Results of palaeomagnetic measurement of "Shinshu Loam".

Horizon	Number of samples	Optimum step	Declination	Inclination	α_{95}	K
SL - 9	10	25 Oe	-120.45°	-26.98°	21.15°	6.18
SL - 10	9	25 Oe	-124.09	-10.33	9.08	33.12
SL - 10'	2	n.r.m.	120.65	30.27	22.03	174.30
SL - 11	10	100 Oe	6.17	52.90	9.31	27.91
SL - 12	11	n.r.m.	125.26	9.80	5.58	68.00
SL - 13	9	25 Oe	126.77	18.92	6.13	71.41
SL - 14	9	25 Oe	113.45	27.43	5.93	76.38
SL - 15	11	n.r.m.	133.49	9.45	7.85	34.80
SL - 16	10	n.r.m.	125.54	9.60	4.47	117.84
SL - 17S	5	25 Oe	126.88	9.68	3.72	424.10
SL - 17N	5	25 Oe	-108.77	-0.50	8.62	79.70
SL - 18	12	n.r.m.	7.61	36.95	1.83	562.32
SL - 19	9	25 Oe	12.14	46.30	5.49	88.96
SL - 20	10	25 Oe	3.02	48.16	6.06	64.59
SL - 21	10	50 Oe	18.57	48.29	8.24	35.32
SL - 22	10	50 Oe	17.26	53.05	6.72	52.66
SL - 23	10	25 Oe	3.45	37.16	7.39	43.67
SL - 24	12	n.r.m.	22.34	50.29	4.08	113.94
SL - 25	11	n.r.m.	25.37	52.71	2.79	268.25
SL - 26	9	25 Oe	5.95	40.73	9.19	32.32
SL - 27	1	n.r.m.	9.48	53.63	-	-
SL - 28	1	n.r.m.	16.55	46.50	-	-
SL - 29	12	n.r.m.	11.41	56.29	3.16	190.00
SL - 30	1	n.r.m.	8.12	56.34	-	-
SL - 31	1	n.r.m.	-1.90	49.54	-	-
SL - 32	12	n.r.m.	11.11	53.20	3.49	155.56

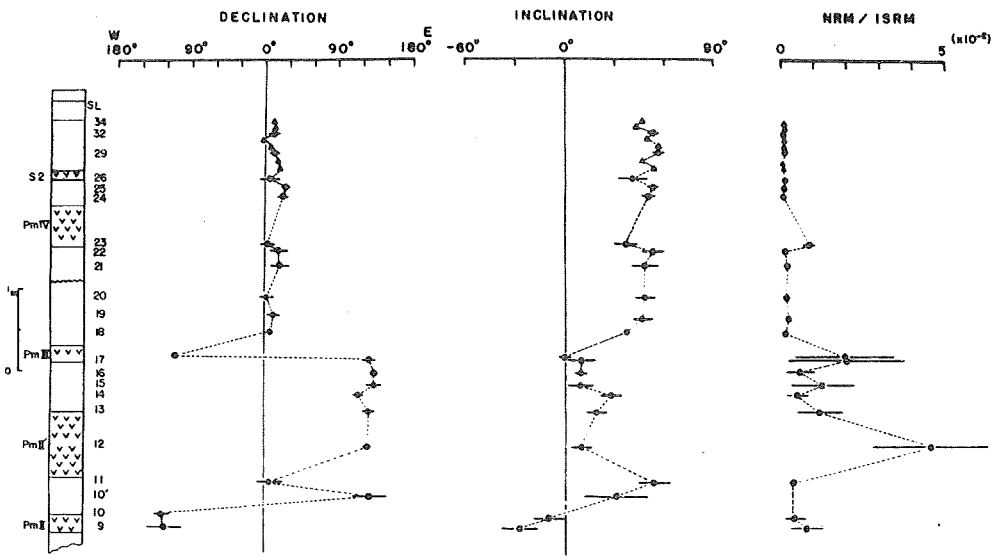

Fig. 3. The results of palaeomagnetic measure ments obtained from "Shinshu Loam". Triangles show the data of single sample horizons.

the excursion of 49,000 years B.P. recorded in the Lake Biwa sediments (Yaskawa et al., 1973) whose pole positions are shown in Fig. 5. The same excursion was recorded in the two different places appart 200 km from each other as Hirooka pointed out (Hirooka, 1977). If we look at the results of Lake Biwa core study precisely, big fluctuations can be found in the inclination and also in the relative declination during a period of about 55,000 to 65,000 years ago. These fluctuations might be correlated to the older half of the excursion of this study. Our recent preliminary measurement of the lower horizons of the Middle Loam unit confirmes that the excursion started at the horizon of Pm-I pumice bed whose age was determined by fission track method. The age is around 80,000 years B.P.

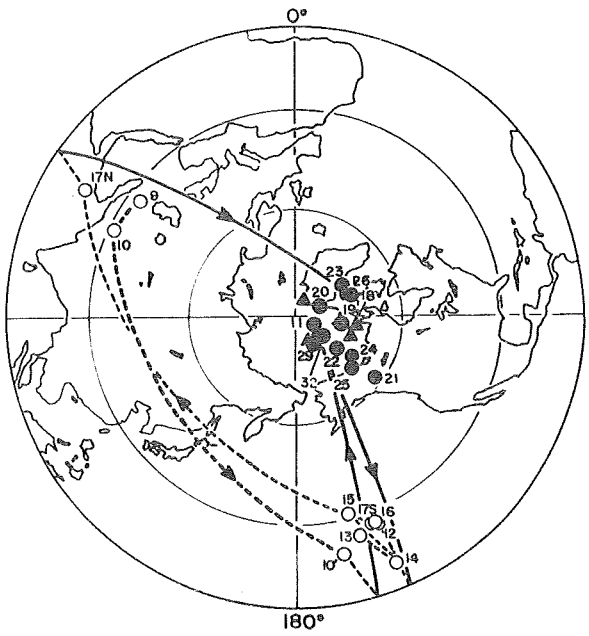

Fig. 4. Virtual pole positions of the latest Pleistocene obtained from "Shinshu Loam". Solid signs show on the northern hemisphere and open ones on the southern hemisphere.

The same excursion starting from Pm-I bed

was reported from the tephra beds of Mt. Yatsgatake recently (Aida, private communication). The site is in the distance of 40 km from our site. It is very possible that the excursion of this period will be found in the other parts in the Japanese Islands.

Upper than Pm-III horizon, a stable normal polarity period lasted until the top surface of the out crop, and no sign of the Laschamp event was found. Fisher's α_{95} and K were calculated for the VGP positions of this normal period, and the varue is found almost same compared with the varue of Japanese archaeosecular variation of recent 1,500 years which was reported by one of the present authors (Hirooka, 1971). In table 2, $_{95}$ and K of Fisher's statistics are tabulated for thearchaeo-secular variation and the palaeo-secular variation of 30,000 to 10,000 years ago.

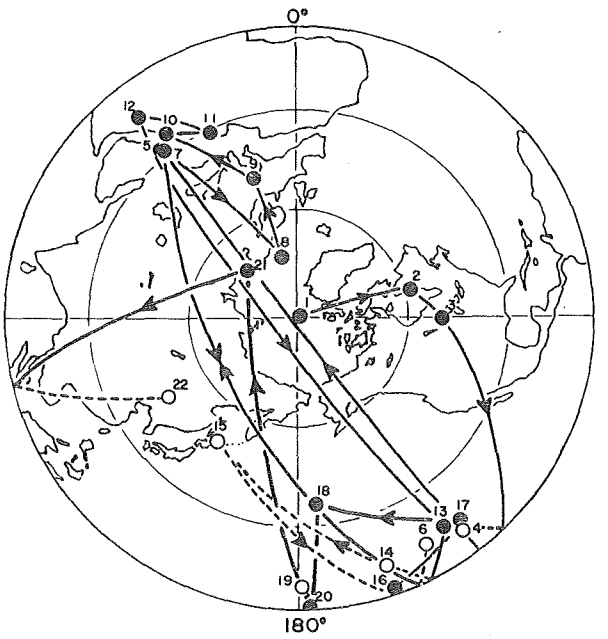

Fig. 5. Virtual pole positions of 49,000 years B.P. excurtion obtained from Lake Biwa 200 m core (after Yaskawa et al., 1973). Solid circles are on the northern hemisphere and open ones are on the southern hemisphere.

Table 2.

	N	α_{95}	K
Archaeo-secular variation (500-1950 A.D.)	30	2.98	78.94
Palaeo-secular variation (10,000-30,000B.P.)	17	3.97	81.65

It seems an important fact from the geomagnetic view point that the secular variation of the geomagnetic field right after an excursion has no big difference from the present geomagnetic secular variation.

References

Hirooka, K. (1971) Mem. Fac. Sci., Kyoto Univ., Ser. Geol. Mineral., 38, 167.
Hirooka, K. (1977) Paleolimnol. Lake Biwa & Japanese Pleistocene, 4, 153.
Hirooka, K., Y. Sakai and T. Yokoyama (1977) Rock Mag. & Paleogeophys., 4, 88.
Kobayashi, K. (1965) Chikyu Kagaku, no.81, 44 (in Japanese).
Kobayashi, K. and H. Shimizu (1962) J. Fac Lib. Arts & Sci., Shinshu Univ., no.12, II, 20.
Kobayashi, K. and H. Shimizu (1965) J. Fac. Lib. Arts & Sci., Shinshu Univ. no.15, 37.
Kobayashi, K., T. Kobayashi and H. Shimizu (1971) Collected Papers for the commemories of Retirement of Prof. Takehara, 191 (in Japanese).
Kobayashi, K., H. Shimizu, K. Kitazawa and T. Kobayashi (1967) J. Geol. Japan,

73, 291 (in Japanese).
Machida, H. and M. Suzuki (1971) Kagaku, 41, 263 (in Japanese).
Nakajina, T. and N. Kawai (1973) Rock Mag. Paleogeophys., 1, 34.
Quaternary Research Group of Kiso Valley and K. Kigoshi (1964) Chikyu Kagaku, no.71, 1.
Sakai, J. and M. Shimono (1972) J. Fac. Sci., Shinshu Unive., 7, 123 (in Japanese).
Yaskawa, K., T. Nakajima, N. Kawai, M. Torii, N. Natsuhara and S. Horie (1973) J. Geomag. Geoelectr., 25, 447.

PALAEOMAGNETIC STUDY OF " KANTO LOAM ", THE LATE PLEISTOCENE VOLCANIC SEDIMENTS

Kimio HIROOKA, Yumiko SAKAI*

Geological Laboratory, Faculty of Education, Fukui University
Bunkyo 3-9-1, Fukui, 910,

and

Takuo YOKOYAMA

Laboratory of Earth Science, Faculty of Technology, Doshisha University,
Kamigyo Ward, Kyoto, 602.

Introduction

Since Smith and Foster (1969) found an excursion, "Blake Event" occurred at about 110,000 years ago, many evidences of this excursion were reported from various places in the world by palaeomagnetic studies of core samples of lake and marine sediments. There are two disadvantages, however, in the study of palaeomagnetism by using cores. One is that only a single specimen can be submitted for each horizon except in the case of giant diameter cores. Within-horizon scattering of magnetic direction is undetectable and the scattering exaggarates the apparent variation of magnetization. The other disadvantage is that the horizontal orientation of a core is unknown. Only the relative declination can be used for the palaeomagnetic data, so that we cannot expect to get accurate virtual geomagnetic pole positions. In order to get rid of these disadvantages, we attempted to study the terrestrial sediments of the late Pleistocene. The sediments sampled here are tephras so-called "Kanto Loam" which contains much volcanic materials such as pumice, scoria and ash. The distribution of this tephra covers a wide area of Kanto District, central Japan. The tephra had been derived from Hakone volcanos and Mt. Fuji.

The palaeomagnetic study of the time younger than the Blake event has a special importance because it acts the role of the link connecting the palaeomagnetism with the geo- and archaeo-magnetism. The mode and the magnitude of secular variation observed in the historical and archaeological time might be extended back to the latest Peistocene. On the other hand, drastic geomagnetic fluctuation such as excursions were recognized during the same period.

Stratigraphy of the Sampling Site

Samples were collected from the tephra layers of about 30m thick which are cropping out at Idenawa, Hiratsuka City, Kanagawa Prefecture, central Japan. The geographical coordinations of the site are 35°19'31" N and 139°18'01" E. Stratigraphy of the sediments in this area was studied by Machida (1971), and Machida and Moriyama (1968). According to their reports, the sediment layers arround Idenawa are divided into two units. The lower is named Kissawa unit, and the upper is Kissawa Loam unit. Kissawa unit is mainly composed of marine sand which is called Kissawa Sand (K-S) and Kissawa Loam unit is subdivided into three parts of the lower, the middle and the upper. So-called "Loam" here, is indicating the sediments containing a big amount of weathered volcanic ash. Pumice tuff beds and "loam" beds are alternating in this unit. A small unconformity is recognized between a thick "loam" bed of about 1.5m thick and the overlying

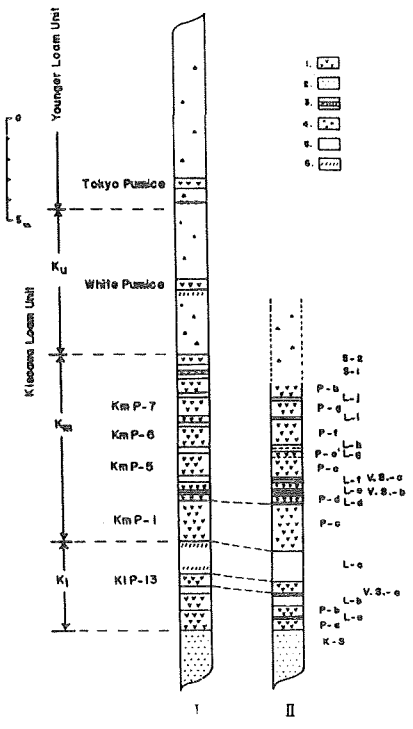

Fig. 1. Stratigraphical sections of "Kanto Loam" around Idenawa and sampling site. I : a typical stratigraphy around Idenawa (after Machida and Moriyama, 1968), II ; the sampling site of this study. 1 : pumice fall deposit, 2 : sand, 3 : volcanic sand, 4 : scoria fall deposit, 6 : black or dark brown humic ash.

white coloured pumice tuff bed (Km P-1). The lower and the middle parts of Kissawa Loam unit are bounded by this unconformity.

Pumice tuff beds and "loam" beds are alternating in the upper Kissawa Loam and those are sometimes intercalated with thin layers of volcanic sand. A typical stratigraphic column around Idenawa area is shown as column I in fig. 1. According to fission track dating of zircons and volcanic glasses (Machida and Suzuki, 1971), the ages of the pumice beds of Kl P-6, Kl P-8 and Kl P-13 in the lower Kissawa Loam are 128,000±11,000, 132,000±10,000 and 117,000±10,000 years B.P. respectively. And the two beds of Km P-1 and Km P-7 in the middle Kissawa Loam show the respective ages of 98,000±12,000 and 89,000±13,000 years B.P.

Sampling and Results of Measurement

243 samples were collected from 28 horizons at the site at Idenawa. Sampling was made from the uppermost horizon of Kissawa Sand to the uppermost horizon of the middle Kissawa Loam. The horizons sampled, therefore, cover a period about from 130,000 to 80,000 years B.P. We expected that the record of the Blake event would be found in those horizons. The samples were taken from 8 horizons of pumice beds which are denominated alphbetical order from the lower to the upper (P-a, b, c, d, e, e', f, and g), 13 horizons of "loam" beds (L-a, b_l, b_u, c_l, c_m, c_u, d, e, f, g, h, i, and j), and 3 horizons of volcanic sand beds(V.S.-a, b and c). Besides these, we obtained samples from 2 horizons of scoria beds (S-1 and 2) and one horizon of Kissawa Sand (K-S).

Between L-c "loam"bed and P-c pumice bed, there is the slight unconformity which is the boundary between the lower Kissawa Loam and the middle Kissawa Loam.

Stabilty of remanent magnetization is checked by both of alternating field (A.F.) demagnetization and 5 months storage test. The practical procedures of sampling and stability tests are the same method as mentioned in the paper of "Ontake Tephra" in this volume (Hirooka et al.,1977). A.F. demagnetization was carried out at the steps of 50, 100, and 150 Oe, and in some cases the additional 25, 200 and 250 steps were applied. The median decay field (MDF) of demagnetization is between 100 and 150 Oe, and the optimum field varies from n.r.m. step to 150 Oe.

The results of magnetic measurements were tabulated in Table 1, and shown in Fig. 2. It is clear that no data indicating the Blake event are obtained.

Since the orientation of samples was measured by referring to the geomagnetic north, we must correct the orientation by the varue of present-day declination at the site. From the observation of the sun's azimuth at the site, the varue of -7.44° was obtained as for the declination. The strata

Table 1. Results of palaeomagnetic measurements of "Kanto Loam".

Horizon	Number of samples	Optimum step	Declination	Inclination	α_{95}	K
S-2	9	n.r.m.	44.8	67.2	2.80	338.24
S-1	4	25 Oe	47.0	70.6	6.32	212.61
P-h	12	n.r.m.	25.2	55.9	4.17	109.48
L-j	6	50 Oe	7.2	49.1	9.15	54.60
P-g	9	25 Oe	0.1	76.0	9.70	33.56
L-i	9	50 Oe	14.8	62.2	5.23	98.05
P-f	3	25 Oe	7.1	64.2	19.51	40.98
L-h	3	50 Oe	6.6	59.2	4.19	865.20
L-g	7	100 Oe	19.4	57.2	4.38	191.31
P-e'	4	25 Oe	4.4	61.6	15.60	35.64
P-e	6	n.r.m.	25.9	42.0	12.16	31.33
V.S.-c	7	100 Oe	16.7	56.2	4.99	147.42
L-f	9	n.r.m.	21.0	47.2	3.81	183.19
L-e	9	50 Oe	14.0	59.0	6.11	71.99
V.S.-b	7	100 Oe	15.3	57.0	3.71	266.21
P-d	5	100 Oe	-0.4	53.7	2.55	899.64
L-d	9	50 Oe	8.7	59.7	2.40	459.39
P-c	12	n.r.m.	13.9	46.8	4.64	88.29
L-cu	9	50 Oe	8.7	53.1	4.15	154.80
L-cm	9	50 Oe	10.6	55.3	3.93	172.81
L-cl	9	100 Oe	12.6	56.1	2.82	333.67
V.S.-a	4	50 Oe	10.2	40.8	6.95	175.72
L-bu	11	50 Oe	13.7	55.1	3.79	146.04
L-bl	11	n.r.m.	9.1	61.8	4.40	108.83
P-b	5	150 Oe	33.6	44.7	10.49	54.12
L-a	9	n.r.m.	7.8	57.0	2.68	369.10
P-a	5	50 Oe	34.3	48.9	12.90	36.11
K-S	9	n.r.m.	26.8	71.0	14.71	13.20

are dipping 8° to the southeast (S 64.5° E), so that the bedding correction was also made on the palaeomagneic data. The corrected varues were tabulated in the table.

Ratio of Intensities of NRM and Saturation IRM

It is a very interesting subject to clarify the variation of the geomagnetic field intensity in the late Peistocene. But, unfortunately, the method of palaeo-intensity study of sediments is not yet established. In this paper, we tried to use the ratio of n.r.m. intensity (NRM) and that of saturation i.r.m. (ISRM) to estimate the palaeointensity variation of the late Pleistocene. As Nakajima and Kawai (1973) suggested, ISRM is a measure of the capacity of magnetization of the sediments. The ratio NRM/ISRM, therefore, expresses the efficiency of acquisition of magnetization. As the efficiency can be considered to depend upon the geomagnetic field intensity at the time of sedimentation, the ratio would be a parameter of the ancient geomagnetic field intensity.

We prepared 1.3 cm cube specimens for each of horizons for the intensity study. After the demagnetization experiments of n.r.m., the specimens were magnetized in the steady field of 5.21×10^3 Oe by an electromagnet. The specimens were again demagnetized and the ratios of NRM/ISRM were calculated for every steps of 0, 50, 100, 150, 200 and 250 Oe. We took the avrage of NRM/ISRM ratios of all steps to compare the results with those of Lake Biwa

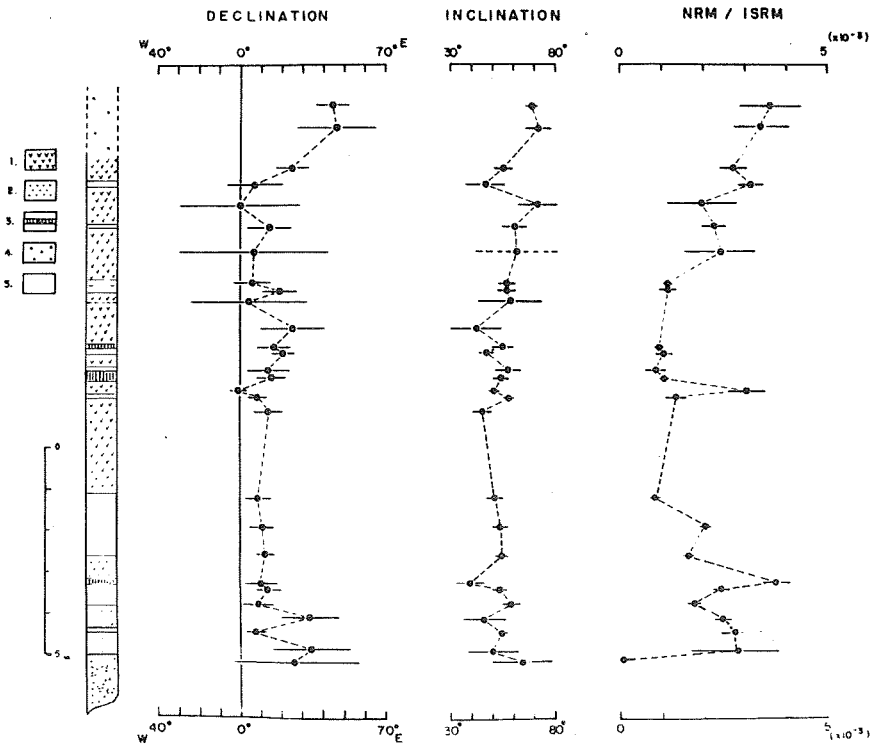

Fig. 2. The results of palaeomagnetic measurements obtained from "Kanto Loam". Sinbols in the stratigraphical column are same as those in Fig. 1.

core which reported by Nakajima and Kawai (1973). Lake Biwa sediments are very fine grained and homogenious. But, in our case, the sediments contain various kinds of materials as well as a big variety in grain size. The results are shown in Fig. 2. It is rather surprising that the obtained ratios show no big differences in spite of a big variety in both of grain size and 6f material kind.

Discussions

Virtual pole positions were calculated for each of 28 horizons and are ploted in Fig. 3. As seen in the figure, all the poles are clustering in a small region near the geographic north pole except the poles of the lower most two and the uppermost two horizons having fairly deviated positions. But it is a noticeable phenomenon that the center of these poles is not coinside with the north pole but it is in the place about 10 degrees off from it.

Continuous sedimentation can not be expected in such tephra sediments. Many time durations of no sedimentation must be involved between layers. Taking the age data of pumice beds into consideration, we correlated the variations of inclination and the ratio of NRM/ISRM to those of the Lake Biwa 200m core results (Kawai et al., 1975). The correlation was done in a way as described in the following. First, we took the Lake Biwa data of the depth between 40 to 60m which is corresponding to the age of our tephras. Next, the sedimentation in the lake was continued by the rate estimated by

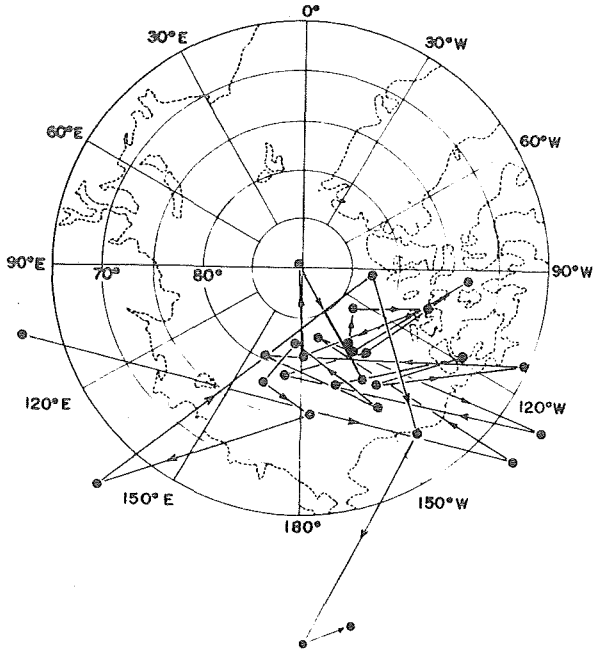

Fig. 3. Virtual geomagnetic pole positions of "Kanto Loam".

Fig. 4. Correlation of the palaeomagnetic data of 40 to 60m depth of Lake Biwa core (after Kawai et al., 1975) and those of "Kanto Loam". Solid circles show the results of Lake Biwa and hollow circles are of "Kanto Loam". It is clear that "Kanto Loam" data fit only before and after the Blake event which was found at about 55m depth of the Lake Biwa core.

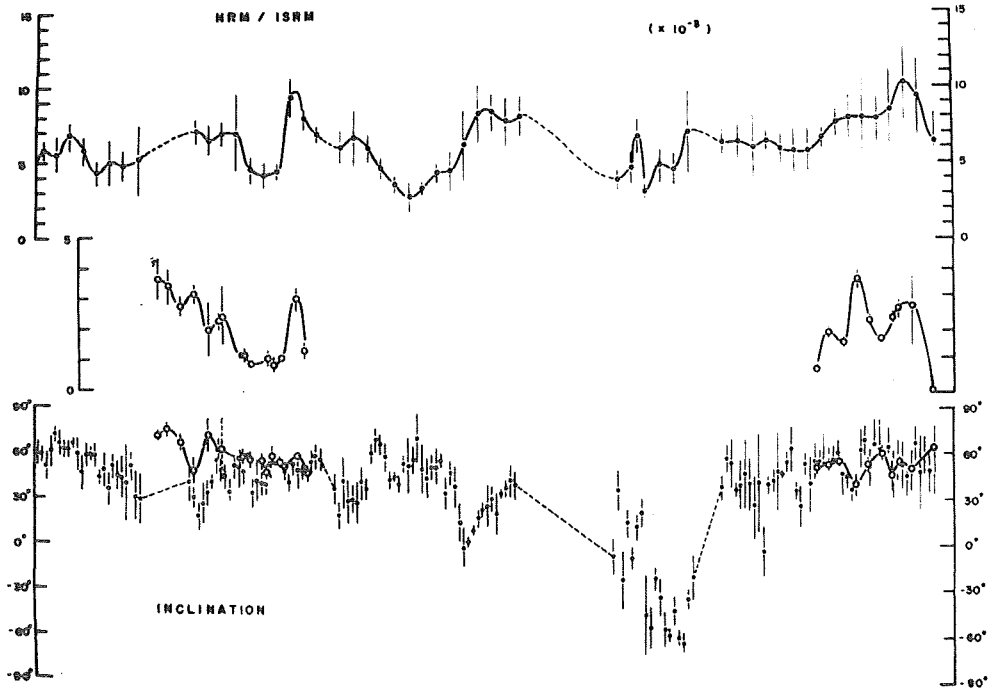

Yaskawa (1973). Then, we sifted the varues of inclination and NRM/ISRM ratio of "Kanto Loam" along the time axis within the range of the age dating errors of pumice beds in order to find the vest fit place of the both varues. The result of the correlation is shown in Fig. 4. In the figure, hollow circles indicate the data of the present study and solid circles express the Lake Biwa data. One can see a conspicuous agreement in both inclination variation and that of NRM/ISRM ratio. Of course, as the magnetic properties and its contents are different, the varues of the ratio of NRM/ISRM of "Kanto Loam" are not the same as the Lake Biwa varues. But the pattern of their variation is very similar. Moreover it is clear that the Blake event found in Lake Biwa sediments is lying between the horizons of L-c and P-c of "Kanto Loam" tephras. As already mentioned, an unconformity is detected the very place between L-c and P-c beds. It is, therefore, the Blake event occurred while the sedimentation was stopping after the sedimentation of L-c bed.

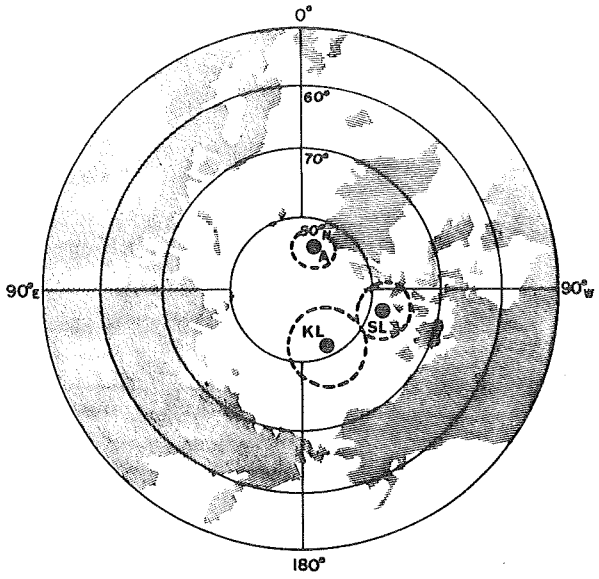

Fig. 5. The mean positions of VGPs of the three periods of archaeomagnetic, the latest Pleistocene and the late Pleistocen normal polarity time. Broken line ovals are Fisher's 95 % circle of confidences for each period. A : archaeomagnetic age, S1 : the latest Pleistocene (Ontake Tephra), KL : the late Pleistocene ("Kanto Loam").

The means of VGP positions, Fishe's 95 % circle of confidence (α_{95}) and the precision parameter (K) were computed for the time of ordinal normal polarity period after the Blake event (P-c to P-h). The period corresponds about 20,000 years. The same computations were carried out about the data of the Ontake tephra (Hirooka et al., 1977) and the archaeomagnetic data of south west Japan (Hirooka, 1971). As for the Ontake tephra, the time duration is also about 20,000 years of the quiet normal polarity period after the newly found excursion which ended at about 35,000 years ago. Because Kawai and Hirooka (Kawai and Hirooka, 1969; Hirooka, 1971) pointed out that the archaeo-secular variation was caused by the geomagnetic dipole wobbling of a period of about 1,500 years, the mean of pole positions of archaeomagnetic age was account for the recent 1,500 years (500 - 1950 A.D.). The computed results are presented in Table 2 and Fig. 5.

It is obvious that the scope of secular variation is not so different among the tree periods of the recent 1,500 years, ca. 30,000 - 10,000 years B.P. and ca. 100,000 - 80,000 years B.P. None of the mean poles of them coincide with the geographic north pole. Moreover, the three mean poles have different positions from each other.

To explain this fact, we need more world-wide knowledges about the past geomagnetic secular variation. But it might be caused by the effect of the predominant standing non-dipole field which situated near Japanese Island at the respective periods.

Table 2. Mean pole position, Fisher's precision parameter and 95 % circle of confidence of archaeo- and palaeo-secular variation.

	N	K	α_{95}	Mean pole position latitude	longitude
Archaeo-secular variation (500 - 1950 A.D.)	30	78.94	2.98°	83.9° N	17.2° W
Palaeo-secular variation of Ontake Tephra (30,000 - 10,000 B.P.)	17	81.65	3.97°	78.0° N	105.0° W
Palaeo-secular variation of "Kanto Loam" (100,000 - 80,000 B.P.)	16	38.87	5.99°	80.9° N	157.0° W

References

Hirooka, K. (1971) Mem. Fac. Sci., Kyoto Univ., Ser. Geol. Mineral., 38,167.
Hirooka, K., C. Tobita, T. Yokoyama and S. Nakaya (1977) Rock Mag. Pleogeophys. 4,81.
Kawai, N. and K. Hirooka (1967) J. Geomag. Geoelectr., 19, 217.
Kawai, N., T.Nakajima, K. Yaskawa, M. Torii and N. Natsuhara (1975) Rock Mag. Palaeogeophys., 3, 24.
Machida, H. (1971) Daiyonki Kenkyu, 10, 1 (in Japanese).
Machida, H. and A. Moriyama (1968) Chirigaku Hyoron, 41, 241 (in Japanese).
Machida, H. and M. Suzuki (1971) Kagaku, 41, 263 (in Japanese).
Nakajima, T. and N. Kawai (1973) Rock Mag. Paleogeophys., 1, 34.
Smith, J.D. and J.H. Foster (1969) Science, 163, 565.
Yaskawa, K. (1973) Rock Mag. Paleogeophys., 1, 39.

*Present address : Kunimi Junior High School, Ayukawa, Fukui, 910-34.

PROGRESS REPORT ON PALEOMAGNETISM IN THE MELANESIA BASIN

Takaharu SATO, Naoto KAWAI

Department of Physics, Faculty of Engineering science,
Osaka University, Toyonaka, Japan

Kazuo KOBAYASHI

Ocean Research Institute, University of Tokyo,
Nakano-ku, Tokyo, Japan

Paleomagnetic studies using sliced thin sections of two deep-sea sediment cores KH 73-4-7 (2°41.3' N, 164°50.2' E) and KH 73-4-8 (1°33.2' S, 167°38.6' E) from the Melanesia Basin have been undertaken since 1974 by Kawai et al (1976, 1977). In the present study upper part (120 - 490 cm) of core KH 73-4-8 is used and 448 specimens are prepared with the same method described by Kawai et al (1976).

Natural remanent magnetization (NRM) vectors are measured with a slow speed spinner magnetometer after AF cleaning in 100 Oe at Ocean Research Institute, University of Tokyo and artificial remanent magnetization vectors are measured with an astatic magnetometer at Osaka University. In order to normalize the NRM intensity for the variations of the magnetic particles isothermal saturation remanent magnetization (ISRM) is produced on every other specimen picked up from successive ones in the 9,000 Oe static field and a ratio of NRM to ISRM (J_N/J_S) is calculated (Fig. 1). In Fig. 1 the results reported by Kawai et al (1976, 1977) are also shown for comparison and the Brunhes-Matuyama boundary and Jaramillo event are shown in it.

Although the NRM intensity of two cores changes similarly with depth below the level of the Brunhes-Matuyama boundary, it is difficult to find any correlation above that level. However, a clear correlation become apparent when we normalize NRM with ISRM intensity. On the other hand a part of large values (310 - 520 cm) in the ratio (J_N/J_S) appears because of small ISRM intensity. The portion in core KH 73-4-7 (160 - 260 cm), which is assumed to correspond to the above part, has smaller values in the ratio.

In order to examine a variation of magnetic property, anhysteretic remanent magnetization (ARM) is produced on 39 specimens in a 0.83 Oe static field and a peak alternating field in 1,000 Oe. The result of ARM measurements shows similar variations to that of ISRM. Parallel variations of ISRM and ARM were reported in the lower part of the both cores (Sueishi, 1977). But a ratio of ARM to ISRM (J_A/J_S) shifts from 7.5 to 6.0 % on an average at the depth of 300 cm as shown in Fig. 2. This difference is statistically significant to the 99 % level. The magnetic grains' size distribution seems to change at the depth abruptly. In this case a better choice for the normalization parameter would be ARM because normalizing with ISRM will overestimate the role of large grain size particles. The similarity of normalized intensity variations seems to be improved although there is a exception at the depth of 310 cm.

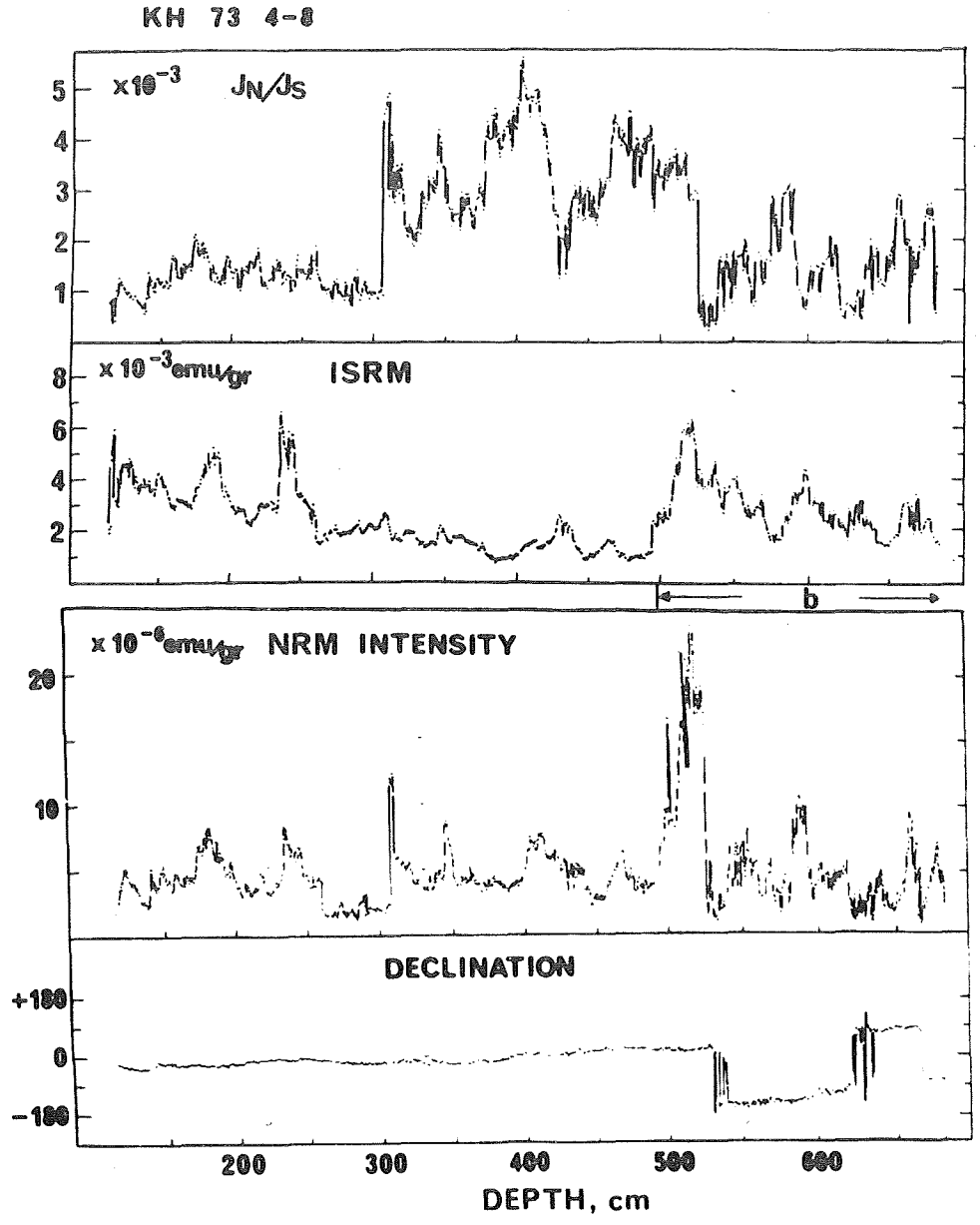
KH 73 4-8
x10⁻³ JN/JS
5
4
3
2
1
x 10⁻³emu/gr ISRM
8
6
4
2
b
x 10⁻⁶emu/gr NRM INTENSITY
20
10
DECLINATION
+180
0
-180
200
300
400
500
600
DEPTH, cm

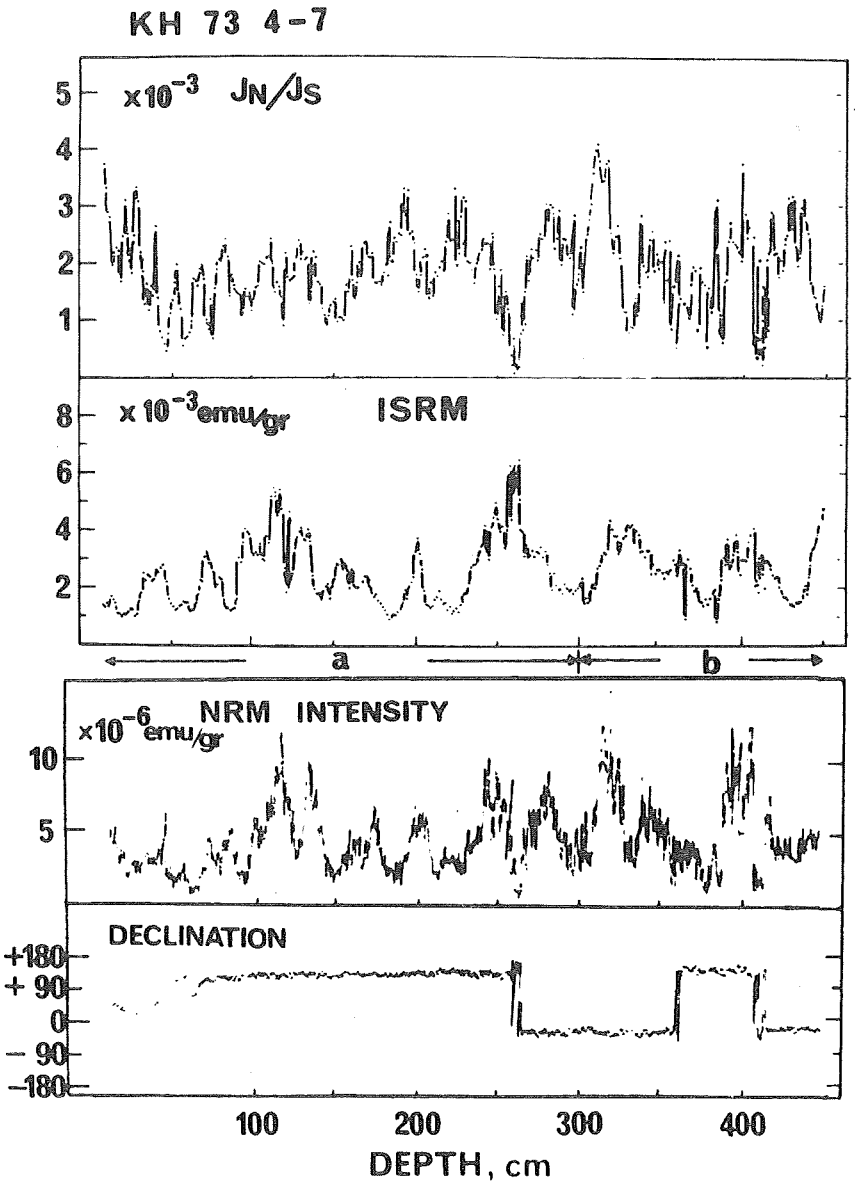

Fig. 1. Results of magnetic measurements in two cores. The data in region (a) are from Kawai et al.(1976) and (b) from Kawai et al.(1977).

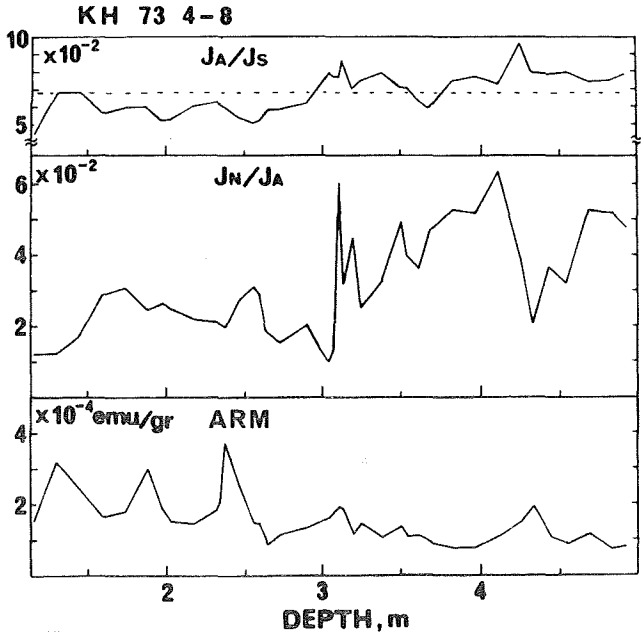

Fig. 2. Result of an anhysteretic remanent magnetization experiment in core KH 73-4-8. A dotted line indicates the average value.

References

Kawai, N., Y. Otofuji and K. Kobayashi (1976) J. Geomag. Geoelectr. 28, 395.

Kawai, N., T. Sato, T. Sueishi and K. Kobayashi (1977) J. Geomag. Geoelectr. 29, 211.

Sueishi, T. (1977) M. Sc. Thesis, Osaka Univ.

DETAILED VARIATIONS OF GEOMAGNETIC FIELD FROM 1 M.Y.BP TO 2 M.Y.BP

Tsutomu SUEISHI, Naoto KAWAI

Department of Physics, Faculty of Engineering Science, Osaka University, Toyonaka, Japan

Kazuo KOBAYASHI

Ocean Research Institute, University of Tokyo, Nakano-ku, Tokyo, Japan

Introduction

Kawai et al. (1976, 1977) have revealed the detailed variations of the past geomagnetic field since 1 million years ago using thin sections of the core KH73-4-7 taken from the equatorial Pacific basin (Lati. 2°41.3'N, Longi. 164°50.2'E, Water Depth 4160 m). For the purpose of continuing the same investigation back to 2.03 m.y.BP, the same core with 6 m length in KH73-4-7 are newly sliced into 1324 sections, each with 4.3 mm in thickness. About 730 years is needed to form one specimen if the constant sedimentation rate is assumed.

This interval of about 6 m is to record the geomagnetic field variation in the period older than Jaramillo event. Its age is in the range from 1.01 m.y.BP to 2.03 m.y.BP if the constant rate of sedimentation is assumed.

The declination and the intensity of all the specimens are measured in the horizontal component using the Schonstedt spinner magnetometer after the AF demagnetization in the field of 100 Oe.

In order to test the homogeneity, the declination of NRM of thin sliced sample has been measured twice for each sections, with its upper surface being approached first and with the lower surface then to the magnetometer. The difference of the declination is called ΔD (Kawai et al. 1976, 1977).

The reverse-normal polarity boundaries we confirmed in the core well coincides with the data by Cox (Kawai et al., 1976).

The core is mainly composed of relics of calcareous foraminifera with small amount of ferromagnetic minerals.

The Stability of NRM

The stability of NRM is tested by the stepwise AF demagnetization method . 24 specimens are selected with an interval of 25 cm throughout entire core. Progressive AF demagnetization has been carried out using three-axis tumbler with peak field from 25 Oe up to 400 Oe.

The change of the normalized intensity is shown in Fig 1. Normally magnetized specimens and reversedly magnetized ones are shown separately.

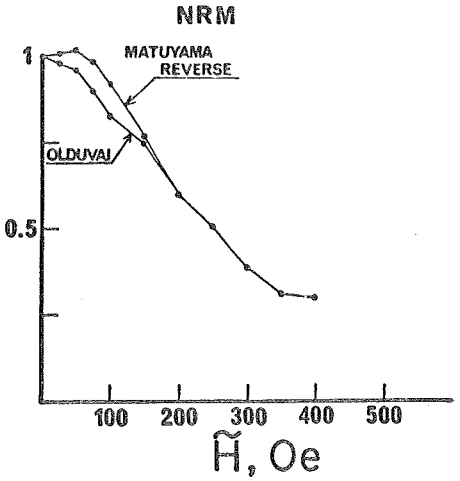

Fig 1. Progressive AF demagnetization of NRM

In the reversedly magnetized samples, the intensity first slightly increased in the region of loe demagnetizing field. This increase is due to the removal of a secondary VRM acquired by the specimen in the opposite direction to the primary field. It can be said that the primary remanence is very stable because a median destructive field is more than 200 Oe and suffered a weak influence of VRM.

Result

The result of the measurement at depths from 449 cm to 1027 cm is shown in Figs 2,3,4 (Sueishi, 1977).

The most striking secular change that this part of the core can depict is the existence of pronounced drop of the intensity at the depth from 461 cm to 482 cm (from 1.05 m.y.BP to 1.07 m.y.BP). The declination is so disturbed that a few polarity change can be seen. In the extremely case, the differencial declination (ΔD) appears even in one section (Fig 2). " A Zone " (1.07 m.y.BP) denoted by Watkins (1968) is in good agreement with our data together with the determined age.

The change in declination at the depth of 812 cm is due to the reversal of the earth's magnetic field at the upper Olduvai boundary (Fig 3). The Gilsa event which is appointed in the table by Cox seems not to exist in our results, but there are some specimens having weak NRM at the depth of around 830 cm. This fact might be correlated with the Gilsa-Olduvai boundary.

The lower Olduvai boundary is found at the depth around 890 cm (Fig 4). The interval of the transitional stage is longer than that we have confirmed at the upper Olduvai boundary, but a few specimens have NRM intensities which are slightly stronger than those at the other boundary.

The interval with normal-polarity is newly found at the depth of around 980 cm, with the intensity distinctly dropped. Such fine successive structure as those we confirmed in this experiment is hard to be achieved if 2 cm-cubic specimens taken at the interval of 10 cm had been measured (Kawai et al., 1976). The age of this anomaly is estimated to be 1.94 m.y.BP from our experiment on the bases of a constant rate of sedimentation . It is thought to correspond to the Reunion event in the table obtained by Cox (1969).

In older period than the Reunion event, the intensity change occured gradually and differently from the other boundaries. A slight but definite shift of declination can be observable. This seems to be due to the misoperation when the core was vertically divided into half with knife.

References

Cox,A. (1969) Science, 163,237.

Kawai,N., Otofuji,Y. and Kobayashi,K. (1976) J.Geomag.Geoelectr.,28,395.

Kawai,N., Sato,T., Sueishi,T. and Kobayashi,K. (1977) J.Geomag.Geoelectr. 29,211.

Sueishi,T. (1977) M.Sc.Thesis, Osaka Univ.

Watkins,N.D. (1968) Earth Planet. Sci. Lett., 4, 341.

(To be submitted to Phys. Earth Planet. Inter.)

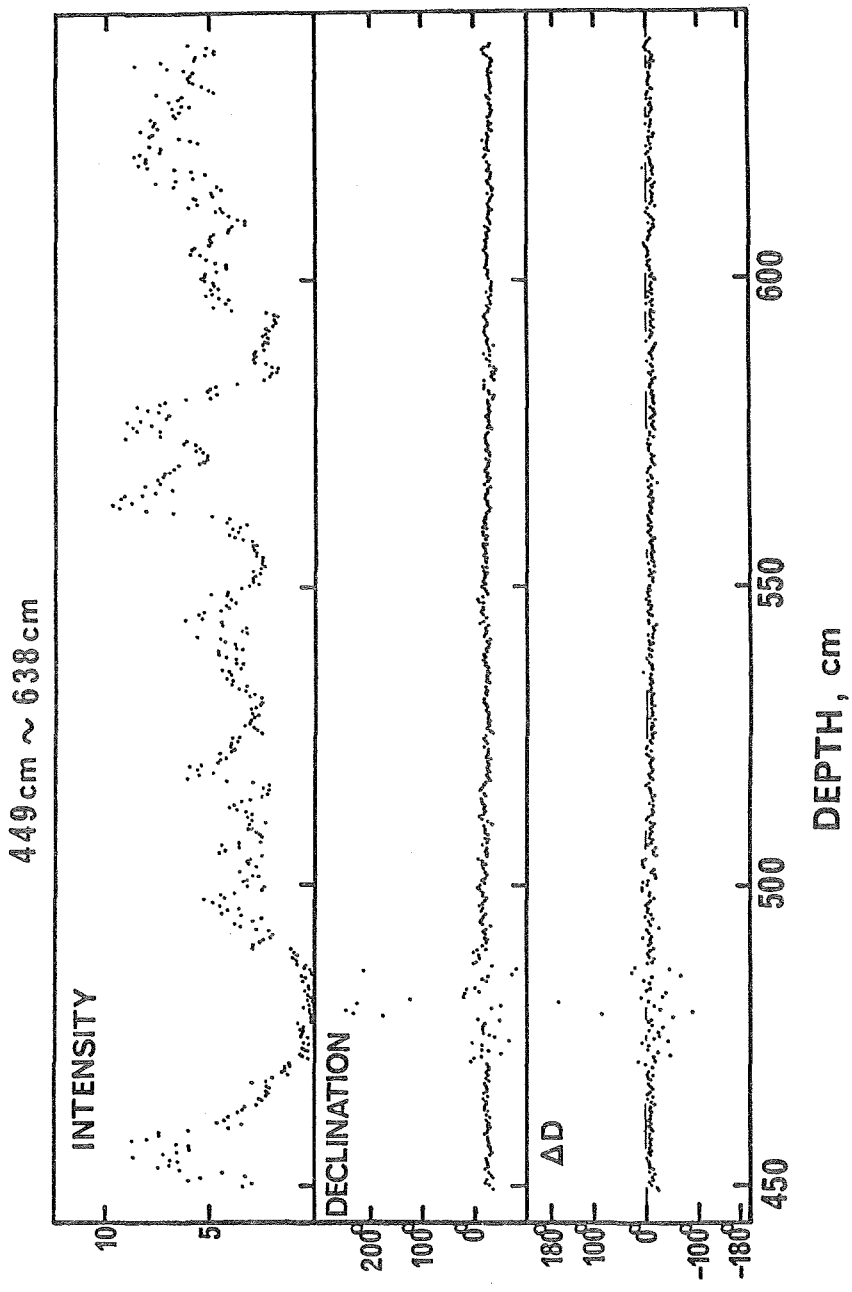

Fig 2. Result of NRM measurement at depths from 449 cm to 638 cm (from 1.01 m.y.BP to 1.35 m.y.BP)
The INTENSITY is in unit of 10^{-6} emu/gr. The angle of the DECLINATION is relative value.

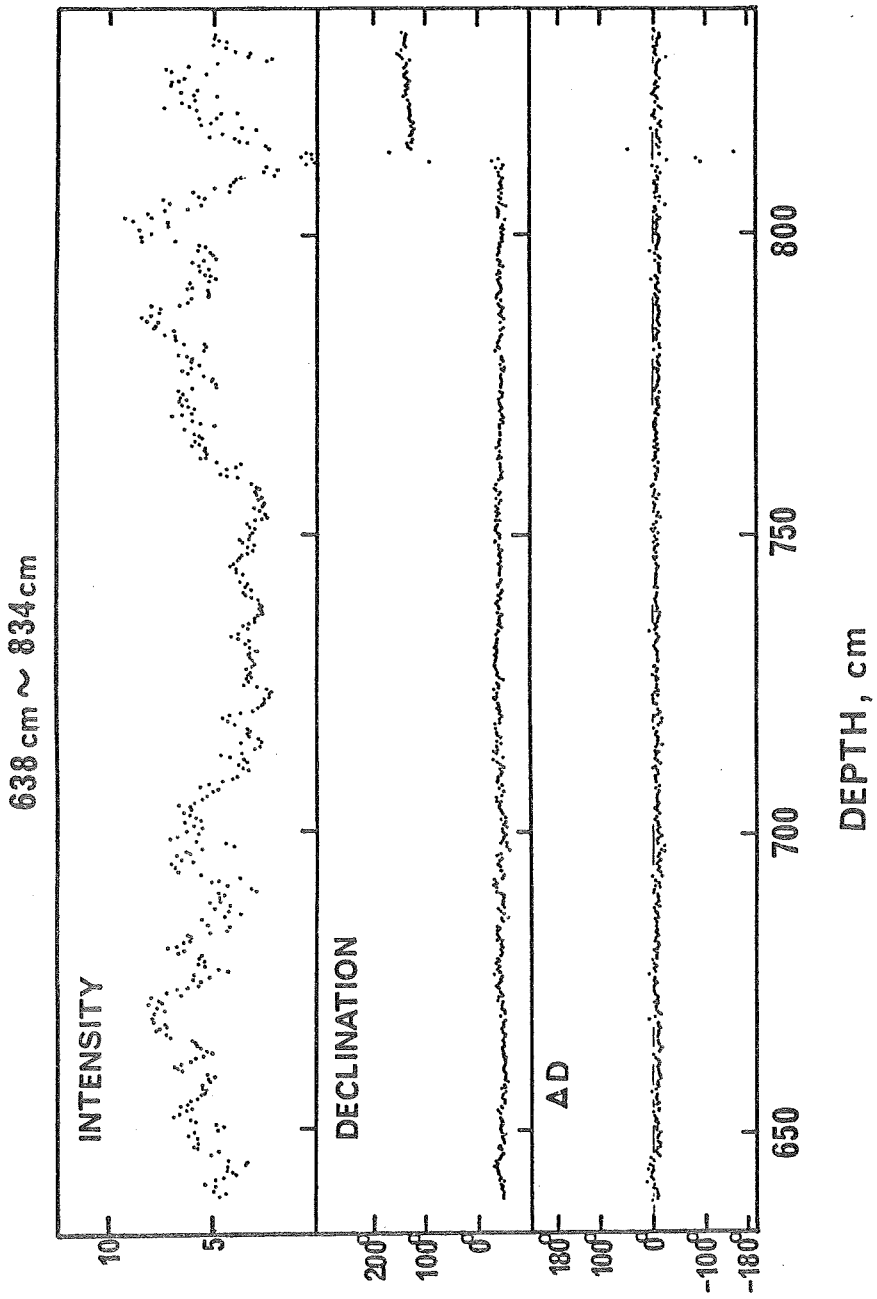

Fig 3. Result of NRM measurement at depths from 638 cm to 834 cm (from 1.35 m.y.BP to 1.69 m.y.BP)
The INTENSITY is in unit of 10^{-6} emu/gr. The angle of the DECLINATION is relative value.

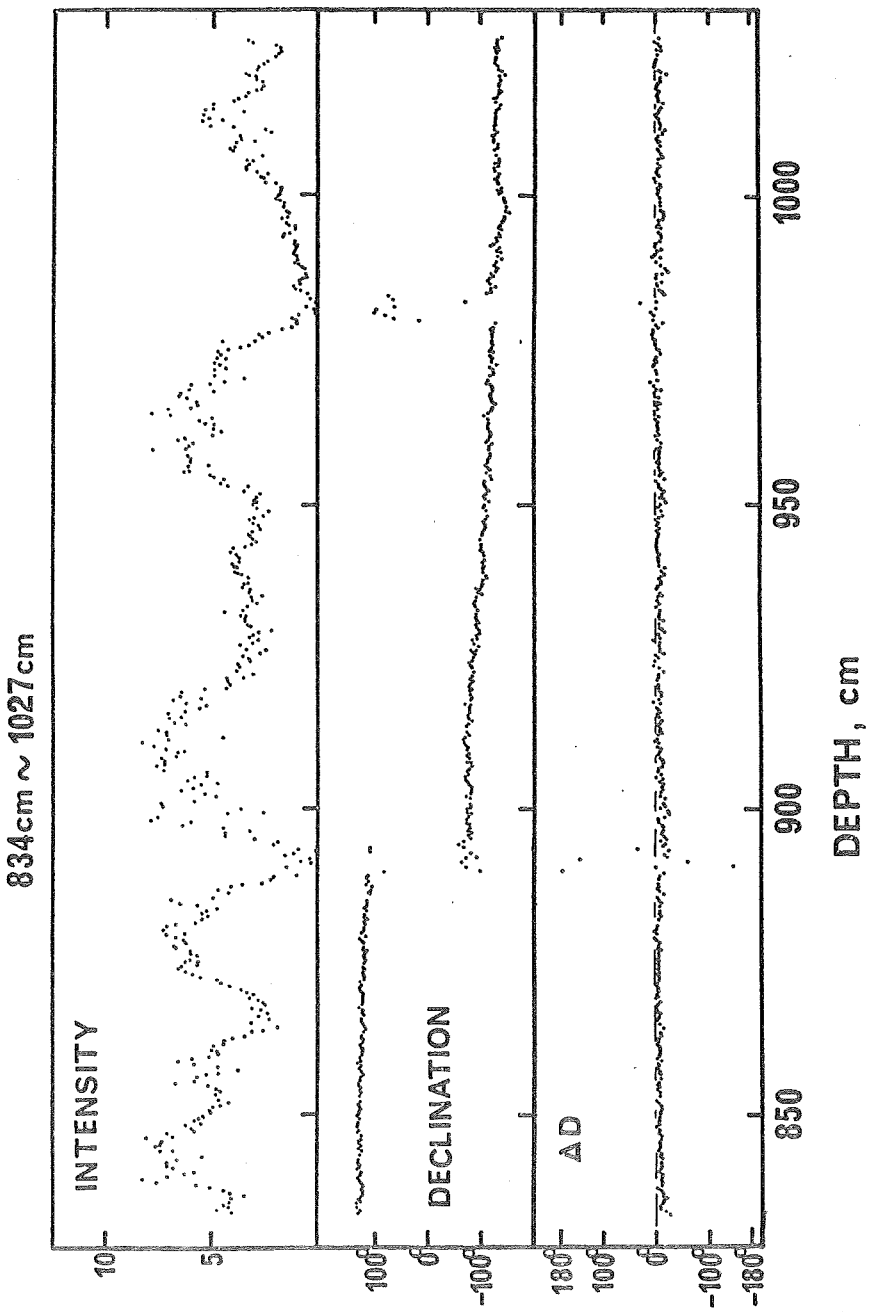

Fig 4. Result of NRM measurement at depths from 834 cm to 1027 cm (from 1.69 m.y.BP to 2.03 m.y.BP)
The INTENSITY is in unit of 10^{-6} emu/gr. The angle of the DECLINATION is relative value.

EXAMPLES OF THE PALEOGEOMAGNETIC FIELD INTENSITY DETERMINATION USING A SINGLE HEATING METHOD.

Haruo DOMEN and Hiroshi MUNEOKA

Institute of Physical Sciences, Faculty of Education,
Yamaguchi University, Yamaguchi 753, Japan.

Recently, one of the present authors (H.D.) has proposed a single heating method for the determination of paleo/archeo geomagnetic field intensity (Domen 1974, 1975a, 1975b, 1977a, 1977b).This newly proposed simple method was applied to two sets of Cenozoic (lower Pleistocene) rocks come from west Japan. This preliminary study on these rocks is presented briefly in this short note.

A set submitted to the present study is andesite come from Choja-ga-Hara in the central Yamaguchi Prefecture, west end of the Main Island and another set is basalt from Karatsu, Saga Prefecture, northern Kyushu Island respectively. The minute on NRM data of the former rocks had been shown in other bulletin (Domen et al 1977), and on the latter, brief report on NRM data has shown by another article separately in this annual report (Domen and Muneoka 1977).

The result thus obtained of paleogeomagnetic field intensity determination on those two sets of Cenozoic rocks is shown in Table 1.

Table 1. Paleogeomagnetic field intensity of Cenozoic rocks in west Japan obtained by a single heating method.

Sample		Ha/Hp*	N R M**	N R M Polarity
a) Choja-ga-Hara, Yamaguchi Pref.				
L. Pleisto. Andesite	(1)	0.806	1.004	N
	(2)	1.891	1.108	N
	(3)	1.168	1.143	N
b) Karatsu, Saga Pref.				
L. Pleisto. Basalt	(1)	0.675	1.074	R
	(2)	1.355	1.104	R
	(3)	1.273	1.188	R

* Paleogeomag. field intensity/present field intensity ratio.
** calculated value (normalized), which is equal to unity gives most reliable estimation of Ha/Hp ratio.

However submitted rock samples come from both locations are not dated absolutely yet, it seems from the geological view points that both rocks consolidated in lower Pleistocene. As shown in Table 1, samples are classified into two groups within each locality; one shows larger intensity ratio compared with the present geomagnetic field, another smaller respectively. This may suggest that there was some fluctuation of the paleogeomagnetic field intensity at that time; lower Pleistocene and this might occur in accordance with the geomagnetic field reversal during lower Pleistocene, if these reversed polariries are true fossils due to the field reversal. However this is still dubious as shown in the separate article by the present authors (Domen and Muneoka 1977).

The secular changes of paleogeomagnetic field intensity has still be veiled over. In order to uncover such hazy circumstances, the present study should be one of stepping-stones.

References.

Domen, H. (1974) Bull. Fac. Educ., Yamaguchi Univ. 24 (Part 2), 7-11.

Domen, H. (1975a) IAGA Bull. No.36, 156.

Domen, H. (1975b) Rock Mag. Paleogeophys. 3, 22-23.

Domen, H. (1977a) Phys. Earth and Planet. Inter. 13, 315-318.

Domen, H. (1977b) Bull. Fac. Educ., Yamaguchi Univ. 26 (Part 2), 33-39.

Domen, H., H. Muneoka and T. Yokoyama (1977) Bull. Fac. Educ., Yamaguchi Univ. 27, in press.

Domen, H. and H. Muneoka (1977) Rock Mag. Paleogeophys. 4 (this annual report)

CLASSIFIED NATURAL REMANENT MAGNETIZATION OF CENOZOIC BASALT COME FROM SHIMONOSEKI CITY, WEST END OF YAMAGUCHI PREFECTURE, WEST JAPAN.

Haruo DOMEN and Hiroshi MUNEOKA

Institute of Physical Sicences, Faculty of Education
Yamaguchi University, Yamaguchi 753, Japan.

Eighteen fist sized samples of upper Pleistocene basalt were taken from Shimonoseki City, in Yamaguchi Prefecture, west Japan. Those NRM were measured by means of an astatic magnetometer. Mean NRM direction is as follows; D(E) = +60° (from the astronomical north), I(D) = -25°, κ = 2 and α = 34°.

As has been seen, the NRM of these basalts show rather wide scattering, then each NRM was classified into six polarity classes according to thier VGP latitudes calculated due to each NRM direction; as N, (N) and O(N) for normal NRM and R, (R) and O(R) for reversed respectively (Domen et al 1977). The classified NRM thus obtained is shown in Table 1.

Table. 1. Classified NRM of Shimonoseki upper Pleistocene basalts (due to VGP latitude).

Polarity Class	D(E)	I(D)	κ	$\alpha_{95\%}$	Nos. of Samples
N	+30°	+56°	-	-	1
(N)	+14	+27	4	55	4
O(N)	+53	-19	3	49	6
R	no sample was found in the present collection				
(R)	+172	-9	-	-	1
O(R)	+97	-56	21	15	6

Such a classification does still not reduce the scattering of NRM directions at this location as shown above. Then the polarity classification in another attempt was made such that the longitudinal situation of VGP is put into six classes; I, +II, +III, -II, -III and IV as shown in Fig. 1. But this classification due to VGP longitude made no improvement. Furthermore, a combination of these classifications due to both latitude and longitude was made, then somewhat concentrated NRM directions were found in two caltgories; -III,O(N) and -III,O(R) which are shown in Table 2.

Table 2. Classified NRM of Shimonoseki basalts (2) (due to both VGP latitude and longitude)

Polarity Class	D(E)	I(D)	κ	$\alpha_{95\%}$	Nos. of Samples
-III, O(N)	+72°	-14°	32	17°	4
-III, O(R)	+100	-53	23	17	5

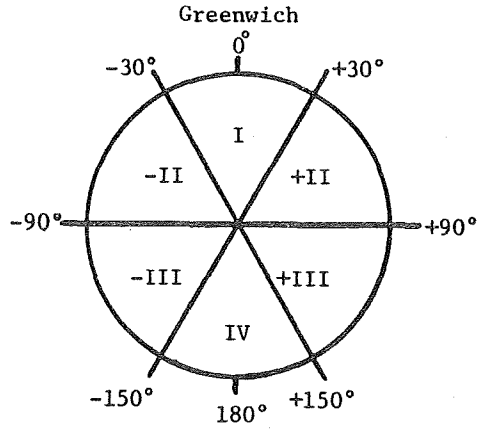

Fig. 1. Polarity classification of NRM by its VGP, which is identified its longitude.

Anyhow most of all specimens are obliquely magnetized *in situ* at this locality, and father investigations such as magnetic stability tests, and Js-T and X-ray analyses etc. should be required in the near future.

Reference.

Domen, H., H. Muneoka and T. Yokoyama (1977) Bull. Fac. Educ., Yamaguchi Univ. 27 (Part 2), in press.

TERTIARY PALEOMAGNETISM OF THE RYUKYU ISLANDS AND ITS RELEVANCE TO THE DEVELOPMENT OF THE PHILIPPINE BASIN

Sadao SASAJIMA

Department of Geology and Mineralogy,
University of Kyoto, 606, Kyoto, Japan

1. Introduction

The paleomagnetic study on the Ryukyu Islands so far published is so scarce compared with that on the Honshu Island. But it is very important not only for comparative study with the Honshu Arc but also to clarifying the origin and development of the marginal seas. Although much progress has been achieved in the marine earth sciences of the Philippine Sea, many problems are still under debate; especially of the West Philippine Basin.

The Eocene and Miocene paleomagnetism on the Ryukyu Islands can be expected to have close relation with the origin of the West Philippine Basin that is determined to be early Eocene in its age. I have carried out paleomagnetic investigations of Eocene rocks in the southwestern part of Ryukyu Islands, including Ishigaki-, Kohama-, and Iriomote-jima. Okinawa-jima which is tectonically separated from the islands mentioned above with the Miyako depression, a prominent structural zone, has been also studied paleomagnetically.

Further works on Miocene rocks of Kumejima island supplementing the previous paleomagnetic result (1965) has been also carried out.

2. Paleomagnetic results

Recently the Nosoko Formation of Ishigaki-jima has been confirmed to be Eocene in age by the discovery of *Nummulites* in several layers (Shirao et al., 1976). About ten years ago when the writer reported paleomagnetic results of the Miocene and Pliocene series of the Ryukyu Islands (Sasajima and Shimada, 1965), the Nosoko Formation was thought presumably Miocene in age. Therefore, the data and discussion described about the Nosoko Formation in that paper should be revised as those appeared in the present paper.

In Kohama- and Iriomote-jima, there distribute pyroxene andesite lavas and sills which are correlated to the Nosoko Formation. Paleomagnetic sampling of the Nosoko Formation in Ishigaki-jima and of its correlatives in Kohama- and Iriomote-jima was undertaken in 1975 and 1976. In the northeastern part of Okinawa-jima, the upper part of the Kayo Formation, Eocene in age (Konishi et al., 1973), was also sampled at 12 sites along near coastline outcrops from Abu to Teima town, east of Nago-city. All of sandstone samples taken from flysh type Kayo Formation were too weak or soft magnetically to get reliable remanence data thus they were discarded. On the contrary, NRMs of most bluish gray siltstone were rather strong and stable after partial AF demagnetization in the peak field of 250∿300 Oe.

The obtained paleomagnetic properties of samples are summarized in Table 1. In this table, NRM data of the Kume-jima

Age	locality		lat.(N)	long.(E)	rock kind	number, Sp. (site no.)	Dec.	Inc.	k	α_{95}	VGP φ(N)	VGP λ		δp	δm
EOCENE	Ishigaki-jima	(1)	24°24'	124°12'	tuff	13	27.1	52.4	71.8	5.1	64.7	172.9	W	4.8	7.0
		(2)			pyroxene And.	4	211.4	27.0	181.8	9.2	58.9	133.0	W	5.4	10.6
		(3)			Welded tuff	6	243.0	-57.3	49.0	9.6	35.4	176.2	W	10.2	14.0
		(4)			Pyroxene And.	7	245.8	-53.4	56.5	6.8	40.8	152.4	W	4.6	10.6
		(5)			ditto	7	229.5	-53.4	80.5	6.7	46.1	170.5	W	6.5	9.3
	Kohama-jima	(6)	24°18'	124°00'	Two Pyr. And.	5	57.7	36.8	64.5	9.1	36.9	154.1	W	6.3	10.9
		(7)			ditto	5	51.3	30.6	93.0	7.9	41.5	148.4	W	4.9	8.8
	Iriomote-jima	(8)	24°24'	124°00'	Two Pyr. And.	19	43.0	31.0	31.6	6.1	49.2	143.3	W	3.8	6.8
	Okinawa-jima	(9)	26°32'	128°05'	Siltstone	14 (4)	5.9	48.3	34.9	6.8	84.1	170.7	W	5.8	8.2
	Mean value					(8)	47.7	43.3	26.0	11.1	46.9	157.8	W	8.6	13.8
MIOCENE	Okinawa-jima	(10)	26°26'	127°54'	Porphylite	21	- 12.5	52.8	14.3	8.7	77.0	74.3	E	8.3	12.0
		(11)	26°26'	127°58'	ditto	10	2.0	46.9	63.2	5.0	87.5	178.0	W	4.3	6.4
		(12)	26°34'	128°00'	Qz-Porphyry	6	155.5	-55.4	78.1	7.6	66.4	71.0	E	7.7	10.9
	Kume-jima	(13)	26°18'	126°48'	Horb. And.	10	- 4.1	26.7	14.2	13.3	77.2	41.1	W	7.8	14.4
		(14)			ditto	12	2.1	47.6	16.3	10.6	87.7	142.6	E	8.9	13.8
		(15)			Pyr. And.	11	2.5	44.1	10.5	15.0	87.3	115.8	W	11.8	18.7
		(16)	26°19'	126°48'	Pyr. And.	10	17.4	36.2	10.4	15.7	72.9	132.2	W	10.6	18.3
		(17)			ditto	7	19.3	34.0	21.9	13.2	70.6	130.0	W	8.6	15.1
		(18)	26°19'	126°46'	Pyr. And.	14	- 9.5	47.4	18.1	9.6	81.3	47.0	W	8.1	12.4
		(19)	26°19'	126°46'	ditto	10	15.8	43.4	169.8	3.7	75.7	144.7	W	2.9	4.6
	Mean value					(10)	5.8	43.4	32.1	9.2	88.5	163.0	W	5.4	11.4

Table 1: (1) Yarabusaki, (2) Miyara, (3) Kabira-ishizaki site 1, (4) ditto site 2, (5) ditto site 3, (6) Komazaki site 1, (7) ditto site 2, (8) Nobaru-zaki, (9) West Abu, (10) Shiokawa, (11) Yabu, (12) Yohuke, (13) Shimaziri site 1, (14) ditto site 2, (15) ditto site 3, (16) Zenda site 1, (17) ditto site 2, (18) South Gima, (19) Ahra-hama

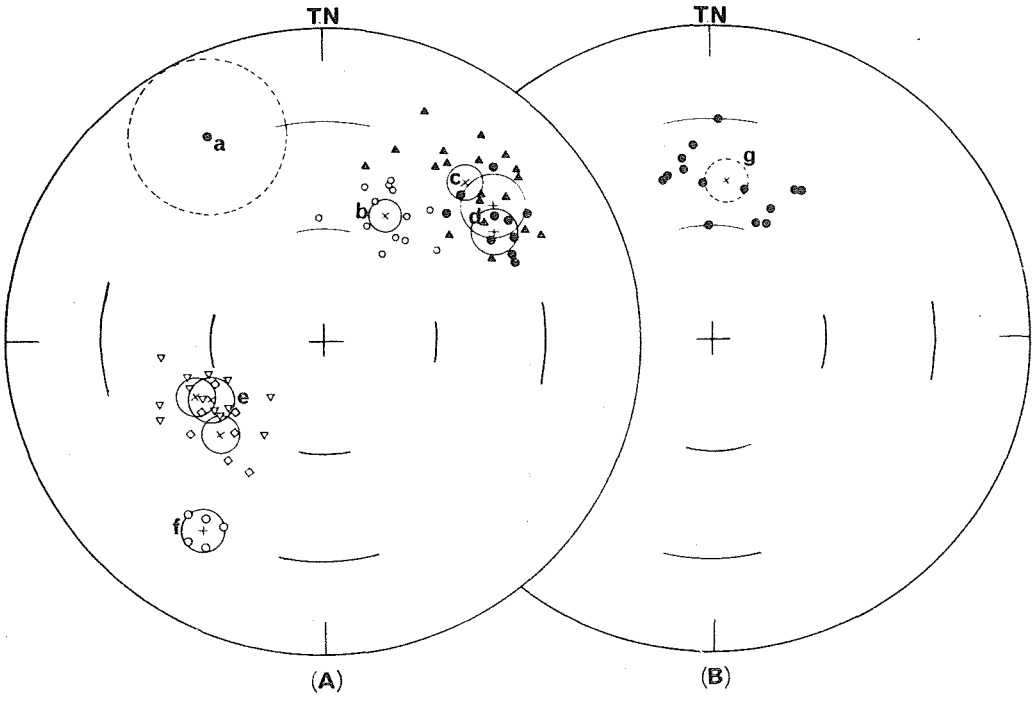

Fig. 1: Directions of NRMs obtained from the S. W. Ryukyu sub-arc (A), and from Okinawa-jima (B).
a: Tamatorizaki, b: Yarabusaki, c: Iriomote-jima, d: Kohama-jima, e: Kabiraishizaki, f: Miyara, g: West Abu.

andesites, Nosoko Formation and its correlatives are those values after the demagnetization of the peak field in 150 Oe. Most of Miocene NRMs are of normal polarity excepting one with reversed polarity, but the average of the all NRMs gives the direction almost parallel with that of the axial dipole field at the area.

Fig. 1-(A) shows direction of NRMs obtained from various sites of the S. W. Ryukyu sub-arc. From the figure it is apparent that the direction from Tamatorizaki (a) is quite anomalous. This datum is quoted to point out the previous erroneous remanent direction by comparing with the other newly obtained reliable directions. The anomalous direction can be regarded as beeing affected by any local fault movement. It is also shown in the figure that about a half directions with normal polarity are almost antipodal with another half with reversed polarity, suggesting a positive evidence of reliability of the paleomagnetic data.

In Fig. 1-(B), direction of NRMs obtained from Okinawa-jima is shown. Virtual geomagnetic pole positions for all these NRMs are shown in Fig. 2, together with the Eocene paleomagnetic pole for Southwest Honshu (A) (Sasajima et al., 1968). In the figure is also plotted the Paleogene geomagnetic pole for Eurasia (B) (McElhinny, 1973).

3. Discussion

As seen clearly in Fig. 2, the Eocene paleomagnetic north pole for the S. W. Ryukyu sub-arc is significantly differ from that for the Okinawa-jima. A simple explanation of the fact is that the striking intra-arc VGP difference has been caused by the 40° clockwise rotation of the S. W. sub-arc relative to the N. E. sub-arc during Eocene through the earliest Miocene. As paleomagnetic inclinations of the two arcs nearly equal for that of the centered axial dipole field, the rotation axis is supposed to be roughly vertical. Such a bending of the Ryukyu Arc might have been controled by the Miyako depression, of which successive activity is found in the extensive oceanographic investigation by Wageman et al. (1970). From the figure it is also apparent that the clockwise rotation of mean VGP for the S. W. Ryukyu sub-arc is larger in magnitude in comparison with that for S. W. Honshu (Sasajima et al., 1968).

If we accept, as a working hypothesis, the assumption that the paleomagnetic directions of the southwestern part of three islands and Okinawa-jima truly represent those for the S. W. sub-arc and N. E. sub-arc respectively, the schematic paleomagnetic relation to the trench-arc system of the Japanese area is drawn as shown in Fig. 3. The differences between the S. W.- and N. E.-Ryukyu sub-arc bear analogy to those existing between the S. W.- and N. E.-Honshu in various geotectonic and geohistoric point of views. Whereas, it should be noted that a basic difference between the two bendings lies on the fact that the age concerned to the former bending is considerably younger than that to the latter ones; the age of the former bending is presumed to be Oligocene (38~26 m.y. BP.), but that of the latter is assigned to the middle of Late Cretaceous (90~80 m.y. BP.) by Kawai et al. (1971).

It may not be fortuitous that the Eocene paleomagnetic directions for the four sub-arcs are in good conformity generally with the related skeletons of both island arcs and trenches respectively. It could be implied that the major part of the present arcuate structure of Japanese islands was almost completed around Oligocene period, and therefore Miocene to Recent paleomagnetic poles for these sub-arc point to around the centered dipolar pole, except for some virtual geomagnetic poles affected by any local tectonic movements. From the presently available knowledges it may be very difficult to explain fully the reason why such zigzag or arcuate structure occurred a series of two connected island arcs. The writer's idea even tentative is that the driving force might be originated from the directional change of Pacific-Philippine plate motion possibly occurred at about 40 m.y. ago.

Kobayashi and Isezaki (1976) has proposed a plausible model to explain the origin and evolution of marginal basins and trench-arc systems around Japan including the Philippine Sea. At about 45 to 40 m.y. BP. they have assumed about 40° anticlockwise rotation of the Philippine Basin caused by the southward drift of the Honshu and Ryukyu Islands, of which driving force has been resulted from the opening of the Japan basin. If we accept this assumption, the clockwise rotation of the S. W. Ryukyu sub-arc can be explained by the suspected right-lateral motion between the S. W. Ryukyu ridge to north and Philippine Sea plate to south. However, the age they assumed seems to be, more or less, older than the period when the clockwise rotation of the S. W. Ryukyu sub-arc is inferred to have occurred.

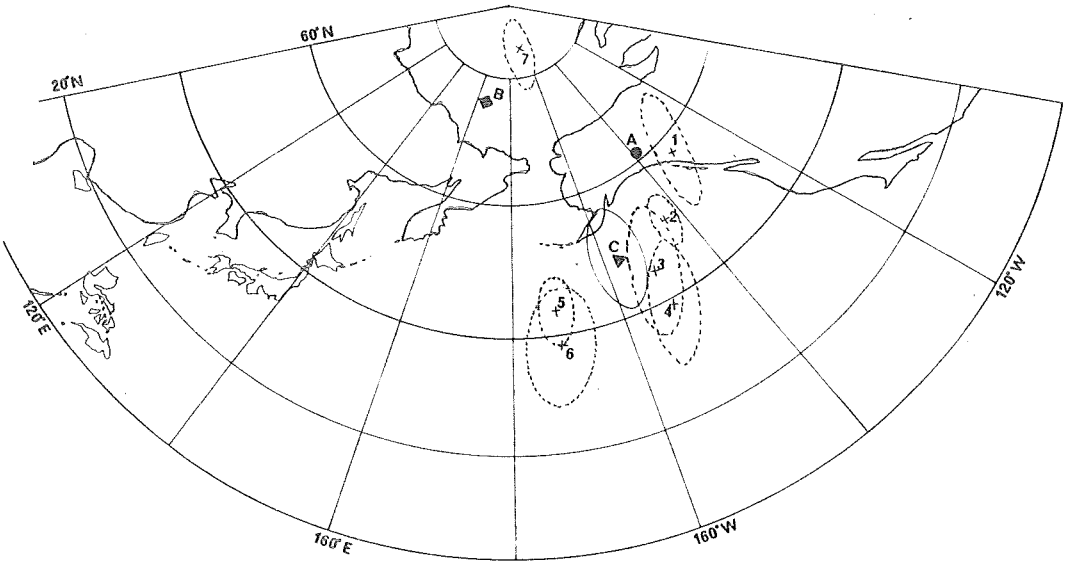

Fig. 2: Map showing VGPs for Ryukyu Islands and S. W. Honshu Island. 1. Miyara, 2. Iriomote, 3, 4. Kohama-jima, 5. Yarabusaki, 6. Kabira, 7. Abu, Okinawa-jima, A. S. W. Honshu, B. Euroasia, C. Mean for S. W. Ryukyu Islands.

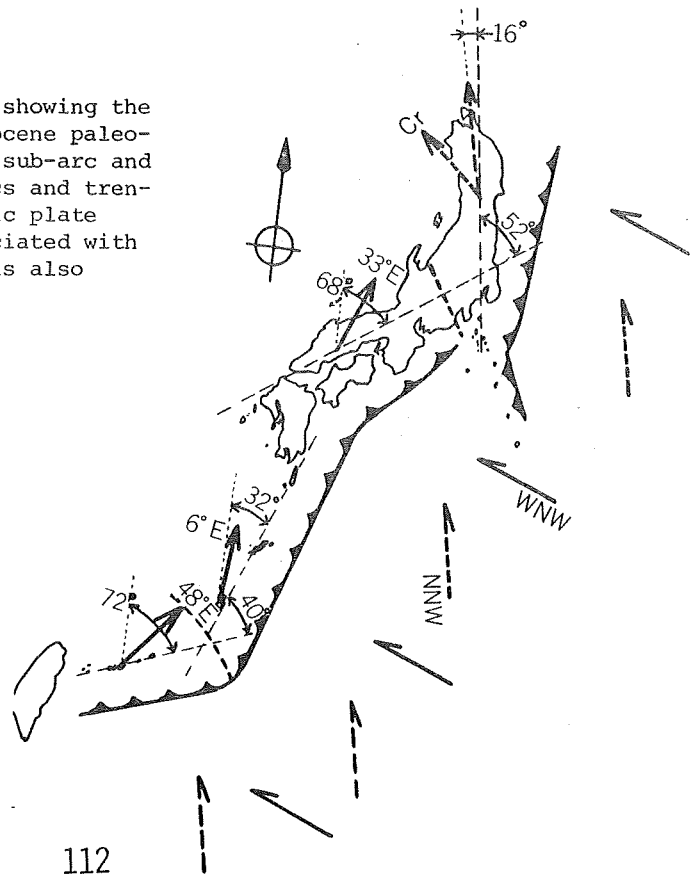

Fig. 3: Schematic tectonic map showing the relation between the Eocene paleomagnetic directions of sub-arc and the skeleton of sub-arcs and trenches. Change of oceanic plate motion presumably associated with the arcuate structure is also shown.

Two years ago the writer made a paleomagnetic summary concerning to the origin and development of the Philippine Sea basing on the data so far available from the surrounding islands (Sasajima and Yaskawa, 1975). From a comparative study of the Paleogene paleomagnetic data, including S. W. Honshu, Ryukyu Islands, Guam, Saipan, Luzon and its neighbouring small island (Hsu and Scharon, 1970), Australia (Wellman et al., 1969), it was suggested that the Philippine Sea was originated at about 20° South Latitude or near equator during Paleogene period. Very recently Louden (1976, 1977) has reported positive evidences supporting the hypothesis on the basis of paleomagnetism of DSDP cores and phase shifting of magnetic anomaliesin the West Philippine Basin.

Another important conclusion of his result is a clockwise rotation of the West Philippine Basin by 60°, supporting the similar rotation of paleomagnetic direction obtained from Guam (Larson et al., 1975) and the hypothetical clockwise rotation of the Philippine Sea previously proposed by Uyeda and Ben-Avraham (1972). Much detailed paleomagnetic studies on many islands in and surrounding the Philippine Sea are required before its origin and development can be understood without any reservation.

References

Hsu, I. and L. Scharon(1970), U. S.-Japan Seminar on Paleomagnetism, Hawaii

Kawai, N., T. Nakajima and K. Hirooka (1971), J. Geomag. Geoelectr. 23, 267-293.

Kobayashi, K. and N. Isezaki (1976), Geophys. Mono. 19, Amer. Geophys. Union, 235-251.

Konishi, K., T. Ishibashi and K. Tsuruyama (1973), Sci. Rep. Kanazawa Univ., 18, 43-53.

Larson, E. E., R. L. Reynolds, M. Ozima, Y. Aoki, H. Kinoshita, S. Zashu, N. Kawai, T. Nakajima, K. Hirooka, K. Merrill and S. Levi (1975), Geol. Soc. Amer. Bull. 86, 346-350.

Louden, K. E. (1976), Geophys. Monograph 19, Am. Geophys. Union. 253-267.

———— (1977), J. Geophys. Res. 82, 2989-3002.

McElhinny, M. W. (1973), Cambridge Univ. Press, 244.

Sasajima, S. and M. Shimada (1965), Mem. Coll. Sci., Univ. Kyoto Ser. B, 32, 89-101.

————, J. Nishida and M. Shimada (1968), Earth Planet. Sci. Lett., 5, 135-141.

———— and K. Yaskawa (1975), The 82th Annual Meeting, Geol. Soc. Japan, 137-145. (in Japanese)

Shirao, M., N. Doi and H. Nakagawa (1976), Geological studies of the Ryukyu Islands, 1, 21-33. (in Japanese)

Wageman, J. M., T. W. C. Hilde and K. O. Emery (1970), Bull. Am. Assoc. Petrol. Geol. 54, 1611-1643.

Wellman, P., M. W. McElhinny and I. McDougall, (1969), Geophys. J. Roy. astr. Soc., 18, 371-395.

Uyeda, S. and S. Ben-Avraham (1972), Nature, 240, 176-178.

ON THE NATURAL REMANENT MAGNETIZATION OF COLUMBIA RIVER TERTIARY BASALT IN WASHINGTON, U. S. A.

Haruo DOMEN and Hiroshi MUNEOKA

Institute of Physical Sciences, Faculty of Education,
Yamaguchi University, Yamaguchi 753, Japan.

Several hand samples were taken from the late-Tertiary lavas in three sections of Columbia River basalts after the previous work (Domen 1965, 1966). The remanent magnetization of these samples has been examined and three polarities for Grande Ronde River section, two polarities for Steptoe Canyon section and two for Asotin Creek section can be added to Campbell's results (Campbell and Runcorn 1956).

Obtained data of NRM directions with statistical treatment that due to Fisher (Fisher 1953) were shown in Table 1; k is a measure of the precision and α is the cone of confidence for 95%.

Table 1. Directions of magnetization of lava flows and those polarity classes.

Site	Elevation in feet	D(E)*	I(D)	k	α	Polarity Class
Grande Ronde River						
1	3,700	-9°	+42°	20	14°	N
2	2,500	-147°	-67	43	8	R
3	1,260	-23	+73	50	9	N
Steptoe Canyon at Snake River						
4	1,580	-77	+82	24	54	(N)
5	740	+130	-32	7	25	O(R)
Asotin Creek						
6	842	-106	+63	6	57	O(N)
7	762	-179	-75	32	22	R

* D(E) is measured from the astronomical north.

The VGP was calculated by each direction of magnetization and according to the obtained VGP, the magnetization of the test specimen is classified into six polarity classes such as N, (N) and O(N) for the normal NRM and R, (R) and O(R) for reversed NRM respectively (Creer and İspir 1970, Domen et al 1977). These classified polarities thus obtained are added to the result given by Campbell and Runcorn mentioned above, as shown in Fig. 1.

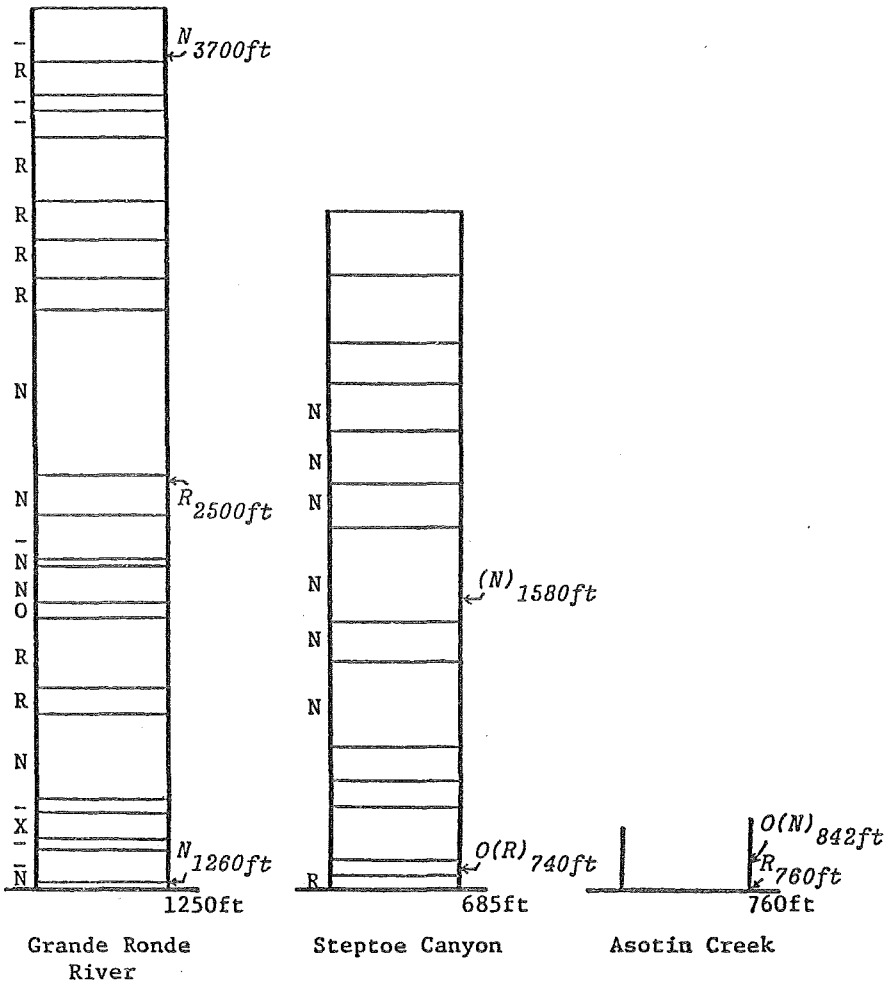

Fig. 1. NRM Polarity of Columbia River Tertiary basalt. Polarity shown at the left side of each column is refered with Campbell and Runcorn, 1956. The right italicized is for this work. Numeral shows the elevation from the sea-level.

References

Campbell, C.D. and S.K. Runcorn (1956) J. G. R. 61, 449-458.
Creer, K.M. and Y. İspir (1970) Geophys. J. R. astr. Soc. 20, 127-148.
Domen, H. (1965) Bull. Fac. Educ., Yamaguchi Univ. 14 (Part 2), 35-44.
Domen, H. (1966) ibid. 15 (Part 2), 9-12.
Domen, H., H. Muneoka and T. Yokoyama (1977) ibid. in press.
Fisher, R.A. (1953) Proc. R. Soc., A, 217, 295-305.

ON NATURAL REMANENT MAGNETIZATION OF KARATSU CENOZOIC BASALT, SAGA PREFECTURE, NORTHERN KYUSHU ISLAND, JAPAN.

Haruo DOMEN and Hiroshi MUNEOKA

Institute of Physical Sciences, Faculty of Education,
Yamaguchi University, Yamaguchi 753, Japan.

Some ten hand samples of Cenozoic basalts come from two separate sites; Tate-Gami and Chinzei, aparted about 5 km each other, at Karatsu Township, east Matsuura Peninsula, Saga Prefecture, northern Kyushu Island, west Japan. The age of those basalt samples submitted to the present study is estimated as the lower Pleistocene from the geological view points.

All of these NRM obtained so far as the present work is concerned are reversed. Mean NRM directions for each site and the grand mean of them are shown in Table 1.

Table 1. Mean NRM for Karatsu Cenozoic basalts.

Site	D(E)*	I(D)	κ	α	Nos. of Samples
Tate-Gami	-179°	-30°	25	8°	15
Chinzei	+173	-54	21	5	50
Grand Mean	+176°	-49°	59	2°	65

* measured from the astronomical north.

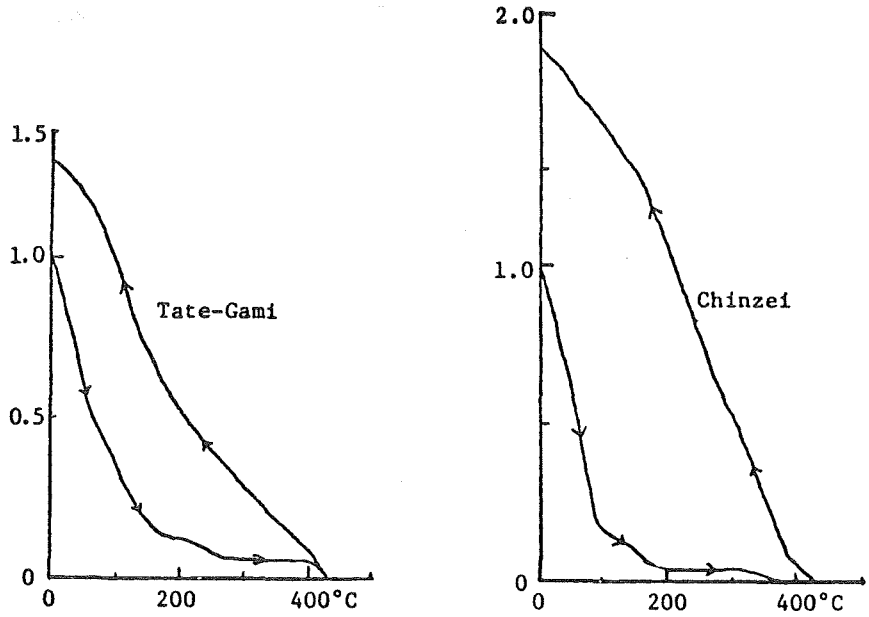

Fig. 1. Typical Js-T curves for Karatsu Cenozoic basalts (carried out in open air).

Js-T analysis was carried out on ferromagnetic minerals extracted from some of these rock smaples. The analysis shows that the main ferromagnetic constituents of test specimens come from both sampling sites have rather low Curie points, say 100 ~ 200°C, as shown in Fig. 1.

As has been seen in Table 1, the NRM of these samples shows the truly reversed polarity with very good concentrations which is due to the phase of low Curie points, and it is not so easily able to draw a conclusion that those NRM are the indication of the geomagnetic field reversals at that time the rocks examined were solidified.

Several stability tests on these samples are now being undertaken.

PALEOMAGNETISM AND CHEMICAL COMPOSITION OF CRETACEOUS GRANITIC ROCKS

H. ITO and K. TOKIEDA
(Physics Department, Shimane University, Matsue)

Natural remanent magnetizations of Cretaceous granitic rocks collected from the southwestern part of Hokkaido, Kitakami and Uetsu Districts have significantly been stable. The mean directions of stable remanent vector of each sampling site are shown in Fig. 1. The mean directions of stable remanent vector from Hokkaido were northeasterly and averaged direction is 62° in declination and 54° in inclination, and those from the Kitakami mountainland were northwesterly and averaged direction is -42° in declination and 48° in inclination. In Uetsu District, the directions of stable remanent magnetization were confusingly distinct from a granitic body to body.

The ratios of Fe_2O_3/Fe_2O_3+FeO were calculated from the published chemical analyses in Japan compiled by Shibata (1967). The ratios of Fe_2O_3/Fe_2O_3+FeO of granitic rocks from the Kitakami mountainland are apparently high as compared with those of rocks from the other regions as seen in Fig. 2. It is particularly striking in the Oshima, Hokubu-Kitakami and Kinkasan granitic bodies. These bodies are significantly exposed in the ocean-side of the Kitakami District.

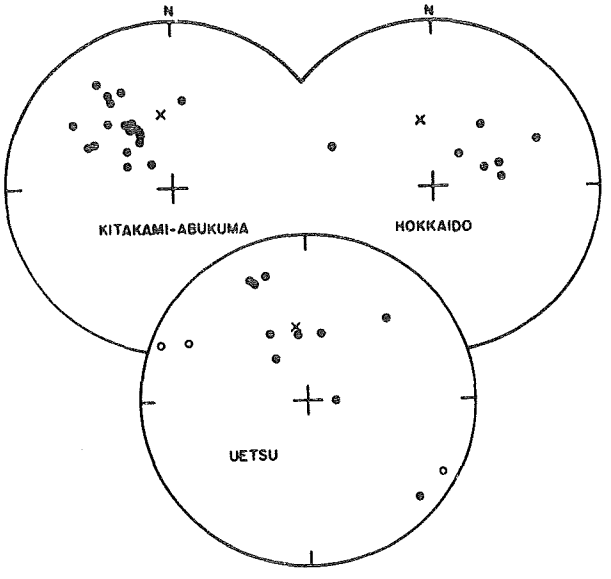

Fig. 1 Mean directions of NRM after A.C. demagnetization of 100 oe or 200 oe.
Solid circles indicate positive inclination.
Open circles indicate negative inclination.
Cross mark is the present geomagnetic field direction.

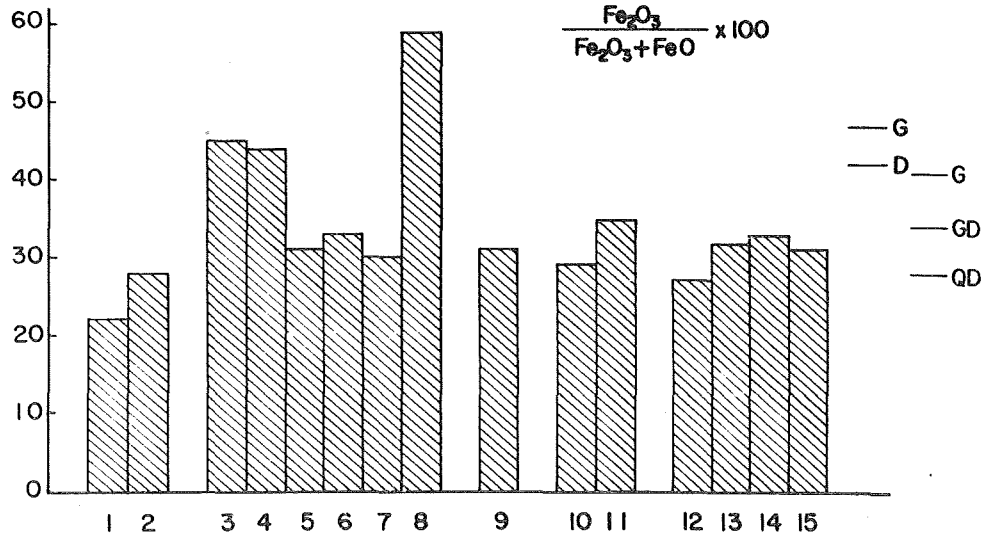

Fig. 2 The ratios of Fe_2O_3/Fe_2O_3+FeO x 100.
1. Southwestern part of Hokkaido 2. Okujiri Island
3. Oshima rock body 4. Hokubu-Kitakami rock body
5. Okirai rock body 6. Kesengawa rock body
7. Senmaya rock body 8. Kinkasan 9. Abukuma
10. Jitsukawa rock type 11. Kusozu rock type
12. Kanmon rock type 13. Inbi rock type
14. San-in rock type 15. San-yo rock type

Kanaya and Ishihara (1973) measured magnetic susceptibility of a large number of granitic rocks in Japan. They noticed that there ia a regional variation of the magnetic susceptibility between the major granitic units in Japan, and also noted that the magnetic susceptibility is high in the ocean-side of the Kitakami mountainland. This is consistent with the result obtained from the ratios of Fe_2O_3/Fe_2O_3+FeO.

If the main constituent of oxide minerals with the high magnetic susceptibility is magnetite (Kanaya and Ishihara, 1973), and if existence of magnetite become an indicator of the depth at which granitic rocks were initially empaced (Kawai, 1957), granitic rocks with the high magnetic susceptibility or high ratio of Fe_2O_3/Fe_2O_3+FeO should be to have initially emplaced at shallow depth below the surface of the earth's crust.

Granitic bodies have usually been situated at the surface of the crust by upward displacements after the formation. In case the depth at which granitic rocks were initially formed was shallow, the upward displacement should not be conspicuous. In the Kitakami mountainland, assuming that the granitic rocks with the high values of the magnetic susceptibility had initially emplaced at the shallow depth below the surface and those with the low values had formed at more deep level, the Kitakami mountainland should be to have tilted to the ocean-side with gradual uplifts of the granitic rocks.

Paleomagnetic data from Northeast Honshu and Hokkaido are likely to be supportive of a working hypothesis mentioned above as shown in Fig. 3. It is therefore concluded from the paleomagnetic data that the Kitakami mountainland had a tilt of about 30° to the ocean-side and a tilting axis is taken in N20°W direction. In contrast with this, it is noted that the southwestern part of Hokkaido had a tilt of about 38° to the Japan Sea side and a tilting axis is taken in N31°E direction. However, we could not observe significant movements of the Uetsu block as a whole from the directions stable remanent vector of the granitic rocks. It means that this region might be affected by more local and complicated movements.

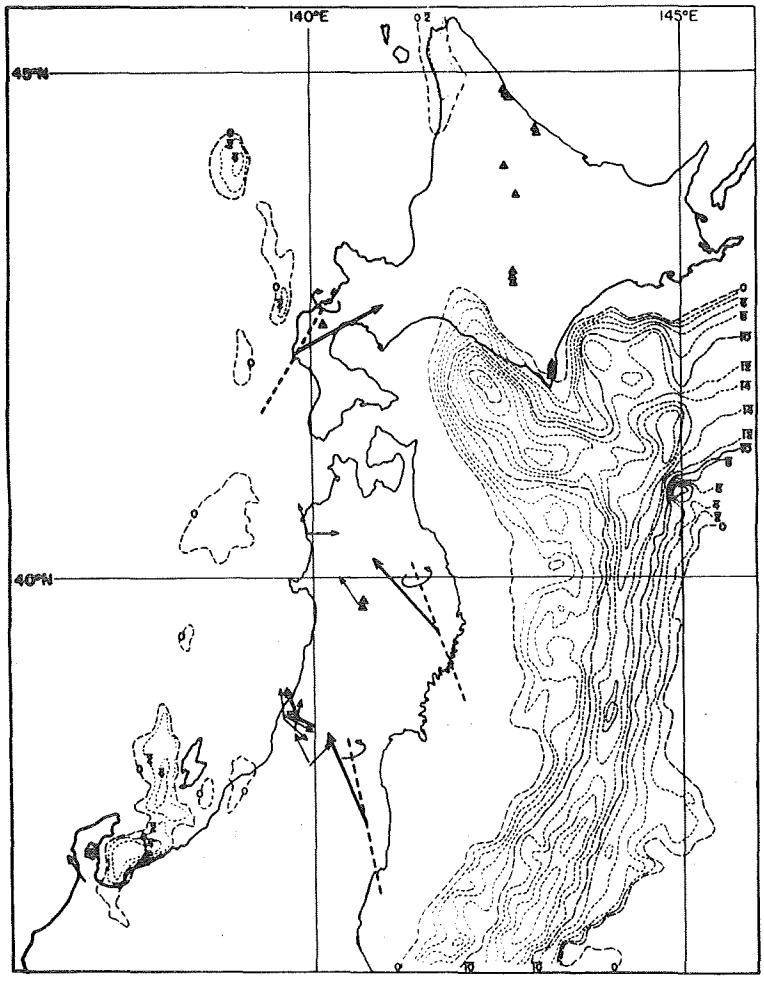

Fig. 3 Schematic tilting direction of the Kitakami mountainland and the southwestern part of Hokkaido. Free Air Anomaly is shown by dotted curves (Tomoda, 1973).

References

Kanaya, H. and S. Ishihara: Regional variation of magnetic susceptibility of the granitic rocks in Japan, Jour. Jap. Assoc. Min. Petr. Econ. Geol., 60, 211-224, 1973, (in Japanese with English abstract).

Kawai, N.: Magnetism of the earth crust, Jour. Geomag. Geoelectr., 9, No 3, 140-156, 1957.

Shibata, H.: Nihon-Gansekishi 2, Plutonic Rocks (2), Asakura Shoten, 1967.

Tomoda, Y.: Maps of Free Air and Bouguer Gravity Anomalies in and around Japan, Univ. Tokyo Press, 1973.

Sr ISOTOPIC STUDIES OF THE VOLCANIC ROCKS FROM THE LINE ISLANDS

Jun-ichi MATSUDA

Department of Earth Sciences, Faculty of Science,
Kobe University, Nada, Kobe 657, Japan

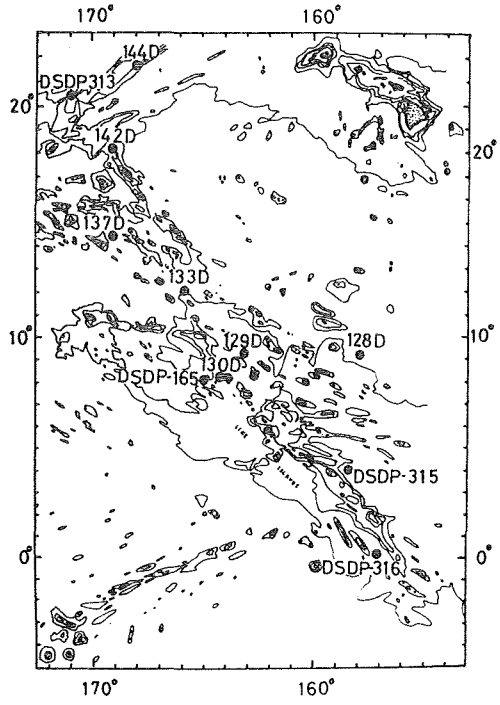

Fig. 1 General map

1. Introduction

A hot spot theory was first proposed for the Hawaiian volcanic chain by Wilson (1963) and then extended by Morgan (1972) to explain other volcanic chains, the Austral-Marchall-Gilbert and the Tuamotu-Line. According to their model, the volcanic chain is formed on the moving lithosphere by a "hot spot" fixed in the lower mantle. The Hawaii-Emperor chain seems to be well explained by the "hot spot" theory. Radiometric ages of volcanic rocks in Hawaii (McDougall, 1971; Clague and Dalymple, 1975) and the fossil ages (DSDP scientific staff, 1971) agree with the results expected from the hot spot origin of the Hawaii-Emperor chain.

However, the fossil ages obtained from DSDP holes in the central and south part of the Line chain were almost the same, suggesting that the Line chain was not originated in the hot spot (DSDP scientific staff, 1974). The ^{40}Ar-^{39}Ar ages obtained by Saito and Ozima (1977) indicated that there is not a simple age progression along the Line chain. Under such circumstances Sr isotope and trace element concentration studies of these rocks should be interesting.

2. Samples

The samples were first used for the ^{40}Ar-^{39}Ar dating. The sampling locations can be found in Table 1 and Fig. 15 in their paper and are shown here again (Fig. 1, Table 1). These samples except DSDP315A are alkali basalts which are common in the seamount.

3. Results

The results are listed in Table 2. The initial ($^{87}Sr/^{86}Sr$) ratios are calculated from Rb/Sr and ^{40}Ar-^{39}Ar ages. In case

Table 1 Sampling locations for rocks from the Line islands

Sample	Rock	Locality	
		long.	lat.
128D	mugearite	9°15'N	158°20'W
129D	olivine-titanaugite basalt	9°20'N	163°10'W
130D	olivine-titanaugite basalt	8°20'N	164°22'W
133D	alkali-olivine basalt	12°04'N	165°50'W
137D-9	aegirine phonolite	14°27'N	168°59'W
137D-10	aegirine phonolite	14°27'N	168°59'W
142D	mugearite	18°00'N	169°05'W
144D	alkali dolerite	21°32'N	167°56'W
DSDP-165	alkali basalt	10°07'N	164°51.6'W

that the ^{40}Ar-^{39}Ar age was not obtained, the fossil age is used for age correction. The initial ($^{87}Sr/^{86}Sr$) ratio is in general low compared with the measured rare ($^{87}Sr/^{86}Sr$) ratio because of large Rb/Sr and old age. The ($^{87}Sr/^{86}Sr$) ratios after HCl leaching are also listed for some samples. This leaching technique is same as that descrived by O'nions and Pankhurst (1976) except that we used about 1 g at the beginning of the chemical treatment. The absence of ($^{87}Sr/^{86}Sr$) ratios after leaching for some samples is due to the failure of the measurement.

4. Discussion

(4-1) Main chain

The measured ($^{87}Sr/^{86}Sr$) ratios of 142D, 133D and 130D which are located at the northern part of the main chain are quite variable. The ($^{87}Sr/^{86}Sr$) ratio (0.7029) of 130D is as low as that of the typical oceanic ridge basalt. The initial ($^{87}Sr/^{86}Sr$) ratio (0.7028) and the ($^{87}Sr/^{86}Sr$) ratio after leaching (0.7031±7) confirm that 130D had certainly low ($^{87}Sr/^{86}Sr$) ratio when it was formed. On K-Rb and K-Sr diagram (Fig.2) 130D occupies the position near that of alkali basalt. The measured ($^{87}Sr/^{86}Sr$) ratio of 142D is 0.7039, but the initial ($^{87}Sr/^{86}Sr$) ratio of it is 0.7033. The ($^{87}Sr/^{86}Sr$) ratio after leaching (0.7031±5) may suggest that HCl treatment leached out the stored radiogenic Sr from the old age sample. As shown later the ($^{87}Sr/^{86}Sr$) ratio after leaching is comparable with or lower than the initial ($^{87}Sr/^{86}Sr$) ratio for most samples. Though HCl leaching is very effective in excluding alteration effect of young basalt (O'nions and Pankhurst, 1976), it is doubtful to apply such old age samples as those of the Line island. An old age sample in oceanic area is more or less altered and HCl leaching may affect not only altered minerals, but also radiogenic Sr because radiogenic Sr occupies unstable position in minerals.

The measured ($^{87}Sr/^{86}Sr$) ratio of 133D is high (0.7052). The initial ($^{87}Sr/^{86}Sr$) ratio is also high (0.7051). The color of 133D was yellow and this sample is thought to be hardly altered. The Sr content of 133D after leaching is

Table 2 ($^{87}Sr/^{86}Sr$) ratios, K, Rb and Sr contents of the rocks from the Line islands

Sample	144D	142D	137D-9	137D-10	133D	129D
Rock type	alkali delerite	mugearite	aegirine phonolite	aegirine phonolite	alkali-olivin basalt	olivin-titanaugite basalt
K (ppm)	11800	28000	45900	51600	12200	10700
Rb (ppm)	39.4	43.3	163.3	187.3	13.6	36.4
Sr (ppm)	432	352	1094	1345	329	628
K/Rb	299	646	281	275	897	294
Rb/Sr	0.0911	0.1229	0.1492	0.1392	0.0413	0.0580
$(^{87}Sr/^{86}Sr)$	0.7039±1	0.7039±2	0.7042±1	0.7050±1	0.7052±2	0.7037±2
$(^{87}Sr/^{86}Sr)_0$	0.7036±1	0.7033±2	0.7039±1	0.7047±1	0.7051±2	0.7035±2
$(^{87}Sr/^{86}Sr)^*$		0.7031±5	0.7041±5	0.7044±8		0.7036±9
Ar-Arage (m.y.)**	82.4±3.7	127.5±5.0	56.6±0.8	55.8±1.8	84.4±0.9	~80 (fossil)
$(^{40}Ar/^{36}Ar)_0^{**}$	277.8±9.1	280.5±6.1	245.8±8.0	277.2±10.9	268.7±2.8	

Table 2 (continued)

Sample	130D	128D	DSDP165	DSDP315A$_{31}$	DSDP315A$_{34}$
Rock type	olivin-titan augite basalt	mugearite	alkali basalt	titanaugite coarse basalt	titanaugite coarse basalt
K (ppm)	11500	7800	17300	3100	1300
Rb (ppm)	33.6	16.1	29.9	3.7	0.9
Sr (ppm)	766	340	758	258	254
K/Rb	342	484	578	838	1444
Rb/Sr	0.0438	0.0473	0.0394	0.0143	0.0035
$(^{87}Sr/^{86}Sr)$	0.7029±2	0.7035±1	0.7039±1	0.7037±1	0.7039±2
$(^{87}Sr/^{86}Sr)_0$	0.7028±2	0.7034±1	0.7038±1	0.7037±1	0.7039±2
$(^{87}Sr/^{86}Sr)$*	0.7031±7	0.7030±9	0.7033±4		0.7027±5
Ar-Arage (m.y.)**	(71.5±3.1)	(49.0±9.2)	(61.1±2.1)	92***	92***
$(^{40}Ar/^{36}Ar)_0$**	298.6±3.2	274.7±9.2	255.5±10.9		

* $(^{87}Sr/^{86}Sr)$ ratio after HCl leaching
** Saito and Ozima (1977)
*** Lanphere and Darymple (1975)

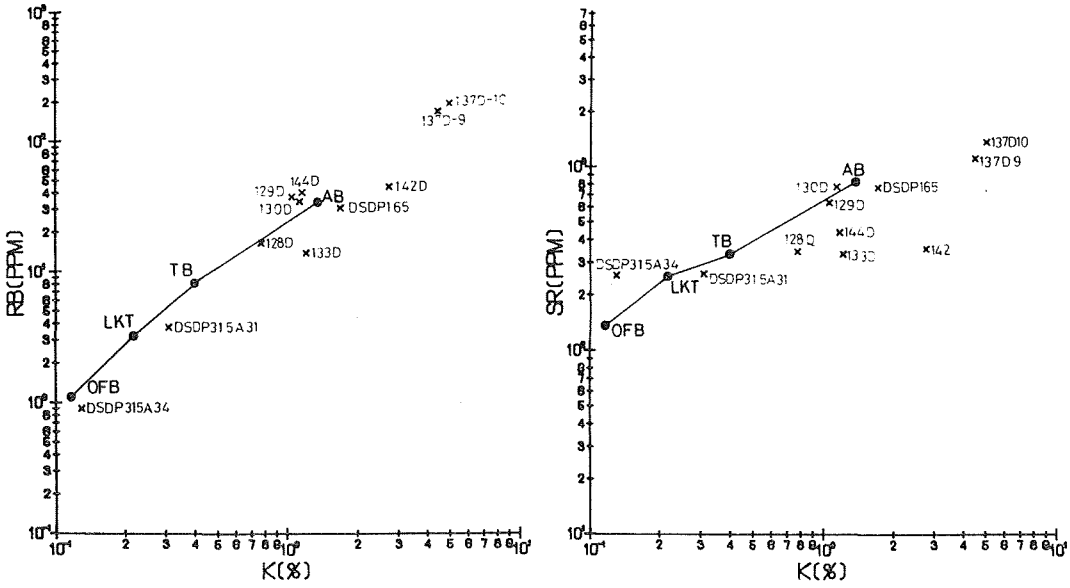

Fig. 2 K content vs. Rb content (left) and K content vs. Sr content (right) for volcanic rocks from the Line islands. OFB, LKT, TB and AB are taken from Hart et al. (1970). OFB = ocean floor basalt (oceanic ridge basalt), LKT = low potassium tholeiite from island arc and oceanic island regions, TB = tholeiitic basalt from island arc and oceanic island regions, AB = alkali basalts mainly from oceanic islands. These are mean values for various rock types of modern basalts, respectively.

very small and the author could not measure the ($^{87}Sr/^{86}Sr$) ratio. Therefore, the high ($^{87}Sr/^{86}Sr$) ratio of 133D is not original and may be due to the sea water alteration.

If these three samples 142D, 133D and 130D were originated in the same hot spot as suggested by the ^{40}Ar-^{39}Ar age data, the ($^{87}Sr/^{86}Sr$) ratio of "hot spot" magma will be about 0.7031 which is a mean ($^{87}Sr/^{86}Sr$) ratio for 142D and 130D. The three samples 142D, 133D and 130D are located near the alkali basalt on K-Rb and K-Sr diagram (Fig. 2). The ($^{87}Sr/^{86}Sr$) ratio is low compared with those of alkali basalts from Tahiti and Samoa (Hedge et al., 1972; Hubbard 1971; Peterman and Hedge, 1971), but same as that of alkali basalts from Hawaii (Powell et al., 1965). The ($^{87}Sr/^{86}Sr$) ratio (0.7031) is quite low for those of alkali basalts from various oceanic islands (Brook et al., 1976).

It is important that the obtained ($^{87}Sr/^{86}Sr$) ratio is

different from that of Tahiti (0.7042). The Tahiti island is located on the curving point of the Tuamotu-Line chain. The change in a direction of the Pacific plate Movement took place about 40 m.y. ago (Clague and Jarrard, 1973). If the Tahiti island originated from the same hot spot as that of the Tuamotu-Line chain, the age of the rock from the Tahiti island must be about 40 m.y., suggesting that the Tahiti island does not belong to the Tuamotu-Line chain.

Another interpretation is that the "hot spot" is only a heat source which is located in the lower mantle and the magma source of each volcano is independent for each island. The ($^{87}Sr/^{86}Sr$) ratios are different between alkali basalt and tholeiite even in a single island. This suggests that at least two magma sources exist under a single island. The "hot spot" only provides heat to generate the magma sources. In this idea the magma sources also move as the plate does, and the life time of the volcanism of each island is variable. It is probable that the volcanism of Tahiti started 40 m.y. ago and still continues. Hence, ($^{87}Sr/^{86}Sr$) ratios of the rocks from various islands could be different from each other, even though they are originated in the same hot spot. Therefore, we can not wholly rule out the possibility that the Tahiti is not originated in the same hot spot as that of the Tuamotu-Line chain. At any rate, the difference in ($^{87}Sr/^{86}Sr$) ratios between Tahiti and the main chain of the Line islands suggests that the magma source is different.

The measured ($^{87}Sr/^{86}Sr$) ratios of 137D-9 and 137D-10 are high compared with those of 142D and 130D which are located in the north of the main chain. The initial ($^{87}Sr/^{86}Sr$) ratio from 137D-9 and 137D-10 are also high, but that of 137D-9 is different from that of 137D-10. After HCl leaching ($^{87}Sr/^{86}Sr$) ratios of two samples became almost the same ($\sim$0.7043). The ^{40}Ar-^{39}Ar ages from 137D-9 and 137D-10 are younger than those of the main chain (Saito and Ozima, 1977). Therefore, it may be concluded that the magma source of 137D-9 and 137D-10 is different from that of the main chain. On K-Rb and K-Sr diagram (Fig. 2) 137D-9 and 137D-10 occupy the right upper position of the OFB-AB trend line.

(4-2) Line Cross chain

The ($^{87}Sr/^{86}Sr$) ratios of 128D and 129D which located in the Line Cross chain are approximately the same. The initial ($^{87}Sr/^{86}Sr$) ratios of two samples are about 0.7034. These initial ($^{87}Sr/^{86}Sr$) ratios are a little higher than those of the main chain. The magma source of the Line Cross chain is different from that of the main chain. The initial ($^{87}Sr/^{86}Sr$) ratio of DSDP165 is 0.7038 and the ($^{87}Sr/^{86}Sr$) ratio after leaching is 0.7033$\pm$4 which is similar to those of the Line Cross chain. This may suggest that DSDP 165 is also originated in the same magma source of the Line Cross chain. The ^{40}Ar-^{39}Ar age of DSDP165 is younger than the fossil age of the overlying sediments. Therefore, DSDP 165 was thought to be a later intrusion or a sill (Saito, 1976). Though DSDP 165 is drilled from a basement, it does not represent a true basement basalt and it is quite probable that the magma source of the sill must be the same as that of the Line Cross chain. These three

samples are also located near the position of the alkali basalt on the K-Rb and K-Sr diagram (Fig. 2). Therefore, the magma source of the Line Cross chain is characterized by a little high ($^{87}Sr/^{86}Sr$) ratio.

(4-3) South part of the Line chain

The samples DSDP315A31 and DSDP315A34 are drilled from the oceanic basement. The measured and initial ($^{87}Sr/^{86}Sr$) ratios of DSDP315A31 and DSDP315A34 are about 0.7038 which is higher than that of the oceanic ridge basalt. After HCl leaching the ($^{87}Sr/^{86}Sr$) ratio of DSDP315A34 became 0.7027±5 which is the same as that of the oceanic ridge basalt. The low K and Rb contents and high K/Rb ratios suggest that DSDP 315A samples are typical oceanic floor basalts formed at the oceanic spreading ridge. On K-Rb and K-Sr diagram (Fig. 2) these samples are located near the position of the ocean floor basalt. The ($^{87}Sr/^{86}Sr$) ratios are probably due to sea water alteration.

5. Conclusion

On the basis of Sr isotope studies the samples from the Line chain may be divided into three regions.

(1) the initial ($^{87}Sr/^{86}Sr$) ratio of the Line chain is about 0.7031 which is the same as that of alkali basalts from Hawaii islands, but different from that of alkali basalts from Tahiti and Samoa. If the Tahiti island is situated on the Tuamotu-Line chain, this may suggest that the Tuamotu-Line chain is not of a simple "hot spot" origin. Otherwise, the "hot spot" may only provide heat to generate magma source of an individual island.

(2) The initial ($^{87}Sr/^{86}Sr$) ratio of the Line Cross chain is about 0.7034 which is distinguished from that of the main chain. Therefore, the magma source of the Line Cross chain is different from that of the Line chain. It is probable that the DSDP165 which is a sill may be derived from the magma source of the Line Cross chain.

(3) The initial ($^{87}Sr/^{86}Sr$) ratios from site 137D which is located off the main trend are about 0.7040. This ratio is different from those of the Line chain or those of the Line Cross chain, and it is similar to that for Tahiti. This suggests that the ($^{87}Sr/^{86}Sr$) ratios of the rocks from the site a little distant from the main chain are higher than those of the rocks from the main chain.

References

Brooks, C., Hart, S.R., Hofmann, A. and James, D.E.(1976) Earth Planet. Sci. Lett. 32, 51.
Clague, D.A. and Jarrard, R. D. (1973) Geol. Soc. Amer. Bull. 84, 1135.
Clague, D.A., Dalrymple, G.B. and Moberly, R. (1975) Geol. Soc. Amer. Bull. 86, 991-998.
DSDP Scientific Staff (1971) Geotimes November, 12.
DSDP Scientific Staff (1974) Geotimes March, 16.
Hart, S.R., Brooks, C., Krogh, T.E., Davis, G.L. and Nava, D. (1970) Earth Planet. Sci. Lett. 10, 17.

Hedge, C.E., Peterman, Z.E. and Dickinson, W.R. (1972) Geol. Soc. Am. Bull. 83, 2709.
Hubbard, N.J. (1971) Pacific Sci. 25, 178.
Lanphere, M.A. and Dalrymple, G.B. (1971) Earth Planet. Sci. Lett. 12, 359.
McDougal, I. (1971) Nature Phys. Sci. 231, 141.
Morgan, W.J. (1972) Amer. Assoc. Petrol. Geologist Bull. 56, 203.
O'Nions, R. K. and Pankhurst, R. J. (1976) Earth Planet. Sci. Lett. 31, 255.
Peterman, Z.E. and Hedge, C.E. (1971) Geol. Soc. Am. Bull. 82, 493.
Powell, J.L., Faure, G. and Hurley, P.M. (1965) J. Geophys. Res. 70, 1509.
Saito, K. (1976) Ph. D. Thesis, Univ. of Tokyo.
Saito, K. and Ozima, M. (1977) Earth Planet. Sci. Lett. 33, 353.
Wilson, J.T. (1963) Can. J. Phys. 41, 863.

$^{40}Ar/^{39}Ar$ ANALYSES OF PHLOGOPITE NODULES AND PHLOGOPITE-BEARING PERIDOTITES IN SOUTH AFRICAN KIMBERLITES

Ichiro KANEOKA* and Ken-Ichiro AOKI**

* Geophysical Institute, University of Tokyo, Bunkyo-ku, Tokyo 113, Japan
** Institute of Mineralogy, Petrology and Economic Geology, Tohoku University, Sendai 980, Japan

1. Introduction

In deep-seated rocks, excess Ar is often found, reflecting the conditions of rock and/or mineral formations (e.g. McDougall and Green, 1964; Lovering and Richards, 1964; Kirsten and Müller, 1967). Since most of deep seated rocks are composed of only K-poor minerals such as olivine and pyroxene, the apparent anomalously high K/Ar ages are probably enlarged due to their low K contents.

Lovering and Richards(1964) reported, however, that the apparent K/Ar ages of phlogopites in eclogite inclusions from Roberts-Victor mine, South Africa and those in pipe filling breccia from Delegate, Australia were older than the ages estimated stratigraphically and/or determined radiometrically for other minerals, which suggests the existence of excess Ar in phlogopite. Since phlogopite is a K-rich mineral, the existence of excess Ar in phlogopite raises interesting problems, including the origin of such excess Ar and the state of rare gases in the upper mantle.

Phlogopite-bearing ultramafic inclusions and phlogopite nodules are sometimes found in South African kimberlites, which are generally regarded to be of upper mantle origin (Kushiro and Aoki, 1968). Concerning the formation ages of ultramafic inclusions in South African kimberlites, several attempts have been made to obtain their radiometric ages by Rb/Sr and U,Th/Pb methods (Allsopp et al., 1969; Manton and Tatsumoto, 1971), but have not succeeded in obtaining meaningful ages probably due to contamination of samples (Barrett, 1974). Only recent results of Rb/Sr isochron ages on phlogopite micas in kimberlites and its associated inclusions have given us useful informations on the ages of the kimberlite pipe emplacement, which range from about 80 to 150 m.y. (Allsopp and Barrett, 1975). However some phlogopite samples do not form such isochron, suggesting the difference of the origin and/or degree of secondary effects for these samples. Petrographically, the origin of phlogopite in peridotite nodules and phlogopite nodules might be different (Aoki, 1974,1975).

In the present study, Ar-40/Ar-39 analyses were applied for phlogopite-bearing peridotite inclusions and phlogopite nodules from South Africa, in order to study the origin of excess Ar in phlogopites together with their formation ages.

2. Samples

Phlogopite-bearing peridotite inclusions (BF-03, BF-05, BF-13) and phlogopite nodules (DU-01, DU-02) in kimberlites were collected

by one of us (K.A.) from Bultfontein and Du Toitspan mines respectively, near Kimberley, South Africa. Petrologically, these peridotite inclusions are estimated to have been derived from a depth of about 100 km or less (Aoki,1975), whereas phlogopite nodules are estimated to have been formed at a shallower region such as in the lower crust or in the upper mantle (Aoki, 1974).

Samples BF-05 and BF-13 are composed of forsterite, enstatite, garnet, phlogopite, diopside and chlorite, whereas the sample BF-03 consists of forsterite, enstatite, phlogopite, potassic-richterite and chlomite in decreasing order of abundance. Phlogopite nodules are composed of phlogopite and potassic-richterite, from which pure phlogopite samples (DU-01, DU-02) were separated with an isodynamic separator. More details on petrology and mineralogy of these rocks are given elsewhere (Aoki, 1974, 1975).

The peridotite inclusions were analysed as whole rocks (48-80 meshes), but pure phlogopites (40-60 meshes) were used for phlogopite nodules.

3. Experimental

Samples and muscovite monitors (Bern 4M) wrapped in Al-foil were stacked in quartz ampoule (10ϕ x 70 mm) and irradiated with fast neutrons in the core of JMTR reactor for 22 days ($\sim 10^{18}$ nvt). The neutron flux gradient along the length of each ampoule amounted up to 20-25%. Hence the interpolated J-values were assigned for each sample to calculate the age. Sample was incrementally heated for one hour at each temperature with an induction heater. Degassing temperature was calibrated with an optical pyrometer for more than 700°C, but the extrapolated value from a calibration curve was used for lower temperature. Hence the ambiguity of about 30°C exists in the degassing temperature. Ar purified by using Ti-Zr alloy at around 800°C was collected in a collector tube with charcoal at liquid nitrogen temperature for mass spectrometry.

Ar isotopes were measured with a 60 degree, 15 cm radius Reynolds type mass spectrometer in static mode. Mass discrimination was about 0.4% for each mass and corrected. Memory effect was also corrected by extrapolating the ratio to time zero.

Correction factors for Ca- and K-derived Ar were determined by irradiating CaF_2 and K_2SO_4, which gave the following values: $(Ar\text{-}39/Ar\text{-}37)_{Ca} = 0.0007$, $(Ar\text{-}36/Ar\text{-}37)_{Ca} = 0.00025$, $(Ar\text{-}40/Ar\text{-}39)_{K} = 0.14$, where suffix Ca and K indicate the factors for Ca and K respectively. Decay of Ar-37 was also corrected, but that of Ar-39 was negligible in the present study.

The amount of Ar was estimated by the peak height comparison between the sample and the standard sample whose total amount of radiogenic Ar-40 is known. Since Ar extraction and mass spectrometry were made separately in the present study, the value have ambiguity of about 20%, which also reflects the K-content estimated from the total amount of Ar-39 in a sample.

4. Results

The analytical results are given in Figs. 1-1$\sim$1-5, where all values were corrected for K- and Ca-derived Ar isotopes. The amount of radiogenic Ar-40 (= $^{40}Ar^*$) is calculated by assuming that all Ar-36 represents the atmospheric component which has the Ar-40/Ar-36 ratio of 295.5 (Nier, 1950). Since there is a possibility for the

Fig. 1

Ar-40/Ar-39 age spectra as a function of Ar-39 released (left) and Ar-40/Ar-36 versus Ar-39/Ar-36 isochron diagram (right).
The band in the Ar-40/Ar-39 age spectra diagram indicated ± 1 standard deviation envelope about the calculated age of each temperature fraction. In the isochron diagram, reference isochrons are drawn, assuming that the initial Ar-40/Ar-36 ratio equals to that of present atmospheric Ar. All temperatures are in degrees Celsius.

Samples:
1, BF-03; 2, BF-05;
3, BF-13; 4, DU-01;
5, DU-02.

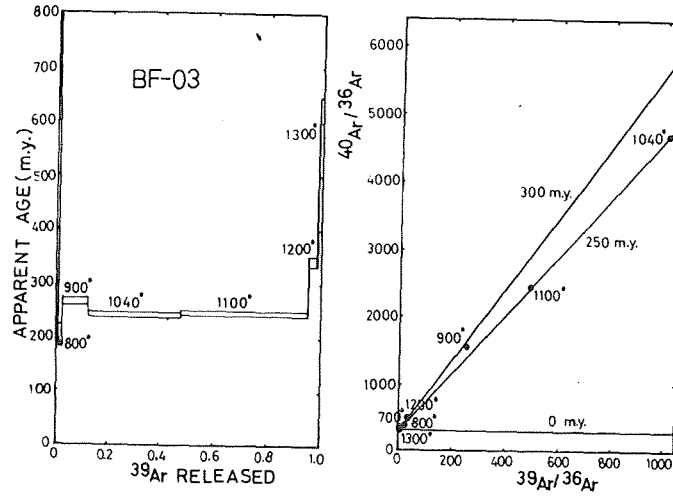

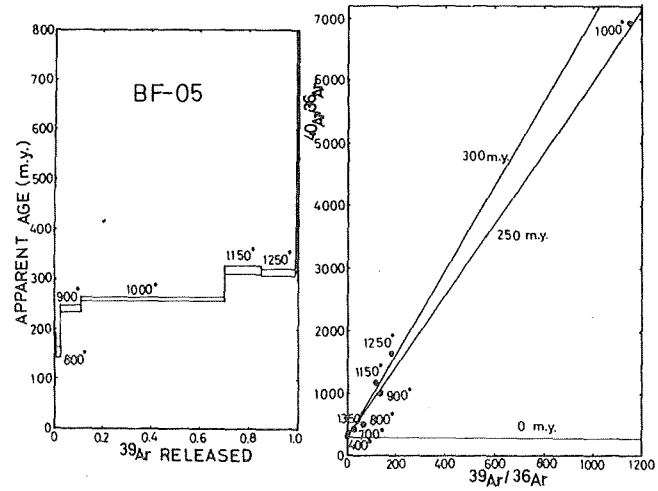

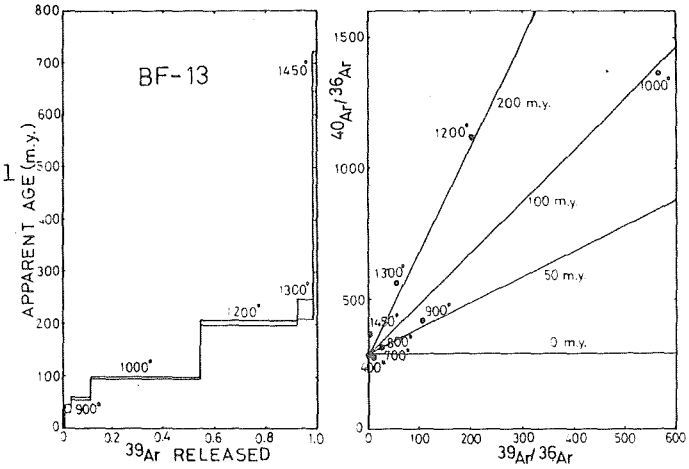

occurrence of non-atmospheric Ar-36 in deep-seated rocks (Kaneoka, 1975), this assumption may not always be valid. To exclude the ambiguity of the assumption, the Ar-40/Ar-36 versus Ar-39/Ar-36 diagram is also adopted, in which an isochron should be obtained foe a sample with unique values for both the initial Ar-40/Ar-36 ratio and the age.

As shown in Figs. 1-1 ~1-5, however, no definite isochron could be obtained for present samples, though some of them show rough correlations between Ar-40/Ar-36 and Ar-39/Ar-36 ratios. Samples which show such correlations seem to have initial Ar-40/Ar-36 ratios of nearly atmospheric values.

Fig. 1 (continued)

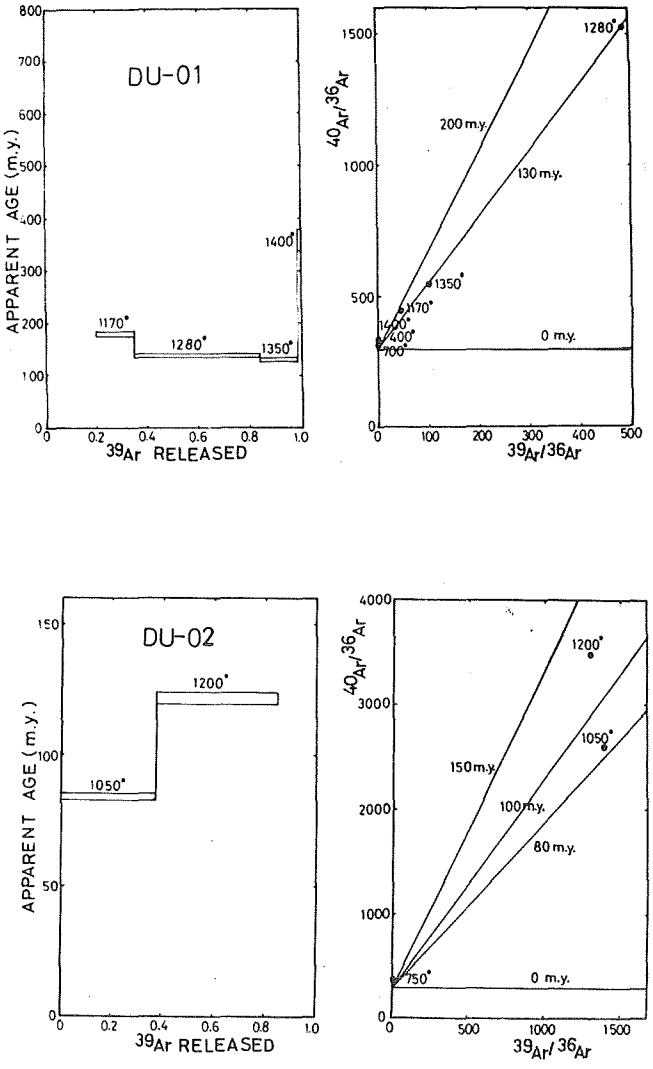

In Fig. 2, the release patterns of Ar isotopes are shown for sample BF-03 as an example, in which most Ar-36 is degassed at the lowest temperature. Furthermore, the release pattern of Ar-36 is clearly differnt from those of the other Ar isotopes: the former has no clear peak through whole temperatures, whereas the latter has a peak around 1100°C. The other samples show similar results. This suggests different trapping sites and origin for Ar-36 from those of the other Ar isotopes. Present blank level is in the order of 10^{-9} cc STPAr-36 at 1400°C for one hour with the isotopic composition of atmospheric Ar and comparable to the amount of Ar-36 in samples estimated from an experiment with different conditions (Kaneoka et al., 1977). Hence most observed Ar-36 might be of secondary atmospheric component, including blanks.

Fig. 2
Release patterns of Ar isotopes in a neutron-irradiated sample (BF-03). $^{40}Ar^{*}$ indicates assumed non-atmospheric Ar-40.

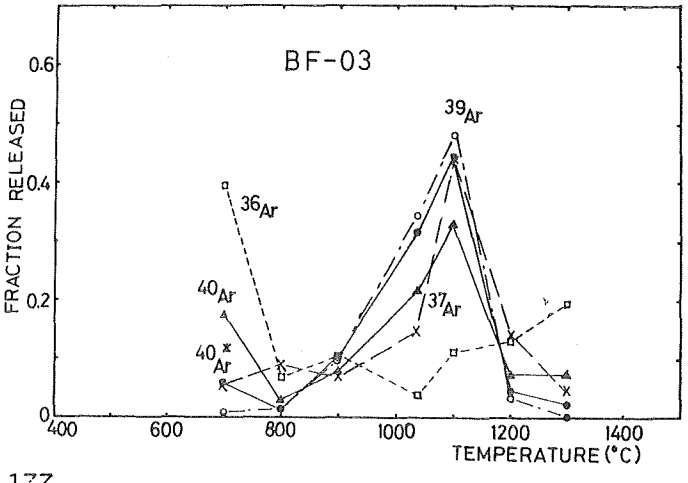

As shown in Fig. 1-1, sample BF-03 shows a rough correlation between Ar-40/Ar-36 and Ar-39/Ar-36 ratios, indicating an apparent plateau age of about 240 m.y. for 1040°C and 1100°C fractions. Except for 800°C fraction, however, lower and higher temperature fractions have older ages. Such age patterns are often observed in igneous rocks which contain excess Ar-40 (Kaneoka, 1974; Lanphere and Dalrym-le, 1976). From the same sample, Rb/Sr age of about 84 m.y. has been determined for phlogopite and K-richterite pair (Shimizu, personal communication). Furthermore, a series of phlogopite samples from Bultfontein indicate a Rb/Sr age of (90±3) m.y. (Allsopp and Barrett, 1975). From the release patterns of Ar isotopes, Ar-40 seems to correlate with Ar-39, implying that Ar-40 is trapped in K- or K similar sites. Since phlogopite and K-richterite are only K-minerals in this sample, most Ar-40 should be retained in these minerals. These evidences suggest that an apparent plateau age of about 240 m.y. cannot be interpreted as a crystallization age of the sample, but indicates a correlation between excess Ar-40 and Ar-39.

Similar results are obtained for sample BF-05, in which 900°C and 1000°C fractions show Ar-40/Ar-39 ages of 240-250 m.y., whereas higher temperature fractions and the lowest temperature fraction show older ages. Even the youngest age of about 150 m.y. obtained in 800°C fraction is older than the Rb/Sr ages reported for phlogopites from this region, suggesting the occurrence of excess Ar-40.

On the other hand, sample BF-13 shows a very different age pattern from samples BF-03 and BF-05. Apparent Ar-40/Ar-39 age increases monotonously with increasing temperature, which suggests serious secondary thermal or mechanical effects on this sample. In 400°C and 700°C fractions, no radiogenic Ar-40 is observed, suggesting that the effects should occur quite recently. The total Ar-40/Ar-39 age is younger than those of the previous two samples, but still older than Rb/Sr ages estimated for phlogopites. At present, we cannot identify the characteristics of the effect definitely.

The results for samples DU-01 and DU-02 are incomplete due to the loss of a few temperature fractions during gas purification procedures. Although 850°C and 1050°C fractions were lost from sample DU-01, it seems to show the youngest age in the intermediate temperature fraction like samples BF-03 and BF-05. However the apparent Ar-40/Ar-39 ages are younger than those of samples from Bultfontein. Total Ar-40/Ar-39 age of about 150 m.y. is younger than those of samples BF-03 and BF-05.

Sample DU-02 lost the highest temperature fraction, but the remaining three temperature fractions also show similar age release pattern to those of the other samples, having the youngest apparent Ar-40/Ar-39 age of about 84 m.y.. This value is quite interesting in relation to the extrusion age of the sample and discussed later. Total Ar-40/Ar-39 age for this sample is about 110 m.y.. By comparing the total amount of Ar-39 in each sample with that of standard sample, K content can be estimated as follows: BF-03 (1.0%), BF-05 (0.89%), BF-13 (0.52%), DU-01 (6.6%<), DU-02 (7.0%<). These values are in agreement with those determined chemically within the error of about 20%.

5. Discussion

5.1 Ages

Present samples show no definite plateau nor isochron ages, though samples BF-03, BF-05 and DU-01 seem to indicate a correlation

between Ar-40/Ar-36 and Ar-39/Ar-36 ratios. Except for sample BF-13, present samples indicate the youngest Ar-40/Ar-39 age in the intermediate temperature fraction. These age patterns are similar to those of igneous rocks which contain excess Ar-40, in which the youngest age generally shows the upper limit for the age of a sample or sometimes corresponds to the age of the sample concerned (Kaneoka, 1974; Lanphere and Dalrymple, 1976). Rb/Sr ages for phlogopites from this region have been interpreted to correspond to the age of the kimberlite pipe emplacement on the earth's surface (Allsopp and Barrett, 1975). Hence older apparent Ar-40/Ar-39 ages of present samples probably reflect the occurrence of excess Ar-40.

From the correlation between Ar-40/Ar-36 and Ar-39/Ar-36 ratios, however, one may argue that the apparent Ar-40/Ar-39 ages reflect the formation ages of peridotitie or phlogopite, which should be older than the extrusion age of samples. In this case, Ar should have been kept in closed system, whereas Sr was reequilibraetd during the extrusion of phlogopite sample to the earth's surface to be compatible with Rb/Sr results. However it does not seem to occur in general case. Furthermore, Ar diffusion coefficient of 10^{-12} 10^{-13} cm^2/sec have been determined for phlogopite at 700-800° C from a diffusion experiment under hydrostatic pressure of 15 kbars (Giletti and Tullis, 1977). If this value is applied for a phlogopite with 1 cm diameter, Ar is lost from phlogopite mineral after 1 m.y.. It seems difficult to keep closed system for Ar in phlogopite in the upper mantle for relatively long time. Hence, the apparent Ar-40/Ar-39 ages for present samples may not directly reflect their formation ages.

Except for sample BF-13, the youngest Ar-40/Ar-39 age obtained in the intermediate temperature fraction probably indicates the upper limit for the extrusion age for these samples. However, the youngest age of about 84 m.y. for sample DU-02 agrees with younger Rb/Sr age data for phlogopites from Kimberley area. It also agrees well with Rb?Sr age for BF-03. Hence the age probably reflects a correct value for the extrusion age of sample DU-02.

Present results reconfirm the phenomenon that in the saddle shaped Ar-40/Ar-39 age spectra the youngest age in the intermediate temperature generally indicates the upper limit for the age of the sample concerned, but sometimes reflects the significant age for the sample. The extrusion age of peridotite nodules from Bultfontein will be represented by reported Rb/Sr ages of 84-90 m.y., whereas that of phlogopite nodules from Du Toispan will be about 84 m.y.suggested from present Ar-40/Ar-39 age analysis. This means that kimberlite pipe emplacement might have occurred at the same age forBultfontein and Du Toitspan.

5.2 Excess Ar-40

As discussed before, present samples seem to contain excess Ar-40. Furthermore, the release patterns of Ar-40 and Ar-39 for sample BF-03 are similar, suggesting that most Ar-40 is trapped in K- or K-similar sites (Fig. 2). Since phlogopite and K-richterite are only K minerals in this sample, excess Ar-40 will be mainly trapped in these minerals. The release patterns of Ar isotopes for the other samples lead to the same conclusion, though they do not contain K-richterite. Olivine and pyroxene probably contain excess Ar-40, but the amount of excess Ar-40 in phlogopite would be much abundant than those in these minerals. Hence excess Ar-40 in phlogopite is confirmed.

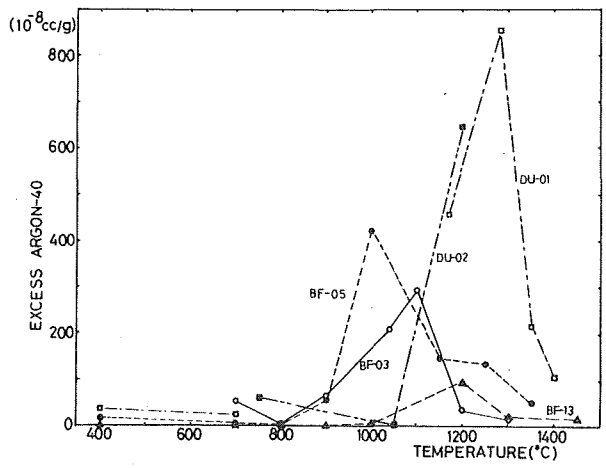

Fig. 3
Release patterns of excess Ar-40.
Excess Ar-40 is calculated by assuming that the extrusion age is 90 m.y. for Bultfotein samples (BF-03, BF-05, BF-13) and 84 m.y. for Du Toitspan samples (DU-01, DU-02). No secondary Ar loss is assumed, though this may not be true for sample BF-13.

By assuming the extrusion age of each sample, the amount of excess Ar-40 can be calculated for each temperature fraction. The release pattern of excess Ar-40 for present samples are shown in Fig. 3, where no secondary Ar loss is assumed. The extrusion ages are assumed to be 90 and 84 m.y. for Bultfontein and Du Toispan samples respectively. This result reveals that most excess Ar-40 is degassed at higher temperature, suggesting that they are probably trapped in mineral lattices. The amount of excess Ar-40 observed in the lower temperature fraction is much lower than those observed in ultramafic xenoliths from Kola Peninsula (Kaneoka, 1974). This may reflect the poor retentivity of phlogopite for trapped Ar which does not locate in lattices.

Furthermore, excess Ar-40 in phlogopite nodule seems to be more degassed at higher temperature than that in peridotite nodules. The averaged grain size of the former is a little larger than that of the latter, which may explain this differnce.

Although apparent total Ar-40/Ar-39 ages for phlogopite nodules from Du Toitspan are much younger than those of peridotite nodules from Bultfontein, the amount of excess Ar-40 is more abundant in phlogopite nodules than in peridotite nodules. This probably reflects the differnce in the amount of phlogopite in these samples, but the difference of phlogopite formation mechanism suggested by petrological consideration (Aoki, 1974, 1975) may have played a role in this connection.

5.3 Excess Ar-40 versus Ar-39

As discussed before, excess Ar-40 seems to correlate with Ar-39 for samples BF-03, BF-05 and DU-01. An example for sample BF-03 is shown in Fig. 4. Although the correlation between Ar-40 Ar-39 is most easily explained by the formation of radiogenic Ar-40 from K-40, it is not compatible with other evidences for present samples.

Several examples have been reported for the correlation between excess Ar-40 and Ar-39. A biotite from the ancient Precambrian gneiss of west Greenland (ca. 3700 m.y.) shows a well-defined plateau age of 5030 m.y, indicating the occurrence of such correlation (Pankhurst et al., 1973). Furthermore, a phlogopitic biotite sample from a kimberlite dyke near Little Falls, New York, seems to show a rough correlation between excess Ar-40 and Ar-39 (Lanphere and Dalrymple, 1976). A Greenland dolerite has also shown an anomalous old age in spite of good correlation in the Ar-40/Ar-36 versus Ar-39/Ar-36 isochron diagram (Brereton, 1972).

These evidences suggest that excess Ar-40 sometimes locates in K- or K-similar sites. In this respect, mica structure may be a typical example for trapping excess Ar in such sites. Mica is a composite sheet in which a layer of octahedrally coordinated cations is sandwiched between two identical layers of linked $(Si,Al)O_4$ tetrahedra. Hence if excess Ar-40 exists during phlogopite formation, Ar atom which has relatively large atomic radius (about 1.4 Å) may mainly replace K-site, because the sites which the other elements occupy are too small to be replaced by Ar atoms. In this case, the correlation between excess Ar-40 and Ar-39 naturally occurs.

From the above discussion, it is inferred that excess Ar-40 has been incorporated into phlogopite during its formation. Secondary incorporation of excess Ar-40 into phlogopite does not well explain the correlation between the excess Ar-40 and Ar-39.

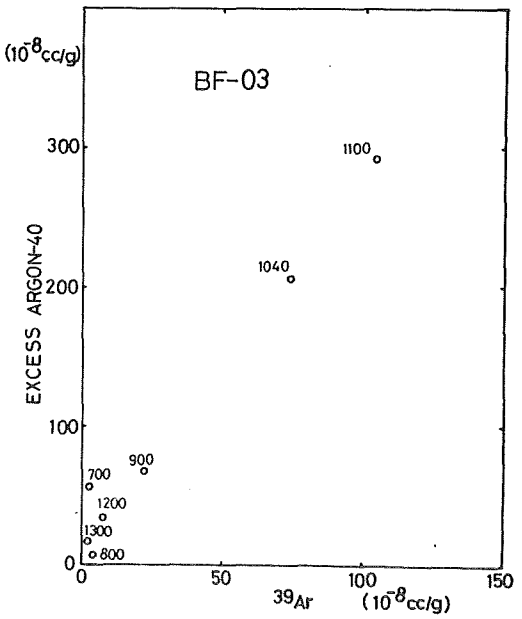

Fig. 4
Excess Ar-40 versus Ar-39 for sample BF-03. Figure at each point indicates extraction temperature in degrees Celsius.

5.4 Excess Ar-40 and the formation of phlogopite

From the correlation between excess Ar-40 and Ar-39, it has been inferred that excess Ar-40 is trapped in K-site in phlogopite and probably incorporated during phlogopite formation.

To form phlogopite, K_2O and H_2O should be enriched in magma. There should be some sources for these elements under South African continent and they might have been also concentrated into a magma from which phlogopite was formed. During the concentration of K_2O, H_2O and other volatile elements, rare gases were also enriched in the magma, including the excess Ar-40. Rare gas analyses in samples BF-03 and DU-02 have proved that phlogopite surely contains large amount of rare gases, including excess Ar-40 (Kaneoka et al., 1977). To keep relatively high partial pressure for these rare gases in the magma, the depth of magma reservoir should not be shallow, which is compatible with petrological observations that these phlogopites were formed in the upper mantle or in the lower crust (Aoki, 1974, 1975).

Thus the occurrence mode of excess Ar-40 gives a good information concerning the condition of mineral and/or rock formation in the earth's deep interior.

6. Coclusions

(1) Phlogopite-bearing peridotites and phlogopite nodules in kimberlites from Kimberley area, South Africa, indicate no definite plateau nor isochron ages, though the rough correlation between Ar-40/Ar-36 and Ar-39/Ar-36 ratios are observed. Total Ar-40/Ar-39 ages are older than the Rb/Sr ages reported for phlogopites from this region. Several evidences suggest the occurrence of excess Ar-40 in phlogopite.
(2) From the youngest Ar-40/Ar-39 age in the intermediate temperature fraction, the age of extrusion for phlogopite nodule from Du Toitspan is estimated to be about 84 m.y..
(3) Excess Ar-40 is degassed mostly at higher temperature, suggesting that they are trapped in crystal lattices of phlogopite.
(4) The correlation between excess Ar-40 and Ar-39 is observed for a few samples, which suggests that excess Ar-40 is trapped in K- or K-similar sites and incorporated during phlogopite formation. Mica structure may be a typical example for the occurrence of such correlation.
(5) The occurrence of excess Ar-40 in phlogopite is compatible with the petrological observation that the phlogopite has been formed in the upper mantle or in the lower crust.

References

Allsopp, H.L. and D.R.Barrett (1975) Phys. Chem. Earth 9, 605.
Allsopp, H.L., O.L.Nicolaysen and P.Hahn-Weinheimer (1969) Earth Planet. Sci. Lett. 5, 231.
Aoki, K. (1974) Contrib. Mineral. Petrol. 48, 1.
Aoki, K. (1975) ibid. 53, 145.
Barrett, D.R. (1975) Phys. Chem. Earth 9, 637.
Brereton, N.R. (1972) Geophys. J. R. Astron. Soc. 27, 449.
Giletti, B.J. and J. Tullis (1977) Earth Planet. Sci. Lett. 35, 180.
Kaneoka, I. (1974) ibid. 22, 145.
Kaneoka, I. (1975) Geochem. J. 9, 113.
Kaneoka, I., N. Takaoka and K. Aoki (1977) Earth Planet. Sci. Lett. 36, 181.
Kirsten,T. and O. Müller (1967) Radioactive Dating and Methods of Low-Level Counting, IAEA 483.
Kushiro, I. and K. Aoki (1968) Am. Mineral. 53, 1347.
Lanphere, M.A. and G.B.Dalrymple (1976) Earth Planet. Sci. Lett. 32, 141.
Lovering, J.F. and J. Richards (1964) J. Geophys. Res. 69, 4895.
Manton, W.I. and M. Tatsumoto (1971) Earth Planet. Sci. Lett. 10, 217.
McDougall, I. and D.H.Green (1964) Norsk geol. Tidsskr. 44, 183.
Nier, A.O. (1950) Phys. Rev. 77, 789.
Pankhurst, R.J., S. Moorbath, D.C.Rex and G. Turner (1973) Earth Planet. Sci. Lett. 20, 157.

(To be submitted to Earth Planet. Sci. Lett.)

EXCESS ^{129}Xe AND HIGH $^{3}He/^{4}He$ RATIOS IN OLIVINE PHENOCRYSTS OF KAPUHO LAVA AND XENOLITHIC DUNITES FROM HAWAII

Ichiro KANEOKA* and Nobuo TAKAOKA**

* Geophysical Institute, University of Tokyo
Bunkyo-ku, Tokyo, 113, Japan
** Department of Physics, Osaka University
Toyonaka-shi, Osaka, 560, Japan

Excess ^{129}Xe has been reported in CO_2 well gas from New Mexico (Butler et al., 1963; Boulos and Manuel, 1972) and in an Hawaiian xenolith (Hennecke and Manuel, 1975), which gives a very important constraint on the evolution of the terrestrial atmosphere provided that it still exists ubiquitously in the earth's interior. Furthermore, the occurrence of primordial ^{3}He has been found in submarine pillow basalts (Lupton and Craig, 1975), volcanic gases (Polak et al., 1975) and some mantle rocks (Tolstikhin, 1974). Craig and Lupton argued the existence of excess ^{20}Ne in Kilauea fumarolic gases and in some submarine pillow basalts (Craig and Lupton, 1976). However, the relationships among isotopic anomalies of rare gases compared to atmospheric values are not yet clear.

Present study includes the measurements for both $^{3}He/^{4}He$ ratios and Xe isotopes in a few Hawaiian samples, which are expected to show very primitive natures with respect to rare gas isotopes from available evidences. Olivine phenocrysts of Kapuho lava, Kilauea, erupted in 1960 are regarded to have crystallized in the magma reservoir. They are hand-picked greenish olivines (1 - 8 mm in size), showing black impurities under a microscope. By examining thin sections, two Hualalai dunites were selected so that they contain CO_2 inclusions as much as possible. They are composed of more than 95% olivine (1 - 10 mm in size) and have been brought to the surface by the 1801 Kaupulehu flow of the Hualalai Volcano, Hawaii. These xenolithic dunites will represent the state of the lithosphere under the Hawaii Island.

Rare gases were analysed with a Nier-type mass spectrometer at the Osaka University, installed with a secondary multiplier and having a resolution power of about 600. Hence the separation of ^{3}He from $HD+H_3$ is complete and Xe isotopes are also measurable with good precision. Blanks were taken before and after each sample measurement. Mass discriminations were corrected by the air standard analyses except for He which was corrected by analysing Bruderheim meteorite standard. More details on experimental conditions are reported elsewhere (Takaoka, 1976).

The results of rare gas concentrations are shown in Table 1. For sample Hualalai 1801b, two extraction temperatures (600 and 1700°C for 30 minutes respectively) were adopted. However the sample was not melted completely even at 1700°C due to relatively large sample size, which was remelted in a separated run. As shown in Table 1, the degassed rate at 600°C is rela-

Table 1. Rare gas concentrations in samples from Hawaii.**

Sample	Temperature (°C)	^{3}He ($\times 10^{-12}$ cm^3STP/g)	^{4}He	^{20}Ne	^{36}Ar	^{40}Ar ($\times 10^{-8}$ cm^3STP/g)	^{84}Kr	^{132}Xe ($\times 10^{-10}$ cm^3STP/g)
Olivine phenocryst, Kapuho lava, Kilauea (4.221 g)	1700 (melted)	1.11	4.43	0.0100	0.0245	18.0	0.0476	0.0058
Hualalai 1801 Dunite, Hualalai (5.764 g)	1700 (melted)	3.75	32.6	0.0209	0.0326	46.7	0.112	0.0159
Hualalai 1801b Dunite Hualalai (22.551 g)	600	< 0.02	0.05	0.0050	0.0149	4.5	0.0146	0.0004
	1700	2.13	14.4	0.0218	0.0186	44.1	0.0706	0.0109
	1700* (remelted)	0.34	2.93	0.0013	0.0061	10.9	0.0243	0.0051
	Total	2.47	17.38	0.0281	0.0396	59.5	0.1095	0.0164
		($\times 10^{-12}$ cm^3STP)		($\times 10^{-8}$ cm^3STP)			($\times 10^{-10}$ cm^3STP)	
Blanks (30 min.)	1700	< 0.56	0.095	0.0010	0.0026	0.55	0.0062	0.0040

* A part of the sample was not melted completely due to relatively large sample size. Hence it was remelted at 1700°C in a separated run.
** Rare gas concentrations were determined by the peak height method with about 10% error, using a calibrated air standard.

tively small except for ^{36}Ar. When 1200°C extraction was added further for similar olivine samples, most rare gases were degassed at 1700°C (Kaneoka and Takaoka, 1976), which suggests that most rare gases are tightly trapped in olivine crystals. Such release patterns of rare gases are completely different from other minerals. For example in phlogopite, lighter rare gases are degassed at lower temperatures (Kaneoka et al., 1977). Relatively large rate of ^{36}Ar at 600°C may be interpreted as the addition of secondary atmospheric contamination. Although total amounts of rare gases in two dunites are roughly similar, the amounts of lighter rare gases are more variable. The rare gas concentrations in peridotites determined by Hennecke and Manuel (1975) are a little different from present samples. These results suggest that some secondary processes and/or the amount of CO_2 inclusions affect such tendencies. The amounts of rare gases in olivine phenocrysts of Kapuho lava are less abundant than those of dunites, which is attributed to their different origin.

In Fig. 1, rare gas abundance patterns are compared among each sample. Present xenoliths are more depleted in Ne, but more enriched in Kr and Xe than those investigated by Hennecke and Manuel (1975). Such difference can be most easily understood in terms of elemental fractionation during introduction of CO_2 into olivine melt, since large amounts of rare gases in dunites are considered to be associated with CO_2 inclusions. This strongly suggests that the abundance patterns of rare gases are largely controlled by secondary processes in addition to its original pattern in the magma reservoir. This situation is also seen for olivine phenocrysts of Kapuho lava, where Ne is more depleted and Xe is more enriched than those of the atmosphere. As discussed later, olivine phenocrysts were surely formed at the deep interior of the earth. Hence in order to discuss the

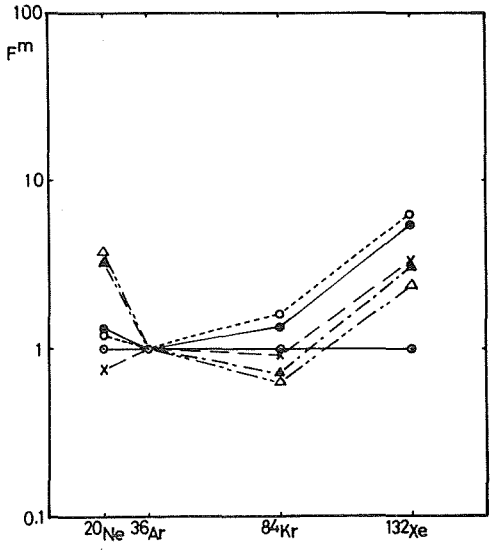

Fig. 1. Rare gas abundance patterns in air (◎), in xenolithic dunites Hualalai 1801 (○), Hualalai 1801b (●) and in olivine phenocrysts of Kapuho lava, Kilauea (×). Hennecke and Manuel's results for xenolithic peridotites (△, ▲) (Hennecke and Manuel, 1975) are included. Relative abundances of ^{20}Ne and ^{132}Xe normalized to ^{36}Ar for their samples are estimated from ^{22}Ne and ^{130}Xe concentrations reported, assuming atmospheric composition of Ne and Xe isotopes.

$$F^m = (^mX/^{36}Ar)_{sample}/(^mX/^{36}Ar)_{air}$$

Table 2. Isotopic compositions of rare gases in samples from Hawaii.

Sample	olivine phenocryst Kilauea	Hualalai 1801	Hualalai 1801b	Atmosphere
Temperature (°C)	1700	1700	1700	——
^{3}He	$(2.51\pm0.34)\times10^{-5}$	$(1.15\pm0.10)\times10^{-5}$	$(1.48\pm0.10)\times10^{-5}$	1.4×10^{-6}
^{4}He	≡1.00	≡1.00	≡1.00	≡1.00
^{20}Ne	9.64 ± 0.19	9.71 ± 0.11	9.76 ± 0.09	9.81
^{21}Ne	0.029 ± 0.004	0.031 ± 0.002	0.029 ± 0.001	0.029
^{22}Ne	≡1.00	≡1.00	≡1.00	≡1.00
^{36}Ar	≡1.00	≡1.00	≡1.00	≡1.00
^{38}Ar	0.187 ± 0.001	0.186 ± 0.003	0.190 ± 0.002	0.187
^{40}Ar	732 ± 2.2	1432 ± 15	2371 ± 27	295.5
^{78}Kr	0.0062 ± 0.0006	0.0063 ± 0.0005	0.0061 ± 0.0005	0.0062
^{80}Kr	0.0409 ± 0.0028	0.0412 ± 0.0012	0.0394 ± 0.0020	0.0396
^{82}Kr	0.204 ± 0.003	0.203 ± 0.002	0.202 ± 0.002	0.202
^{83}Kr	0.203 ± 0.004	0.202 ± 0.002	0.202 ± 0.001	0.202
^{84}Kr	≡1.00	≡1.00	≡1.00	≡1.00
^{86}Kr	0.311 ± 0.010	0.307 ± 0.004	0.309 ± 0.002	0.306
^{124}Xe	<0.01	<0.01	0.0038 ± 0.0002	0.0036
^{126}Xe	<0.01	<0.01	0.0035 ± 0.0002	0.0034
^{128}Xe	0.0706 ± 0.0030	0.0729 ± 0.0014	0.0716 ± 0.0018	0.0713
^{129}Xe	1.014 ± 0.009	1.022 ± 0.014	1.007 ± 0.009	0.983
^{130}Xe	0.154 ± 0.004	0.154 ± 0.002	0.152 ± 0.003	0.152
^{131}Xe	0.799 ± 0.022	0.795 ± 0.011	0.785 ± 0.004	0.788
^{132}Xe	≡1.00	≡1.00	≡1.00	≡1.00
^{134}Xe	0.391 ± 0.007	0.399 ± 0.007	0.392 ± 0.003	0.389
^{136}Xe	0.327 ± 0.009	0.335 ± 0.004	0.332 ± 0.002	0.329

± represents one standard deviation.

elemental abundance ratios, the effect of secondary processes should be very carefully evaluated especially for terrestrial samples. For present samples, $Ne/^{36}Ar$ and $Kr/^{36}Ar$ ratios normalized to those of the atmosphere are variable. $Xe/^{36}Ar$ ratio is, however, always larger than that of the atmosphere, which suggests that the ratio in the earth's interior is higher than that of the present atmosphere. This may mean the selective adsorption of atmospheric Xe on shales (Fanale and Cannon, 1971) and/or insufficient degassing of Xe from the interior of the earth to the atmosphere.

Rare gas isotopic compositions of 1700°C fraction for each sample are shown in Table 2, where high $^3He/^4He$ ratios of the order of 10^{-5} and the occurrence of excess ^{129}Xe are identified for present samples. Except for ^{40}Ar, however, the other isotopes are almost atmospheric within the experimental error, including Ne isotopes. In the analyses of Ne isotopes, the correction of $^{40}Ar^{2+}$ and $^{44}CO_2{}^{2+}$ effects on ^{20}Ne and ^{22}Ne reduces its precision. The effect of $^{20}NeH^+$ on ^{21}Ne is not negligible and has been corrected by using air standard. Although there may be signs for the occurrence of fissiogenic components in Xe and Kr isotopes, they cannot be distinguished from the atmospheric values within the experimental error.

The occurrence of excess ^{129}Xe in xenolithic rocks was firstly identified by Hennecke and Manuel (1975) and present results have reconfirmed their results. Furthermore, olivine phenocrysts of Kapuho lava have been revealed to contain excess ^{129}Xe. Excess ^{129}Xe has been regarded to represent the decay product of extinct ^{129}I ($T_{1/2} = 17$ my). Hence the occurrence of excess ^{129}Xe indicates that the juvenile gases in the magma source still keep its very primitive state. As suggested by Green (1972), CO_2 observed in olivine crystals of dunites as inclusions might have been brought to the surface from a CO_2-charged asthenosphere. If this is the case and the magma of ridge basalts are also formed in the asthenosphere, such excess ^{129}Xe should be identified in submarine pillow basalts too. However no definite evidence for the excess ^{129}Xe has been reported so far in submarine pillow basalts. In such a case, the occurrence of excess ^{129}Xe might be very limited even in the asthenosphere. Further work should clarify this point. On the other hand, the occurrence of excess ^{129}Xe in olivine phenocrysts of Kapuho lava suggests that juvenile gases are still remained in its magma reservoir.

The $^3He/^4He$ ratio for olivine phenocrysts of Kapuho lava, Kilauea is about 2.5×10^{-5}, whereas those of xenolithic dunites from Hualalai are $(1.2 - 1.5) \times 10^{-5}$. It is noteworthy that the $^3He/^4He$ ratio of Kilauea fumaroles has been reported to be about 2×10^{-5}, whereas those in pillow basalts are around 1.4×10^{-5} (Lupton and Craig, 1975). Although the data are very limited, the high $^3He/^4He$ ratio for Kilauea samples seems to be real, reflecting the different character of its magma reservoir from that of xenolithic dunites. This may indicate the vertical heterogeneity of rare gas state in this region. A hot spot has been suggested under the Hawaii Island (Morgan, 1972). Samples from Kilauea may reflect the characteristics of the hot spot, whereas xenolithic rocks those of spreading area, from which such upper mantle materials were formed. If this conjecture is

true, similar isotopic ratios should be found in samples from the other Hawaiian Islands.

Furthermore, the occurrence of excess ^{129}Xe and high $^{3}He/^{4}He$ ratio in olivine phenocrysts of Kapuho lava implys that the phenocrysts should have been formed at the relatively deep part. Although a definite estimate is difficult, we can at least say that it was not formed at a so shallow depth as a few kilometers from the surface. Because it is very difficult to imagine that such excess ^{129}Xe still remains for relatively long time without any secondary contamination at a shallow depth. Further detailed work on rare gas isotopes will clarify the state of juvenile gases and contribute to disclose magma genesis.

References

Boulos, M.S. and O.K. Manuel (1972) Nature, 235, 150.

Butler, W.A., P.M. Jeffery, J.H. Reynolds, and G.J. Wasserburg (1963) J. Geophys. Res., 68, 3283.

Craig, H. and J.E. Lupton (1976) Earth Planet. Sci. Lett., 31, 369.

Fanale, F.P. and W.A. Cannon (1971) Earth Planet. Sci. Lett., 11, 362.

Green, H.W., II (1972) Nature Phys. Sci., 238, 2.

Hennecke, E.W. and O.K. Manuel (1975) Nature, 257, 778.

Kaneoka, I. and N. Takaoka (1976) unpublished results.

Kaneoka, I., N. Takaoka and K. Aoki (1977) Earth Planet. Sci. Lett., 36, 181.

Lupton, J.E. and H. Craig (1975) Earth Planet. Sci. Lett., 26, 133.

Morgan, W.J. (1972) Amer. Ass. Petrol. Geol. Bull., 56, 203.

Polak, B.G., V.I. Kononov, I.N. Tolstikhin, B.A. Mamyrin, and L.V. Khabarin (1975) Proc. Grenoble Symp., Int. Assoc. Hydrol. Sci., Pub. No. 119, 15.

Takaoka, N. (1976) Mass Spectroscopy, 24, 73.

Tolstikhin, I.N., B.A. Mamyrin, L.B. Khabarin, and E.N. Erlikh (1974) Earth Planet. Sci. Lett., 22, 75.

(Submitted to Earth Planet. Sci. Lett.)

RARE GAS ISOTOPIC COMPOSITIONS IN DIAMONDS

Nobuo TAKAOKA* and Minoru OZIMA**

* Department of Physics, Osaka University, Toyonaka 560
** Geophysical Institute, University of Tokyo, Tokyo 113

Rare gas isotopic compositions such as $^{40}Ar/^{36}Ar$, $^{3}He/^{4}He$ and $^{129}Xe/^{132}Xe$ in the earth have proved to provide a powerful tool to understand the origin and evolution of the terrestrial atmosphere (Ozima, 1975; Schwarzman, 1973; Tolstikhin, 1975; Boulos, 1971). The isotopic information may be obtained from rare gases trapped in some mantle-derived materials such as volcanic rocks, volcanic xenoliths or volcanic gases. Among these mantle-derived materials, diamond seems to be unique owing to its almost perfect inertness to any known chemical and to its enormous stability against high temperature. Existence of O_2, H_2, CH_4, H_2O, CO, N_2, Ar and CO_2 in diamonds has been reported (Melton and Giardani, 1974, 1976). However, no measurement has so far been made either on elemental compositions or on isotopic ratios of rare gases in diamonds. This is the first report of rare gas elemental composition and isotopic ratios in diamond. We found that $^{3}He/^{4}He$ ratio is more than an order of magnitude larger than the atmospheric value and also $^{40}Ar/^{36}Ar$ ratio is significantly higher.

Industrial diamonds we studied are believed to come from Kimberley Mines, South Africa. The size of the diamonds ranges from about 1 mm to about 5 mm. Some contain black inclusions, some of which are ferromagnetic and appears to be pyrrhotite under a microscope. Existence of phrrhotite inclusions in diamond is not unusual (Sharp, 1960). The black inclusions seem to be syngenetic with diamonds from the reason discussed below. Diamonds are crashed to a few meshes in a stainless steel mortar. Step-heating was made on two batches of samples at 800°C, 2000°C and 2100°C in a high vacuum tantalum furnace (Takaoka, 1976). Only visible difference between the two batches is that batch 1 is richer in black inclusions than batch 2.

Rare gas elemental abundance and their isotopic ratios are shown in Table 1. Batch 1 gave almost three times as abundant rare gases as batch 2. Also isotopic ratios, $^{40}Ar/^{36}Ar$ and $^{3}He/^{4}He$, are quite different between the two batches. We believe that the difference is mainly due to difference in an amount of the black inclusions, that is, rare gases in batch 1 may be mostly from the black inclusions, while those in batch 2 are more representative of diamonds. In both cases major degassing are observed at 2000°C heating. In third batch of sample which were heated at 1500°C gave off ^{40}Ar of about 1×10^{-8} ccSTP/g which is less than 10% of rare gases degassed in batch 1 and 2 at 2000°C heating. X-ray analyses on heated samples showed that 1500°C heating for 1 hour (batch 3) did not result in graphitization, but 2000°C heating for 1 hour (batch 1 and batch 2) have completely converted diamonds to graphite. From these experimental results we conclude that graphitization which accompanies density change of by more than 30% must be responsible to the major degassing of diamonds.

Table 1. Elemental and isotopic compositions of rare gases in diamond.

SAMPLE	Batch 1			Blank 1	Batch 2			Blank 2
Weight (g)	1.98				2.61			
Temperature (°C)	800	2000	2100	2000	800	2000	2100	2000
Time of heating (min.)	30	60	5	60	30	60	60	60
	ccSTP/g							
$^{3}He \times 10^{-13}$	<3	286	<10	<20	<10	179	<10	<20
$^{4}He \times 10^{-9}$	1.36	3480	0.09	1.1	1.57	918	0.37	2
$^{20}Ne \times 10^{-12}$	6.3	20.7	< 0.1	20	2.1	10.2	< 0.1	20
$^{36}Ar \times 10^{-11}$	3.35	36.7	10	2.4	1.54	9.37	1.90	2
$^{84}Kr \times 10^{-12}$	1.8	3.6	< 0.02	0.6	1.0	2.9	0.26	0.8
$^{132}Xe \times 10^{-13}$	3.5	9.1	< 2	2	4.4	7.3	1.0	2
$^{3}He/^{4}He$	$<2 \times 10^{-4}$	$(8.23 \pm .35) \times 10^{-6}$				$(1.95 \pm .07) \times 10^{-5}$		
$^{40}Ar/^{36}Ar$	359 ± 2	436 ± 2			574 ± 14	1121 ± 8		
$^{128}Xe/^{132}Xe$		0.0754 ± .0011				0.0718 ± .0037		
$^{129}Xe/^{132}Xe$		0.996 ± .019				0.978 ± .004		
$^{130}Xe/^{132}Xe$		0.161 ± .007				0.149 ± .006		
$^{131}Xe/^{132}Xe$		0.786 ± .023				0.779 ± .014		
$^{134}Xe/^{132}Xe$		0.391 ± .012				0.386 ± .009		
$^{136}Xe/^{132}Xe$		0.328 ± .012				0.318 ± .018		

Other isotopic ratios are indistinguishable from atmospheric values.

Except for He, other rare gases show similar thermal release pattern. In the case of He, more than 99% was degassed at 2000°C suggesting that most of He resided at low temperature sites had already been degassed prior to the experiment, perhaps under high temperature mantle condition. From the very similar thermal release pattern of rare gases between batch 1 and batch 2, we conclude that rare gases in the black inclusions occupies similar residing sites as those in batch 2, the latter being more likely to represent diamond rare gases. The result suggests syngenetic origin of the black inclusions with diamonds.

Potassium contents were measured on evaporates which were deposited on the inner wall of a high vacuum extraction furnace during the graphitization. The deposits were washed by dil. HNO_3 and potassium content in the washed solution was measured with an isotope dilution method. The amount of potassium are 8.22 ppm and 1.97 ppm for batch 1 and batch 2 respectively. Since radiogenic ^{40}Ar which would have been produced in batch 1 diamonds by this amount of K will exceed the total amount of ^{40}Ar if the age of the diamonds is older than 2.8 b.y. Hence, the age of the diamonds can not be older than 2.8 b.y. If the maximum age of 2.8 b.y. is assumed, this will give minimum

$^{40}Ar/^{36}Ar$ ratio of 670 for the trapped Ar in the batch 2 diamonds. The observed $^{3}He/^{4}He$ ratio is also minimum, since the diamonds must contain some U as well as K. From these we conclude that $^{3}He/^{4}He$ and $^{40}Ar/^{36}Ar$ in the diamonds must be larger than 1.95×10^{-5} and 670. The $^{3}He/^{4}He$ retio is significantly higher than those observed in ridge submarine glasses (Craig and Lupton, 1976), which is generally regarded to be derived from oceanic upper mantle. The high $^{3}He/^{4}He$ ratio may suggest that the diamonds were derived from a region different from source regions for oceanic ridge basalts, most likely from deeper region in the mantle. In this connection it is interesting to note that similar high $^{3}He/^{4}He$ (2.09×10^{-5}) are observed in Hawaiian volcanic gases (Craig and Lupton, 1976), which may be derived from deeper mantle through a hot spot.

Although origin of diamonds is not fully understood yet, it is generally assumed that diamonds crystallized from CO_2 saturated fluid phase in the mantle, probably deeper than 100 km or even more. The syngenetic black inclusions occluded in diamonds appear to have been derived from mantle region in which diamonds crystallized. The present results then lead us to an interesting speculation that rare gases observed in batch 2 may be representative of those carried by CO_2 phase, whereas rare gases in batch 1, or more specifically rare gases in the black inclusions, is rather indicative of a region where the diamonds occluded the former.

Ar isotopic ratios observed in diamonds do not seem to support a speculation (Frank, 1967) that diamonds were formed from materials in subducting ocean sediments, since even very small amount of sea water contamination (say less than 0.1%) which would necessarily accompany ocean sediments would reduce $^{40}Ar/^{36}Ar$ isotopic ratio to almost atmospheric value (295.5) because of relatively very high Ar content (about 0.03%) in sea water. The observed $^{40}Ar/^{36}Ar$ is much higher than the atmospheric ratio, ruling out any noticeable amount of sea water contamination.

References

Boulos, M.S. and O.K. Manuel (1971) Science, 174, 1334-1336.

Craig, H. and J.E. Lupton (1976) Earth Planet. Sci, Lett., 31, 369-385.

Frank, F.C. (1967) in Science and Technology of Industrial Diamonds, 1, ed. by J. Burls.

Melton, C.E. and A.A. Giardani (1976) Nature, 263, 309-310.

Melton, C.E. and A.A. Giardani (1974) Amer. Mineral., 59, 775-782.

Ozima, M. (1975) Geochim. Cosmochim. Acta, 39, 1127-1134.

Schwarzman, D.W. (1973) Nature Phys. Sci., 245, 20.

Sharp, W.E. (1960) Nature, 211, 402-403.

Takaoka, N. (1976) Mass Spectroscopy, 24, 73-86.

Tolstikhin, I.N. (1975) Earth Planet. Sci. Lett., 26, 88-96.

RARE GAS OCCLUSION INTO GRAINS DURING ITS GROWTH — AN APPROACH TO STUDY THE PLANET FORMATION

Masahiko HONDA and Minoru OZIMA

Geophysical Institute, University of Tokyo
Bunkyo-ku, Tokyo 113

1. Introduction

"Primordial" rare gases found in meteorites are generally classified in two groups; solar and planetary types. The formar represents solar wind trapped on the surface of the meteorites after the accretion. The latter is found in relatively undifferentiated meteorites, and seems to have been incorporated before accretion from the solar nebula. However, the occlusion mechanism in the latter case is not well understood. To explain this, the following three features must be accounted for.

1. Elemental abundances; when normarized to Ar, the heavier rare gases (Kr, Xe) of a planetary type show a progressive enrichment relative to the solar abundances, and the lighter one (Ne) depletion (Fig. 1).

2. Amounts; meteorites contain large amounts of rare gases. Average amounts of 'primordial' ^{20}Ne, ^{36}Ar, ^{84}Kr, and ^{132}Xe in carbonaceous chondrites are 64, 89, 0.82, and 0.58 with the unit of 10^{-8} ccSTP/g respectively. (Mazor et al., 1970) They are two to three orders of magnitude larger than those in terrestrial volcanic rocks.

3. Rare gas trapping sites; the planetary type rare gases appear to be uniformly distributed throughout the host crystals. Stepheating experiment suggests that such retentive sites are associated with the crystal lattice. Most rare gases are not released until the lattice is broken.

In order to explain the rare gas occlusion into grains three models have been presented; 1. solubility model 2. Adsorption model 3. implantation model

Kirsten (1968) made an experiment on solubility of rare gases in enstatite melts.

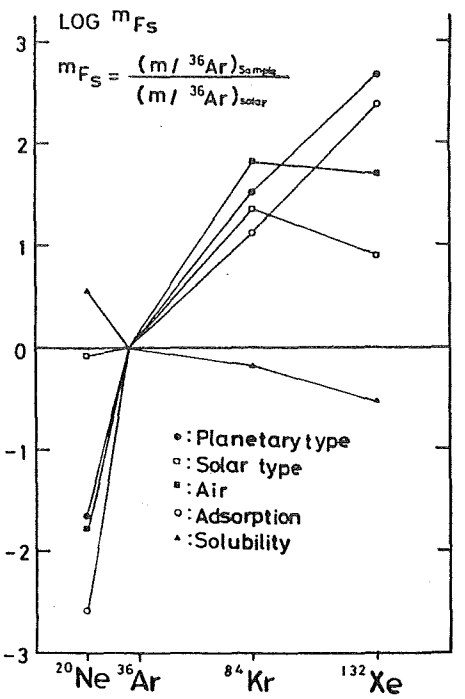

Fig. 1

Enstatite melts were quenched in the presence of He, Ne and Ar in different partial pressures. The amounts of the included gas were found to be proportional to the applied partial pressure. Henry constant for rare gas solubility is expressed as $K_i = a \exp(-b r_i^2)$, where a and b are constants and r_i is a gas kinetic radius of the rare gas atom. One can, then, calculate the similar constants for Kr and Xe from their atomic radius. The solubility constants for the lighter rare gases are larger relative to the heavier ones. The resultant rare gas pattern is opposite to those observed in meteorite (Fig. 1).

Fannale and Cannon (1972) examined the adsorption of Ne, Ar, Kr and Xe on pulverised samples of the Allende meteorite at 113°K. The observed rare gas elemental abundance pattern after adsorption is similar to that of the planetary rare gases (Fig. 1). Although adsorption model explains the elemental abundances and amounts, it does not appear to explain the trapping sites characteristics, since adsorped gases on the surface of grains can be easily degassed even at moderate temperatures. Moreover, the temperature of the pre-planetary nebula may have been higher than 113°K. If so, amounts of adsorped rare gases may decrease drastically compared to those adsorped at 113°K.

The third model is the implantation model. Arrhenius and Alfvén (1971) suggested that the crystal growth by condensation from a medium containing rare gases leads to the incorporation of rare gas atoms in the solid. By an implantation of rare gas atoms on or into the surfaces of a growing crystal, rare gas will be occluded at thermally retentive sites in a relatively larger quantity.

Since an experiment of rare gas occlusion into grains during crystal growth has not been reported so far, we have carried out an experiment to resolve these questions.

2. Experiment

We have chosen telluric cadmium alloy (CdTe) for the study, because CdTe can be easily made in the rare gas atmosphere (sublimation method) as well as by melting method. The melting temperature of CdTe is 1090°C. After making CdTe crystals by the both methods, we compared the amounts of rare gases trapped, and their thermal release patterns. In the sublimation method we may simulate the rare gas occlusion into grains during a crystal growth from gas phase, whereas in the melting method that from liquid phase. We have investigated the difference of the amounts and the released patterns of occluded rare gases between the samples prepared by the two methods.

Fig. 2 shows the equipment for preparing CdTe. Lumps of Cd and Te were put in a combution boat. The temperature of a combusion boat was maintained at 900°C (which is well below the melting temperature of CdTe) by a temperature controller. The quartz tube was filled with argon gas of 99.99% purity, which had a flowing rate of 150 cc/min.. Vapourized Cd and Te were carried to the cooler place by argon gas and the crystals of CdTe educed in the interior of the quartz tube. The mean grain size of CdTe made by sublimation method was about 1 μm. In the melting method, Cd, Te and $CdCl_2$ were put in the combusion boat. CdTe was in a melting state with $CdCl_2$ at more than 500°C.

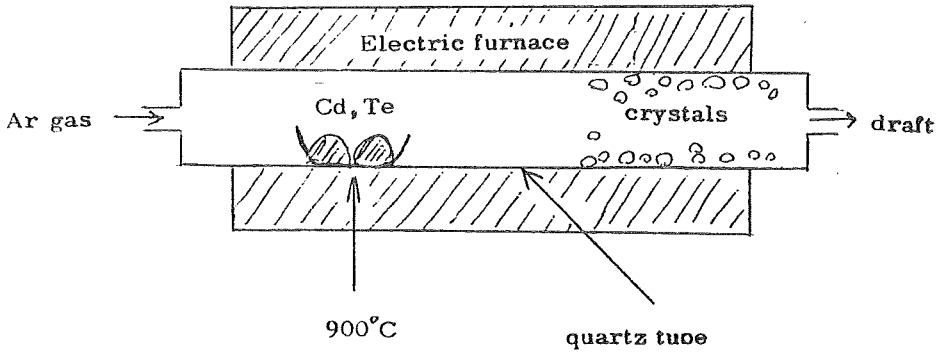

Fig. 2

After the combusion boat was heated up to 900°C, the electric furnace was put off and CdTe was quenched. There were only CdTe crystals in the combusion boat. CdTe was checked by X ray diffraction and it was confirmed that no other crystals were formed but CdTe. The size of CdTe prepared by a melting method ranges from 1 μm to 1 mm.

Argon was analysed by a quadrupole mass spectrometer, which has an accuracy of about 5% for a quantitative analysis of argon for the present sample size. The samples were heated for 30 minutes by an induction heater at each step (500°C, 750 °C, 900°C, 1000°C, 1200°C). The amount of argon released at each temperature fraction was calibrated against known amounts of the standard gas.

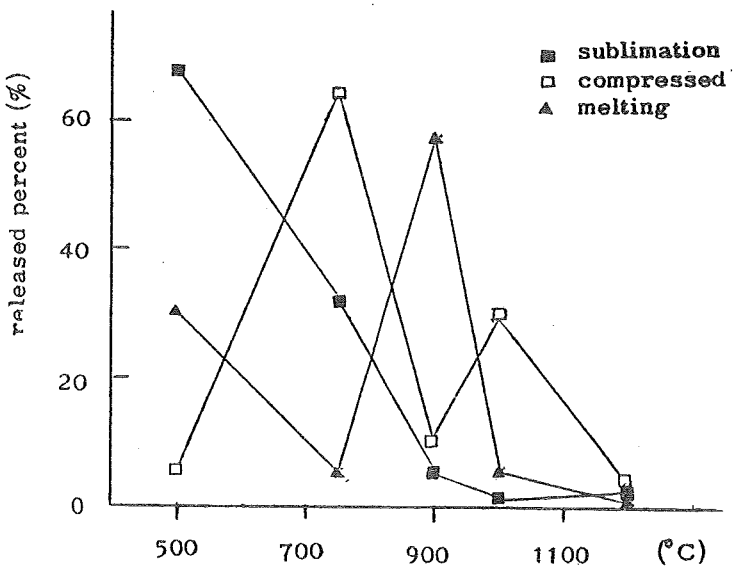

Fig. 3

3. Results and discussion

Released patterns are shown in Fig. 3. In the case of a sample prepared by a sublimation method, argon was mostly degassed at lower temperatures; it was completely degassed much below the melting temperature of CdTe. In the case of sample prepared by a melting method, argon was mostly degassed at the melting temperature, which means that argon was trapped very tightly in crystal lattices. In the case of sublimation method, contrary to Arrhenius and Alfvén's speculation, argon was trapped at thermally very loose sites. More argon may have been trapped even at lower temperatures.

We have also examined rare gas redistribution in crystals after the crystal growth. Rare gases which were firstly trapped in loose sites, such as ultrafine cavities in crystals (Abadi et al., 1976), might have been redistributed to more retentive sites caused by a shock effect (Davis, 1977) during the accretion process and/or hydrostatic pressure within the meteorite parent body. So we have made an experiment to check this suggestion. We pressed fine grains of CdTe prepared by a sublimation method at 3 Kbar for 5 minutes by a piston cylinder. Released patterns of argon for the compressed samples is also shown in Fig. 3, which is cleary different from that for the original unpressed fine grains. Hence, the experiment seems to support the suggestion that compaction would stabilize the retentivity of rare gas atoms in a crystalline powder.

Amounts of argon in CdTe crystals made by a sublimation method and by a melting method were 65 and 6.1 with the unit of 10^{-6} ccSTP/g respectively. The amount of argon made by a sublimation method was one order of magnitude more than those made by a melting method. However, if we assume that the amount of rare gases trapped in crystals during a sublimation process is proportional to the partial pressure of the rare gases, the expected amount of Ar trapped in a solar nebula (a total pressure $\sim 10^{-3}$ torr) would be almost six orders of a magnitude less than those commonly observed in meteorites. It is important to make crystals under various partial pressure of argon to check whether this characteristics is true in different conditions.

References

Abadi, H., P. Joshi, S. Ramadurai and N.C. Wickramasinghe (1976) Nature, 263, 214.

Arrhenius, G. and H. Alfvén (1971) Earth Planet. Sci. Letters, 10, 253.

Davis, P.K. (1977) Geochim. Cosmochim. Acta, 41, 195.

Fannale, F.P. and W.A. Cannon (1971) Geochim. Cosmochim. Acta, 36, 319.

Kirsten, T. (1968) J. Geophys. Res., 73, 2807.

Mazor, E., D. Heymann and E. Anders (1970) Geochim. Cosmochim. Acta, 34, 781.

IMPLICATION OF PRIMORDIAL ^{3}He DEGASSING ON AN ATMOSPHERIC EVOLUTION

Minoru OZIMA* and Sadao MATSUO**

* Geophysical Institute, University of Tokyo
Bunkyo-ku, Tokyo 113
** Department of Chemistry, Tokyo Institute of Technology
Meguro-ku, Tokyo 152

1. Clark, et al. (1969) and Mamyrin, et al. (1969) found that ^{3}He is currently being degassed from the mantle. The ^{3}He flux was estimated to be about 2 atom/cm^2·s. Lately, Lupton and Craig (1975) estimated ^{3}He flux on the basis of ^{3}He inventory on oceanic ridge basalts, suggesting a value for ^{3}He flux of about 5 atoms/cm^2·s. The latter estimation, however, was derived rather indirectly with some unwarranted assumptions. We therefore take a value for ^{3}He flux to be

$$f\ (^3He) = 2\ \text{atom/cm}^2\cdot\text{s} = 2.4 \times 10^{-12}\ \text{ccSTP/cm}^2\cdot\text{y}.$$

2. Assuming $f\ (^3He) = 2\ \text{atom/cm}^2\cdot\text{s}$, we obtain a total flux $F(^3He)$ from the entire earth's surface,

$$F\ (^3He) = 4\pi R^2 \times f\ (^3He) = 17.4 \times 10^{-6}\ \text{moles/s} = 12 \times 10^6\ \text{ccSTP/y}.$$

3. We assume a first order rate process for ^{3}He degassing, that is,

$$F\ (^3He) = \frac{d}{dt}\ (^3He)_E = -k\ (^3He)_E \qquad (1)$$

$$(^3He)_{E,P} = (^3He)_{E,0}\ e^{-k\cdot T_0} \qquad (2)$$

where suffixes p and o denote the present time and 4.5 b.y. ago and T_0 is 4.55×10^9 y.
From Eq. (1) and (2), we have

$$(^3He)_{E,p} = \frac{1}{k}\ F\ (^3He) \qquad (3)$$

$$(^3He)_{E,0} = \frac{1}{k}\ F\ (^3He) \times e^{k\,T_0} \qquad (4)$$

4. From Eq. (3) and (4) and with the use of $F\ (^3He) = 1.2 \times 10^7$ ccSTP/y, we can estimate $(^3He)_{E,p}$ and $(^3He)_{E,0}$ for various values of k;

$k(y^{-1})$	$(^3He)_{E,p}$	$(^3He)_{E,0}$
10^{-10}	2×10^{-11} ccSTP/g	3.2×10^{-11} ccSTP/g
10^{-9}	2×10^{-12}	1.9×10^{-10}
10^{-8}	2×10^{-13}	12×10^6
10^{-7}	2×10^{-14}	

5. We may make an estimate on ^3He content in the present mantle from ^3He content trapped in xenoliths in volcanic rocks, the latter giving about 1.4×10^{-12} ccSTP/g (Gramlich and Naughton, 1972).

Comparing this value with those in Table 1, we see that if ^3He degassing follows a first order rate process as we have assumed above, the degassing coefficient k must be about $10^{-9}y^{-1}$ and the originally trapped ^3He in the earth would be about 2×10^{-10} ccSTP/g. The latter value is still much less than ^3He trapped in C-chondrite, i.e., $10^{-9} \sim 10^{-8}$ ccSTP/g. Hence, ^3He which has been degassed by a continuous process, i.e., by a first order rate process, must be only a small (say less than 10%) fraction of total ^3He initially trapped in the earth. The rest of ^3He must have been degassed catastrophically. Hence, observed ^3He degassing is not inconsistent with an early sudden and later continuous degassing model of the terrestrial atmosphere as concluded by Ozima (1975).

References

Clark, W.G., M.A. Beg and H. Craig (1969) Earth Planet. Sci. Lett., 6, 213.

Gramlich, J.W. and J.J. Naughton (1972) J. Geophys. Res., 77, 3032.

Lupton, J.E. and H. Craig (1975) Earth Planet. Sci. Lett., 26, 133.

Mamyrin, B.A., I.N. Tolstikhin, G.S. Anufriev and I.L. Kamensky (1969) Dokl. Akad. Nauk. S.S.S.R., 184, 1197.

Ozima, M. (1975) Geochim. Cosmochim. Acta, 39, 1127.

TRANSPORT MECHANISM OF TRACE ELEMENTS FROM THE MANTLE TO THE CRUST

Minoru OZIMA

Geophysical Institute, University of Tokyo
Bunkyo-ku, Tokyo 113

Transport of trace-elements such as U, Pb, Rb, Sr and so on from the mantle to the crust is conventionally represented by a phenomenological first order rate process, that is, a rate of the transport of elements is assumed to be proportional to the total amount of the elements. Below, we show that a first order rate process can be interpreted in terms of partition of trace elements between liquid and solid phases, therefore giving a firm physical basis for the phenomenological theory.

Applying a first order rate process for transport of trace element A and B, we have the following phenomenological equation,

$$\begin{aligned} \frac{d(A)_M}{dt} &= -k_A (A)_M \\ \frac{d(B)_M}{dt} &= -k_B (B)_M \end{aligned} \tag{1}$$

where k denotes a first order rate coefficient or a transport coefficient and subscript M denotes a value in the mantle. Denoting $(A)_C$ and $(B)_C$ for values in the crust, from Eq. (1) we have,

$$\begin{aligned} d(A)_C &= -d(A)_M = -k_A (A)_M dt \\ d(B)_C &= -d(B)_M = -k_B (B)_M dt \end{aligned} \tag{2}$$

Hence,

$$\frac{d(A)_C}{d(B)_C} = \left(\frac{k_A}{k_B}\right) \frac{(A)_M}{(B)_M} \tag{3}$$

As an transport mechanism, we assume that trace elements were transported with magma ascending from the mantle to the crust. Trace elements which were transported with magma must be those which were in liquid phase during a partial melting for the magma generation. Hence, we have

$$\begin{aligned} (dA)_C &= (dA)_L \\ (dB)_C &= (dB)_L \end{aligned} \tag{4}$$

in which subscript L indicates a liquid phase. Trace elements in a solid phase then correspond to residuals in the mantle, that is,

$$\begin{aligned} (A)_S &= (A)_M \\ (B)_S &= (B)_M \end{aligned} \tag{5}$$

By definition of partition, from (4) and (5) we have

$$\frac{(dA)_L}{(A)_S} = \frac{(dA)_C}{(A)_M} = \alpha_A \tag{6}$$

$$\frac{(dB)_C}{(B)_S} = \frac{(dB)_C}{(B)_M} = \alpha_B$$

where α_A and α_B indicate partition coefficients between a liquid and solid phases. Consequently, we have from (6)

$$\frac{d(A)_C}{d(B)_C} = \left(\frac{\alpha_A}{\alpha_B}\right) \frac{(A)_M}{(B)_M} \tag{7}$$

Eq. (7) is exactly the same form as Eq. (3), and from a comparison of these equations, we have

$$k_A/k_B = \alpha_A/\alpha_B \tag{8}$$

or the phenomenological transport coefficient is given a physical significance. As an example we will examine a case for U-Pb systematics.

Both U and Pb are incompatible trace elements and are enriched in the crust. Systematic transport of these elements from the mantle to the crust should be reflected in Pb isotopic ratios in basalts, which may be regarded to be representative of the mantle isotopic ratios. From a study on oceanic basalt Pb isotopes, Russell (1972) obtained a transport coefficients for U and Pb, i.e., $k_{Pb} \simeq 1.6 \times 10^{-9}$ yr^{-1} and $k_U \simeq 2.6 \times 10^{-9}$ yr^{-1} which give a ratio $k_U/k_{Pb} = 1.6$.

Experimental results on partition of Pb and U between melt and residual solid phases (Onuma, et al., 1968) give $\alpha_U/\alpha_{Pb} \simeq 7$. Although the above discussion suggests that α_U/α_{Pb} should be equivalent to k_U/k_{Pb}, the experimentally estimated ratios for U-Pb systematics differ significantly. The difference may be due to inadequacy in either of the experimental estimates α_U/α_{Pb} or k_U/k_{Pb}, or in the both.

References

Onuma, N., H. Wakita and H. Nagasawa (1968) Earth Planet. Sci. Lett., 5, 47.

Russell, R.D. (1972) Rev. Geophys. Space Phys., 70, 529.

AUTHOR INDEX